Influence of selenium on pancreatic carcinogenesis and the role of the selenoproteins cytosolic and mitochondrial thioredoxin reductase in the pancreas

Dissertation zur Erlangung des Doktorgrades
der Naturwissenschaften (Dr. rer. nat.)

Fakultät Naturwissenschaften
Universität Hohenheim

Institut für Biologische Chemie und Ernährungswissenschaften

und

Abteilung für Vergleichende Medizin,
Helmholtz Zentrum München –
Deutsches Forschungszentrum für Gesundheit und Umwelt (GmbH)

vorgelegt von

Michaela Yvonne Aichler

aus Backnang

2007

Dekan:	Prof. Dr. rer. nat. H. Breer
1. berichtende Person:	Prof. Dr. rer. nat. L. Graeve
2. berichtende Person:	Dr. vet. med. M. Brielmeier
Eingereicht am:	21.12.2007
Mündliche Prüfung am:	08.05.2008

Die vorliegende Arbeit wurde am 25.03.2008 von der Fakultät Naturwissenschaften der Universität Hohenheim als „Dissertation zur Erlangung des Doktorgrades der Naturwissenschaften“ angenommen.

To my parents.

Preliminary remarks

The present work has in part be published or presented as follows:

Publications in peer-reviewed journals

Aichler, M., Algül, H., Behne, D., Hölzlwimmer, G., Michalke, B., Quintanilla-Martinez, L., Schmidt, J., Schmid, R.M., Brielmeier, M.
Selenium status alters tumour differentiation but not incidence or latency of pancreatic adenocarcinomas in *Ela*-TGF-α $p53^{+/-}$ mice.
Carcinogenesis, 28 (9), 2002-2007, 2007.

Talks

Aichler, M., Algül, H., Behne, D., Hölzlwimmer, G., Michalke, B., Quintanilla-Martinez, L., Schmidt, J., Schmid, R.M., Brielmeier, M.
Does the selenium status influence the incidence of pancreatic carcinomas and hematopoietic tumours in tumour prone p53-hemizygous mice?
(Danish –German Symposium, June 27th – 28th, 2006, Environmental Research Station Schneefernerhaus – Zugspitze, Garmisch)

Aichler, M., Algül, H., Behne, D., Hölzlwimmer, G., Michalke, B., Quintanilla-Martinez, L., Schmidt, J., Schmid, R.M., Brielmeier, M.
Effect of selenium on incidence, latency and tumour differentiation in pancreatic cancer.
(8th International Symposium on Selenium in Biology and Medicine, July 25th – 30th, 2006, University of Wisconsin, Madison WI, USA)

Poster presentations

Brielmeier, M., Aichler, M., Behne, D., Schmid, R., Schmidt, J.
The selenium platform: selenium deficiency as pathogenic factor.
(Gemeinsame Herbsttagung, 24th-25th November, 2005, Hahn-Meitner-Institut, Berlin, Germany)

Aichler, M., Algül, H., Behne, D., Hölzlwimmer, G., Michalke, B., Quintanilla-Martinez, L., Schmidt, J., Schmid, R.M., Brielmeier, M.
Effect of selenium on incidence, latency and differentiation in pancreatic cancer prone mice.
(Gemeinsame Herbsttagung “Metallobiolomics”, 6th – 7th December, 2006, Hahn-Meitner-Institut, Berlin, Germany)

Aichler, M., Algül, H., Behne, D., Hölzlwimmer, G., Michalke, B., Quintanilla-Martinez, L., Schmidt, J., Schmid, R.M., Brielmeier, M.
Selenium supplementation in mice influences the malignancy of pancreatic adenocarcinomas.
(FELASA-ICLAS Joint Meeting, 11th – 14th June, 2007, Villa Erba, Cernobbioa (CO), Italy)

Aichler, M., Algül, H., Behne, D., Hölzlwimmer, G., Michalke, B., Quintanilla-Martinez, L., Schmidt, J., Schmid, R.M., Brielmeier, M.
Selenium supplementation in mice influences the tumour differentiation of pancreatic adenocarinomas.
(1st Life-Science PhD Symposium, 7th December, 2007, MPI of Neurobiology/Biochemistry, Munich, Germany)

Index

1 Introduction

1.1 Selenium

Selenium was discovered by the Swedish chemist Brezelius in 1817 when he investigated intoxications in sulphuric acid plant workers. Contamination with arsenic was the problem, but he also recognized that a new element was involved, which he named selenium after the Greek goddess of the moon Selene. For many years selenium remained unappreciated, until it was recognized in forages that caused livestock poisoning in South Dakota (Franke, 1934). The understanding of the significance of selenium changed dramatically with the discovery, that minute amounts of selenium were protective against a type of liver necrosis in laboratory rats fed vitamin E deficient diets (Schwartz and Foltz, 1957). Since this finding selenium is considered as an essential trace element.

Selenium is involved in various biological processes. It accesses the food chain from soil sources through plants into animals and humans, and as a consequence the selenium soil content influences selenium intake by the nutrition route (Moxon *et al*., 1939). In Germany, the selenium content of the soil is poor. Subsequently, the intake of selenium by nutrition in humans and animals is low (Sill, 1999). About 40 µg/day is the suggested minimum requirement of selenium in humans (Whanger, 2004). In Germany the selenium intake is about 47 µg/day, which is very low compared to many other countries (Surrai, 2006). An intake of less than 11 µg/day results in severe deficiency problems, while an intake of 3200-5000 µg/day results in selenosis (Reid *et al*., 2004; Whanger, 2004). Selenium intake in toxic amounts leads to alkali disease (selenosis), associated with symptoms like loss of hair and nails and dermatitis (Vinceti *et al*., 2001). Selenium deficiency leads to different metabolic disorders in animals and humans. One of these, a localized myopathy involving depigmentation and calcification called “white muscle disease”, occurs in most of agriculturally and commercially used animals (Van Vleet and Ferrans, 1977; Poston *et al*., 1976; Walter and Jensen, 1964; Calvert *et al*., 1962; Hartley and Grant, 1961; Dodd *et al*., 1960; Muth *et al*., 1958; Eggert *et al*., 1957). Pancreatic atrophy in chicken, fragility and brakeage of spermatozoa and cataracts in rats are other signs of selenium deficiency (Whanger and Weswig, 1975; Wu *et al*., 1973; Thompson and Scott, 1970). In humans, selenium deficiency-related diseases for example are Keshan disease, a cardiomyopathy, Kaschin-Beck disease with necrosis of cartilage and dystrophy of skeletal muscle and myxoedematous endemic cretinism, a thyroid atrophy of young children in areas of selenium and iodine deficiency and overload of thiocyanate (Surrai, 2006; Contempre *et*

al., 2004; Goyens *et al*., 1987). Further insight into the physiological role of selenium came after the discovery of its essential role in various selenoproteins like glutathione peroxidase, thioredoxin reductase or thyroid deiodinase, where it is incorporated as the 21st proteinogenic amino acid selenocysteine (Koehrle, 2000; Williams *et al*., 2000; Zhong *et al*., 1998; Rotruck *et al*., 1973). The physiological functions of selenium derive from the catalytic and physical properties of such selenoproteins which will be described in detail in this work.

1.1.1 Selenium metabolism

Selenium enters the food chain via plants, which absorb the element in its inorganic forms from the soil and convert it into organic forms. In food, selenium exists mostly in organic forms, mainly as selenomethionine, selenocysteine, selenmethylseleno-methionine and selenmeythylselenocysteine, whereas inorganic selenium forms either selenites or selenates, are found in plants in very low amounts (Surrai, 2006). In mammals, organic selenium forms are actively transported through the intestinal membranes during digestion and are actively accumulated in tissues like liver and muscle. Selenomethionine, for example, cannot be synthesized in animals or humans and must be derived from feed sources (Schrauzer, 2003; 2000). In contrast, selenium from inorganic forms is absorbed as a mineral and only little is stored in tissues. Therefore, most of it is excreted with urine in non-ruminants or with faeces in ruminants (Surrai, 2006). Both forms can be used in the body to produce selenoproteins and selenium enters the metabolism at different points depending on its chemical form (Meuillet *et al*., 2004; Shiobara *et al*., 1998; Lu *et al*., 1995). Selenite (Na_2SeO_3) and selenate (Na_2SeO_4), with a valence of +4 and +6 respectively, are reduced by glutathion. After a number of intermediate metabolic steps hydrogen selenide (H_2Se) is generated. Alternatively, they enter directly the metabolic pool (Lu *et al*., 1995; Foster *et al*., 1986). The reduction of inorganic selenium to hydrogen selenide via selendiglutathion involves the production of superoxide radicals (Hsieh and Ganther, 1975; Ganther, 1971). Organic selenium compounds are also metabolized to hydrogen selenide (Tanaka *et al*., 1985; Esaki *et al*., 1982). Hydrogen selenide is the intermediate compound connecting the reductive metabolism of selenium and its methylation pathway. Hydrogen selenide can be either a selenium donor for the production of selenoproteins or can be methylated by the enzyme thiol S-methyltransferase to

generate mono-, di- and tri-methylated forms of selenium and can be either exhaled as dimethylselenide or excreted into urine as trimethylselenonium (Meuillet *et al*., 2004; Ip *et al*., 1991). At low selenium intake monomethylated forms of selenium are excreted into urine, while trimethylated forms are predominantly excreted at high selenium doses. Also, as a monomethylated metabolite of the selenium metabolism selenosugars in urine have been identified (Kobayashi *et al*., 2002).

Among the organic selenium compounds selenomethionine has a special role, which is due to the fact that cells do not distinguish between methionine and selenomethionine during protein synthesis, so that selenomethionine can get incorporated unspecifically into any protein and is therefore a selenium storage form. Selenium accumulation in the body depends on many factors including selenium-content in the diet. In selenium deficiency mainly liver, kidney and skeletal muscle are reduced in the selenium content, whereas brain, endocrine and reproductive organs do hardly react in this way (Hill *et al*., 1992; Behne *et al*. 1988). In these organs, the activity of thioredoxin reductase (Txnrd), selenoprotein W (SelW) and others selenoproteins is hardly affected (Whanger, 2001; Yeh, 1997). Furthermore, within selenoprotein family there is a hierarchy in selenoprotein expression in various conditions. In selenium-deficiency, the levels of glutathione peroxidase 1 (GPx1) and selenoprotein P (SePP) are drastically reduced, while iodothyronine deiodinase 1 (DIs1) and glutathione peroxidase 4 (GPx4) are nearly unaffected (Brigelius-Flohe, 1999; Bermano *et al*., 1995).

It has been reported, that selenium is efficiently passed from mother to offspring via the milk. This could be shown in a rescue experiment of SePP knockout mice where lactating mice were supplemented with sodium selenite, which then passed to offspring via the milk (Schweizer *et al*., 2004).

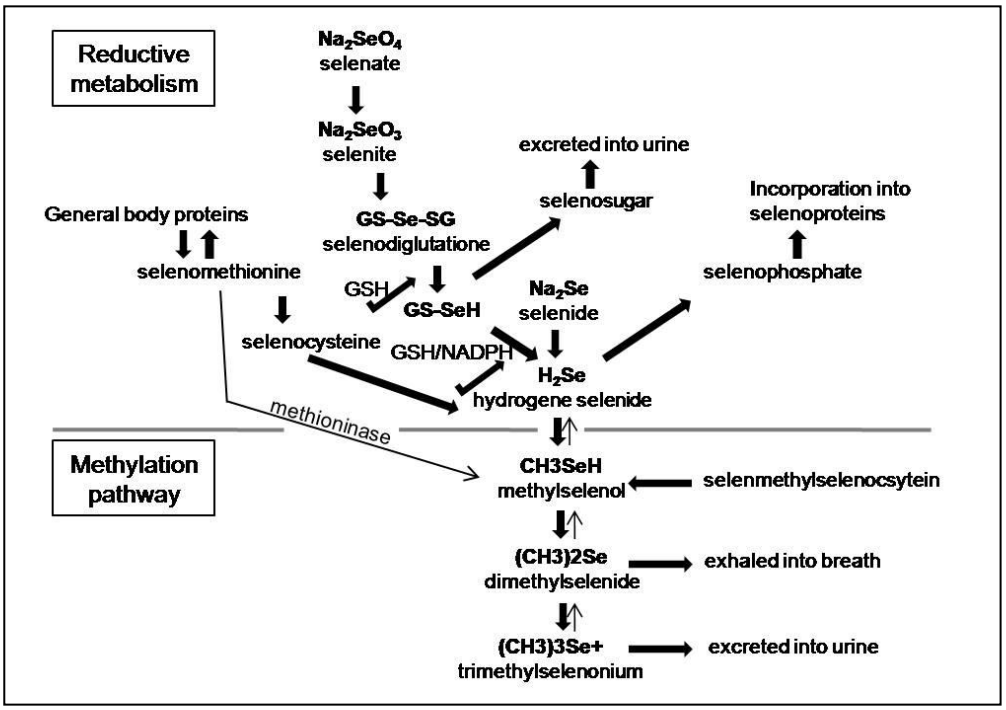

Fig.1: Selenium metabolism. Schematic representation of the selenium metabolic pathway (adapted from Meuillet *et al*., 2004; Lu *et al*., 1995; modified according to Kobayashi *et al*., 2002). (GSH=Glutatione, NADPH=nicotinamide adenine dinucleatide phosphate)

1.1.2 Selenium in cancer prevention

The first hints that there is a correlation between low selenium status and high incidence of certain types of cancer came from epidemiological studies, which showed a significant inverse correlation between selenium intake and age-adjusted mortality for cancers of the colon, prostate, breast, ovary, lung, and weak correlations for cancers of the pancreas, skin and bladder (Clark *et al*., 1991; Schrauzer *et al*., 1977 a, b; Shamberger *et al*., 1976; Yu *et al*., 1997). Clinical data showed cancer-preventive properties of selenium, when added to the normal diet, in all and particularly in gastrointestinal cancers (Rayman, 2005; Bjelakovic *et al*., 2004; Whanger, 2004). First chemopreventive trials have been carried out in China in a study with 130,000 people from a region with low selenium intake and high hepatocellular carcinoma incidence. In the population, one group received table salt fortified with sodium selenite (15 mg/kg), the control group received unfortified salt. After 6 years, the incidence of hepatocellular carcinoma decreased by 35% in the selenium-supplemented group compared to the unsupplemented group (Yu *et al*., 1997). Another important clinical trial tested the hypothesis that selenium supplementation may reduce the risk of skin cancer in a placebo-controlled study in the USA (Clark *et al*., 1996). There was

no effect on the primary endpoint on non-melanoma skin cancers, but individuals in the selenium-supplemented group had a reduced risk of primary cancers of the colon, rectum, prostate and lung. Today, several large interventional studies with different forms of selenium are under way in Europe and in the USA to assess the effect of selenium supplements on the incidence of cancer and other diseases (Burk *et al*., 2006; Sabichi *et al*., 2006; Drake, 2006; Luty-Frackiewicz, 2005). So far, no controlled or randomized interventional studies have been published proving the specific effect of selenium on pancreatic cancer, but data from epidemiological and case-control studies support a protective effect in this context (Knekt *et al*., 1990; Burney *et al*., 1989). A systematic analysis of published trials focussing on the effect of antioxidants in the prevention of gastrointestinal cancers including pancreatic cancer revealed no effect of beta-carotene, vitamin A, vitamin C, and vitamin E given alone or in combinations. These antioxidants may even increase overall mortality (Bjelakovic *et al*., 2004). Selenium, however, represents an exception among the antioxidants leading to a reduction of gastrointestinal cancers in recent studies. Effects of antioxidants on pancreatic cancer in animal studies were described by the use of two models. Hamsters which developed pancreatic tumours after injection of *N*-nitrosobis(2-oxopropyl)amine had a decreased number of advanced ductular lesions after supplementation with vitamin C, whereas beta-carotene, vitamin E or sodium selenite had no effects (Appel *et al*., 1996; Nishikawa *et al*., 1992; Birt *et al*., 1988). In rats, the incidence of azaserine-induced preneoplastic acinar lesions was lower in groups maintained on sodium selenite and also on beta-carotene and vitamin C, whereas vitamin E had no effect (Woutersen *et al*., 1999). In other studies using this model no effects of sodium selenite were observed (Curphey *et al*., 1988).

The suggested mechanisms of selenium in cancer prevention include its effect on DNA repair, the immune system, angiogenesis, inhibition of tumour cell growth and programmed cell death (Whanger, 2004). Selenoproteins play a key role in most of these mechanisms.

1.1.3 Selenoproteins

Selenoproteins are defined as proteins in which selenium is cotranslationally inserted as the 21st amino acid selenocystein (Sec) (Hatfield and Gladyshev, 2002; Low and Berry, 1996; Stadtman, 1996; Boeck *et al*., 1991). So far, 25 human and 24 mouse genes coding for selenoproteins have been identified (Kryukov *et al*., 2003). Sec is encoded by UGA which normally functions as a stop-codon (Voet and Voet, 2004; Boeck *et al*., 1991, Lee *et al*., 1989). In the case of selenoproteins Sec is incorporated by a tRNA molecule with an anti-codon complementary to UGA (Leinfelder *et al*., 1988). Unlike the other 20 amino acids Sec is synthesized universally on its own tRNA by using serine as an intermediate. As a first step in the Sec biosynthesis pathway serine is attached to the Sec tRNA$^{[Ser]Sec}$ by seryl tRNA synthetase to yield seryl- tRNA$^{[Ser]Sec}$. This seryl- tRNA$^{[Ser]Sec}$ is phosphorylated by phosphoseryl tRNA kinase and is then replaced by the selenium donor selenide (H_2Se-P), which is thought to be activated by selenophosphate synthetase 2. Selenocysteyl-tRNA$^{[Ser]Sec}$ is the resulting molecule, which delivers Sec into the growing peptide chain (Fig.2) (Papp *et al*. 2007).

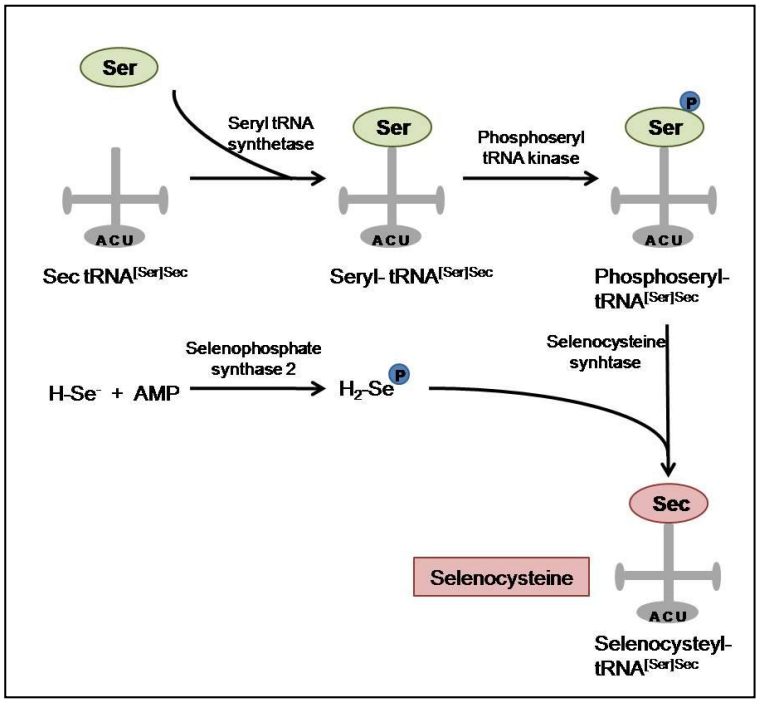

Fig.2: Selenocysteine biosynthesis pathway in mammalian cells. Selenocysteine biosynthesis initiates with the attachment of serine to the Sec tRNA$^{[Ser]Sec}$ by seryl tRNA synthase to yield seryl-tRNA$^{[Ser]Sec}$. The phosphoseryl tRNA kinase phosphorylates the complex. The phosphate is then replaced by the selenium donor selenide (H_2Se-P), which is thought to be activated by selenophosphate synthetase 2. The resulting molecule is selenocysteyl-tRNA$^{[Ser]Sec}$, which delivers the selenocysteine into the growing polypeptide chain (adapted from Papp *et al*., 2007; modified).

The selenocysteyl-tRNA$^{[Ser]Sec}$ is necessary but not sufficient for decoding UGA codons as Sec. A secondary RNA stem-loop structure, the selenocystein insertion sequence (SECIS), is the determinant for read-through of the Sec codon. In eukaryotes the SECIS element is located within the 3´-untranslated region (UTR) of the mRNAs (Berry *et al*., 1993, 1991). This SECIS element functions by recruiting SECIS-binding protein 2 (SBP2) to form a tight SECIS-SBP2 complex (Copeland *et al*., 2001, 2000; Low *et al*., 2000). SBP2 is stably associated with ribosomes via 28S rRNA, independent of its Sec insertion function, suggesting that SBP2 preselects ribosomes for Sec insertion (Copeland *et al*., 2001). The SECIS-SBP2 complex also binds to the Sec-specific elongation factor (EFSec), which recruits Sec tRNA$^{[Ser]Sec}$ and inserts Sec into nascent polypeptides in response to UGA codons (Fagegaltier *et al*., 2000; Tujebajeva *et al*., 2000).

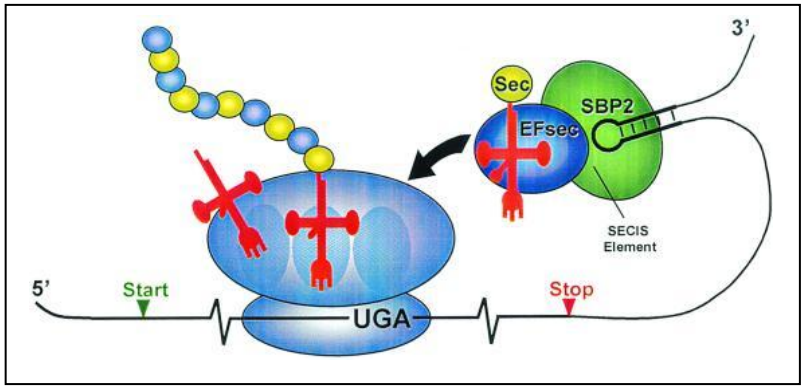

Fig.3: Mechanism of selenocysteine insertion in eukaryotes. The selenocysteyl-tRNA (red, with selenocystein Sec, yellow) is shown in complex with Sec-specific elongation factor (EFSec, dark blue) and SECIS-binding protein 2 (SBP2, green) and the selenocystein insertion sequence (black, SECIS, hairpin loop). Sec tRNA$^{[Ser]Sec}$ is transferred to the ribosomal peptidyl site and Sec is incorporated into the nascent selenopeptide. The growing selenopeptide is shown (alternating blue and yellow balls) attached to the tRNA in the peptidyl site. The mRNA (black, with start and stop codons indicated) is attached to the smaller of the two ribosomal subunits, and the unacetylated tRNA is shown leaving the ribosomal exit site (adapted from Hatfield and Gladyshev, 2002).

1.1.4 Thioredoxin reductases

In mammals, the selenoprotein thioredoxin reductase was first purified from calf liver and described by Holmgren (Holmgren, 1977). Now, three distinct thioredoxin reductases are known in mammals, each encoded by individual genes and located in different cellular compartments. Thioredoxin reductase 1 (Txnrd1) is located in the cytosol (Gasdaska *et al*., 1995; Gladyshev *et al*., 1996), thioredoxin reductase 2 (Txnrd2) in the mitochondria

(Gasdaska *et al*., 1999a), and thioredoxin reductase 3 (Txnrd3), also called thioredoxin-glutathione-reductase (TGR), is mainly expressed in testis (Sun *et al*., 2001). Thioredoxin reductases are part of the thioredoxin system, which is additionally comprised of thioredoxins and NADPH and is ubiquitously present in organisms ranging from Archaea to man (Arner and Holmgren, 2000).

Thioredoxin contains a redox-active dithiol/disulfide centre and therefore acts as an electron donor for essential enzymes such as ribonucleotide reductase. It is a general protein disulfide reductase with numerous functions controlling the intracellular redox potential, signal transduction by thiol redox control and defence against oxidative stress (Arner and Holmgren, 2000). Thioredoxins have a cytokine-like influence on blood cells and modulate the activity of redox-regulated transcription factors such as NF-κB and AP-1 (Karimpour *et al*., 2002; Nishinaka *et al*., 2002; Qin *et al*., 1995). They are also involved in DNA syntheses, as well as in protection of cells from oxidative damage by acting through peroxiredoxins (Nordberg and Arner, 2001; Rhee *et al*., 2001). There are cytosolic (Txn1) and mitochondrial (Txn2) expressed Txn, which are both indispensable for murine embryonic development (Nonn *et al*., 2003; Matsui *et al*., 1996).

Thioredoxin reductases from mammals and higher eukaryotes are selenoenzymes (Zhong *et al*., 1998; Tamura and Stadtman, 1996). They are homodimeric flavoproteins, members of the pyridine nucleotide-disulfide oxidoreductase family and possess two N- and C-terminally located interacting redox-active centres (Mustacich and Powis, 2000; Gromer *et al*., 1998). Reducing equivalents from NADPH are transferred to the prosthetic group FAD, from where they are passed to the N-terminal-catalytic centre of one subunit and then to the C-terminally located redox-active selenylsulfide of the other subunit (Sandalova *et al*., 2001; Zhong *et al*., 1998). Selenocystein is required for the activity of the enzyme, since cysteine variants of the protein loos activity (Zhong and Holmgren, 2000). Rats fed a Se-deficient diet for several weeks showed decreased Txnrd activity in the liver, kidney and lung, but activity in the brain was unchanged (Berggren *et al*., 1999; Hill *et al*., 1997). From *in vitro* data it is known that thioredoxin reductases have a broad range of substrates including selenite, hydrogen peroxide, lipoic acid, ascorbate, ubiquinone, NK-lysine and their main substrate thioredoxins (Txn) (Xia *et al*., 2003; Nordberg and Arner, 2001; Anderson *et al*., 1996). Interestingly, with respect to the following work, also selenite is a direct substrate for thioredoxin reductase as well as an efficient oxidant of thioredoxin (Kumar *et al*., 1992).

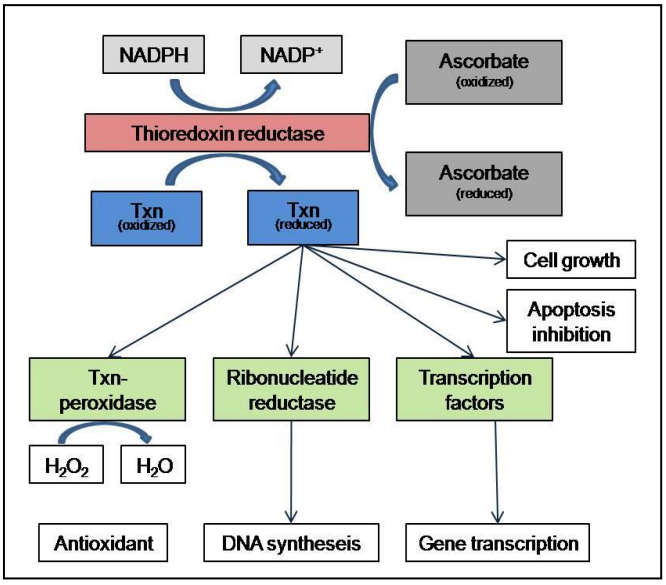

Fig.4: Reactions and functions of thioredoxin reductase. NADPH is needed as a cofactor when oxidized Txn or oxidized ascorbate are reduced by Txnrd. Reduced Txn can reduce Txn-peroxidase, which breaks down H_2O_2 into H_2O, ribonucleotide reductase, which is needed for DNA synthesis, transcription factors, which leads to increased DNA binding and altered gene transcription. Txn increases cell growth and inhibits apoptosis. Major downstream pathways are indicated (adapted from Mustacich and Powis, 2000; modified).

In the case of thioredoxin reductases, little is known about their physiological functions in mammals. Two knockout mouse models brought more light into this issue.

The *Txnrd1* gene consists of 15 exons. The last exon encodes the final 22 amino acids including the C-terminally located Sec-containing redox-centre. The 3´untranslated region contains the SECIS element, AU-rich mRNA instability elements and the endogenous transcription termination signal (Gasdaska *et al*., 1999b). This last exon of *Txnrd1* was flanked with *loxP* sites in mice by gene targeting. Crossing such mice with Cre deleter mice resulted in hemizygous knockout mice without a phenotype. These mice were intercrossed to get homozygous knockouts. With these breedings it was demonstrated that knockout of *Txnrd1* results in death and resorption of the mouse embryo around gestational day (embryonic day) 9.5 (E 9.5), which was due mainly to disturbed development of the nervous system (Jakupoglu *et al*., 2005).

The *Txnrd2* gene consists of 18 exons. It lacks AU-rich mRNA elements. Exon 17 encodes the Sec codon, exon 18 the SECIS element and the poly-adenylation signal. For knockout generation in mice, the last four exons were flanked with *loxP* sites and the same breeding strategy was executed as described for Txnrd1 knockout mice. Homozygous *Txnrd2* knockout in mice was embryonic lethal, too. Embryos were resorbed at E 13.5, due to

reduced heart function and perturbed haematopoiesis. Electron microscopic analysis showed swelling and destruction of mitochondrial cristae in cardiomyocytes of heart specific *Txnrd2* knockout mice (Conrad *et al*., 2004).

1.1.5 The thioredoxin/thioredoxin reductase system in carcinogenesis and tumour progression

A range of human diseases and conditions like rheumatoid arthritis, Sjörgen´s syndrome, AIDS and cancer, are related to the activity of thioredoxin reductases (Becker *et al*., 2000). In respect to cancer, the thioredoxin system supports growth and antioxidant defence in tumour cells, but it also prevents normal cells from getting malignant by protecting them against certain mutagens (Arner and Holmgren, 2000; Sun *et al*., 1999; Tamura and Stadtman, 1996; Gasdaska *et al*., 1994). Therefore, the involvement of the thioredoxin system is far from being clear and is also suspected to vary between cancer types.

In a study with lung carcinoma cells in which *Txnrd1* was knocked down, for example, it could be demonstrated that *Txnrd1* expression is necessary for cancer cell growth. After mice were injected with those lung tumour cells a dramatic reduction in tumour progression and metastasis compared to mice injected with control lung tumour cells, which carried only the vector, was observed (Yoo *et al*., 2006). This study implements the assumption that TXNRD1 is a key enzyme in the tumour phenotype and tumourigenisis. In an earlier study it was shown that in diffuse astrocytoma, the expression of Txnrd was associated with tumour grading, a study which also indicated that the thioredoxin system has an influence on tumour progression (Haapasalo *et al*., 2003).

Txnrd1 is also one of the genes strongly associated with tumour proliferation. Inhibition of Txnrd by antisense RNA in human hepatocellular carcinoma cells resulted in inhibition of growth with increased *p53* mRNA levels and reduced telomere length (Gan *et al*., 2005).

Furthermore, the Txn1/Txnrd1 system is involved in the redox regulation of the tumour suppressor p53. In Txnrd-deficient yeast p53 accumulates as an inactive, oxidized form. Inhibition of Txnrd in mammalian cells using RNA interference leads to increased p53 DNA-binding activity (Seemann and Hainaut, 2005). The DNA-binding activity of the transcription factor p53 is controlled by the thiol redox status of some critical cysteinyl residues in its DNA-binding domain (Hainhaut *et al*., 1993; Parks *et al*., 1997). The redox state of these residues appears to be regulated by thioredoxin (Ueno *et al*., 1999). In

addition, tumours like glioblastomas, which are prone to have p53 mutations show increased Txnrd levels (Haapasalo *et al*., 2003). Oxidative stress promotes nuclear translocation of thioredoxin 1 and activates various kinases phosphorylating p53, resulting in stabilization and activation of p53 in the nucleus (Bode and Dong, 2004).

The thioredoxin-dependent redox regulation of p53 is thus coupled with oxidative stress response and p53-dependent DNA repair and apoptosis.

Also, other selenoproteins like SePP and redox active proteins like manganese superoxide dismutase (MnSOD) are strongly connected with carcinogenesis and tumour phenotype. In the APC^{min} model of colon carcinoma, mice hemizygously knocked out for selenoprotein P, a selenium transport protein, develop more malignant tumours than APC^{min} mice, which are wild type for SePP (L. Schomburg, personal communication). In men with a homozygous mutation of MnSOD, an enzyme functionally linked to Txnrd2, an increased risk for high-grade prostate cancer could be observed. A positive correlation between low/baseline selenium levels in these patients and the development of more aggressive cancer was observed in this study (Li *et al*., 2005). In an in vitro study with pancreatic adenocarcinoma cell lines, a correlation between decreased activity of MnSOD and grade of differentiation of the tumour cell lines was shown (Cullen *et al*., 2003).

All these findings indicated that a lack in selenium/selenoproteins especially thioredoxin reductases, possibly in combination with other redox-regulating factors might drive tumours to a more malignant phenotype.

1.2 Pancreas

The pancreas is a glandular organ associated with the alimentary tract. The bulk of the organ is an exocrine gland producing digestive enzymes in which an endocrine gland is embedded that functions to maintain energy metabolite homeostasis.

1.2.1 Pancreatic organogenesis

Embryonic development of the pancreas is not the focus of this work, but it is important to know about the expression patterns of several genes involved in this process. In the mouse, the three germ layers, endoderm, ectoderm and mesoderm, are formed by the end of gastrulation at E 7.5 and derive from pluripotent cells (Downs and Davies, 1993). The digestive tract and derivates of the respiratory system develop from the endodermal germ layer. Factors produced in the adjacent mesoderm and ectoderm subdivide the endoderm into anterior and posterior domains along the anterior-posterior axis, including a broad endodermal region susceptible to subsequent induction towards a pancreatic fate (Wells and Melton, 2000). In the absence of mesodermal signals the dorsal endoderm develops to intestine instead of pancreas, whereas the ventral endoderm develops to pancreas. The signals from the dorsal mesoderm ensure absence of Hedgehog expression in the pancreatic endoderm, permitting *Ipf1* (insulin promoter factor 1) expression also called *Pdx1* (pancreas duodenum homeobox 1) (Hebrok *et al.*, 2000; Kim *et al.*, 1997). The ventral pancreas does not express Hedgehog molecules and signals from the adjacent cardiogenic mesoderm and the septum transversum are required to activate *Ipf1/Pdx1* (Deutsch *et al.*, 2001). The role of the signals from the ventral mesoderm is to promote hepatic development at the expense of pancreatic development. In the region of the foregut, which will become the duodenum, at E 8.5 to E 9.5, two dorsal and ventral buds crop out (Spooner *et al.*, 1970; Wessels and Cohen, 1967). In both buds *Hlxb9* (= *Mnx1* = motor neuron and pancreas homeobox 1) is expressed. Mice lacking *Hlxb9* fail to express *Ipf1/Pdx1* and have no formation of the dorsal pancreatic bud (Li and Edlund, 2001; Harrison *et al.*, 1999; Li *et al.*, 1999). From E 9.5 until E 10.5 *Ipf1/Pdx1* and *Ptf1a* (pancreas-specific transcription factor 1a) are required for the onset of branching of the pancreatic buds (Kawaguchi *et al.*, 2002). There will be an extra chapter about *Ptf1a*, a gene whose expression pattern is important in this work. From E 10.5 on, growth and early morphogenesis are promoted basically by three major genes. *Ipf1/Pdx1* function is

continuously required for epithelial proliferation and for islet cell differentiation and morphogenesis (Holland *et al.*, 2002). *Hlxb9* is also required for β-cell maturation (Harrison *et al*., 1999). The two buds undergo branching morphogenesis into a ductal tree which by E 12.5 results in the formation of two primordial pancreatic organs consisting predominantly of an undifferentiated ductal epithelium (Pictet *et al*., 1972). At about E 13.5 acinar-islet precursor cells expressing *Ipf1/Pdx1* together with *Ptf1a* differentiate to exocrine cells (Kawaguchi *et al.*, 2002; Krapp *et al.*, 1996). *Ipf1/Pdx1* and *Pbx1* form a complex which is necessary for the expansion of the pancreatic buds but not for the specification of the different pancreatic cell types (Kim and MacDonald, 2002). Between E 13 and E 14 the dorsal and ventral pancreata rotate and fuse into a single organ. Acinar and ductal cells differentiate between E 14.5 and E 15.5 (Pictet *et al*., 1972). Islet cells organise into islet-like clusters at E 16 and undergo additional remodulation until 2-3 weeks after birth.

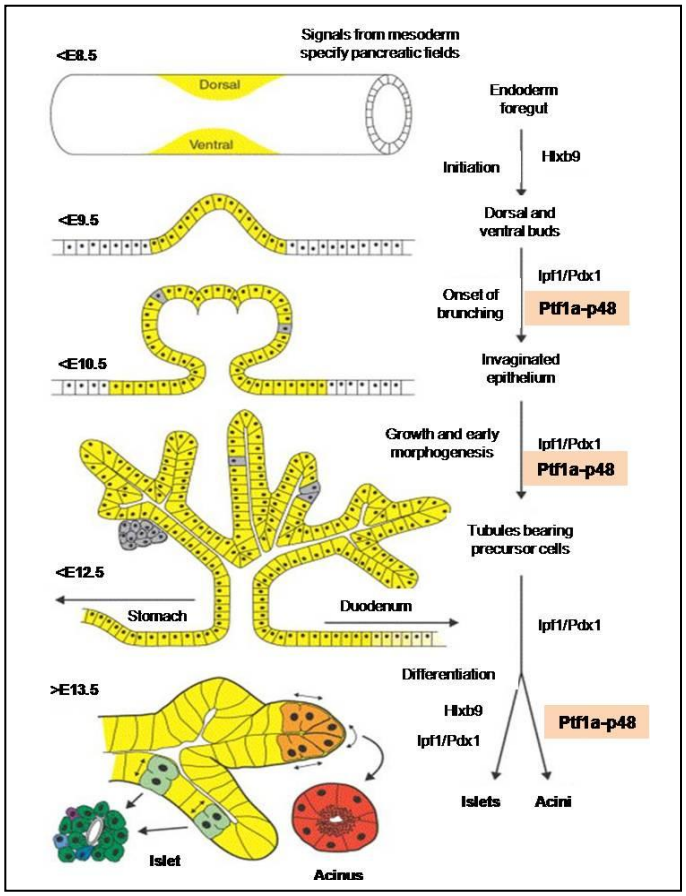

Fig.5: Pancreatic organogenesis. The pancreas starts to develop from a dorsal and ventral pancreatic anlage deriving both from the endodermal germ layer. Important transcription factors are depicted on the right site. (yellow = Ipf1/Pdx1 expression, grey = early-differentiated endocrine cell clusters) (adapted from Kim and MacDonald 2002; modified)

1.2.2 *Ptf1a-p48* as a promoter for *Cre*-expression

In this work, the *Cre-/loxP* technology was used to induce tissue specific knockout in the pancreas. To this end, a transgenic mouse with the gene encoding *Cre*-recombinase inserted into exon 1 of the pancreas transcription factor 1 (*Ptf1*) locus was used (Nakhai *et al*., 2007). Ptf1 is a hetero-oligomeric protein complex, which binds to and activates the transcriptional enhancers of pancreatic acinar hydrolytic enzyme genes (Rose *et al*., 2001; Krapp *et al*., 1996). Ptf1a-p48 is a basic helix-loop-helix (bHLH) protein and a subunit of Ptf1 (Rose *et al*., 2001; Krapp *et al*., 1996). Although Ptf1a-p48 has been detected as early as E9.5 in the dorsal and ventral pancreatic buds, it was proposed to be required only for acinar cell differentiation from E13.5 on (Obata *et al*., 2001; Krapp *et al*., 1996) (also see fig.5). Yet, it was shown by a lineage tracing study in mice that all three major epithelial pancreatic cell lineages derive from a *Ptf1a-p48* expressing progenitor cell population (Kawaguchi *et al*., 2002). Mice homozygously depleted for *Ptf1a-p48* lack the exocrine pancreas whereas endocrine pancreatic function persists throughout the entire lifespan (Krapp *et al*., 1998). It could be shown that Ptf1a-p48 is needed for converting intestinal to pancreatic progenitors (Kawaguchi *et al*., 2002). The *Ptf1a-p48* gene is also involved in GABAergic neuronal cell specification in the cerebellum and in the neuroretina of developing mice (Nakhai *et al*., 2007; Hoshino *et al*., 2005).

1.2.3 Pancreas anatomy, morphology and physiology

The pancreas is located in the abdominal cavity posterior to the stomach and in close association with the duodenum. It is connected via the main pancreatic duct (duct of Wirsung) to the duodenum with the ampulla of Vater, where the main pancreatic duct joins with the bile duct. In humans the four regions head, neck, body and tail of the pancreas can be designated from proximal to distal while in rodents the shape of the pancreas is rather less defined (Richards *et al*., 1964). In comparison to other organs, the pancreas does not present a complete fibrous capsule on its outer limit, but it is covered by a thin layer of loose connective tissue, from which septa extend to divide the organ into lobules. Blood and lymph vessels, nerves and excretory ducts run in the connective tissue septa. The pancreas consists of two different types of glandular tissues, the exocrine part that secretes enzymes into the intestine, and the endocrine part that secretes hormones into the bloodstream.

The exocrine pancreas comprises about 90% of the gland and consists primarily of clusters of acinar cells which are grouped together in grape like structures called acini. These acinar cells appear by light microscopy as pyramid-shaped cells showing a polarized cytoplasm. A round nucleus with a predominant nucleolus and filamentous mitochondria is present on the basal portion of acinar cells. The apical portion of the cells is filled with secretory granules, usually called zymogen granules because they contain precursors of the enzymes of the pancreatic juice (Pavelka and Roth, 2005; McCuskey and Chapman, 1969). The acinar cells produce a number of enzymes which are able to process nearly all digestible macromolecules into forms that are capable, or nearly capable of being absorbed. One group of enzymes are the pancreatic proteases with trypsin and chymotrypsin which are synthesized and packaged into secretory vesicles as the inactive proenzymes trypsinogen and chymotrypsinogen. Once these proenzymes are released into the lumen of the small intestine trypsinogen is activated by the enzyme enterokinase, which is present in the intestinal mucosa. Trypsin in turn activates chymotrypsinogen and these enzymes digest proteins into small peptides. Another important enzyme is the pancreatic lipase which hydrolyses triglyceride into 2-monoglyceride and two free fatty acids. Pancreatic α-amylase is important for the digestion of carbohydrates. The major dietary carbohydrate is starch as a storage form of glucose in plants. α-amylase hydrolyses starch to maltose, maltotriose and α-limit dextrin, which are further digested by enzymes of the intestinal epithelium. In contrast to pancreatic proteases pancreatic lipase and α-amylase are secreted as active enzymes (Silbernagel and Despopoulos, 2001). Although many enzymes that originate from the pancreas have been evaluated as diagnostic tests of pancreatic disease, none have been clearly shown to be such as superior as either amylase or lipase (Loeb and Quimby, 1999). In mice amylase in the serum is predominantly of salivary gland origin, while urine contains only pancreatic amylase. When pancreatic amylase was injected into the blood of mice, it rapidly cleared through the urine (MacKenzie and Messer, 1976). Injury of the pancreas results in increased amylase as well as lipase in the blood (Loeb and Quimby, 1999).

Ductal cells of the pancreas form the epithelial lining of the branched tubes that deliver enzymes produced by the acinar cells into the duodenum. Via centroacinar cells the lumen of the acinus is connected to an intercalated duct. Ductal cells of intercalated ducts shape a squamous cuboidal epithelium surrounded by little connective tissue. These ducts empty into intralobular and then interlobular ducts which join the main pancreatic duct. As ducts become larger the epithelium becomes either cuboidal or columnar and surrounded by

connective tissue (Grapin-Botton, 2005). This network formed by ducts delivers enzymes from acini into the duodenum. Bicarbonate is produced by the ductal cells as a buffer for the enzymes when they are flushed out of the pancreas.In the larger ducts goblet cells are present which produce mucin.

Pancreatic stellate cells characterized by long cytoplasmic processes are present in the periacinar space, perivascular and periductal regions (Apte *et al*., 1998; Bachem *et al*. 1998; Ikejiri, 1990; Watari *et al*., 1982). Normally pancreatic stellate cells are quiescent but they can be activated as a consequence of pancreatic injury (Apte *et al*., 1998; Bachem *et al*. 1998). These activated pancreatic stellate cells participate in tissue repair processes which are known for example from experimental acute pancreatitis in rodents (Lugea *et al*., 2006; Kishi *et al*., 2003; Yokota *et al*., 2002). Activated pancreatic stellate cells express α-SMA and collagen type I, which gives a hint that these cells could be a source of fibrosis in chronic pancreatitis and adenocarcinoma (Apte *et al*., 2004; Casini *et al*., 2000; Haber *et al*., 1999).

The endocrine pancreas consists of the islets of Langerhans, embedded in the exocrine tissue. Four endocrine cell types that produce insulin (β-cells), glucagon (α-cells), somatostatin (δ-cells) and pancreatic polypeptide (PP-cells) are present in the islets of Langerhans, which comprise 1-2% of the cellular mass of the adult pancreas. Insulin is secreted in response to high glucose levels and stimulates muscle, liver and adipose tissue to store glucose by synthesizing glycogen, protein, and fat. Glucagon is secreted in response to low blood glucose and stimulates the liver to release glucose through glycogenolysis and gluconeogenesis and stimulates adipose tissue to release fatty acids through lipolysis. Somatostatin is also released by the hypothalamus and inhibits release of insulin and glucagon (Voet and Voet, 2004). Pancreatic polypeptide is secreted in response to food intake and functions as a regulator of pancreatic exocrine secretion and gallbladder motility (Hazelwood, 1993; Adrian *et al*., 1976). All these hormones are processed in the rough endoplasmic reticulum and, packed into secretory granules to await the signals for their release by exocytose (Voet and Voet, 2004).

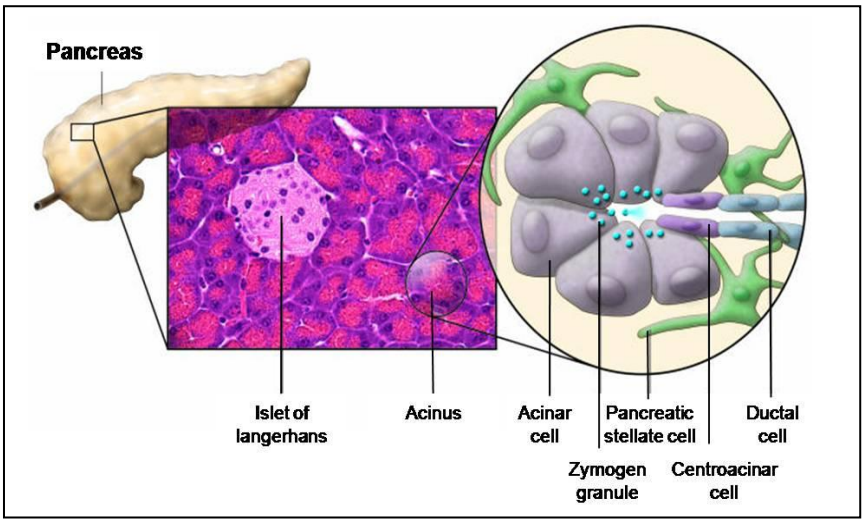

Fig.6: Schematic representation of the secretory cellular components of the pancreas. The pancreas consists of an exocrine (acinar and ductal part of the pancreatic parenchyma) and an endocrine (islets of Langerhans) part. Zymogen granules in the acinar cells of the exocrine part release their contents of digestive enzymes into the pancreatic ductal system which starts with the centroacinar cells. Endocrine cells present in the islets of Langerhans secrete hormone into the bloodstream. Pancreatic stellate cells are present in the periacinar space (adapted from Omary *et al*., 2007; modified).

1.2.4 Pancreatic disorders

Pancreatic disorders are manifested predominantly by either dysfunction of the exocrine or endocrine component and rarely by a combination of both.
In the following only pancreatic disorders relevant for this work will be described.

Acute and chronic pancreatitis:

Pancreatitis is defined as an inflammatory condition of the exocrine pancreas that results from injury to acinar cells (Rubin and Farber, 1990). There is an acute and a chronic course of disease.

Acute pancreatitis is a common clinical problem which can appear in a mild form or develops to a severe disease with systemic inflammatory response, multiorgan dysfunction and acute respiratory distress syndrome in approximately 25% of patients (Baron and Morgan, 1999). Pancreatic hyperstimulation, biliary disease and alcohol abuse are the major causes of acute pancreatitis. There are also hereditary forms of pancreatitis comprising rare cases of acute and chronic pancreatitis (Whitcomb, 1996; Rubin and Farber, 1990).

The exact mechanisms that provoke acute pancreatitis are unknown. It is believed that intra-acinar cell activation of digestive enzymes is an early event of acinar and ductal cell injury (Rubin and Farber, 1990). Inappropriate activation of trypsinogen to trypsin causes autodigestion of the organ which leads to pancreatic inflammation. An *in vitro* study with rat acinar cells and *in vivo* studies with rats, in which cell damage was initiated by treatment with caerulein, showed that cell damage is a secondary effect of trypsin activation (Bockman *et al*., 2004; Saluja *et al*., 1999). Cerulein is a cholecystokinin analogue that induces secretion of pancreatic enzymes which leads to acute or chronic pancreatitis in rodents, depending on the application scheme of cerulein. In the course of hyperstimulation the intra-acinar cell calcium levels rise, especially in the apical region where zymogen granules are stored. This intracellular hypercalcaemia leads to ectopic trypsinogen activation in the acinar cells (Krüger *et al*., 2000; Raraty *et al*., 2000). Intracellular hypercalcaemia can also be a reaction of acinar cells to the exposure to bile acids (Voronina *et al*., 2002). Alcohol abuse affects the acinar cells through different mechanisms like toxic-metabolic injury and oxidative stress (Gukovskaya *et al*., 2002; Li *et al*., 2001; Grattagliano *et al*., 1999).

Trypsin autocatalytically activates trypsinogen. To prevent autodigestion of the acinar cells, pancreatic secretory trypsin inhibitor (PSTI or SPINK1) binds to intrapancreatically activated trypsin (Voet and Voet, 2004). The molar ratio of pancreatic secretory trypsin inhibitor to trypsin is estimated 1:10 (Pubolos *et al*., 1974). When more than 10% of trypsinogen is activated, this inhibitory mechanism is no longer effective (Naruse, 2003). Another self-defending mechanism is rapid flushing of the pancreatic duct by fluids excreted by the duct cells. Duct flushing depends on cystic fibrosis transmembrane conductance regulator (CFTR) (Marino *et al*., 1991). Disruption of any of these protective mechanisms causes an increased risk to acute or even chronic pancreatitis. Hereditary pancreatitis in most cases is associated with mutations in the cationic trypsinogen gene (PRSS1) (Whitcomb *et al*., 1996; Applebaum-Sapiro *et al*., 2001). Gain-of-function mutations in this gene are associated with autocatalysis and/or cause premature trypsinogen activation (Sahin-Tóth and Tóth, 2000; Whitcomb, 1999). Loss-of-function mutations of the PSTI/SPINK and CFTR gene were also found to be associated with chronic pancreatitis (Witt *et al*., 2000; Sharer *et al*., 1998; Cohn *et al*., 1998).

Reactive oxygen species (ROS) attack polyunsaturated fatty acids, which results in peroxidation of lipids (Slater, 1984; Stocks and Dormandy, 1971; Frees *et al*., 1967). Polyunsaturated fatty acids are present in high concentrations in cellular membranes and

are most susceptible to free radical attacks. Reactions of ROS with these membrane constituents can lead to disintegration of the cells and subsequently cell death (Slater, 1984). Oxidative damage by ROS has been implicated in the induction of acute human or experimental pancreatitis (Dabrowski *et al*., 1999; Tsai *et al*., 1998). At an early stage of acute pancreatitis, before morphological alterations could be observed, lipid peroxidation products were found to be increased. It has also been shown, that oxidized glutathione (GSSG) increased at the expense of reduced glutathione (GSH) at an early stage of cerulein induced pancreatitis, which was interpreted as a manifestation of oxidative stress (Dabrowski and Chwiecko, 1990).

Damage of acinar cells leads to release of pancreatic enzymes like amylase and lipase into the blood stream. These two parameters can be measured in blood serum as a diagnostic tool for pancreatitis. In experimentally induced acute pancreatitis in mice amylase and lipase are commonly used standard parameters, which significantly increase in the serum within a few hours, as shown in recent publications (Genovese et al., 2006; Kubisch *et al*., 2006).

Respiratory dysfunction in severe acute pancreatitis precedes heart, liver and kidney failure and is the cause of early mortality (Basran *et al*., 1987). It is assumed from mouse models that thickening of the alveolar-capillary membrane which can be observed during the acute respiratory distress syndrome might be a result of increased myeloperoxidase activity. Myeloperoxidase produced by neutrophil granulocytes increases pulmonary permeability (Pastor *et al*., 2006).

Morphologically, acute pancreatitis is characterized by oedematous fluid in the extracellular space which causes separation of lobules and acini. Usually, there is also invasion by neutrophil granulocytes or lymphocytes into the connective tissue and altered acini. There are no further major changes in the parenchyma (Bockman, 1997). Inflammation of the pancreas can result in the formation of metaplastic lesions called tubular complexes (Willemer and Adler, 1989; Bockman *et al*., 1982). These metaplastic lesions are more common in chronic pancreatitis and will be described in that context.

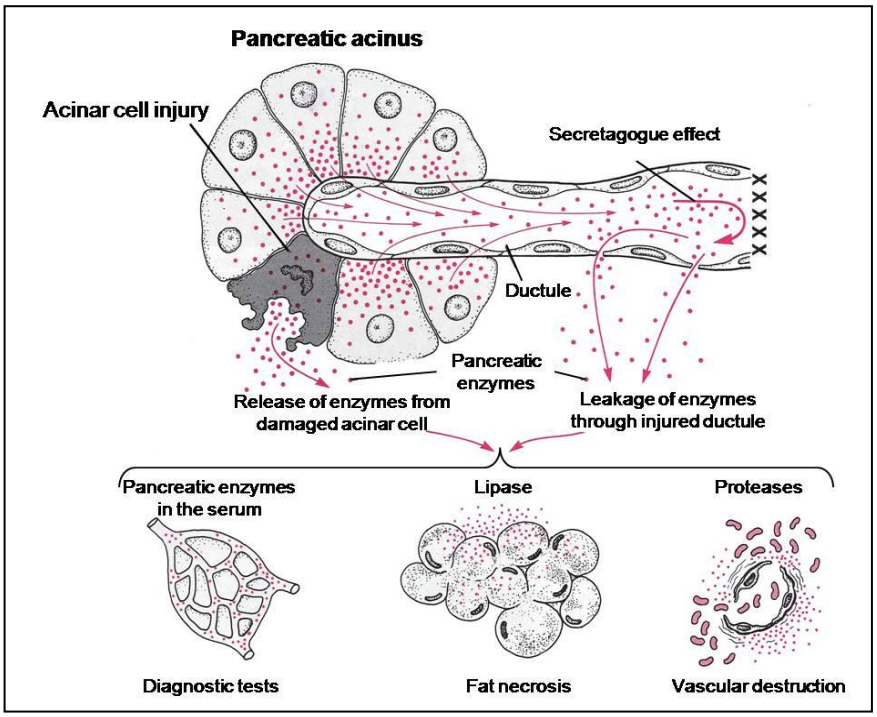

Fig.7: Pathogeneses of acute pancreatitis. Injury to acinar cells or ductules leads to release of pancreatic enzymes. Lipases and proteases destroy surrounding tissue and this autolysis causes pancreatitis. The presence of pancreatic enzymes in the blood serum can be used as a diagnostic test (adapted from Rubin and Farber, 1990; modified).

The course of chronic pancreatitis is characterized by recurrent episodes of acute pancreatitis, which cause parenchymal injury and necrosis, increasing amounts of fibrosis, chronic inflammation, and parenchymal cell loss (Omary *et al*., 2007). The disease often leads to total destruction of the pancreas and results in malabsorption of dietary nutrients, diabetes mellitus, and severe unrelenting pain (Etemad and Whitcomb, 2001). About 70% of cases can be attributed to alcohol abuse, the remaining cases can be classified as idiopathic chronic pancreatitis, tropic pancreatitis, which is the major cause of childhood chronic pancreatitis in tropic regions, hereditary pancreatitis, cystic fibrosis, and chronic pancreatitis associated with metabolic and congenital factors (Etemad and Whitcomb, 2001). The development of chronic pancreatitis requires environmental factors (e.g. alcohol, tobacco smoking, fat/protein rich diet) leading to recurrent pancreatic injury or an altered immune response leading to chronic inflammation and fibrosis (Whitcomb, 2004; Durbec and Sarles, 1978). Based on observations in hereditary and alcoholic chronic pancreatitis, the Sentinel Acute Pancreatitis Event (SAPE) hypothesis gives a good idea of the events required for progression from acute towards chronic pancreatitis and fibrosis (Schneider and Whitcomb, 2002; Whitcomb, 1999): Acinar cells under metabolic stress

produce cytokines and other signals in the absence of histopathological changes. At some point in time, for unknown reasons, acute pancreatitis occurs, which is called the Sentinel Acute Pancreatitis Event. Acute pancreatitis has an early pro-inflammatory phase and a late anti-inflammatory phase in which the healing process is initiated by anti-inflammatory cytokines (e.g. IL-10, TGF-ß) secreted by macrophages and activated stellate cells. Generally, acute pancreatitis resolves, the pancreas returns towards normal function, but the anti-inflammatory cells remain activated for a substantial amount of time. If activated stellate cells become restimmulated by a state of oxidative stress, the response of releasing cytokines and other factors differs compared to the first event (sentinel event). The resident macrophages and pancreatic stellate cells respond differently to these factors. The result is synthesis and deposition of collagen, fibronectin and other matrix proteins characteristic of fibrosis (Schneider and Whitcomb, 2002; Whitcomb, 1999).

There is a strong association between chronic pancreatitis and an increased risk of developing pancreatic ductal adenocarcinoma (PDA) (Howes *et al*., 2004; Malka, *et al*., 2002; Whitcomb and Pogue-Geile, 2002; Lowenfels *et al*., 1997, 1993). In mice, an activating *K-ras* mutation expressed under the control of an inducible elastase promoter did not lead to development of PDA or precursor lesions in adult mice as was shown for *K-ras* mutations under the control of embryonically expressed promoters. But, when these mice were challenged with cerulein they developed the full spectrum of pancreatic precursor lesions and invasive PDA, showing, that the cerulein-induced pancreatitis was a prerequisite for the development of premalignant lesions in this model (Guerra *et al*., 2007; Aguirre *et al*., 2003; Grippo *et al*., 2003; Hingorani *et al*., 2003). The mechanism how chronic pancreatitis can develop to PDA is still unclear. It is assumed that pancreatic stellate cells play a key role in this process (Algül *et al*., 2007; Omary *et al*., 2007).

Morphologically, chronic pancreatitis is characterized by acinar atrophy with fatty necrosis, fibrosis and formation of metaplastic lesions of a ductal phenotype. The origin of these ductal metaplastic lesions is unknown. However, they can be grouped in two different types, tubular complexes and mucinous metaplasia including pancreatic intraepithelial neoplasia (Bockman *et al*., 2003; Hruban *et al*., 2001). The tubular complexes are defined as cylindrical tubes with a wide lumen lined by a monolayer of flat duct-like cells (Iovanna, 1996; Lechene *et al*., 1991; Willemer and Adler, 1989) and can also be found in pancreatic development, regeneration and cancer (Hisaoka *et al*., 1993; Lechene *et al*., 1991; Elsässer *et al*., 1986; Bockman *et al*., 1982). Tubular complexes can additionally be

distinguished into tubular complexes with a wide, empty lumen lined by a few large, flat cells and tubular complexes with an empty lumen lined by many small cells (Strobel *et al*., 2007). Mucinous metaplastic lesions are characterised by a variable lumen, sometimes containing secreted mucin. The lumen is lined by epithelial cells that vary in height according to the extent of mucin expression (Strobel *et al*., 2007). Some of these lesions produce abundant supranuclear mucin and have flat, basally located nuclei, which are also characteristic of early pancreatic intraepithelial neoplasia (Hruban *et al*., 2006 a,b). Typical infiltrating cells which can be found in chronic pancreatitis are lymphocytes, macrophages and plasma cells (Rubin and Farber, 1990).

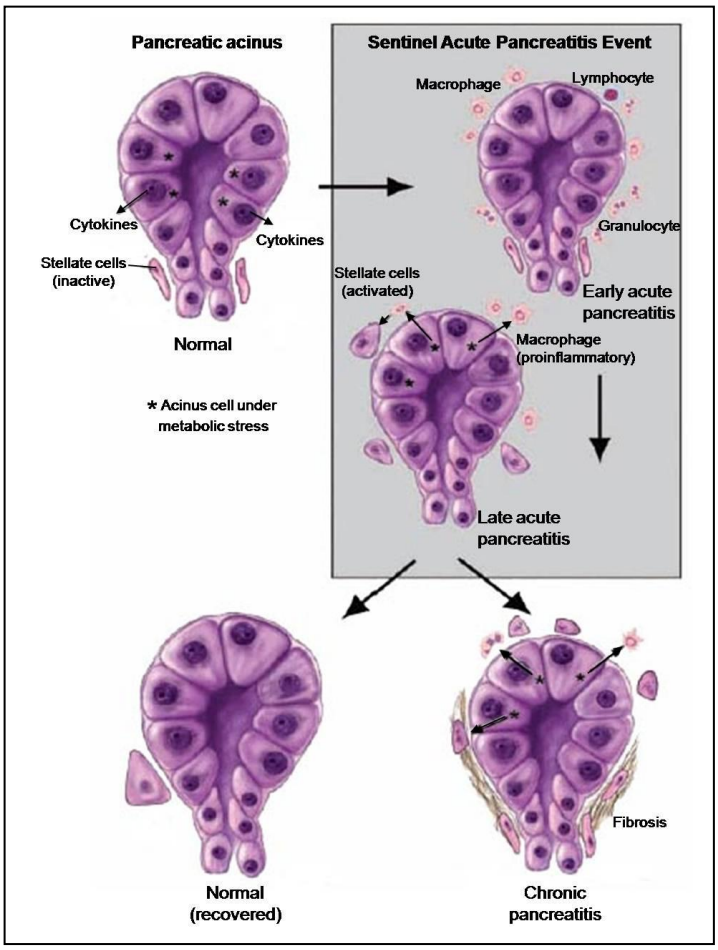

Fig.8: Development from acute to chronic pancreatitis. Acinar cells release cytokines under metabolic stress. No histopathology is observed at this stage. The Sentinel Acute Pancreatitis Event, highlighted in gray, is characterized by a massive inflammatory response: invasion of proinflammatory cells, release of cytokines and finally attraction of anti-inflammatory cells. Pro-fibrotic cells like stellate cells are activated. If stressing factors are removed the pancreas recovers to its normal state. If the acinar cells or primed stellate cells are further stressed, this leads to chronic pancreatitis (adapted from Stevens *et al*., 2004, modified).

Pancreatic ductal adenocarcinoma:

Pancreatic cancer is the fourth leading cause of cancer-related deaths in Germany and in the United States (Jemal *et al*., 2007; DKFZ, 2006). Most pancreatic cancers are ductal adenocarcinomas with a very aggressive course of disease. Nearly all patients diagnosed with pancreatic ductal adenocarcinoma (PDA) will die from this disease. The 5-year survival rate is less than 5% which is also a result of ineffective early detection methods, nonspecific symptoms hampering diagnosis and poor efficacy of the therapies for advanced disease (Hruban *et al*., 2006b; Welch *et al*., 2000). Most PDA occurs sporadically, but there are also approximately 5-10% of patients with a family history of pancreatic cancer (Klein *et al*., 2001). The genetic abnormalities in familial pancreatic carcinoma are unknown in most cases, but PDA shows a characteristic pattern of genetic alterations involving mutations of K-RAS, CDKN2a, TP53, BRCA2 and SMAD4/MADH4/DPC4 at different stages (Hahn *et al*., 1996; Caldas *et al*., 1994; Barton *et al*., 1991b; Almoguera *et al*., 1988). Typically, precursor lesions can be observed before PDA develops (Cubilla and Fitzgerald, 1976, 1975). These hyperplastic non-invasive lesions are named pancreatic intraepithelial neoplasia (PanIN) (Klimstra and Longnecker, 1994). These lesions simultaneously express epidermal growth factors (EGF) like transforming growth factor-α (TGF-α) and EGF receptors like ERBB2 forming autocrine loops (Day *et al*., 1996; Barton *et al*., 1991a). One of the first mouse models mimicking human pancreatic carcinogenesis was the EL-TGFα-hGH;*p53*$^{+/-}$ mouse (Schreiner *et al*., 2003; Wagner *et al*., 2001). In this mouse TGF-α is overexpressed under the control of the rat elastase promoter (Sandrgren *et al*., 1993, Ornitz *et al*., 1985). The EL-TGFα-hGH mice showed transdifferentiation of acinar cells to duct-like cells, which represents premalignant lesions and developed invasive PDA with metastasis in lung and liver when combined with a homozygous knockout of the tumour suppressor p53 (Wagner *et al*., 2001; Wagner *et al*., 1998; Sandrgen *et al*., 1990). As a result of the p53-deficiency these mice also developed lymphomas and sarcomas (Jacks *et al*., 1994).

1.2.5 Thioredoxin reductases in the pancreas

There is very little knowledge about the expression and function of thioredoxin reductases in the pancreas. Early immunohistochemical studies in mice showed strong staining in the islets of Langerhans and less pronounced staining in the acinar cells of the pancreas for thioredoxin reductase. Within the islets of Langerhans the β-cells showed a moderate cytoplasmic, while the δ-cells revealed a very intense cytoplasmic and fine granular staining. In the acinar cells, staining was distinctly enriched in a cytoplasmic zone close to the plasma membrane (Hansson *et al*., 1986). But these studies did not provide detailed information on cytosolic or mitochondrial localization of thioredoxin reductase. Recently, a novel variant of the human TXNRD3 gene was found by Affymetrix DNA chip analysis of psoriatic tissue. The TXNRD3NT1 gene was down-regulated in this tissue. After screening different tissues by reverse transcription-polymerase chain reaction (RT-PCR) it was found out, that this gene was expressed in oesophagus, bone marrow, skin keratinocytes and pancreas (Matsuzaka *et al*., 2005). The nucleotide sequence of TXNRD3NT1 was found to spread four exons of the TXNRD3 gene. Exon 1 and 2 overlap with exon 15 and 16 of the TXNRD2 gene. The function of this gene in the pancreas is unknown.

1.3 Aim of this thesis

Pancreatic ductal adenocarcinoma (PDA) is one of the most aggressive cancers in humans. Despite the rapid progress in understanding molecular mechanisms in PDA, this cancer is still a fatal disease. The high mortality of PDA is attributed to a lack of early detection methods and poor efficacy in therapies for advanced disease (Hruban *et al*., 2003). Most PDA occurs sporadically, but there are also approximately 5-10% of patients with a family history of pancreatic cancer (Klein *et al*., 2001). As an alternative, preventive strategies in individuals with familial pancreatic carcinoma should be considered.

Several epidemiological studies and chemoprevention trials showed an inverse correlation between dietary intake of selenium and cancer risk (Rayman, 2005; Bjelakovic *et al*., 2004; Whanger, 2004; Yu *et al*., 1997, 1985; Clark *et al*., 1996, 1991; Schrauzer *et al*., 1977 a,b; Shamberger *et al*.,1976). Supplementation of selenium has been found to reduce the incidence and mortality of liver, stomach and colon cancer in humans (Bjelakovic *et al*., 2004; Yu *et al*., 1997; Blot *et al*., 1993). Until now there were no controlled or randomized

interventional studies proofing the specific effect of selenium on pancreatic cancer, albeit data from etiological and case-control studies support a protective effect (Knekt *et al*., 1990; Burney *et al*., 1989).

To this end, the aim of the first part of this thesis was to investigate the influence of selenium as a potential preventive micronutrient in a genetically defined pancreatic cancer mouse model, the EL-TGFα-hgH$^{tg/+}$;*p53*$^{+/-}$ mouse strain (Schreiner *et al*., 2003; Wagner *et al*., 2001). In this study sodium selenite was chosen as selenium source. Cancer prone mice (EL-TGFα-hGH$^{tg/+}$;*p53*$^{+/-}$) with low selenium status were compared to such mice replenished with non-toxic adequate amounts of sodium selenite.

Among the suggested mechanism of selenium in cancer prevention, selenoproteins play a key role (Whanger, 2004). The redox-active cytosolic (Txnrd1) and mitochondrial (Txnrd2) thioredoxin reductases are linked in several ways to selenium and cancer, albeit the exact mechanisms are mostly unknown (Arner and Holmgren, 2000; Sun *et al*., 1999; Tamura and Stadtman, 1996; Gasdaska *et al*., 1994). One proposed mechanism is the link of thioredoxin with the function of the tumour suppressor p53.

In order to assess the importance of cytosolic and mitochondrial thioredoxin reductase in the pancreas, in the second part of this thesis, their enzymatic activity was determined in the pancreas and several other organs and the influence of the selenium-status was tested.

In part three and four of this study, a knockout strategy was the method of choice to investigate the *in vivo* role of Txnrd1 and Txnrd2 in the pancreas. To bypass embryonic lethality associated with the complete knockout of Txnrd1 and as well of Txnrd2 (Jakupoglu *et al*., 2005; Conrad *et al*., 2004), the *Cre*/*loxP* technology was used to create pancreas-specific knockout mice. These two knockout mouse strains were characterized in detail to start unravelling the role of these enzymes in the pancreas.

2 Materials and methods

2.1 Materials

2.1.1 Chemicals

All supplies of chemicals were German companies, except when indicated.

Acetic acid	Merck KGaA, Darmstadt
Agarose	Biozym, Hess. Oldendorf
Ampuwa	Fresenius Kabi GmbH, Bad Homburg
Anilin blue solution	Sigma-Aldrich GmbH, Taufkirchen
Bieberich scarlet acid fuchsin solution	Sigma-Aldrich GmbH, Taufkirchen
β-mercaptho-ethanol	Carl-Roth GmbH+CoKG, Karlsruhe
Boric acid	NeoLab GmbH, Heidelberg
Bovine serum albumin	ICN Biomedicals GmbH, Meckenheim
Bradford reagent	Sigma-Aldrich GmbH, Taufkirchen
5-Bromo-4-chloro-3-indolyl-B-D-galactopyranosidase (X-Gal)	Sigma-Aldrich GmbH, Taufkirchen
5-Bromo-2´-deoxyuridine (BrdU)	Sigma-Aldrich GmbH, Taufkirchen
Citric acid monohydrate	Merck KGaA, Darmstadt
Dextrose	Carl-Roth GmbH+CoKG, Karlsruhe
N,N-Dimethylformamide (DMF)	Sigma-Aldrich GmbH, Taufkirchen
Disodiumhydrogenphosphate (Na_2HPO_4)	Merck KGaA, Darmstadt
DNA Ladder, Low Range, 100 bp	Fermentas GmbH, St. Leon-Rot
Deoxnucleioside triphosphates (dNTPs)	Fermentas GmbH, St. Leon-Rot
5,5´-Dithio-bis-(2-Nitrobenzoic Acid) (DTNB)	Sigma-Aldrich GmbH, Taufkirchen
Ethanol	Merck KGaA, Darmstadt
Ethidiumbromide	Sigma-Aldrich GmbH, Taufkirchen
Ethylenediamine-tetraaceticacid (EDTA)	Carl-Roth GmbH+CoKG, Karlsruhe
Eosin	Carl-Roth GmbH+CoKG, Karlsruhe
Formaldehyde 40 %	Bilgram Chemikalien, Ostrach
Goat serum	Sigma-Aldrich GmbH, Taufkirchen

2.5 % glutaraldehyde in 0.1 M sodium buffer, pH 7.4	Electron Microscopy Sciences, cacodylate Hatfield,USA
Hematoxylin acc. Gill III	Merck KGaA, Darmstadt
4-(2-hydroxyethyl)-1-piperazine-ethanesulfonic acid (HEPES)	Carl-Roth GmbH+CoKG, Karlsruhe
Hydrochloric acid 32 % (HCl)	Merck KGaA, Darmstadt
Hydrogen peroxide 30 % (H_2O_2)	Sigma-Aldrich GmbH, Taufkirchen
Magnesium chloride	Sigma-Aldrich GmbH, Taufkirchen
NADPH	Sigma-Aldrich GmbH, Taufkirchen
Oil red O	Sigma-Aldrich GmbH, Taufkirchen
Paraffin	Merck KGaA, Darmstadt
Paraformaldehyde	Sigma-Aldrich GmbH, Taufkirchen
Periodic acid solution	Sigma-Aldrich GmbH, Taufkirchen
Phospatase inhibitor cocktail 1	Sigma-Aldrich GmbH, Taufkirchen
Phospatase inhibitor cocktail 2	Sigma-Aldrich GmbH, Taufkirchen
Phosphomolybdic acid solution	Sigma-Aldrich GmbH, Taufkirchen
Phosphotungstic acid solution	Sigma-Aldrich GmbH, Taufkirchen
Picric acid solution 1,2 %	Sigma-Aldrich GmbH, Taufkirchen
Potassium ferricyanide crystalline	Sigma-Aldrich GmbH, Taufkirchen
Potassium ferricyanide trihydrate	Sigma-Aldrich GmbH, Taufkirchen
Potassium phosphate	Merck KGaA, Darmstadt
Propylene glycol, 100%	Carl-Roth GmbH+CoKG, Karlsruhe
Protease inhibitor cocktail	Sigma-Aldrich GmbH, Taufkirchen
Rabbit Serum	Sigma-Aldrich GmbH, Taufkirchen
RLT-buffer	Qiagen GmbH, Hilden
Roti®-Clear	Carl-Roth GmbH+CoKG, Karlsruhe
Roti®-Phenol	Carl-Roth GmbH+CoKG, Karlsruhe
Roti®-Histol	Carl-Roth GmbH+CoKG, Karlsruhe
Roti®-Histokitt II	Carl-Roth GmbH+CoKG, Karlsruhe
Schiff´s reagent	Sigma-Aldrich GmbH, Taufkirchen
Sodium chloride (NaCl)	Merck KGaA, Darmstadt
Sodium hydroxide (NaOH)	Merck KGaA, Darmstadt
Sodiumdihydrogenphosphate (NaH_2PO_4)	Merck KGaA, Darmstadt
Sodium dodecylsulfat (SDS)	Fluka Chemie AG, Buchs

Succrose	Sigma-Aldrich GmbH, Taufkirchen
Tris(hydroxymethyl)-aminomethane (Tris)	Merck KGaA, Darmstadt
Tissue Tec O.C.T. Compound	Miles Inc., Elkhart, USA
Trisodium citrate dehydrate	Merck KGaA, Darmstadt
Weigert´s iron hematoxylin part A	Sigma-Aldrich GmbH, Taufkirchen
Weigert´s iron hematoxylin part B	Sigma-Aldrich GmbH, Taufkirchen

2.1.2 Desoxyoligoribonucleotides

The following primers were used for genotyping of the transgenic mice or for gene expression studies.

Name	Sequence 5´-3´
Aldolase1	AGC TGT CTG ACA TCG CTC ACC G
Aldolase2	CAC ATA GTG GCA GCG CTT CAA G
GAPDH1	CTC ACT CAA GAT TGT CAG CAA TG
GAPDH2	GAG GGA GAT GCT CAG TGT TGG
Rosa1	AAA GTC GCT CTG AGT TGT TAT
Rosa2	GCG AAG AGT TTG TCC TCA ACC
Rosa3	GGA GCG GGA GAA ATG GAT ATG
TetO-Cre1	ACC AGC CAG CTA TCA ACT CG
TetO-Cre2	TTA CAT TGG TCC AGC CAC C
TetO-Cre3	CTA GGC CAC AGA ATT GAA AGA TCT
TetO-Cre4	GTA GGT GGA AAT TCT AGC ATC ATC C
TR1E13f	TTG GCC ATT GGA ATG GAC AGT CC
TR1E15r	AGC ACC TTG AAT TGG CGC CTA GG
TR1_59	CGA AGA CAC AGT GAA GCA TGA CTG
TR1_60	TCC CCT CCA GGA TGT CAC CGA TGG CG
TR1floxf1	TCC ACC TCA CAG GAG TGA TCC C

TR1floxr1	TGC CTA AAG ATG AAC TCG CAG C
TR1wtfor2	GGT CTG AGC TAG CGT GAA GTG TTC C
TR2E6	CAG CTT TGT GGA TGA GCA CAC AGT TCG
TR2E10	GAT CCT CCC AAG TGA CCT GCA GCT GG
TR2_15	TTC ACG GTG GCG GAT AGG GAT GC
TR2_18	TGC CCA GGC CAT CAT CAT CTG ACG
TR3Del1	TGC TTC CAG GCC CAG TGC TCT GAC TGG
TR3Del2	CAG GCT CCT GTA GGC CCA TTA AGG TGC
TR3flox1	CAG GTC ACT AGG CTG TAG AGT TTG C
TR3flox2	ATG TCC CAG TGT ACT TAT GAT GAA TC
Neopromrev1	AGG TGC TAC TTC CAT TTG TCA CGT CCT
3´hGH2TGFα	TAG GAG GTC ATA GAC GTT GC
5´hGH2TGFα	GGC TTT TTG ACA ACG CTA TG
036P53	ACA GCG TGG TGG TAC CTT AT
037P53	TAT ACT CAG AGC CGG CCT
038P53	CTA TCA GGA CAT AGC GTT GG

Table1: Primer sequences.

2.1.3 Enzymes

Proteinase k	peqLab GmbH, Erlangen

2.1.4 Kits

Avidin/Biotin Blocking-Kit	Vector Laboratories, Inc, Burlingame, UK
PCR-Kit	Qiagen GmbH, Hilden
PCR-Kit	Invitrogen GmbH, Karlsruhe
Peroxidase Substrate Kit DAB SK-4100	Vector Laboratories, Inc, Burlingame, UK
Vectastain® ABC-Kit Elite®PK-6100 Standard	Vector Laboratories, Inc, Burlingame, UK

RNeasy® Mini Kit	Qiagen GmbH, Hilden
RNase-Free DNase Set	Qiagen GmbH, Hilden
Reverse Transkription System	Promega Corporation, Madison, USA

2.1.5 Antibodies for immunohistochemistry

The following antibodies were used for immunohistochemical studies in dilutions as indicated.

Primary antibodies	Manufacturer	Dilution
Rabbit anti-α-amylase	Sigma, Saint Louis, USA	1:200
Rat anti-BrdU	Biozol Diagnostica Vertrieb, Eching	1:250
Rabbit anti-cytokeratin19 (TromaIII)	Max-Planck-Institute, Freiburg	1:250
Rabbit anti-CD3	Dako Cytomation, Hambug	1:50
Rat anti-CD45R/B220	BD Pharmingen, Heidelberg	1:200
Rabbit anti-glucagon	Abcam, Cambridge, UK	1:50
Guinea pig anti-insulin	Abcam, Cambridge, UK	1:50
Rabbit anti-human myeloperoxidase	Dako Cytomation, Hambug	1:200
Rat anti-F4/80 – BM8	BMA Biomedicals, Augst, CH	1:50
Rabbit anti-calbindin	Chemicon/Millipore GmbH, Schwalbach	1:500

Secondary antibodies	Manufacturer	Dilution
Goat anti-rabbit (biotin-linked)	Vector Laboratories, Inc, Burlingame	1:300
Rabbit anti-rat (biotin-linked)	Vector Laboratories, Inc, Burlingame	1:250
Goat anti-guinea pig (biotin-linked)	Vector Laboratories, Inc, Burlingame	1:500

Table2: Primary and secondary antibodies.

2.2 Transgenic mice

2.2.1 EL-TGFα-hGH

The EL-TGFα-hGH transgenic mouse was created by Sandgren and colleagues (Sandgren *et al.*, 1993). In this mouse a rat elastase enhancer/promoter was fused to a TGFα cDNA-human growth hormone (hGH) gene construct. A high transgene expression is targeted to pancreatic acinar cells (Ornitz *et al.*, 1985). EL-TGFα-hGH mice were kept as a heterozygous line on a C57BL/6 background.

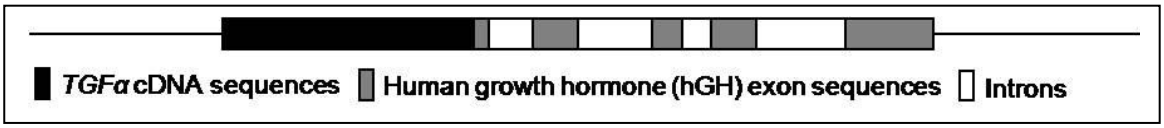

Fig.9: EL-TGFα-hGH transgene construct. A rat elastase enhancer/promoter was fused to a TGFα cDNA-hGH gene construct (EL-TGFα-hGH) (Sandgren *et al.*, 1990). A highly specific transgene expression is targeted to pancreatic acinar cells (Ornitz *et al*,. 1985).

2.2.2 *P53*$^{+/-}$

The *p53*$^{+/-}$ knockout mouse was published by Jacks and colleagues (Jacks *et al*., 1994). Homologous recombination between a *p53* knockout targeting vector and one allele of the endogenous *p53* gene leads to the replacement of *p53* coding sequences between exons 2 and 6 with a neomycin gene expression cassette and the formation of the p53 mutant allele. *P53*$^{+/-}$ mice were bred on a BALB/c background and kept as a hemizygous line.

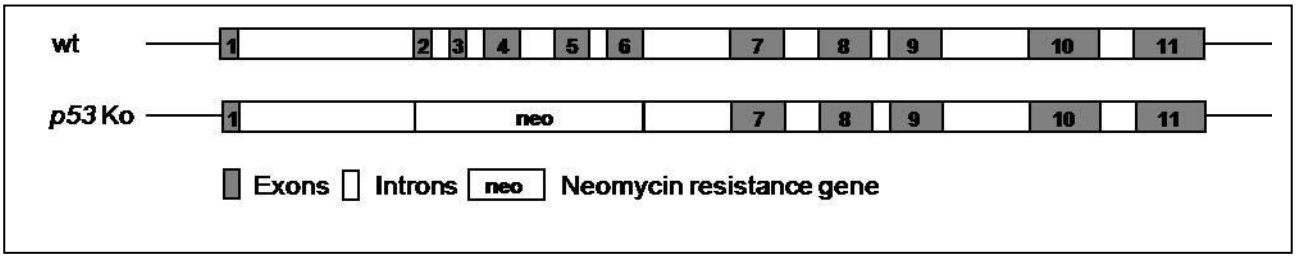

Fig.10: *p53* knockout construct. Homologous recombination was used to inactivate one *p53* allele. A neomycin cassette, present in the gene targeting vector replaced exon 1 to 6 of the endogenous *p53* locus (Jacks *et al*., 1994).

2.2.3 Floxed cytosolic thioredoxin reductase mouse

To create a conditional cytosolic thioredoxin reductase (*Txnrd1*) knockout mouse, the Txnrd1 mouse created by Jakupoglu and colleagues (Jakupoglu *et al.*, 2005) with floxed alleles was used. In this mouse exon 15 was flanked with *loxP* sites (open triangles). Exon 15 harbours the coding region for the redox centre, including the Sec codon UGA (marked with an asterisk), the SECIS element, the AU-rich elements, and the endogenous transcription termination signal. Also a neomycin gene cassette was inserted and flanked by frt sites (black triangles). The Cre-mediated deletion of exon 15 leads to inactivation of cytosolic thioredoxin reductase. These mice were bred on a C57BL/6 background.

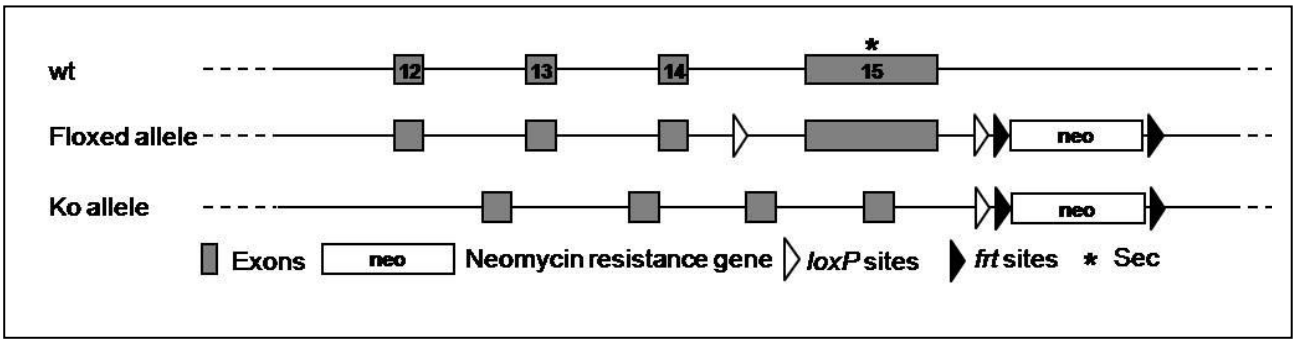

Fig.11: Gene targeting of *Txnrd1*. Txnrd1 exon 15, harbouring the coding region for the redox centre, including the Sec codon UGA (marked with an asterisk), the SECIS element, the AU-rich elements, and the endogenous transcription termination signal was flanked by *loxP* sites (open triangles). A neomycin gene cassette flanked by frt sites (black triangles) was inserted. Cre-mediated deletion of exon 15 leads to inactivation of thioredoxin reductase 1 (knockout allele) (Jakupoglu *et al*, 2005).

2.2.4 Floxed mitochondrial thioredoxin reductase mouse

For studies with a conditional mitochondrial thioredoxin reductase (*Txnrd2*) knockout mouse, a mouse with floxed Trxnrd2 alleles was used. This mouse was published by Conrad and colleagues (Conrad *et al.*, 2004) and bred on a C57BL/6 background. In this mouse exons 15 to 18 were flanked by *loxP*-sites (open triangles). Exon 17 harbours the Sec codon UGA (marked with an asterisk). The neomycin cassette was removed by homologous subsequent Flp-mediated recombination. Cre-mediated deletion of the C-terminally located redox centre leads to inactivation of mitochondrial thioredoxin reductase.

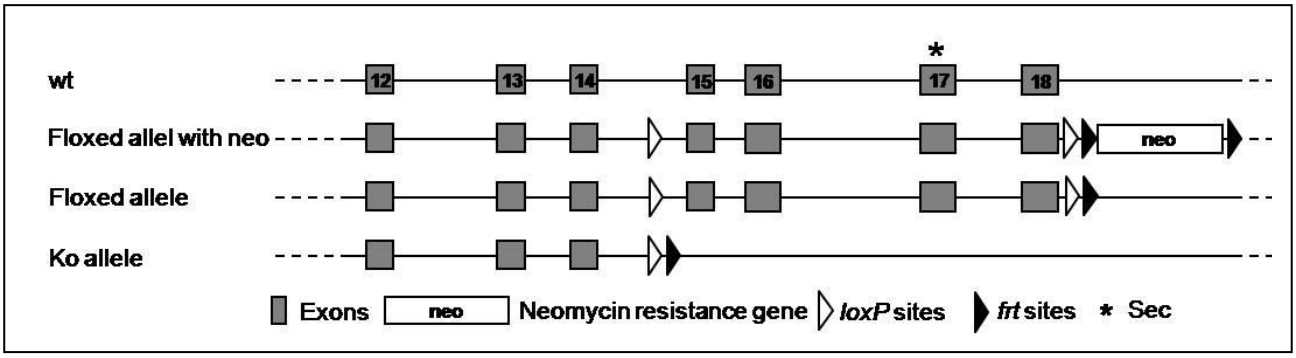

Fig.12: Gene targeting of *Txnrd2*. Exons 15 to 18 harbouring the Sec codon UGA (marked with an asterisk), the SECIS element and the transcription termination signal, were flanked by *loxP*-sites (open triangles). The neomycin cassette necessary for selection of embryonic stem cell clones was subsequently removed by homologous Flp-mediated recombination. Cre-mediated deletion of the C-terminally located redox-centre leads to inactivation of thioredoxin reductase 2 (Conrad *et al.* 2004).

2.2.5 ROSA26 Cre reporter

The ROSA26 Cre reporter strain (R26R), developed by Soriano (Soriano, 1999), is a mouse line for monitoring *Cre*-expression in cells by expression of *lacZ*. Therefore a ßgeo reporter, *lacZ*, was targeted into the ROSA26 locus. Upstream of *lacZ* stop-sequences including a polyadenylation sequence and a neomycin expression cassette flanked by *loxP* sites was inserted. In cells expressing Cre-recombinase the stop-elements and the neomycin cassette are removed and *lacZ* is expressed. lacZ expression than can be visualized by X-Gal staining (chapter 2.6.9).

2.2.6 *Ptf1a-Cre*^{ex1}

To direct *Cre* expression to the exocrine and endocrine pancreas, a knockin mouse with the gene encoding for Cre recombinase within the *Ptf1a* locus was created by Nakhai and colleagues (Nakhai *et al.*, 2007).

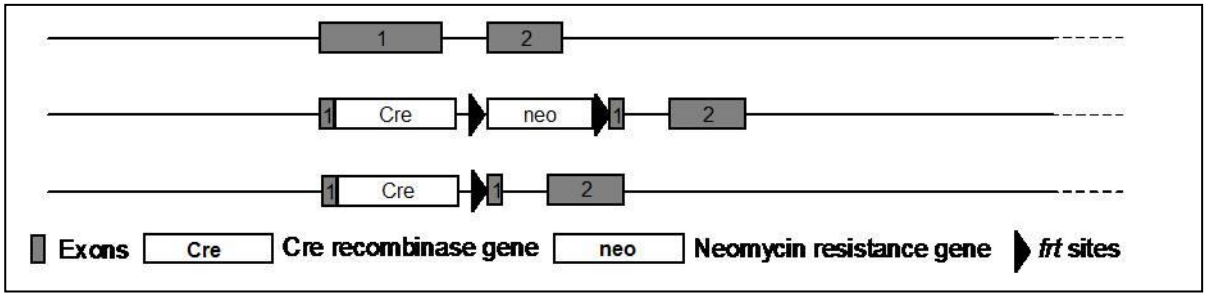

Fig.13: *Ptf1a-Cre*^{ex1} construct. To direct *Cre* expression to the exocrine and endocrine compartment of the pancreas, *Ptf1a* exon 1 was replaced in frame with the gene encoding the Cre recombinase (Nakhai *et al.*, 2007). The neomycin cassette necessary for selecting positive embryonic stem cell clones after homologous recombination was subsequently removed using Flp-mediated recombination.

2.3 Experimental groups and breeding

2.3.1 Pancreatic cancer mouse model

The EL-TGFα-hGH$^{tg/+}$;*p53*$^{+/-}$ mouse is a well established mouse model for pancreatic adenocarcinoma (Wagner *et al*., 2001; Schreiner *et al*., 2003). The parental generations were kept as heterozygous or hemizygous lines on C57BL/6 or BALB/c background, respectively. For the production of selenium-deficient mice, the parental mouse lines were depleted of selenium for three generations by feeding a commercially available (MP Biomedicals, Inc., Aurora, OH, USA) selenium-depleted (mean basal selenium: 22 µg/kg) semi-purified diet (Behne *et al*., 1991). The diet was composed of torula yeast, sucrose, lard, minerals and vitamins (Fig.17). For adequate selenium supply in the control groups the same diet supplemented with 300 µg/kg selenium as sodium selenite was used. The two parental and the tumour-prone experimental F1 mouse lines were kept in parallel on the two diets.

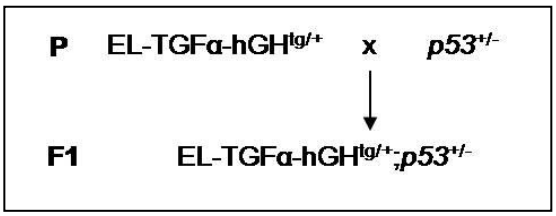

Fig.14: Breeding scheme of EL-TGFα-hGH$^{tg/+}$;*p53*$^{+/-}$. The parental EL-TGFα-hGH$^{tg/+}$ and *p53*$^{+/-}$ generations were bred as hetero-/ hemizygous mouse lines on C57BL/6 or BALB/c background, respectively. The double transgenic F1 generation provided the experimental groups.

Contents	Behne selenium depleted	Behne selenium adequate
Torula yeast	300 g/kg	300 g/kg
Sucrose	586,10 g/kg	586,10 g/kg
Lard, tocopherol stripped	50 g/kg	50 g/kg
Salt mix, HMW	50 g/kg	50 g/kg
Vitamin mix, w/o Vit E and Vit C	10 g/kg	10 g/kg
DL-Methionine	3 g/kg	3 g/kg
Zink carbonate	95,88 mg/kg	95,88 mg/kg
DL-alpha-Tocopherol acetate powder (250U/g)	800 mg/kg	800 mg/kg
Sodium selenite (selenium)	0 µg/kg (0 µg/kg)	660 µg/kg (300 µg/kg)

Table3: Selenium diets. The semi-purified experimental diets are based on torula yeast as protein source. The selenium-deficient diet (Behne selenium depleted) contains mean basal selenium of 22 µg/kg, the selenium-adequate (Behne selenium adequate) diet was supplemented with 300 µg/kg selenium as sodium selenite.

2.3.2 Pancreas-specific *Txnrd1* knockout mouse strain

In a first breeding step heterozygous floxed Txnrd1 mice were mated with heterozygous *Ptf1a-Cre*^{ex1} mice. The heterozygous Txnrd1$^{+/fl}$;*Ptf1a-Cre*^{ex1} mice of the F1 generation were mated in a second breeding step with homozygous floxed *Txnrd1* mice to get the experimental generation with the pancreas-specific *Txnrd1* knockout *Txnrd1*$^{fl/fl}$;*Ptf1a-Cre*^{ex1} and the heterozygous floxed *Txnrd1* mice *Txnrd1*$^{+/fl}$ as a control. After genotyping of the puppets at the age of 3 weeks, the offspring were separated into groups of the same genotype.

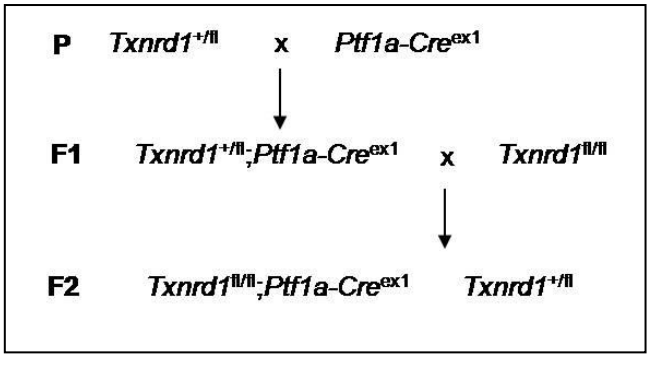

Fig.15: Breeding scheme for pancreas-specific *Txnrd1* knockout mice. Conditional cytosolic thioredoxin reductase knockout mice were bred in two breeding steps. The F2 generation provided the experimental generation with conditional knockout and control. In F1 and F2, only the genotype combinations important for the studies are shown.

2.3.3 Pancreas-specific *Txnrd2* knockout mouse strain

Pancreas-specific *Txnrd2* knockout mice *Txnrd2*$^{fl/fl}$;*Ptf1a-Cre*^{ex1} and their controls *Txnrd2*$^{+/fl}$ were bred in 2 breeding steps. In the first breeding step the heterozygous floxed parental generation of *Txnrd2* and *Ptf1a-Cre*^{ex1} were mated to get heterozygous conditional knockouts of *Txnrd2* which were mated in a second breeding step with homozygous floxed *Txnrd2* mice. This second breeding step led to the experimental generation. After genotyping of the puppets at the age of 3 weeks, the offspring were separated in groups of the same genotype.

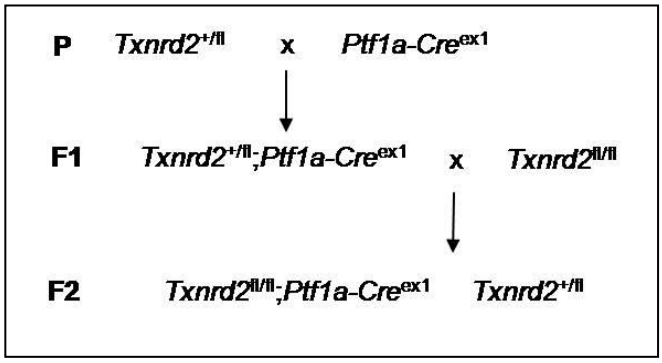

Fig.16: Breeding scheme for pancreas-specific *Txnrd2* knockout mice. Conditional mitochondrial thioredoxin reductase knockout mice were bred in two breeding steps. The F2 generation provided the experimental generation with conditional knockout and control. In F1 and F2, only the genotype combinations important for the studies are shown.

2.3.4 Pancreas-specific knockout mouse strains with *Cre* reporter

To monitor specificity of *Cre*-expression in the pancreas of *Txnrd1* or *Txnrd2* knockout mice, the ROSA26 *Cre* reporter strain (R26R) (Soriano, 1999) was crossed into the Txnrd1 and Txnrd2 mouse strains.

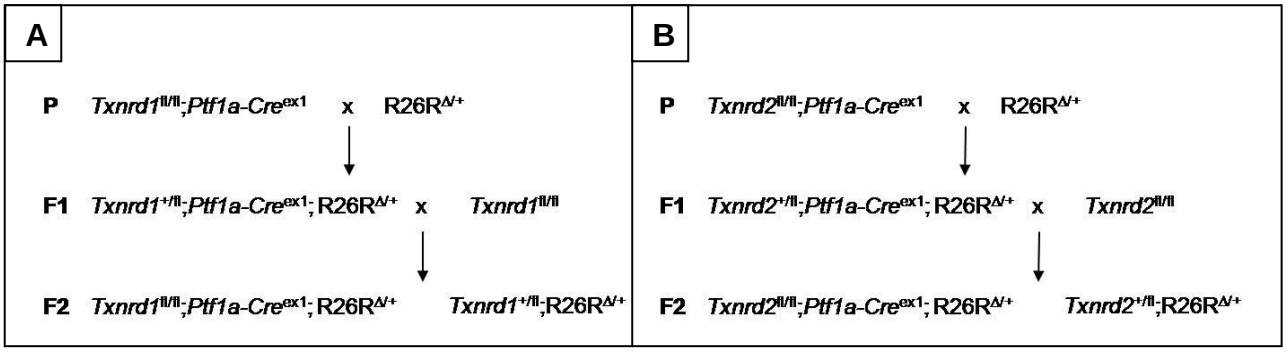

Fig.17: Breeding schemes for Txnrd1 and Txnrd2 mouse lines with R26R Cre reporter mouse line. For monitoring *Cre*-expression the Cre reporter mouse strain R26R (Soriano, 1999) was crossed into the Txnrd1 (A) and Txnrd2 (B) mouse lines. Only the genotype combinations important for the studies are shown.

2.3.5 Genotyping

At the age of three weeks young mice were weaned from their mothers. Their ears were punched with continuous numbers for identification and a 3 mm long piece of the tail was cropped for DNA extraction and subsequent genotyping by polymerase chain reaction (PCR) as described in 2.5.2.

2.4 Animal husbandry

All mice were kept at the animal facilities of the Helmholtz Center Munich – German Research Center for Environmental Health. The animals were housed in groups of up to five in type II polycarbonate cages on wood shavings (Altromin, Lage, Germany) at 20 to 24 ^{o}C, 50% to 60% humidity, 20 air exchanges per hour, and a 12/12-hour light/dark cycle. Sterile filtered water was given *ad libitum.*

All mice were kept on a standard diet (Altromin type 1314 GmbH, Lage, Germany) except those mice which were fed with selenium diets as indicated in 2.3.1.

The animals were kept under SPF (specific pathogen free) conditions according to the recommendations of the *Federation of European Laboratory Animal Science Associations* („FELASA“) and sentinel mice were examined for hygiene monitoring every three month (Nicklas, 2002). The mice were free of all tested pathogens except Mouse hepatitis virus (MHV) which was first detected in August 2005*,* as well as *Helicobacter spp*. and *Syphacia spp*. in August 2005. Treatment with Fenbendazol eliminated the helminths. Mouse norovirus (MNV) was first detected in December 2006.

All animal experiments were performed in compliance with the German animal welfare law and have been approved by the institutional animal care and use committee on animal experimentation and the Government of Upper Bavaria.

2.5 Molecular biological methods

2.5.1 Preparation of genomic DNA

Tail biopsies or organ samples were incubated in 500 µl lysis buffer at 55 °C for 3 hours on a shaker. The lysate was mixed with 500 µl Roti®-Phenol, vortexed and centrifuged at room temperature for 6 minutes at 16000 x g. For DNA precipitation 200 µl of the upper aqueous phase were taken and mixed with 500 µl ethanol / NaCl. After centrifugation for 10 minutes at 16000 x g and 4 °C the supernatant was rejected and the DNA pellet was washed twice in 70 % ethanol. After drying the pellet at room temperature it was resuspended in 80 µl TE-buffer.

Ethanol/NaCl: per 500 µl 100 % ethanol 15 µl 5 M NaCl

Lysis buffer: 10 mM Tris/HCL pH 7.6, 10 mM EDTA pH 8.0, 10 mM NaCl, 0.5 % SDS, 200 µg/ml proteinase k

TE-buffer: 10 mM Tris/HCL pH 7.5, 1 mM EDTA

2.5.2 Preparation of RNA

Quantification of gene expression was carried out on mRNA level by semiquantitative reverse transcription-polymerase chain reaction (RT-PCR).

To this end, RNA of the organ tissue was prepared. A 2 x 2 x 2 mm piece of organ tissue was homogenised (Ultra Turex T18 Basic, IKA, Staufen) in 1.2 ml RLT-buffer with β-mercapthoethanol (1:1000), frozen in liquid nitrogen immediately after preparation and stored at -80°C. RNA was prepared with the RNeasy® Mini Kit. 600 µl of the homogenized tissue were carefully mixed with 600 µl ethanol (70% ethanol in Ampuwa) after thawing. Twice 600 µl were loaded together with all precipitates on RNeasy-columns (provided in the RNeasy® Mini Kit) and centrifuged for 15 seconds at 11000 x g. In a first washing step 350 µl RW1-buffer (provided in the RNeasy® Mini Kit) were given on the column and centrifuged for 15 seconds at 11000 x g. For digestion of DNA 70 µl RDD-buffer were mixed with 10 µl DNase stock solution (all provided in RNase-Free DNase Set) and were incubated on the column for 15 minutes. A washing step with 350 µl RW1-buffer and 15 seconds centrifugation at 11000 x g followed. Afterwards two washing steps with 500 µl RPE-buffer (provided in the RNeasy® Mini Kit) with centrifugation at 11000 x g for 15 seconds and 2 minutes at 11000 x g followed. The column was dried with an additional

centrifugation step for 1 minute at 19000 x g. The RNA was eluted from the column with 30 µl RNase free water (provided in the RNeasy® Mini Kit) after incubation for 1 minute and 1 minute centrifugation at 11000 x g and put on ice.

By gel electrophoreses, the quality of the RNA was analyzed. For this purpose a 0.8% agarose gel in Tris-Borate-EDTA (TBE) -buffer containing 0.5 µg/ml ethidiumbromide was used and loaded with a 1:10 dilution of the prepared RNA. As a fragment length standard a 100 bp DNA-leader was taken. The gel was run with 140 V and RNA was detected with a UV-gel-detection-system (Vilber Lourmat, Marne LA Vallee, France).

The quantity of RNA was determined in a 1:50 dilution by spectrophotometrical analysis (SmartSpec™Plus, Biorad, München) in disposable cuvettes (trUView™ Disposable Cuvettes. BioRad, Munich, Germany).

2.5.3 Polymerase chain reaction (PCR)

For the PCRs two different mastermixes were used. For genotyping of EL-TGFα-hGH$^{tg/+}$;*p53*$^{+/-}$ mice a PCR kit from Qiagen was used, while all other PCRs were performed with a PCR kit from Invitrogen. The PCR conditions were adjusted for the annealing temperature according to the melting temperature of the primers and for the elongation time according to the length of the template. All PCRs were carried out in thermocyclers (T1 Thermocycler, Biometra GmbH, Göttingen, Germany). The following table depicts the gene specific PCR conditions (Fig.21).

hot start	denaturation	annealing	elongation	final elongation	cycles
EL-TGFα-hGH (Primer pair: 3´hGH2TGFα / 5´hGH2TGFα)					
95 °C, 4 min	95 °C, 45 sec	58 °C, 1 min	72 °C, 75 sec	72 °C, 7 min	40
p53$^{+/-}$ (Primer pairs: transgenic: 037P53 / 038P53, wt: 036P53 / 037P53)					
95 °C, 5 min	95 °C, 45 sec	59 °C, 1 min	72 °C, 75 sec	72 °C, 7 min	40
Floxed *Txnrd1* allele (Primer pair: TR1floxf1 / TR1floxr1)					
95 °C, 4 min	95 °C, 45 sec	63 °C, 30 sec	72 °C, 20 sec	72 °C, 7 min	40
Deleted exons in the knockout *Txnrd1* allele (Primer pair: TR1wtfor2 / Neopromrev1)					
95 °C, 5 min	95 °C, 20 sec	64 °C, 50 sec	72 °C, 1 min	72 °C, 7 min	40
Floxed *Txnrd2* allele (Primer pair: TR3flox1 / TR3flox2)					
95 °C, 4 min	95 °C, 45 sec	60 °C, 30 sec	72 °C, 30 sec	72 °C, 7 min	40
Deleted exons in the knockout *Txnrd2* allele (Primer pair: TR3Del1 / TR3Del3)					
95 °C, 5 min	95 °C, 20 sec	65 °C, 50 sec	72 °C 1 min	72 °C, 7 min	31
R26R (Primer triplet: Rosa-1 / Rosa-2 / Rosa-3)					
94 °C, 15 min	94 °C, 30 sec	58 °C, 30 sec	72 °C, 30 sec	72 °C, 7 min	35
***Ptf1a-Cre*^{ex1}** (Primer pairs: transgenic: TetO-Cre1 / TetO-Cre2, wt: TetO-Cre3 / TetO-Cre4)					
94 °C, 3 min	94 °C, 1 min	60 °C, 3 min	72 °C, 3 min	72 °C, 7 min	35

Table4: PCR-conditions for genotyping.

Mastermix with Qiagen-PCR-kit: 12.5 µl distilled water, 6 µl Solution Q, 3 µl 10x PCR buffer, 3 µl dNTP (aqueous solution of dATP, dCTP, dGTP, dTTP each 0.5 mM), 0.18 µM forward-5´primer, 0.18 µM reverse-3´primer, 2.5 U taq-polymerase (all provided in the kit except the primers and dNTPs); Per 27 µl mastermix, 1 µl DNA was added.

Mastermix with Invitrogen-PCR-kit: 14 µl distilled water, 5 µl dNTP (aqueous solution of dATP, dCTP, dGTP, dTTP each 0.5 mM), 0.3 µM forward-5´primer, 0.3 µM reverse-3´primer, 2.5 µl 10x PCR buffer without $MgCl_2$, 3 mM $MgCl_2$, 0.5 U taq-polymerase (all provided in the kit except primers and dNTPs). Per 25 µl mastermix, 1 µl DNA was added.

2.5.4 Semiquantitative reverse transcription-polymerase chain reaction (RT-PCR)

For preparation of cDNA a reverse transcription system (Promega Corporation, Madison, USA) was used. A first incubation step for 10 minutes at room temperature was followed by incubation for 1 hour at 42°C, 5 minutes at 95°C and 5 minutes on ice.
For validation of the knockouts, the expression of two housekeeping genes (aldolase and GAPDH) were taken as controls in addition to the genes of interest, *Txnrd1* and *Txnrd2*. Figure 22 depicts the PCR-conditions for the genes tested. The PCRs were carried out as described in 2.5.3 for the Invitrogen-PCR-kit.

hot start	denaturation	annealing	elongation	final elongation	cycles
Aldolase (Primer pair: Aldolase1 / Aldolase2)					
95°C, 4 min	95°C, 20 sec	58°C, 20 sec	72°C, 1 min	72°C, 7 min	35
GAPDH (Primer pair: GAPDH1 / GAPDH2)					
95°C, 4 min	95°C, 20 sec	58°C, 20 sec	72°C, 1 min	72°C, 7 min	35
Cytosolic thioredoxin reductase containing exon 15 (Primer pair: TR1E13f / TR1E15r)					
94°C, 5 min	94°C, 20 sec	66°C, 20 sec	72°C, 1 min	72°C, 7 min	34
Cytosolic thioredoxin reductase upstream knockout region (Primer pair: TR1_59 / TR1_60)					
94°C, 5 min	94°C, 20 sec	66°C, 20 sec	72°C, 1 min	72°C, 7 min	34
Mitochondrial thioredoxin reductase containing exon 15 to 18 (Primer pair: TR2_15 / TR2_18)					
95°C, 4 min	95°C, 20 sec	64,5°C, 1 min	72°C, 1 min	72°C, 7 min	34
Mitochondrial thioredoxin reductase upstream knockout region (Primer pair: TR2E6 / TR2E10)					
95°C, 4 min	95°C, 20 sec	65°C, 1 min	72°C, 1 min	72°C, 7 min	36

Table5: PCR-conditions for RT-PCR.

Mastermix for cDNA synthesis: 4 µl magnesium-chloride, 2 µl reverse transcription buffer (10x), 2 µldNTPs (dATP, dTTP, dCTP, dGTP each 10 mM), 1 µl Oligo(dT) primer, 0,625 µl RNasin, 0,5 µl AMV (*avian myoblastosis virus*) reverse transcriptase; all provided in the kit. Per 10,125 µl mastermix, 1µg RNA was used.

2.5.5 Gel electrophoresis and detection

PCR products were controlled by gel electrophoresis. Therefore, 2% agarose gels in Tris-Borate-EDTA (TBE) -buffer containing 0.5 µg/ml ethidiumbromide were used. As length standard a 100 bp DNA-leader was used. DNA was separated by 140 V and resulting bands were detected with a UV-gel-detection-system (Vilber Lourmat, Marne LA Vallee, France).

Tris-Borate-EDTA (TBE) –buffer: 89 mM Tris base, 89 mM boric acid, 2 mM EDTA pH 8.0, 100 ml distilled water.

2.5.6 Preparation of cytosolic and mitochondrial protein fractions

Txnrd1 is expressed in the cytosol of cells and *Txnrd2* in the mitochondria. In several experiments the two proteins needed to be analyzed separately.
Therefore, organs were prepared freshly and washed in ice cold PBS. The whole organs were homogenised with a hand glass / glass homogeniser in 1.5 ml homogenising-buffer. After 7 strokes the homogenate was centrifuged for 10 minutes at 700 x g and 4°C. The supernatant was than centrifuged at 11000 x g for 10 minutes at 4°C to separate the mitochondria from the cytosolic fraction. The supernatant which means the cytosolic fraction was centrifuged again at 11000 x g for 10 minutes at 4°C as a cleaning step. Again the supernatant received was transferred in a new reaction tube and stored at -20°C. The pellet containing the mitochondrial fraction was washed in 200 µl homogenising-buffer and centrifuged at 11000 x g for 10 minutes at 4°C to retain a more concentrated mitochondrial fraction. The supernatant was discarded and the pellet resuspended in 60 µl homogenising-buffer. The pellet was shock-frosted in liquid nitrogen to break the mitochondria membranes. After thawing on ice the mitochondrial fraction was sonicated twice for 10 seconds keeping it on ice and then stored at -20°C.

Homogenising-buffer: 250 mM sucrose, 20 mM HEPES, 1mM EDTA, 1:100 protease inhibitor cocktail, 1:100 phosphatase inhibitor cocktail 1, 1:100 phosphatase inhibitor cocktail 2.

2.5.7 Protein quantification according to Bradford

For quantification of protein the Bradford reagent was mixed 1:1 with distilled water. 1 ml of the premix was mixed with 3 µl of the protein sample, incubated for 5 minutes at room temperature in the dark and then measured in disposable cuvettes (Plastibrand® 1.5 ml semi-micro, Brand GmbH, Wertheim, Germany) with a spectrophotometer (SmatSpec™Plus, BioRad GmbH, Munich, Germany) at 595 nm. A standard curve was obtained using 0.5 – 6.5 mg bovine serum albumin (BSA) /ml.

2.5.8 Thioredoxin reductase activity assay

For determination of enzymatic activity of either TXNRD1 or TXNRD2, a colorimetric NADPH-dependent DTNB reduction assay (Holmgren and Bjornstedt, 1995) was performed. To this end, protein was prepared as described in 2.4.5 and quantified by the Bradford assay as described in 2.4.6. 100 µg of the cytosolic or mitochondrial fraction, respectively, was added to the reaction mix. Thereafter the reaction mix was adjusted to room temperature for 30 minutes. Absorption was measured at 412 nm for 3 minutes in intervals of 10 seconds immediately. Thioredoxin reductase activity was calculated as follows and was expressed in nmol reduced DTNB/min/mg protein: mean of slope of extinction out of triplet measurement per organ x reaction volume (1000 µl) /DTNB extinction coefficient (13,6 ml/nmol) x sample volume (100 µl) x 10.

Reaction mix: 0.1 M potassium phosphate, pH 7.0, 1 mM EDTA, 2 mg/ml DTNB, 0.2 mg/ml NADPH, 0.2 mg/ml BSA.

2.6 Histological methods

2.6.1 Preparation and fixation of organs for paraffin sections

EL-TGFα-hGH$^{tg/+}$;*p53*$^{+/-}$ mice were euthanized by cervical dislocation. The pancreatic tumours, liver, spleen, duodenum and altered organs were prepared, washed in PBS and fixed in 4% buffered formalin over night at 4°C in a tissue processing/embedding cassette (Histosette®I with lid, Simport, Bernard-Pilon, Canada). For getting a better fixation of the tumour tissue, the tumours were cut in pieces.

Pancreas, liver, spleen and duodenum of the thioredoxin reductase knockout mice and controls were prepared after CO_2 euthanasia, washed in PBS and fixed in 4% buffered formalin over night at 4°C in tissue processing/embedding cassettes.
For the preparation of the lung its vessels were flushed with PBS by punctuation of the right heart ventricle until the lung changed colour from light red to white. Thereafter the trachea was prepared and a lung lavage with PBS was performed followed by injection of 4% buffered formalin into the lung, incubation for 10 seconds and fixation in 4% buffered formalin in a tissue processing/embedding cassette at 4°C over night.
For preparation of the brain the skullpan was taken off and the brain was carefully prepared from the skull and fixed in 4% (w/v) paraformaldehyde in PBS at 4°C over night.
The fixed organs were stored in 70% ethanol at 4°C until they were dehydrated in a vapuro infiltration processor (Sakura 510, Tissue Tek, Miles Inc., Elkhart, USA). After dehydration the organs were incubated in paraffin at 60°C over night.

4% buffered formalin: 4 % formaldehyde, 64 mM NaH_2PO_4, 90 mM Na_2HPO_4
4% (w/v) paraformaldehyde in PBS: 40 g paraformaldehyde, 1000 ml PBS, 100 µl 1 M NaOH
PBS: 50 mM potassium phosphate, 150 mM NaCl, pH 7.2

2.6.2 Preparation and fixation of organs for cryosections

After preparation of the organs intended for cryosections, the organs were washed in ice-cold PBS and fixed overnight in 4% (w/v) paraformaldehyde in PBS at 4°C. The next day, organs were partially dehydrated in a 30% sucrose solution in PBS until they sank to the bottom of the reaction tube to prevent formation of ice crystals in frozen tissue. Then they were incubated in 30% sucrose / 30% Tissue Tec O.C.T. Compound in PBS solution for 2 hours and afterwards for 30 minutes in 100% Tissue Tec O.C.T. Compound.

4% (w/v) paraformaldehyde in PBS: 40 g paraformaldehyde, 1000 ml PBS, 100 µl 1 M NaOH
PBS: 50 mM potassium phosphate, 150 mM NaCl, pH 7.2

2.6.3 Paraffin sections

Fixed and dehydrated organs were incubated in 60°C paraffin over night, paraffin-embedded with a paraffin embedding station (Typ pec 3003-D, Tespa GmbH, Gießen,

Germany) and stored at –20°C until they were cut into sections of 3.5 µm with a microtome (HM 355S, Microm, Walldorf, Germany) and mounted on special glass slides (Superfrost plus, Menzel-Gläser, Braunschweig, Germany). The sections were dried over night at 37°C.

2.6.4 Cryosections

Cryoprotected organs were frozen in 100% Tissue Tec O.C.T. Compound on dry ice. The frozen organs were cut into sections of 20 µm in a cryostat, post fixed for 10 minutes in ice cold 4% (w/v) paraformaldehyde in PBS, washed in PBS and stained immediately.

4% (w/v) paraformaldehyde in PBS: 40 g paraformaldehyde, 1000 ml PBS, 100 µl 1 M NaOH
PBS: 50 mM potassium phosphate, 150 mM NaCl, pH 7.2

2.6.5 Hematoxylin and Eosin (H&E) staining

Organ samples were prepared and embedded in paraffin as described in 2.5.1 and 2.5.3. Each organ sample was stained with hematoxylin and eosin (H&E) as a standard stain for histological evaluation. The sections were deparaffinised in Roti®-Histol for 10 minutes twice and rehydrated in graded ethanol series (2x 100%, 2x 96%, 2x 70%) each for 3 minutes. The sections were stained with hematoxylin according to Gill III for 3 minutes, rinsed in water for 5 minutes, stained with 1% eosin for 30 seconds and washed in distilled water. The sections were dehydrated in graded ethanol series (2x 70%, 2x 96%, 2x 100%) each for 5 seconds, treated with Roti®-Clear twice for 5 minutes and mounted in Roti®-Histokitt II. H&E-stained nuclei are coloured in blue, the cytosol in light red.

1% eosin: 1 g eosin, 100 ml distilled water, 1 ml acetic acid

2.6.6 Immunohistochemistry

Organ samples were prepared and embedded in paraffin as described in 2.5.1 and 2.5.3. The paraffin sections were deparaffinised in Roti®-Histol for 10 minutes twice and rehydrated in graded ethanol series (2x 100%, 2x 96%, 2x 70%) each for 3 minutes and 5

minutes in distilled water. For antigen retrieval, microwave treatment in 0.01 M sodium citrate buffer pH 6.0 for 10 minutes on a sub boiling temperature in a plastic jar was required. This was necessary because methylene bridges are formed during fixation, which cross-link proteins and therefore mask antigenic sites. Afterwards, the sections were left for 20 minutes in the buffer to cool down. Another antigen retrieval method was required for the rat anti-F4/80 – BM8 antibody. For this staining, the sections were digested with proteinase K in 20mM Tris-HCl for 10 minutes. After antigen retrieval, sections were washed in distilled water for 5 minutes three times and put into a slide rack (Sequenza™Slide Rack and Coverplate™ system, TedPella, Inc., Redding, USA). To block endogenous peroxidases the sections were incubated in 3% hydrogen peroxide for 15 minutes and then washed in distilled water and PBS. To block unspecific epitopes the sections were incubated for 1 hour in 5% serum in PBS of the species in which the secondary antibody was made. The Avidin/Biotin blocking kit was used when the primary antibody had to be incubated over night. The blocking solution and the blocking solution for overnight incubation were incubated for 1 hour. The primary antibody dilutions are given in table 2. They were diluted in 5% serum in PBS and incubated for 90 minutes at room temperature. Antibodies with overnight incubations were diluted in 5% serum solution with biotin or over night at 4°C. After incubation with the primary antibody, the sections were washed three times in PBS. The secondary biotin-labled antibody was diluted according to the manufactures instruction (Tab.2) in 1 % serum in PBS and incubated for 30 minutes at room temperature. After the incubation the sections were washed in PBS three times. For signal detection the Avidin-Biotin Complex (ABC)-technique was used. As multiple avidin molecules bind to a single biotin molecule, this gives a stronger signal than simply using an enzyme-chromogen system. Therefore, the ABC-solution was preincubated for 30 minutes at 4 °C and then the sections were incubated with this solution for 30 minutes at room temperature. After incubation the sections were washed in PBS three times and once in distilled water. For final signal detection, the Peroxidase Substrate Kit DAB SK-4100 was used. The slides were incubated in the staining solution until a light brown colour was perceptible or for a maximum of 2 minutes and the enzyme reaction was stopped by washing in distilled water. The sections were counterstained with hematoxylin according to Gill III for 3-5 seconds, rinsed in water for 5 minutes, dehydrated in graded ethanol series (2x 70%, 2x 96%, 2x 100%) each for 5 seconds, incubated twice in Roti®-Clear for 5 minutes and mounted in

Roti®-Histokitt II. Positive cells or structures are stained in brown, negative structures in blue.

ABC-solution: 2.5 ml PBS, 1 drop solution A, 1 drop solution B

Blocking solution for overnight incubation: 1 ml 5 % serum in PBS, 4 drops avidin

Dilution solution with biotin: 1 ml 5 % serum in PBS, 4 drops biotin

3 % hydrogen peroxide: 1 ml 30% H_2O_2, 9 ml ddH_2O

Proteinase K antigen retrieval: 20 mg/ml proteinase K in 20mM Tris-HCl, pH 8.0, 1:50 diluted in 20mM Tris-HCl

0.01 M sodium citrate buffer pH 6.0: 1.8 mM citric acid monohydrate, 8.2 mM trisodium citrate dehydrate

Staining solution: 2.5 ml distilled water, 1 drop buffer solution, 2 drops 3,3´-Diaminobezidine, 1 drop H_2O_2

Tris-HCl: 121 mg / 50 ml Tris(hyoroxymethyl)-aminomethane (Tris), pH 8.0

2.6.7 Masson-Trichrom staining

Masson-Trichrom stains connective tissue and allows examination of developing fibrosis. Organ samples were prepared and embedded in paraffin as described in 2.5.1 and 2.5.3. The section were deparaffinised in Roti®-Histol for 10 minutes twice and rehydrated in graded ethanol series (2x 100%, 2x 96%, 2x 70%) each for 3 minutes and 5 minutes in distilled water. Incubation in Bouin fixative over night lead to more intense staining. Second day started with incubation in Weigert´s iron hematoxylin for 10 minutes subsequently rinsed in water for 5 minutes and washed in distilled water. Then the sections were stained with Bieberich Scarlet acid fuchsin solution for 5 minutes and washed in distilled water. An incubation in phosphotoungstic-/phosphomolybdic acid solution for 5 minutes followed. After that the sections were stained in aniline blue solution for 7 minutes, washed shortly in distilled water and incubated in 1% acetic acid. After a final washing step in distilled water the sections were dehydrated in graded ethanol series (2x 70%, 2x 96%, 2x 100%) for 5 seconds each, incubated twice in Roti®-Clear for 5 minutes and mounted in Roti®-Histokitt II. In this staining cytoplasm is stained in red, nuclei in dark grey and collagen in blue.

Bouin fixative: 15 ml picric acid solution 1.2%, 9% formaldehyde, 1 ml acetic acid

Phosphotoungstic-/phosphomolybdic acid solution: 10 ml phosphotoungstic acid, 10 ml phosphor-molybdic acid, 20 ml distilled water

Weigert´s iron hematoxylin: 50 % weigert´s iron hematoxylin part A, 50 % weigert´s iron hematoxylin part B

2.6.8 Periodic Acid Schiff (PAS) staining

The periodic acid schiff staining is a method for detection of mucopolysccharides in tissues.

Organ samples were prepared and embedded in paraffin as described in 2.5.1 and 2.5.3. The sections were deparaffinised in Roti-Histol for 10 minutes twice and rehydrated in graded ethanol series (2x 100%, 2x 96%, 2x 70%) each for 3 minutes and 5 minutes in distilled water. The sections were incubated in periodic acid solution for 5 minutes at room temperature and washed three times in distilled water for 5 minutes. An incubation in Schiff´s reagent for 15 minutes at room temperature followed and the sections were rinsed in water for 5 minutes. Counterstaining was performed with hematoxylin for 3-5 seconds, rinsed in water for 5 minutes, dehydrated in graded ethanol series (2x 70%, 2x 96%, 2x 100%) each for 5 seconds, incubated twice in Roti®-Clear for 5 minutes and mounted in Roti®-Histokitt II. Glycogen or mucin producing cells are stained in purple, nuclei in blue.

2.6.9 X-Gal detection of β-galactosidase

B-galactosidase was detected in whole organs and on cryosections. Organs or sections were washed 3 times for 5 minutes in PBS and once in distilled water. After these washing steps organs were incubated for 90 minutes and cryosections for 24 hours at 37 °C in X-Gal working solution, then washed twice in PBS. Afterwards cryosections were counter-stained with nuclear fast red for 1 minute, washed in distilled water, dehydrated in graded ethanol series (2x 70%, 2x 96%, 2x 100%) each for 5 seconds, incubated twice in Roti®-Clear for 5 minutes and mounted in Roti®-Histokitt II. Tissues with β-galactosidase activity were stained in dark blue, in cryosection the remaining tissue was stained in red.

X-Gal dilution buffer: 10 µl 5 mM potassium ferricyanide crystalline, 10 µl 5 mM potassium ferricyanide trihydrate, 10 µl 2 mM magnesium chloride, 970 µl PBS

X-Gal stock solution: 4 % 5-Bromo-4-chloro-3-indolyl-β-D-galactopyranoside (X-Gal) in N,N-Dimethyl-formamide

X-Gal working solution: X-gal stock solution 1 : 40 in X-Gal dilution buffer

2.6.10 Transmission electron microscopy

To evaluate ultrastructural changes in the pancreas of *Txnrd1* and *Txnrd2* knockout mice and controls, pancreatic samples were examined by transmission electron microscopy with the kind assistance of Luise Jennen, Institute of Pathology, Biomedical Imaging, Helmholtz Center Munich – German Research Center for Environmental Health. Therefore 1 mm x 1 mm x 1 mm pieces of the pancreas of one-year-old mice were cut immediately after preparation in the fixative 2.5 % glutaraldehyde in 0.1 M sodium cacodylate buffer and fixed for a minimum of one day at 4°C until dehydration and embedding in plastic medium. Preparation of sections for TEM as well as staining of semi thin slides was performed by Luise Jennen.

2.7 Physiological and metabolic screens

2.7.1 Body weight

Mice were fasted over night and weighed the next morning (Compact scale CS200, Ohaus Corporation, Pine Brook, USA). Data were expressed as means ± standard deviation.

2.7.2 Blood glucose

Mice were fasted over night. The next morning from the tail vain a blood drop was taken. Blood glucose levels were measured with a glucometer (Ascensia Contour®, Bayer Vital GmbH, Leverkusen). Data were expressed as means ± standard deviation.

2.7.3 Blood serum analysis for amylase and lipase

Blood samples were taken from the vena cava after euthanizing mice with CO_2. Blood samples were collected in micro tubes for blood samples (Sarstedt, Nümbrecht, Germany) and left for 20 minutes at room temperature to allow coagulation. Samples were centrifuged for 10 minutes at 4000 x g and blood serum was stored at -80°C. The parameters amylase and lipase were measured by Vet Med Labor GmbH, Division of

IDEXX Laboratories, Ludwigsburg in 1 : 3 diluted blood serum samples in PBS. Data were expressed as means ± standard deviation.

2.7.4 Lipid absorption test

Mice were kept singles, fasted for 18 hours and then fed with a 30% High Fat Diet (Ssniff EF R/M with 30% fat, Sniff Spezialdiäten GmbH, Soest, Germany) for two consecutive days. Stool samples were collected for 24 hour-periods. The stool was homogenized after adding 10 µl distilled water per mg stool. After centrifugation at 200 x g for 5 minutes to remove insoluble material, 5 µl of the supernatant were mixed with 5 µl of freshly prepared and filtered 0,5% Oil Red O solution and the whole volume was prepared as stool smears on slides and examined by light microscopy. For quantification, from the centre of the coverslip 20 consecutive fields of sights were counted. Data were expressed as means ± standard deviation.

Oil Red O solution: 5 % Oil Red O in propylene glycol (100 %)

2.7.5 Intraperitoneal glucose tolerance test (IP-GTT)

Following an 18 hour fast, baseline blood glucose levels were measured by scratching the tail vain with an injection needle, a blood drop was taken. Blood glucose levels were measured with a glucometer (Ascensia Contour®, Bayer Vital GmbH, Leverkusen). After the first measurement, dextrose (2 mg / g body weight) was injected intraperitoneal and blood glucose was measured again immediately after injection and then after 15, 30, 60, 90 and 120 minutes. Data were expressed as means ± standard deviation.

2.7.6 Relative pancreatic weight

Gross anatomical observation of pancreatic development in the knockout mice and controls was made by weighing the whole mouse and the pancreas. Determination of relative pancreatic weight was calculated as follows: relative pancreatic weight [%] = body weight / weight of the pancreas x 100. Data were expressed as means ± standard deviation.

2.7.7 Proliferation index

Determination of the number of dividing cells of the pancreatic tissue as a marker for growth and regeneration was done by a BrdU proliferation assay. BrdU is a thymidin derivate which is incorporated into the DNA of dividing cells. Mice were injected intraperitoneally with 50 µg/mg body weight 90 minutes before they were sacrificed. Pancreas and duodenum as control were fixed in 4% buffered formalin over night at 4°C, dehydrated and paraffin embedded as described in 2.5.1 and 2.5.3. 3.5 µm slides were stained by immunohistochemistry with a rat anti-BrdU antibody. Per slide 10 fields of vision were photographed and all brown (proliferating cells) and blue (non-proliferating cells) nuclei were counted. The proliferation index was calculated as follows: proliferation index [%] = all cells / proliferating cells x 100. Data were expressed as means ± standard deviation.

2.7.8 Selenium analysis

All selenium analyses were done by Bernhard Michalke (Institute of Ecological Chemistry, Helmholtz Center Munich – German Research Center for Environmental Health, Neuherberg, Germany).

Serum samples were analysed by means of a Perkin Elmer graphite furnace atomic absorption spectrometer (4100 ZL) with $Mg(NO_3)_2$ and $Pd(NO_3)_2$ (each 0.2%) as matrix modifier. The samples also contained 0.3 HCL and 0.4% Triton X100.

Solid samples were dissolved in HNO_3 for 10 hours at 170°C in a pressure digestion system (Seif, Unterscheißheim, Germany) and measured by ICP-AES (Inductively Coupled Plasma atomic Emission Spectrometry) in a Spectro Ciros Vision-System (SPECTRO Analytical Instruments). Sample introduction was based on hydride generation with 10% HCL and $NaBH_4$ solution using Argon as plasma and introduction gas. All selenium contents were expressed as µg/kg wet mass.

$NaBH_4$ solution: 1% $NaBH_4$ in 0.3% NaOH

2.8 Analysis of tumour prone mice

2.8.1 Observation of tumour progression

EL-TGFα-hGH$^{tg/+}$;*p53*$^{+/-}$ mice were checked daily for clinical signs of illness (Hawkins, 2002) and killed for necropsy after reaching the hyper-acute phase of disease. The lifespan was noted as parameter for tumour latency for 60 selenium-deficient and 71 selenium-supplemented mice.

2.8.2 Tumour nomenclature and grading

H&E stained slides of tumours of EL-TGFα-hGH$^{tg/+}$;*p53*$^{+/-}$ mice were analyzed with the help of two experienced pathologists (Dr. Gabriele Hölzlwimmer and Dr. Leticia Quintanilla-Martinez, Institute of Pathology, Helmholtz Center Munich – German Research Center for Environmental Health, Neuherberg, Germany). Pancreatic tumour description was performed according to the consensus report and recommendations for mouse models of exocrine pancreatic cancer (Hruban *et al*., 2006a).

2.9 Analysis of eyesight

As a consequence of the expression of *Cre*-recombinase under the *Ptf1a*-promoter in GABAeric cells (Nakhai *et al.*, 2007), possible phenotypes of the eye were examined. Therefore one year old conditional cytosolic and mitochondrial thioredoxin reductase knockout mice as well as their heterozygous floxed controls were taken for the following tests which were all done in the German Mouse Clinic by the group of Prof. Dr. Joachim Graw, Institute of Mammalian Genetics, Helmholtz Center Munich – German Research Center for Environmental Health. In the routine eye screen of the German Mouse Clinic the anterior part of the eye, mainly cornea and lens, were examined by slit lamp biomicroscopy according to Favour (Favor, 1983). The posterior parts of the eye were examined by funduscopy (ophthalmoscopy) checking the retina and optic nerve. Laser interference biometry was used for determination of eye size parameters (e.g. axial length) using the “ACMaster” (Meditec, Carl Zeiss, Jena, Germany) adapted for short measurement distances (Schmucker and Schaeffel, 2004) (Fig.23,A). Vision tests were

performed with an optokinetic drum setup as described by Schmucker (Schmucker *et al*., 2005) (Fig.23,B). Function of the retina was tested by electroretinography according to Dalke (Dalke *et al*., 2004) by measuring the nerval reaction of the retina on stimulating flashlights (Fig.23,C) by the use of an ESPION ColorBurst Handheld Ganzfeld LED stimulator (Diagnosys LLC, Littleton, MA, USA).

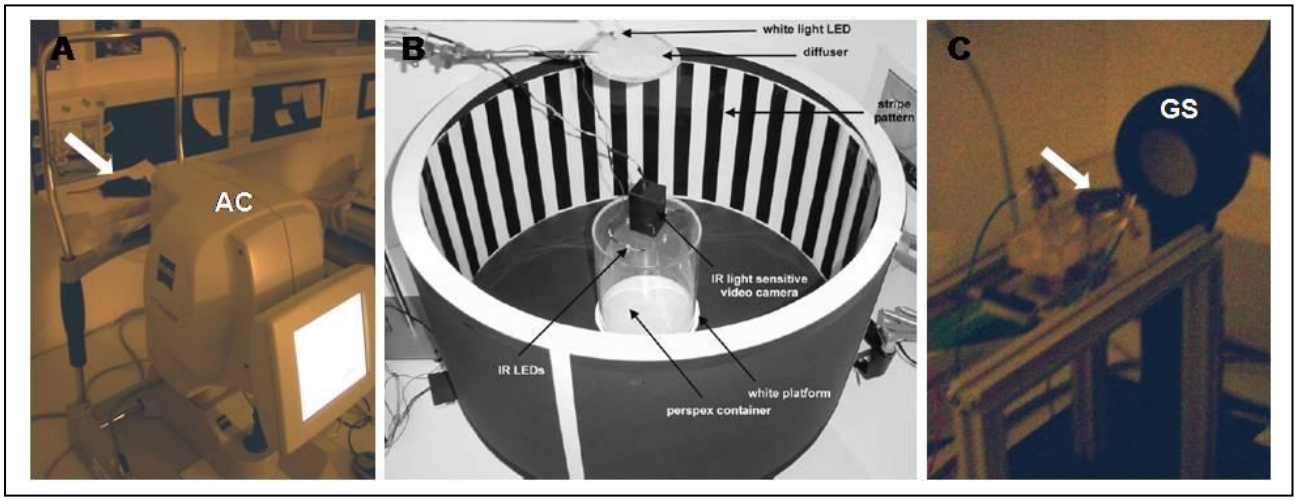

Fig.18: Experimental setup for eye examination. (A) Laser interference biometry (AC = ACMaster, arrow = mouse). (B) Optokinetic drum (adapted from Schmucker *et al*., 2005). (C) GS = Electroretinography (ESPION ColorBurst Handheld Ganzfeld LED stimulator), arrow = mouse.

2.10 Statistical analysis

Mean tumour latency of EL-TGFα-hGH$^{tg/+}$;*p53*$^{+/-}$ mice was calculated with the Log-Rank test (proc lifetest, SAS 9.1). Tumour type proportions of EL-TGFα-hGH$^{tg/+}$;*p53*$^{+/-}$ mice in the selenium-deficient and selenium-adequate groups were calculated by an exact randomized version of the Fisher-test (Scherb, 2001) and selenium concentration differences in several organs were calculated with paired student t-test (Sigma Plot). Thioredoxin reductase activities in relation to selenium-status are calculated with a paired student t-test, whereas all other statistics were calculated with student t-test (Sigma Plot). Data are expressed as means ± standard deviation.

3 Results

3.1 Effect of selenium on pancreatic carcinogenesis

In the first part of this study the tumour pattern of pancreatic cancer-prone mice (EL-TGFα-hGH$^{tg/+}$;*p53*$^{+/-}$) with low selenium status (designated below as selenium-deficient) was compared to that of mice replenished with non-toxic amounts of sodium selenite (designated below as selenium-adequate). The amount of selenium was sufficient to support maximal tissue activities of selenoproteins. Sodium selenite was chosen as selenium source since, in contrast to selenomethionine, it cannot be incorporated non-specifically into proteins. Instead, selenium from selenite is predominantly incorporated as selenocysteine into selenoproteins (Rayman, 2004).

3.1.1 Selenium status of the parental strains and experimental generation

Selenium is stored and retained very efficiently in organs and can be passed from the mother to the offspring via the milk. To this end, mice were bred on a selenium-deficient diet for three consecutive generations. In order to confirm selenium-deficiency in the third selenium-depleted parental generation, several organs (testis: n = 4, all other organs: n = 8) were measured for their selenium content. As a control, the third selenium-adequate fed parental generation was taken. The selenium status of pancreas, liver, serum and skeletal muscle in the selenium-deficient group was 10- to 20- fold lower than those of the selenium-adequate group and confirmed successful deprivation of selenium in these mice ($p < 0.001$, student t-test). In brain and testes the selenium content of the selenium-depleted mice was about 2-fold lower than in adequately selenium-fed mice, but this meant also a statistically significant reduction ($p < 0.01$, student t-test) (Fig.19).

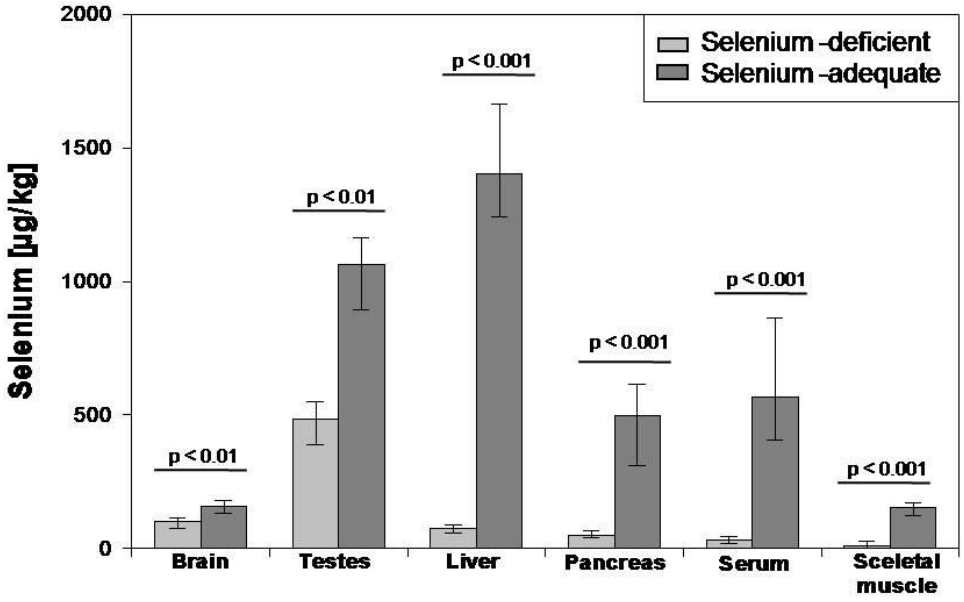

Organ	Selenium-deficient [µg/kg wet mass]	Selenium-adequate [µg/kg wet mass]
Brain	95.3 ± 18.6	157.4 ± 23.4
Testes	467.2 ± 80.8	1027.9 ± 136.4
Liver	72.9 ± 14.9	1453.8 ± 210.6
Pancreas	53.6 ± 11.4	463.8 ± 153
Serum	32.3 ± 13.5	634.5 ± 229
Skeletal muscle	14.0 ± 15.4	147.2 ± 22.8

Fig.19: Selenium content in different organs of the third parental generation. In the third parental generation a significant reduction of the selenium content in different organs had been reached. Data are expressed as means ± standard deviation in µg/kg wet mass.

The selenium content of the liver was chosen as surrogate reference marker for the selenium status at time of necropsy of all experimental mice used in the study. The selenium-content in this organ was highly significant reduced in the selenium-deficient group ($p < 0.001$, student t-test) (Fig.20).

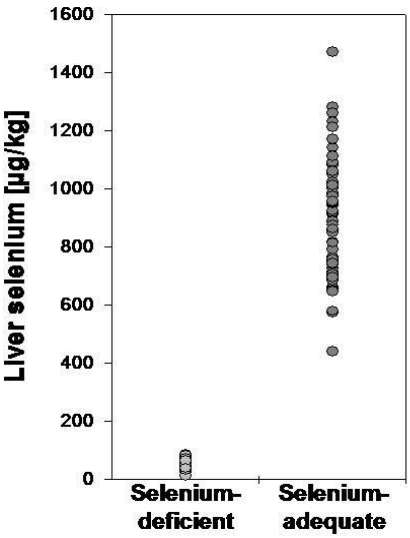

Experimental group	number of animals	Amount of Selenium in the liver [µg/kg]
Selenium-deficient	60	47.6 ± 16.9
Selenium-adequate	71	923 ± 224

Fig.20: Selenium status of experimental mice. The mean amount of selenium in the liver of the experimentally used mice was about 20-fold lower in the selenium-deficient group compared to the selenium-adequate group ($p < 0.001$). Data are expressed as means ± standard deviation in µg/kg wet mass.

3.1.2 Tumour latency

At the hyper-acute phase of disease all experimental mice (n=131) showed malignant tumours. The mouse with the shortest lifespan in the selenium-deficient group died at an age of 188 days of a haematopoietic tumour, the one with the longest lifespan at an age of 797 days of pancreatic carcinoma. In the selenium adequate group the youngest mouse died 187 days old of pancreatic carcinoma and the oldest at an age of 743 days also of pancreatic carcinoma. The mean latency for all tumour types in the selenium-deficient compared to the selenium-adequate group was 470.9 ± 128 days compared to 471.5 ± 113 days, respectively, showing that the selenium status of the mice had no effect on the total tumour latency (Fig.21).

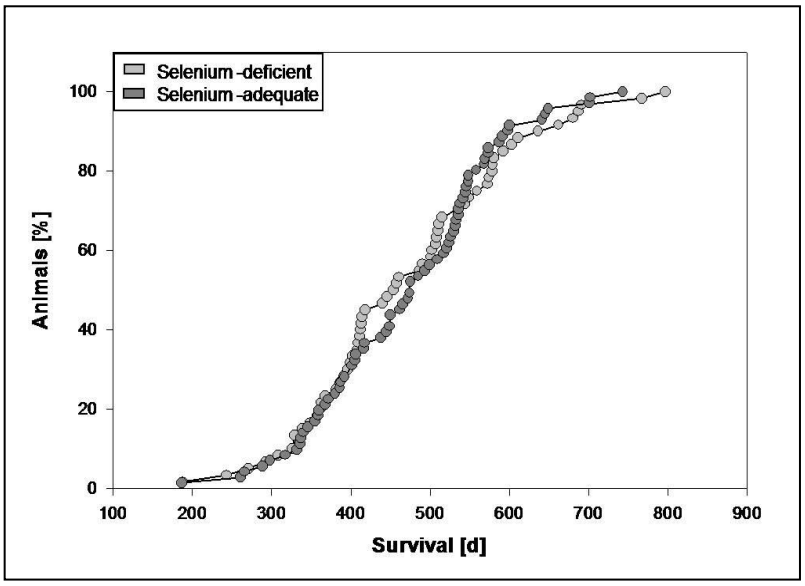

Fig.21: Incidence of all tumours found in EL-TGFα-hGH$^{tg/+}$;*p53*$^{+/-}$ mice. The selenium status did not affect the incidence of the tumours observed in the experimental mice over the whole experimental period of 800 days. Each dot represents one mouse.

Although pancreatic carcinoma, as primary experimental outcome, showed a tendency for a benefit of the selenium-adequate group at an age interval between 400 and 600 days, but over the whole experimental period the selenium status did not have an effect on the incidence of pancreatic carcinoma (Fig.22). The mean latency of pancreatic carcinoma in the selenium-deficient group was 464.3 ± 117 days (n = 33) and in the selenium-adequate group 466.1 ± 112 days (n = 50).

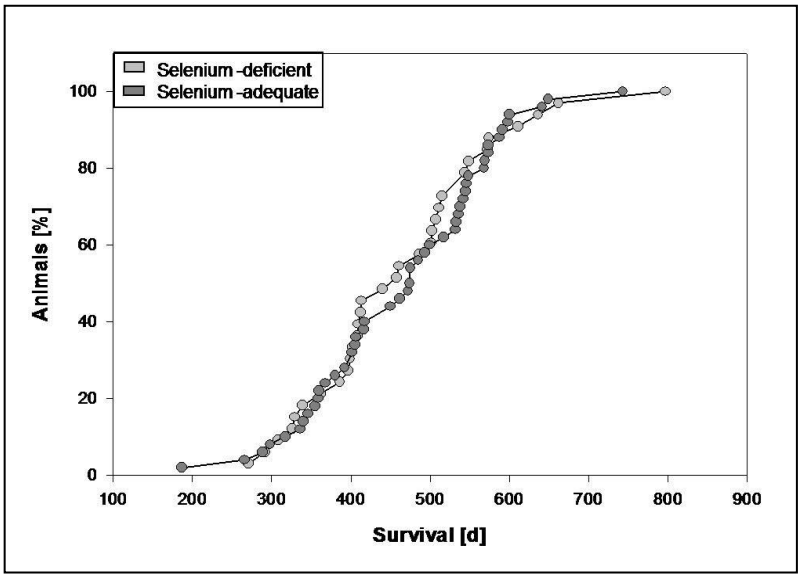

Fig.22: Incidence of pancreatic carcinoma in EL-TGFα-hGH$^{tg/+}$;*p53*$^{+/-}$ mice. The selenium status did not affect the incidence of pancreatic carcinoma. Each dot represents one mouse.

3.1.3 Tumour spectrum

Beside pancreatic carcinomas the experimental mice developed a wide spectrum of tumours. This is due to the *p53* hemizygosity of the mice which caused mostly hematopoietic tumours, mammary and bone tumours, and few cases of tumours of the lung, liver, skin and muscle (Donehower *et al*., 1992; Jacks *et al*., 1994). Interestingly, the tumour spectrum was influenced by the selenium status (Fig.23). In the selenium-deficient group, only 50.0% of all tumours were pancreatic carcinomas, which was a lower percentage than in the selenium-adequate group (70.4%), but this difference was not statistically significant (p = 0.07, fisher-exact-test). In the selenium-deficient group, 40% were hematopoietic tumours in contrast to 33.8 % in the selenium-adequate group.

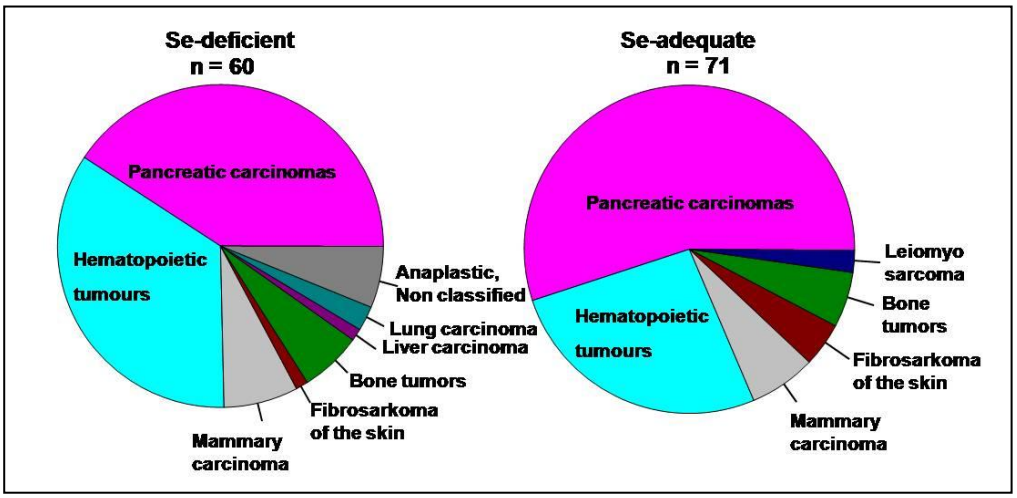

Fig.23: Tumour spectrum of EL-TGFα-hGH$^{tg/+}$;*p53*$^{+/-}$ mice. Influence of selenium on the tumour spectrum. Fewer pancreatic carcinomas were found in the selenium-deficient group.

3.1.4 Morphological analysis of pancreatic carcinomas

EL-TGFα-hGH$^{tg/+}$;*p53*$^{+/-}$ mice showed a palpable drastically enlarged and fibrotic pancreas as premalignant alteration, sometimes with large cysts. In selenium-deficient as well as in selenium-adequate mice, pancreatic carcinomas did not show any gross morphological differences. Figure 24 depicts examples of pancreatic tumours from the selenium-deficient and selenium-adequate group.

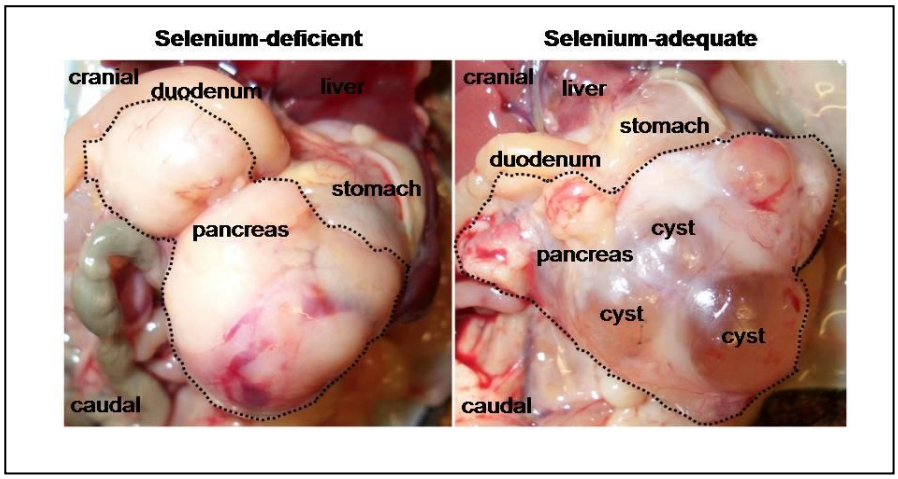

Fig.24: Examples of pancreatic tumours found in EL-TGFα-hGH$^{tg/+}$;*p53*$^{+/-}$ mice *in situ*. Both tumours show similar gross morphology. Dotted lines demark the pancreatic tumour. In the tumour of the selenium-adequate fed mouse some pancreatic cysts are present which also were commonly found in selenium-deficient mice.

After mice were sacrificed, tumour samples were processed for histological analysis and stained with H&E. Tumour morphology was analyzed together with Dr. Leticia Quintanilla-Martinez and Dr. Gabriele Hölzlwimmer, Institute of Pathology, Helmholtz Center Munich – German Research Center for Environmental Health. EL-TGFα-hGH$^{tg/+}$;*p53*$^{+/-}$ mice spontaneously develop pancreatic adenocarcinoma (Wagner *et al*., 2001). Nodular pancreatic hyperplasias were found (Fig.25,B), as well as transdifferentiation of acinar cells to ductal cells to tubular complexes (Fig.25,C). The acinar-ductal metaplasias were surrounded by massive expanding fibrosis (Fig.25,D). Also cystic ossificated metaplasias (Fig.25,E) and serous or mucous cystic adenomas were found (Fig.25,F,G).

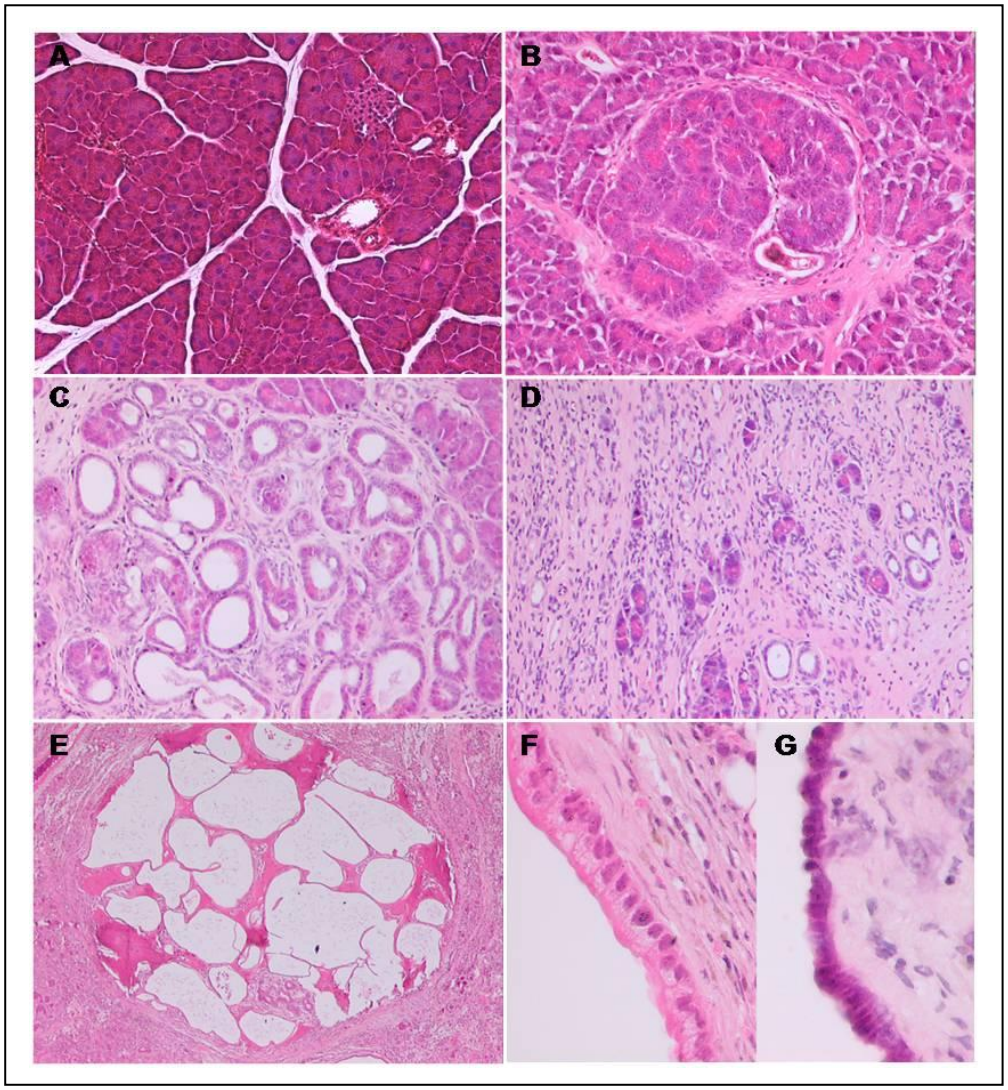

Fig.25: Premalignant lesions of pancreatic adenocarcinomas in EL-TGFα-hGH$^{tg/+}$;*p53*$^{+/-}$ mice. (A) Normal pancreatic tissue (H&E, 200x). (B) Nodular acinar hyperplasia (H&E, 100x). (C) Acinar-ductal metaplasia with fibrosis (H&E, 160x). (D) Massive fibrosis (H&E, 160x). (E) Cystic ossificated metaplasia (H&E, 40x). (F) Serous cystic adenoma (H&E, 500x). (G) Mucous cystic adenoma (H&E, 500x). Pancreatic carcinomas in this model developed via formation of tubular complexes, which were surrounded by massive fibrosis.

The pancreatic carcinomas found could be differentiated in their cellular origin and grade of differentiation. Figure 26 depicts representative samples of pancreatic carcinomas found in EL-TGFα-hGH$^{tg/+}$;*p53*$^{+/-}$ mice of both experimental groups. The acinar cell carcinoma depicted in figure 26,A showed a well-differentiated acinar arrangement of the tumour cells. Cytological, the tumour was characterized by round to oval nuclei, a single prominent nucleolus and abundant eosinophilic cytoplasm with mild pleomorphism and moderate mitotic activity (arrows). The invasive ductal adenocarcinoma shown in figure 26,B

consisted of enlarged irregular ducts with epithelial folding into the lumen (arrows). A high degree of cytological atypia was present, including hyperchromasia and high mitotic activity. Beside the well differentiated carcinomas also poorly differentiated or anaplastic carcinomas were found. Figure 26,C depicts an area of poorly differentiated carcinoma, which in most cases was alternating with areas of well-differentiated acinar tumours. These carcinomas were characterized by cellular crowding, pleomorphism and increased mitotic activity. Anaplastic carcinomas (Fig. 26,D) showed high degree of cellular pleomorphism. High rates of mitoses, apoptotic cells, giant cells, and multinucleated cells as well as cytoplasmic vacuolization were observed.

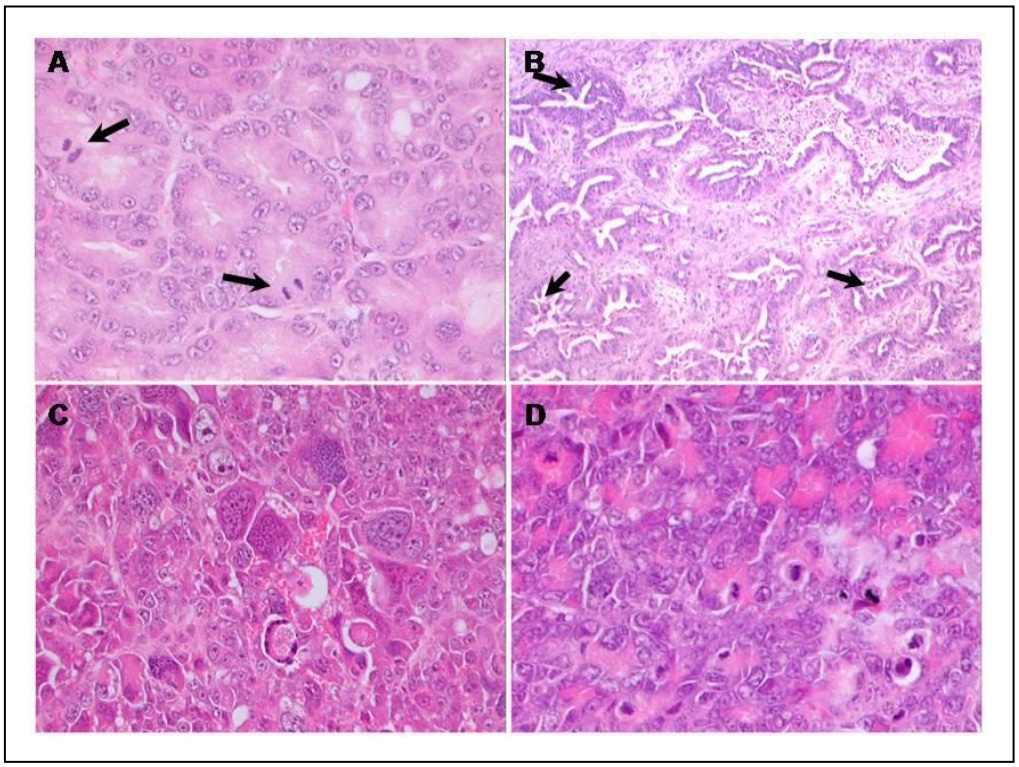

Fig.26: Malignant lesions of pancreatic adenocarcinomas in EL-TGFα-hGH$^{tg/+}$;p53$^{+/-}$ mice. (A) Well-differentiated acinar cell carcinoma with low mitotic activity (arrows) (H&E, 400x). (B) Well-differentiated ductal cell carcinoma with typical epithelial folding into the lumen (arrows) (H&E, 160x;). (C) Poorly differentiated carcinoma (H&E, 400x). (D) Anaplastic carcinoma (H&E, 500x). Pancreatic adenocarcinomas could be distinguished by their cell type of origin and by their differentiation grade.

Distant metastases and/or local invasion were also found in some mice with similar incidence in the selenium-deficient and selenium-adequate group. In gross morphology, metastases appeared as small, greyish, firm nodules in the mesentery and on the surface of abdominal organs or the lung. In figure 27,A the local invasion of a ductal carcinoma into the regional lymph node is depicted. Most distant metastases were found in the lung

or in the liver, a few in the mesentery, diaphragm or in the spleen. Figure 27,B depicts a neoplastic thrombus of an acinar carcinoma in a lung blood vessel (arrow). In Figure 27,C a metastasis of an anaplastic carcinoma in the adjacent spleen is shown. The liver metastasis of an anaplastic carcinoma depicted in figure 27,D had variable cell sizes, including giant cells, numerous mitoses and apoptotic cells and highly necrotic areas with masses of cell debris (arrow).

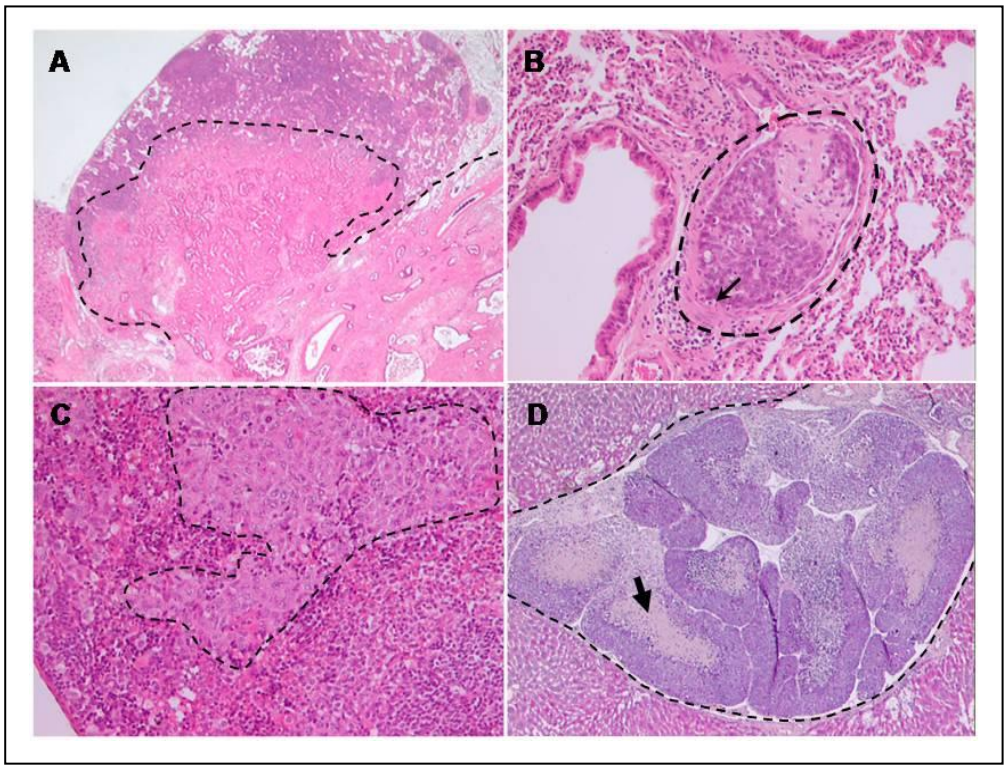

Fig.27: Local and distant metastatic invasion of pancreatic carcinomas. (A) Invasion of ductal carcinoma into a regional lymph node (H&E, 15x). (B) Neoplastic thrombus of an acinar carcinoma in the lung blood vessel (arrow) (H&E, 160x). (C) Metastasis of an anaplastic carcinoma in the spleen (H&E, 160x). (D) Metastasis of an anaplastic carcinoma in the liver with necrotic cell debris (arrow) (H&E, 400x). Dotted lines demark the border between metastasis and normal tissue.

3.1.5 Differentiation grades of pancreatic carcinomas

The percentage of pancreatic carcinomas within all types of tumours was higher in the selenium-adequate compared to the selenium-deficient group, although the difference was not statistically significant as already shown in chapter 3.1.3. Most interestingly, the grade of differentiation of the pancreatic carcinomas showed a highly significant difference between the selenium-deficient and selenium-adequate group (Fig.28). In the selenium-

deficient group, the proportion of differentiated pancreatic carcinomas was 21.2% compared to that of the selenium-adequate group with 60.0% ($p < 0.001$, fisher-exact-test). The differentiated carcinomas were also classified by their cell of origin, but there was no significant difference. 57.1% of the pancreatic carcinomas in the selenium-deficient group were of acinar origin versus 76.7% in the selenium-adequate group ($p = 0.07$, fisher-exact-test).

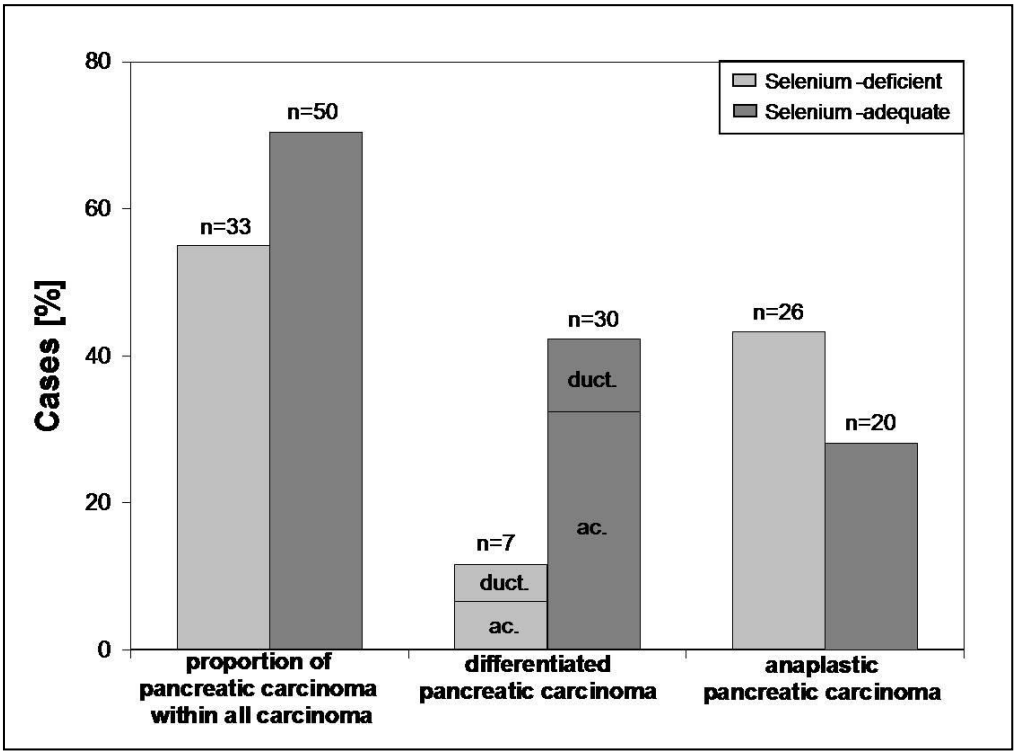

Fig.28: Differentiation grade of pancreatic carcinomas. The selenium-adequate group showed a tend towards a higher percentage of pancreatic carcinomas ($p = 0.07$). Classification into differentiated and anaplastic carcinomas revealed a highly significant difference ($p < 0.001$) between the two groups. More differentiated pancreatic carcinomas were found in the selenium-adequate group. Partition of differentiated carcinomas into acinar or ductal origin did not reveal a significant difference.

These results highlight an impact of selenium on tumour differentiation. Low levels of selenium and subsequently also low levels of selenoproteins may therefore impair differentiation processes in the tumour or in tumour precursor cells.

3.2 TXNRD1 and TXNRD2 activity in the pancreas

Selenoproteins are the effector molecules that translate the mechanism of action of selenium in the mammalian organism (Whanger, 2004). Among the selenoproteins the thioredoxin reductases are linked in several ways to cancer, albeit the mechanisms are unknown as outlined in chapter 1.1.5 (Arner and Holmgren, 2000; Sun *et al*., 1999; Tamura and Stadtman, 1996; Gasdaska *et al*., 1994). In order to clarify the role of thioredoxin reductases in the pancreas under normal and selenium- deficient conditions, the activity of cytosolic (TXNRD1) and mitochondrial (TXNRD2) thioredoxin reductases was measured in different organs of mice fed with a standard diet (Altromin type 1314 GmbH, Lage, Germany). The influence of the selenium status on TXNRD1 and TXNRD2 activity in mice fed the selenium-deficient or selenium-adequate diet was also determined.

3.2.1 TXNRD1 and TXNRD2 activity in the pancreas compared to other organs

The activity of thioredoxin reductase in the cytosol (TXNRD1) of different organs in 6 months old male C57BL/6 mice (n = 5) was measured with the thioredoxin reductase activity assay. The highest activity was found in the liver and the small intestine. Heart, brain and spleen had lower enzyme activities (Fig.29). Intermediate activities of thioredoxin reductase were found in the pancreas, kidney and lung.

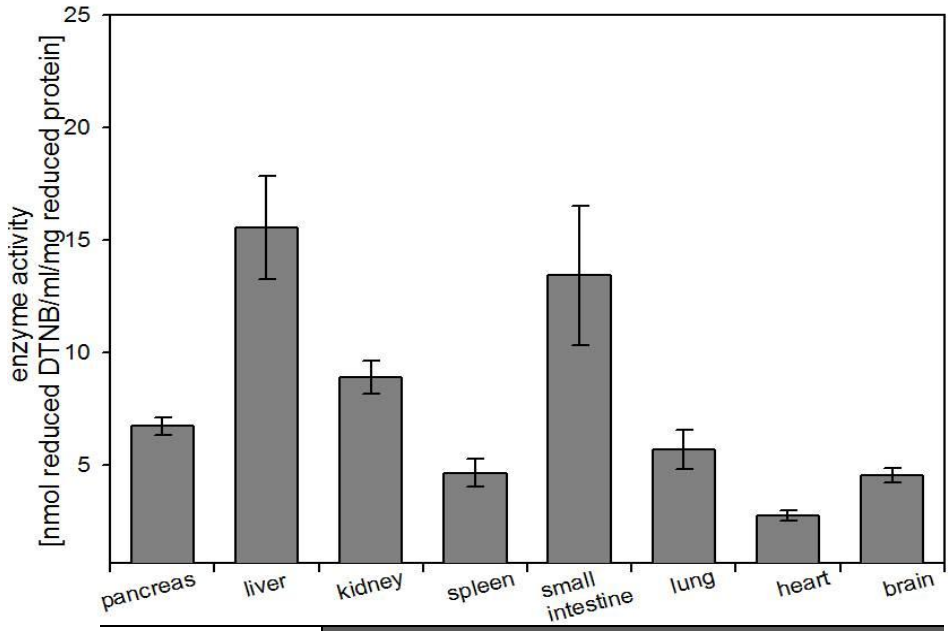

Organ	Txnrd activity [nmol red. DTNB/ml/mg protein]
pancreas	6.7 ± 0.4
liver	15.5 ± 2.3
kidney	8.9 ± 0.7
spleen	4.7 ± 0.6
small intestine	13.4 ± 3.1
lung	5.7 ± 0.9
heart	2.8 ± 0.2
brain	4.6 ± 0.3

Fig.29: Thioredoxin reductase activity in the cytosol of different organs of C57BL/6 mice. Cytosolic thioredoxin reductase activity was highest in the liver and in the small intestine and lowest in the heart, brain and spleen. The activity in the pancreas was moderate. Data are expressed as means ± standard deviation.

The activity of thioredoxin reductase in mitochondria (TXNRD2) isolated from different organs of 6 months old male C57BL/6 mice (n = 5) was highest in the pancreas. The other organs had much lower activity. Thioredoxin reductase activity in the liver and kidney was moderate followed by spleen and heart (Fig.30). In the small intestine, lung and brain comparably very low enzyme activity was found.

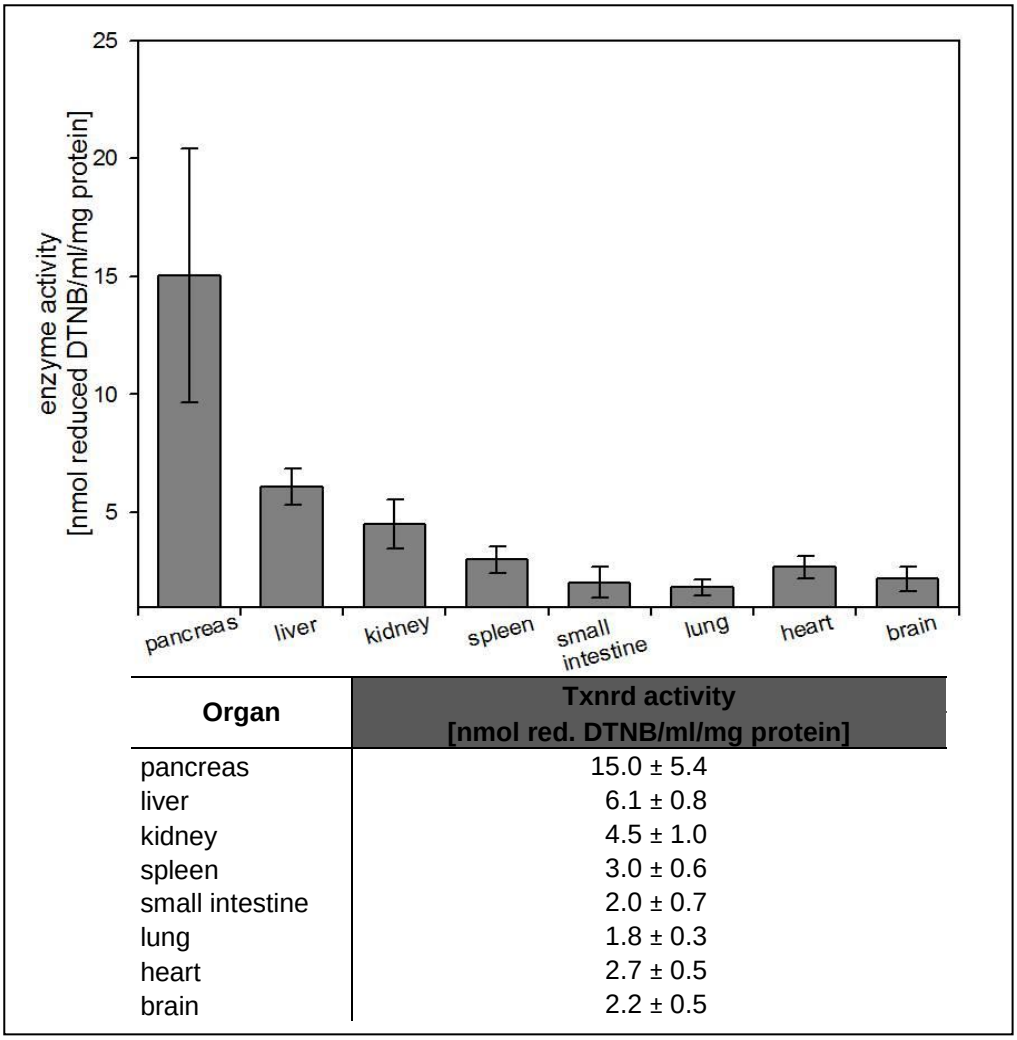

Organ	Txnrd activity [nmol red. DTNB/ml/mg protein]
pancreas	15.0 ± 5.4
liver	6.1 ± 0.8
kidney	4.5 ± 1.0
spleen	3.0 ± 0.6
small intestine	2.0 ± 0.7
lung	1.8 ± 0.3
heart	2.7 ± 0.5
brain	2.2 ± 0.5

Fig.30: Thioredoxin reductase activity in the mitochondria of different organs of C57BL/6 mice. The highest thioredoxin reductase activity in the mitochondria was found in the pancreas, whereas the other organs showed a moderate or low activity. Data are expressed as means ± standard deviation (n=5).

From these results it may be assumed that thioredoxin reductase plays an extraordinary role in pancreatic mitochondria.

3.2.2 Influence of the selenium status on TXNRD1 and TXNRD2 activity in the pancreas in relation to different organs

TXNRD1 activity was again measured in the cytosol, TXNRD2 activity in the mitochondria of the pancreas, as well as in the liver and the kidneys as reference organs in selenium depleted (n = 5) and selenium-adequate (n = 5) 4 month old male C57BL/6 mice.
TXNRD1 activity in the cytosol was significantly reduced in the pancreas of selenium-depleted mice compared to selenium-adequate mice ($p < 0.01$, student t-test). A highly significant reduction of enzymatic activity was also found in the liver and in the kidney of selenium-deficient mice ($p < 0.001$, student t-test) (Fig.31).

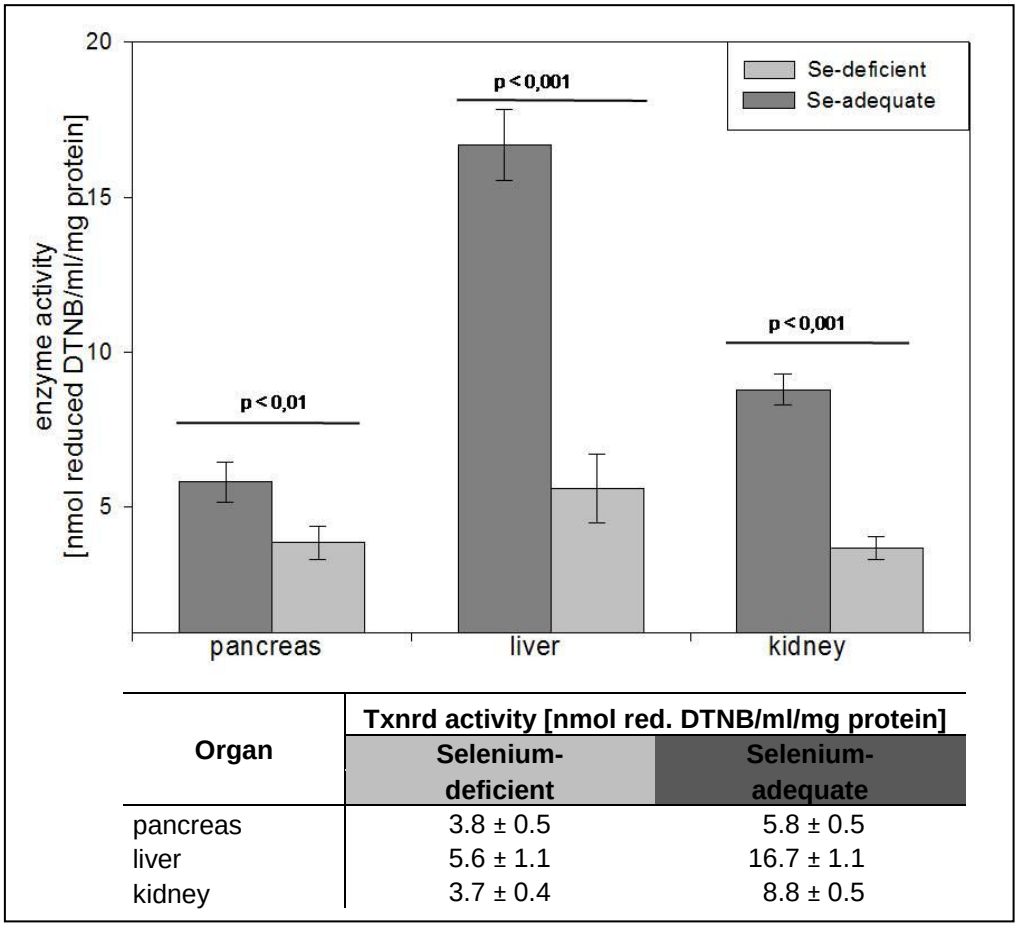

Organ	Txnrd activity [nmol red. DTNB/ml/mg protein]	
	Selenium-deficient	Selenium-adequate
pancreas	3.8 ± 0.5	5.8 ± 0.5
liver	5.6 ± 1.1	16.7 ± 1.1
kidney	3.7 ± 0.4	8.8 ± 0.5

Fig.31: TXNRD1 activity in relation to selenium-availability. In the pancreas, liver and kidney, the activity of thioredoxin reductase in the cytosol was significantly reduced in selenium-deficient fed mice. Data are expressed as means ± standard deviation (n=5).

Thioredoxin reductase activity in the mitochondria showed a completely different picture. As in the cytosol, mitochondrial thioredoxin reductase (TXNRD2) activity in the liver and in

the kidney in selenium-deficient compared to that found in selenium-adequate mice showed significant reduction (both $p < 0.01$, student t-test). In the pancreas, the enzyme activity was not reduced in selenium-deficiency. Instead, thioredoxin reductase activity increased ($p = 0.09$, student t-test) (Fig.32).

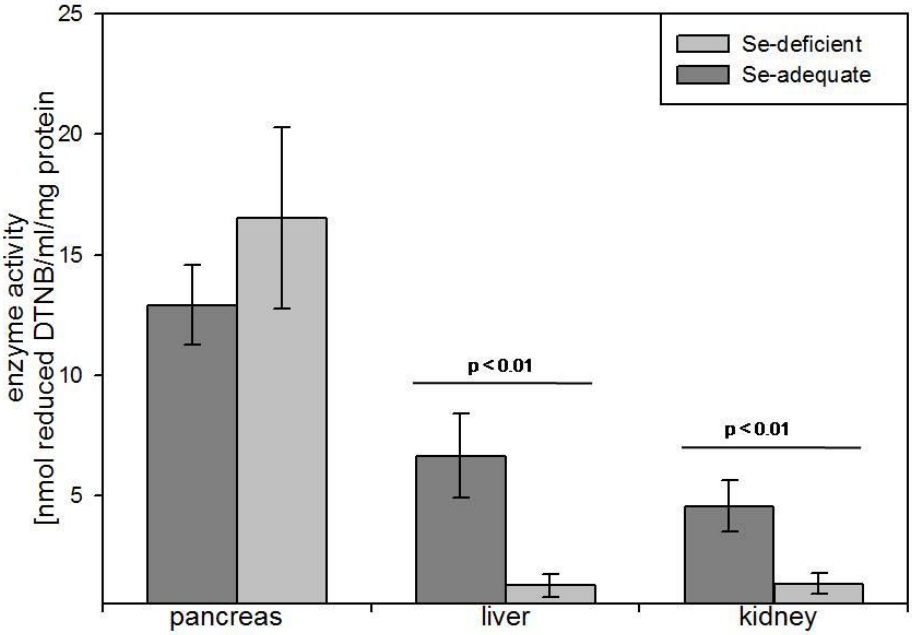

Organ	Txnrd activity [nmol red. DTNB/ml/mg protein]	
	Selenium-deficient	Selenium-adequate
pancreas	12.9 ± 1.6	16.5 ± 3.8
liver	1.3 ± 0.5	6.7 ± 1.8
kidney	1.4 ± 0.4	4.6 ± 1.1

Fig.32: TXNRD2 activity in relation to selenium-availability. In liver and kidney the mitochondrial thioredoxin reductase activity was reduced in selenium deficiency, whereas in the pancreas the activity increased. Data are expressed as means ± standard deviation (n=5).

In order to confirm selenium deficiency, the selenium content of the liver was measured in these mice. Mean concentrations in this organ showed a statistically significant reduction of selenium in selenium-deficiency ($p < 0.001$, student t-test) (Fig.33).

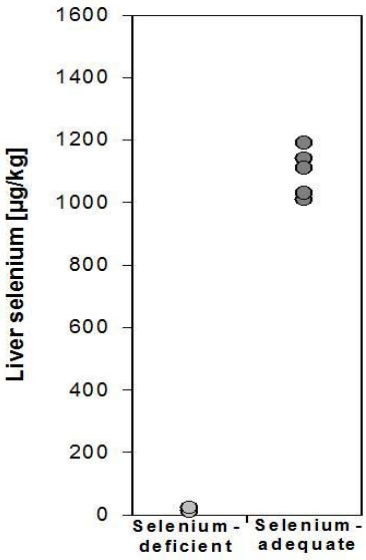

Experimental group	number of animals	Amount of Selenium in the liver [µg/kg]
Selenium-deficient	5	14.6 ± 0.7
Selenium-adequate	5	1096 ± 33.7

Fig.33: Selenium status of experimental mice used for TXNRD1 and TXNRD2 activity analysis. Liver selenium contents confirmed selenium deficiency or adequacy. Data in the table are expressed as means ± standard deviation in µg/kg wet mass.

These results pointed to an important function in the pancreas of mitochondrial thioredoxin reductase, and to a lesser extent of cytosolic thioredoxin reductase. They showed no or only small down-regulation during selenium deficiency in comparison to the liver and kidney, where they were strongly down regulated.

3.3 Pancreas-specific knockout of *Txnrd1*

The results presented in 3.2 demonstrated thioredoxin reductase activity in the cytosol of pancreatic cells that was only weakly influenced by selenium deficiency. Homozygous knockout mice for cytosolic thioredoxin reductase (*Txnrd1*) died around embryonic day (E) 9.5-10.5 (Jakupoglu *et al*., 2005). To clarify the role of TXNRD1 in the pancreas, the *Cre*/*loxP* technology was used to bypass embryonic lethality. A floxed conditional knockout mouse strain was crossed with a Cre-recombinase transgenic mouse strain, expressing Cre-recombinase under the control of the *Ptf1a-p48* promoter to generate pancreas-specific *Txnrd1* knockout mice. For the mice examined in this part of the study the designation "*Txnrd1* knockout mouse" was used for the genotype *Txnrd1*$^{fl/fl}$;*Ptf1a-Cre*^{ex1}, whereas "*Txnrd1* control" was used for the genotype *Txnrd1*$^{+/fl}$. In case other genotypes were used, they were indicated separately.

3.3.1 Validation of pancreas-specific *Txnrd1* knockout

Organ specificity of *Cre*-expression was demonstrated by crossing the knockout strain *Txnrd1* with the Cre reporter mouse ROSA26R (R26R) (Soriano, 1999). The validation of the conditional knockout was done on three levels: genomic DNA, mRNA and enzyme activity.

To monitor pancreas-specific *Cre*-expression, the *Txnrd1* strain was crossed with the ROSA26 Cre reporter strain (R26R) (Soriano, 1999). Three-weeks-old pancreas-specific *Txnrd1* knockout mice from this cross (*Txnrd1*$^{fl/fl}$;*Ptf1a-Cre*^{ex1};R26R$^{\Delta/+}$) and heterozygous floxed controls(*Txnrd1*$^{+/fl}$;R26R$^{\Delta/+}$) were sacrificed and the pancreas as well as a part of the duodenum were prepared. The whole organs as well as cryosections were stained for β-galactosidase expression. The pancreas of the knockout mouse stained blue for β-galactosidase activity as a sign for positive *Cre*-expression, whereas the duodenum remained unstained (Fig.34,A), as well as the pancreas and the duodenum of the control mouse (Fig.34,B). These observations were confirmed in the cryosections. Also here, the pancreatic tissue stained positive for β-galactosidase activity in the knockout pancreas, whereas the intra-pancreatic lymph node (Ln) (Fig.34,C) as well as the pancreatic tissue of the control mouse (Fig.34,D) remained unstained. These results supported specific *Cre*-expression in the pancreas.

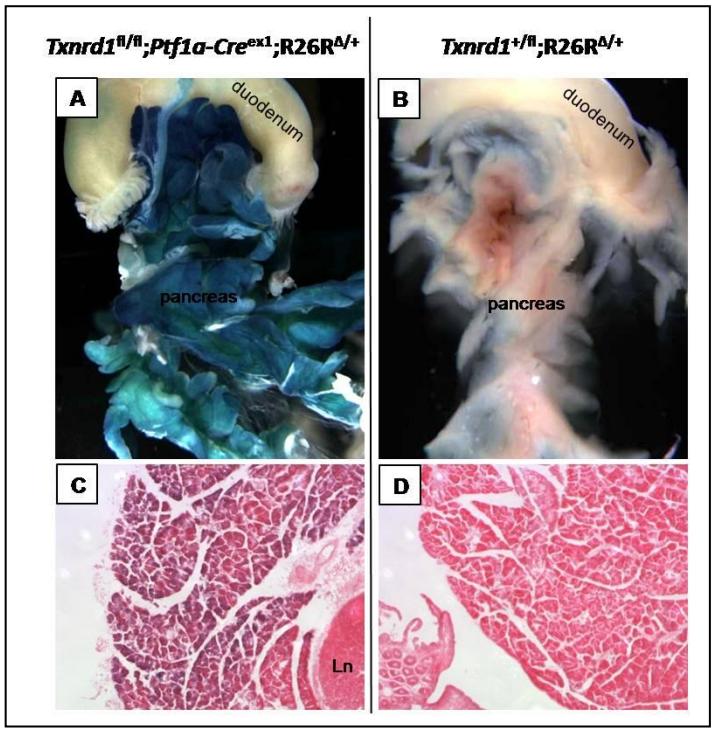

Fig.34: Cre-recombinase expression in pancreatic *Txnrd1* knockout tissue. (A) Pancreas and duodenum of a *Txnrd1* knockout mouse. (B) Pancreas and duodenum of a *Txnrd1* control mouse. (C) Cryosection of pancreatic tissue of a *Txnrd1* knockout mouse. The intra-pancreatic lymph node remained unstained (Ln = lymph node; 100x). (D) Cryosection of pancreatic tissue of a *Txnrd1* control mouse (100x). Blue staining of the pancreas as a result of *Cre*-induced β-galactosidase activity in *Txnrd1* knockout mice (*Txnrd1*$^{fl/fl}$;*Ptf1a-Cre*^{ex1};R26R$^{\Delta/+}$). The pancreas of control mice (*Txnrd1*$^{+/fl}$;R26R$^{\Delta/+}$) remained unstained.

On the level of genomic DNA, the knockout was validated by PCR with specific primer pairs. DNA from the pancreas as target organ and the tail as representative non-pancreatic tissues was isolated. The floxed allele was amplified by a primer pair (TR1floxf1/TR1floxr1) covering the *loxP*-site and adjacent genomic sequences. The corresponding wild type (wt) allele lacked the *loxP*-site and therefore was 64 base pairs (bp) shorter (Fig.: 35,B; floxed and wild type allele). In the knockout mice all tissues contained two floxed *Txnrd1* alleles, whereas in the control mice there was only one floxed and one wild type allele (Fig.: 35,A; floxed allele). To show deletion of exon 15 in the pancreas of knockout mice, a primer pair (TR1wtfor2/Neopromrev1) was used which amplified the deleted region and adjacent sequences (Fig.35,B). The deleted allele was present only in the pancreas but not in the tail (Fig.35,A). This pointed to a successful pancreas-specific knockout. The *Cre*-transgene was present only in the knockout but not in the control mice as shown by a primer pair (TetO-Cre1-4) amplifying the *Cre*-sequence or a slightly longer wild type (wt) sequence (Fig.35,A).

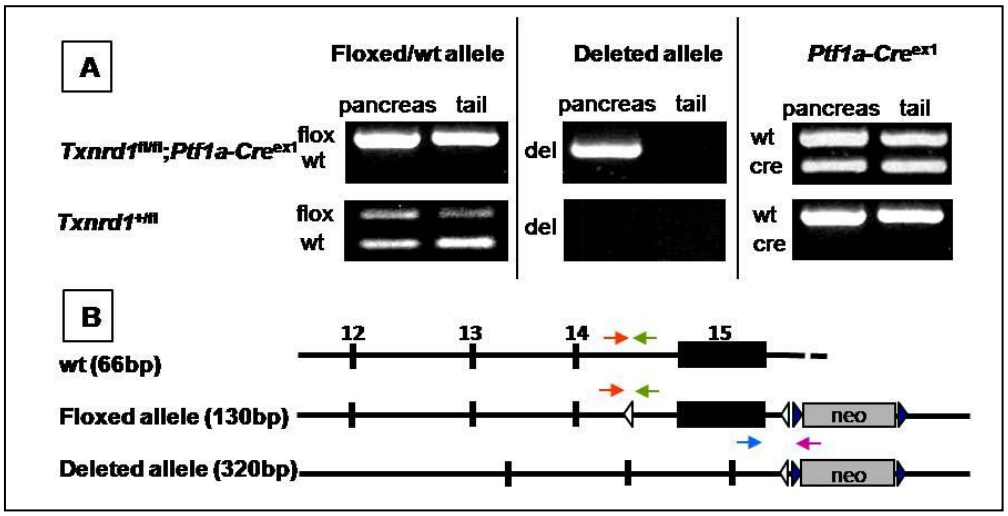

Fig.35: *Txnrd1* knockout validation on DNA level. The pancreas-specific knockout was first verified on DNA level by PCR with specific primer pairs. (A) PCR results for the floxed and deleted allele or Cre-recombinase in pancreas and tail. Knockout mice showed two floxed *Txnrd1* alleles together with one *Ptf1a-Cre* allele. Excision of *Txnrd1* exon 15 was restricted to the pancreas. *Txnrd1*$^{+/fl}$ mice showed one floxed and one wt *Txnrd1* allele together with a wt allele in the *Ptf1a* locus. (B) Primer binding sites.

The expression of *Txnrd1* in knockout and control mice on mRNA level was validated by semiquantitative reverse transcription-PCR (RT-PCR) (each genotype n = 3) (Fig.36). RNA was isolated from the pancreas as the target organ. Liver was used as a control organ. Oligo(dT) primer were used to transcribe mRNA into cDNA. The housekeeping genes *aldolase* and *GAPDH* were used as standards. The primer pair TR1 59 / 60 bound upstream of the knockout region, whereas TR1 E13 / E15 synthesized a template spanning the deleted exon 15. *Aldolase* and *GAPDH* were expressed in the same quantity in the knockout and control mice in pancreas and liver. mRNA upstream of the knockout region was slightly reduced in the knockout pancreas in comparison to the controls. The expression in liver remained unaffected. Expression of mRNA containing exons 13 to 15 was reduced in the pancreas of knockout mice but not in the liver or in controls. These results showed effective knockout of cytosolic thioredoxin reductase in the pancreas.

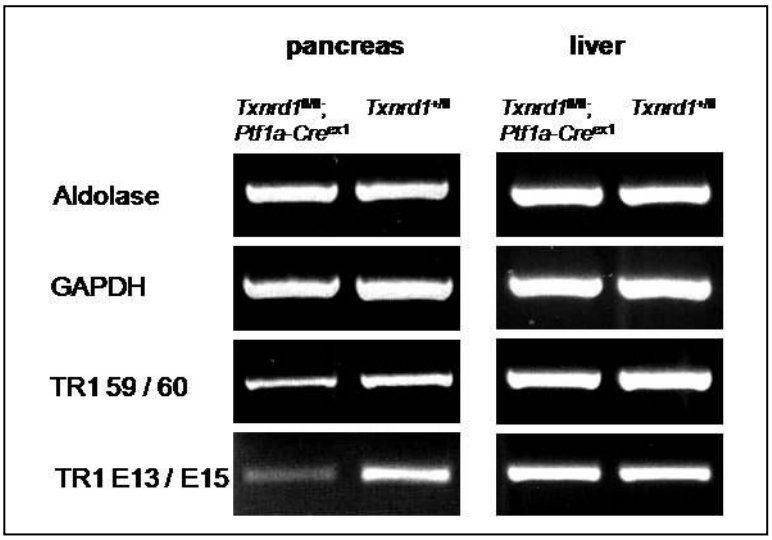

Fig.36: *Txnrd1* knockout validation on mRNA level. *Txnrd1* mRNA containing the deleted region was strongly reduced, truncated mRNAs detected by primers TR1 59/60 was moderately reduced and *Txnrd1* expression in the liver was not affected in knockout mice.

To proof a reduction of the enzymatic activity of TXNRD1 in the pancreas, protein was prepared and measured freshly from the pancreas as well as from liver and kidney as reference organs (all n = 5). In the pancreas of knockout mice, enzymatic activity was significantly reduced by 52% compared to the control mice ($p < 0.01$, student-t-test) (Fig.37). Cytosolic thioredoxin reductase activity in the control organs liver and kidney remained unaffected.

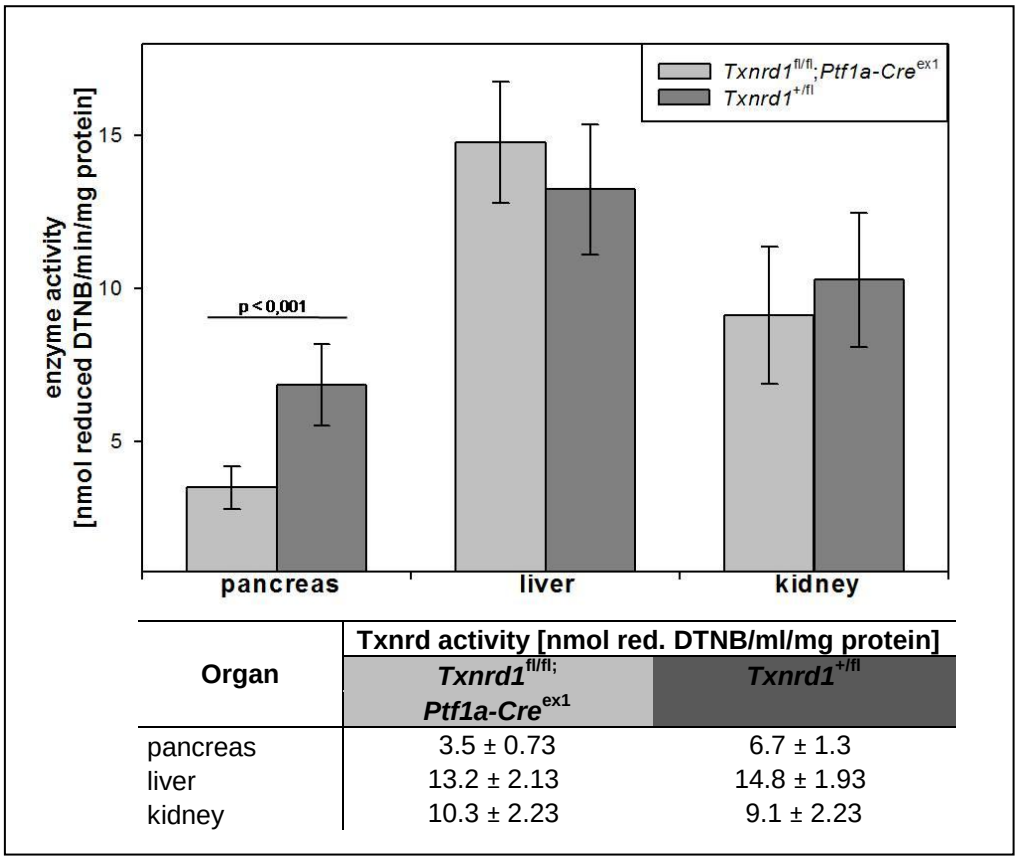

Organ	Txnrd activity [nmol red. DTNB/ml/mg protein]	
	***Txnrd1*$^{fl/fl;}$ *Ptf1a-Cre*^{ex1}**	***Txnrd1*$^{+/fl}$**
pancreas	3.5 ± 0.73	6.7 ± 1.3
liver	13.2 ± 2.13	14.8 ± 1.93
kidney	10.3 ± 2.23	9.1 ± 2.23

Fig.37: TXNRD1 activity in *Txnrd1* knockout mice. Enzymatic activity of thioredoxin reductase in the cytosol was significantly reduced in the knockout pancreas compared to the controls. Liver and kidney as reference organs remained unaffected. Data are expressed as means ± standard deviation.

3.3.2 General observations

The pancreas-specific *Txnrd1* knockout mice did not show any obvious clinical or behavioural changes in comparison to the controls over an observation period of one year. They were also fertile.

Txnrd1 knockout and control mice were weighed every two weeks over an observation period of one year. Mice were fasted overnight to avoid influence of individual differences in amounts of eaten chow. Body weight curves did not differ in knockout and control mice (Fig.38). Even when sexes were analyzed separately, there was no difference (Fig.38).

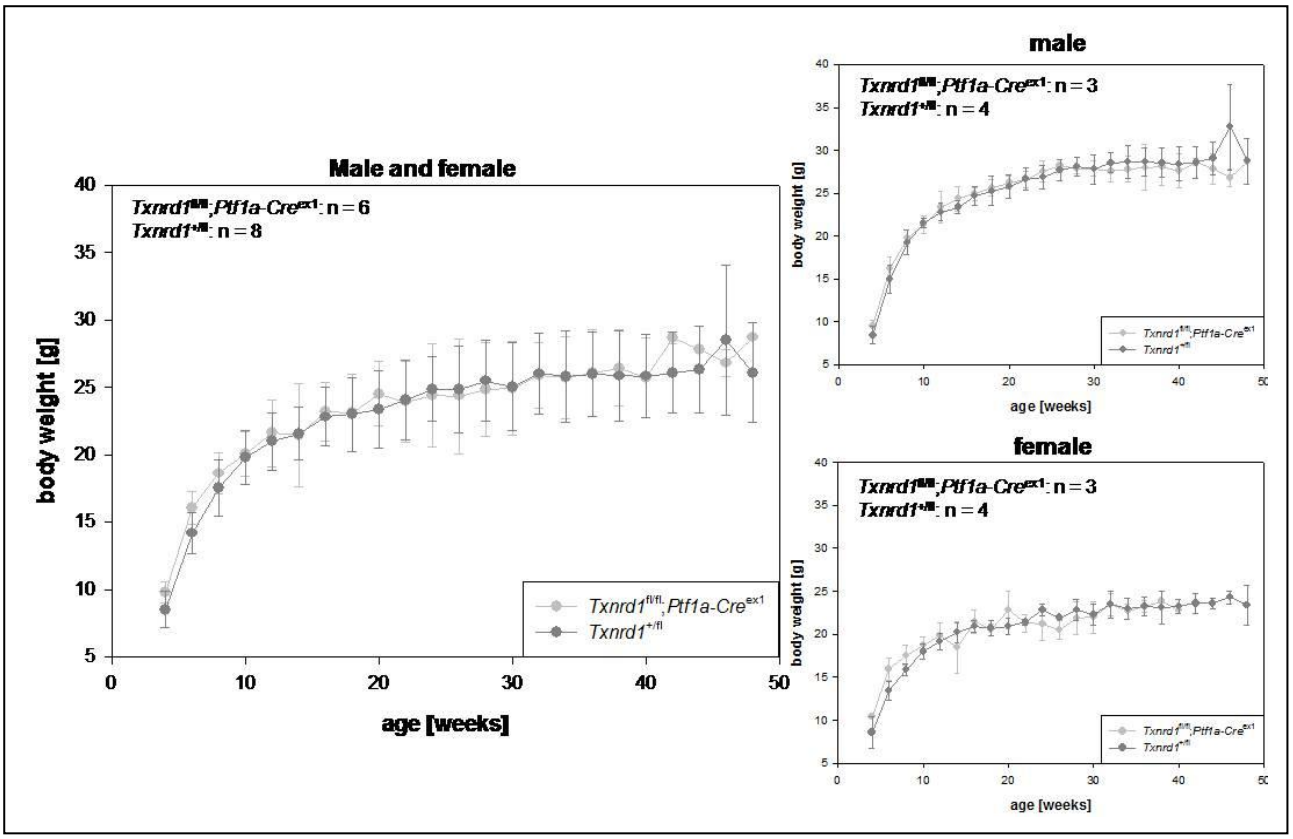

Fig.38: Body weight development in *Txnrd1* knockout and control mice. Mice were fasted over night and weight in the morning. Each dot represents the mean body weight of the mouse group ± standard deviation observed over one year. Data showed no difference in weight development in knockout (*Txnrd1*$^{fl/fl}$;*Ptf1a-Cre*^{ex1}) and control (*Txnrd1*$^{+/fl}$) mice.

3.3.3 Pancreatic gross morphology

Mice were sacrificed at an age of four, twelve and twenty-four weeks and one year (each age and genotype n = 4 males and n = 4 females except at the age of one year knockout mice n = 3 males and n = 3 females). Mice were examined for gross morphological changes in the whole body and especially in the pancreas. Figure 39,A shows the pancreas *in situ* in relation to liver, duodenum and stomach as indicated. At all ages there were no gross morphological differences observable in comparison of *Txnrd1* knockout mice and controls fig.39,A). Also, in direct comparison of knockout and control pancreata from these ages, no gross morphological changes were observed (Fig.39B). Here spleen was used as a size standard.

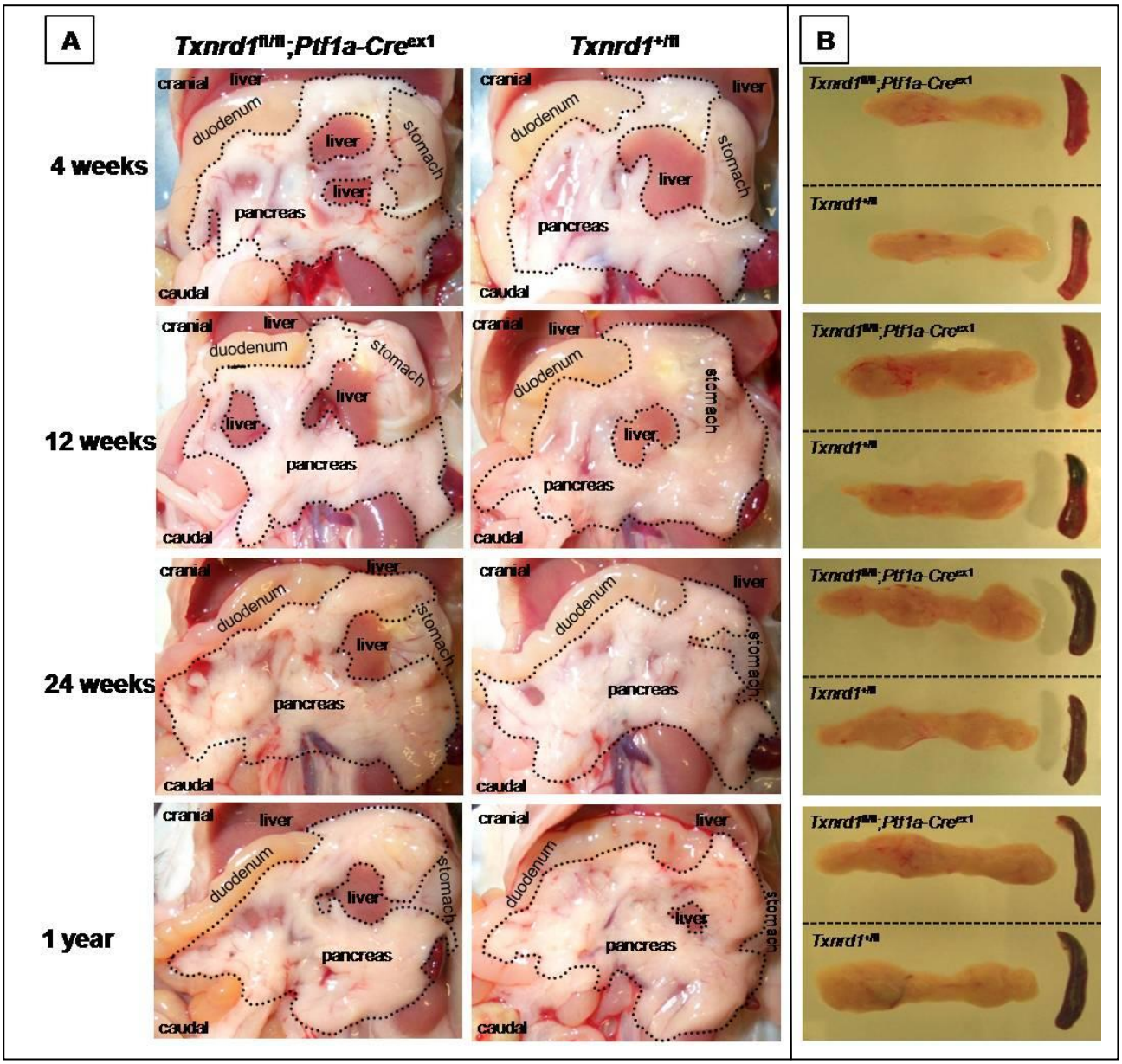

Fig.39: Gross morphological analysis of *Txnrd1* knockout and control mice. (A) Morphological situation of the abdomen *in situ* in knockout (*Txnrd1*$^{fl/fl}$;*Ptf1a-Cre*^{ex1}) and control (*Txnrd1*$^{+/fl}$) mice. (B) Direct comparison of knockout and control pancreata with spleen as a size standard. Gross morphological changes were not observed in *Txnrd1* knockout mice.

The relative pancreatic weight was determined as a parameter for pancreatic integrity during an observation period of one year with samples from mice at an age of four, twelve and twenty-four weeks and one year. There was no significant difference in comparison of *Txnrd1* knockout and control mice (Fig.40).

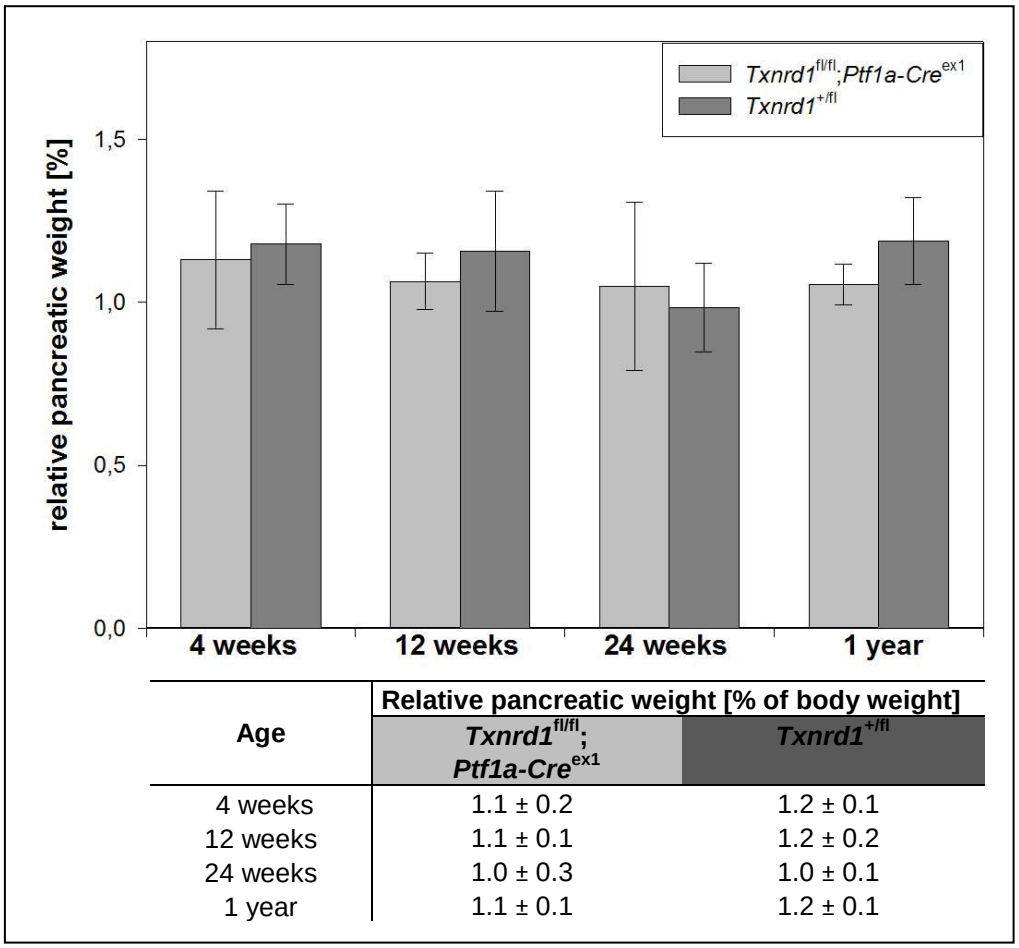

Age	Relative pancreatic weight [% of body weight]	
	***Txnrd1*$^{fl/fl}$; *Ptf1a-Cre*^{ex1}**	***Txnrd1*$^{+/fl}$**
4 weeks	1.1 ± 0.2	1.2 ± 0.1
12 weeks	1.1 ± 0.1	1.2 ± 0.2
24 weeks	1.0 ± 0.3	1.0 ± 0.1
1 year	1.1 ± 0.1	1.2 ± 0.1

Fig.40: Relative pancreatic weight in *Txnrd1* knockout and control mice. The relative pancreatic weight of *Txnrd1* knockout (*Txnrd1*$^{fl/fl}$;*Ptf1a-Cre*^{ex1}) or control mice (*Txnrd1*$^{+/fl}$) was not influenced by the genotype. Data are expressed as means ± standard deviation in % of body weight.

3.3.4 Pancreatic tissue morphology

Histological morphology of the pancreas was analyzed at the age of four, twelve and twenty-four weeks and one year. The same mice as in 3.3.3 were used. Histological samples were prepared and sections were stained with H & E and examined for histological changes. Figure 41 depicts pancreatic section of analyzed ages. In both, knockout and control mice, the exocrine pancreas with the acinar and ductal cell compartments as well as the endocrine part with the islets of Langerhans was without pathological findings throughout the examined period of one year.

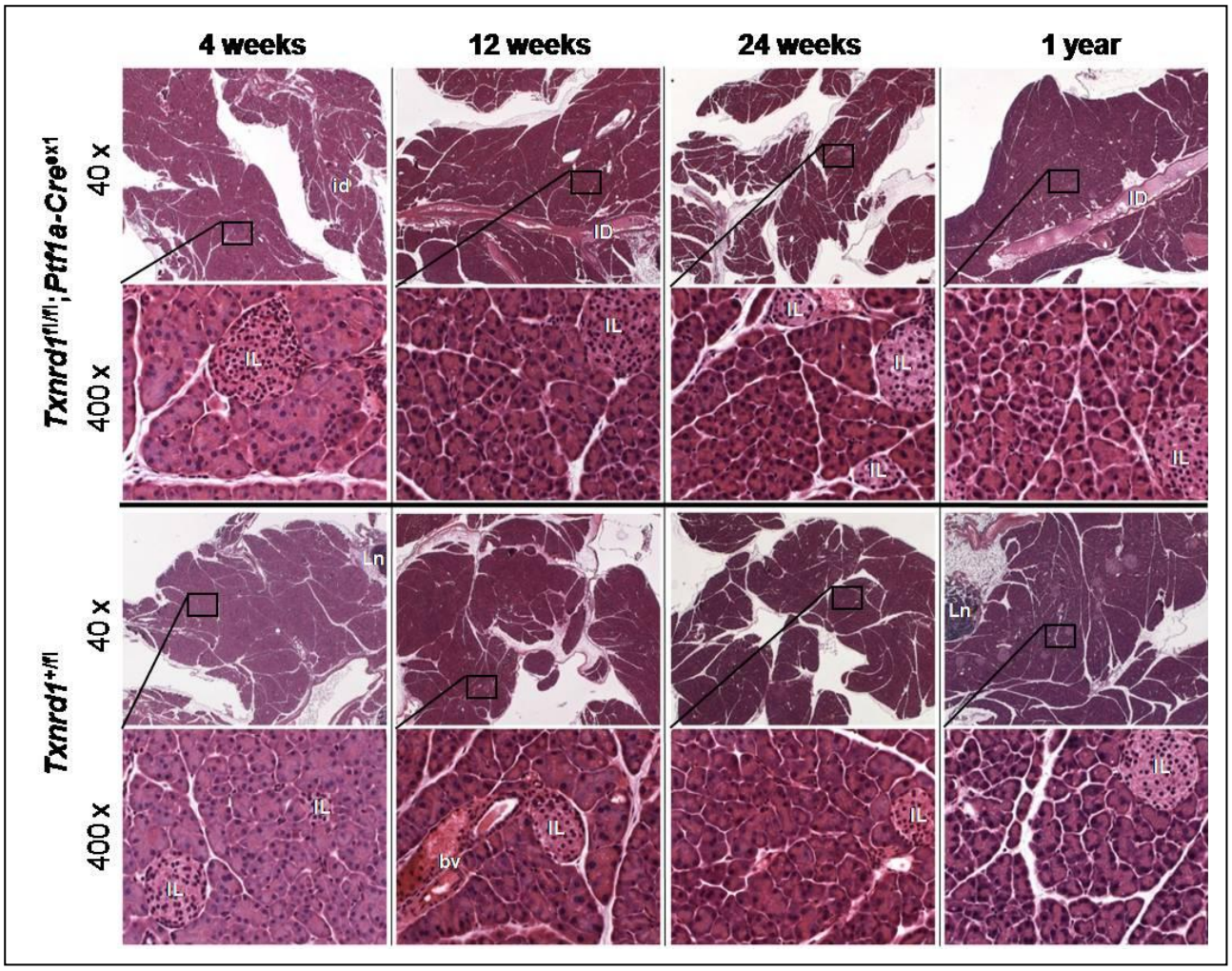

Fig.41: Pancreatic tissue morphology of *Txnrd1* knockout and control mice. *Txnrd1* knockout mice (*Txnrd1*$^{fl/fl}$;*Ptf1a-Cre*^{ex1}) (upper two rows) did not show differences in histological analysis in direct comparison to control mice (*Txnrd1*$^{+/fl}$) (lower two rows). The knockout as well as the control pancreata were characterized by the full development of the endocrine and exocrine pancreas without pathological changes during the observation period of one year. Rectangles indicate the areas chosen for higher magnifications. (bv = blood vessels, ID = interlobular duct, id = intralobular duct, IL = islets of Langerhans, Ln = lymph node)

3.3.5 Characterisation of exocrine functional parameters

The exocrine pancreas was characterised by histological methods and by analysis of enzymatic parameters in serum samples. Also a lipid absorption test was performed.

Histological, the same samples as described in 3.3.3 were used for immunohistological analysis. Acinar cells were immunohistochemically stained with rabbit anti-α-amylase as.

At all analyzed stages the exocrine pancreas stained positive for α-amylase and differences of *Txnrd1* knockout and control mice have not been observed (Fig.42).

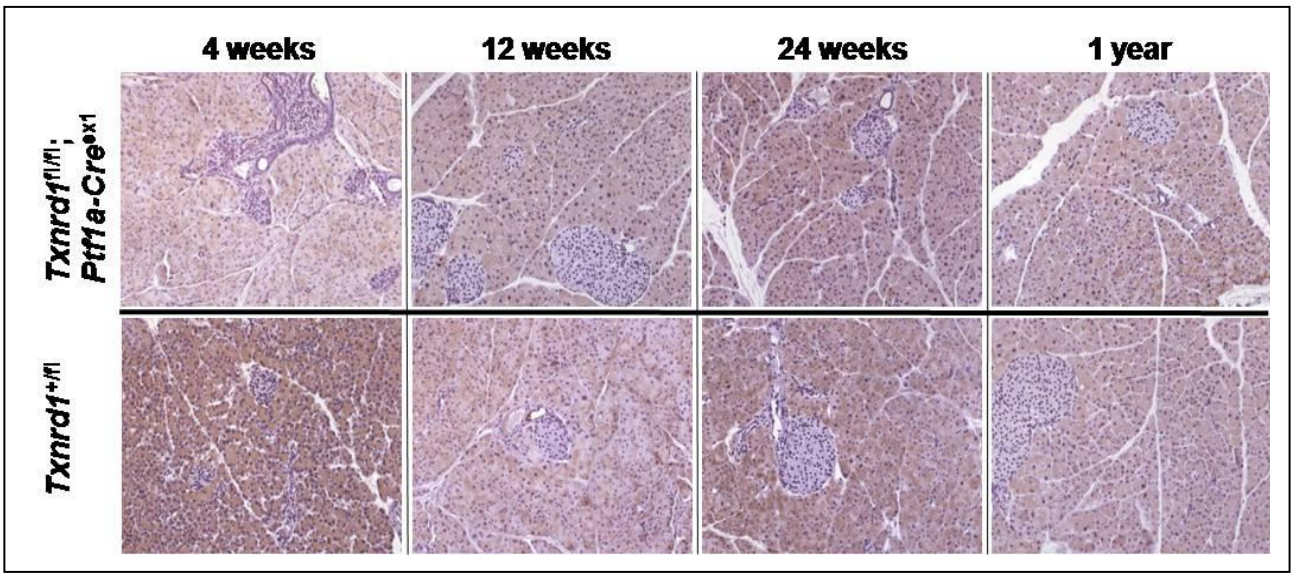

Fig.42: Amylase expression in the pancreas of *Txnrd1* knockout and control mice. At all stages examined the acinar cells of the pancreas were positively stained for α-amylase with similar expression in knockout (*Txnrd1*$^{fl/fl}$;*Ptf1a-Cre*^{ex1}) and control (*Txnrd1*$^{+/fl}$) mice. (Rabbit anti-α-amylase; 200x)

The ultrastructure of the acinar cells of one-year-old *Txnrd1* knockout and control mice was analyzed by transmission electron microscopy (TEM). In figure 43,A and E H&E stained paraffin sections are depicted for an overview. Fig.43 B and F show toluidine blue stained plastic embedded semi thin cuttings of the analyzed regions by TEM. Already in these stainings, in the *Txnrd1* knockout mice, a mosaic of light and dark blue cells was observed, which were not seen in control pancreata, which showed a homogenous picture of the acinar cells. This mosaic-like picture of the acinar cells was also seen in ultrastucture analysis, where differences in electron density between adjacent cells were observed (Fig.43,C). This difference was absent in control cells (Fig.43,G). In a higher magnification in the bright cells a dilated rough endoplasmic reticulum (rER) was observed, characterized by enlarged cisternal lumina between the rER membranes (Fig.43,D). In the control mice such alterations were not observed (Fig.43,H).

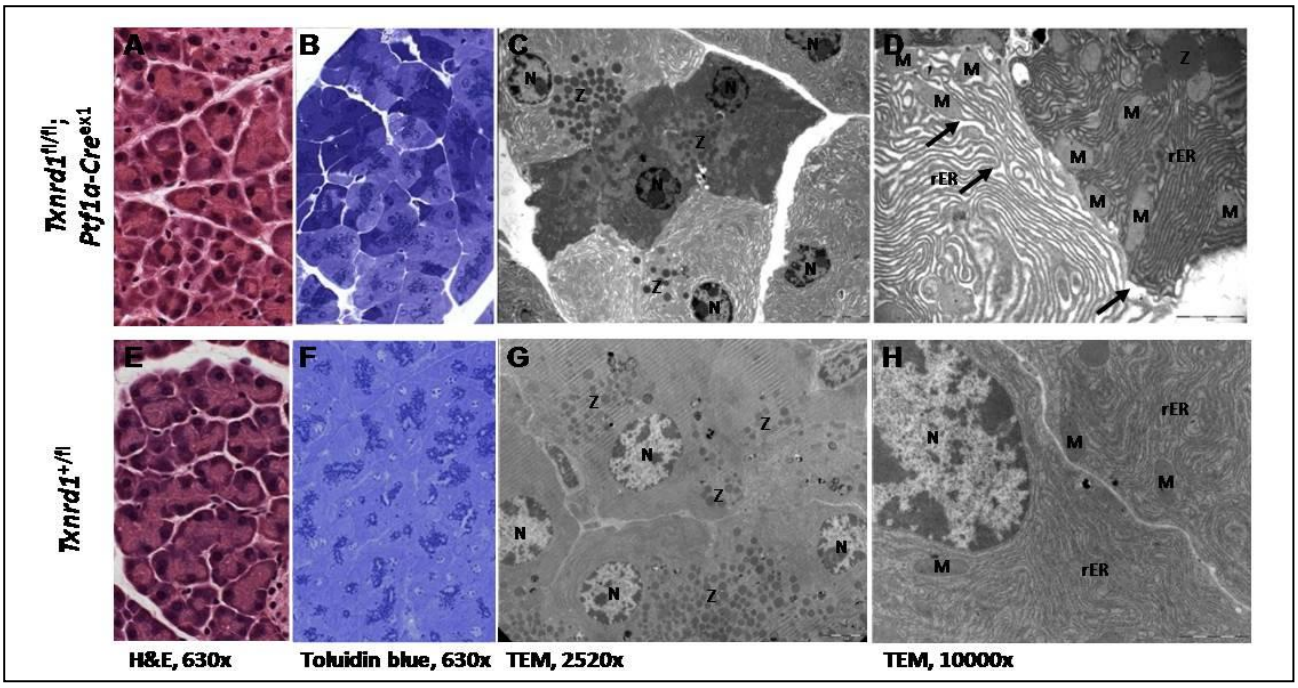

Fig.43: Ultrastructural analysis of *Txnrd1* knockout and control pancreata. (A,E) H & E stained paraffin-embedded knockout and control tissue. (B,F) Toluidine blue stained plastic embedded semi thin slices. (C,G) Acinus cells of 250x magnification and at 10000x magnification (D,H). Note the electron dense and electron light cells in C and D and the dilated rough endoplasmic reticulum. (L = lumen of an acinus, N = nucleus, M = mitochondria, cristae type, rER = rough endoplasmic reticulum, Z = zymogen granules)

The rough endoplasmic reticulum was also analyzed in higher magnification by TEM. Figure 44 depicts representative examples of rER of *Txnrd1* knockout and control mice. In the control mice, the rER showed the typical picture of an ergastoplasm, with stratified rER (arrowhead) and narrow cisternal lumen (asterix). The rER in acinar cells of knockout mice showed a dilated rER in the brighter cells with extended cisternal lumen (Fig.44 cell 1, arrows). On the left side of cell 1 a nearly normal rER was seen, whereas on the right side the rER seems to lose its membrane. This picture also was observed in the electron dense cells (Fig.44 cell 2), where on the right side a normal rER, and on the left side a total loss of the rER structure was seen.

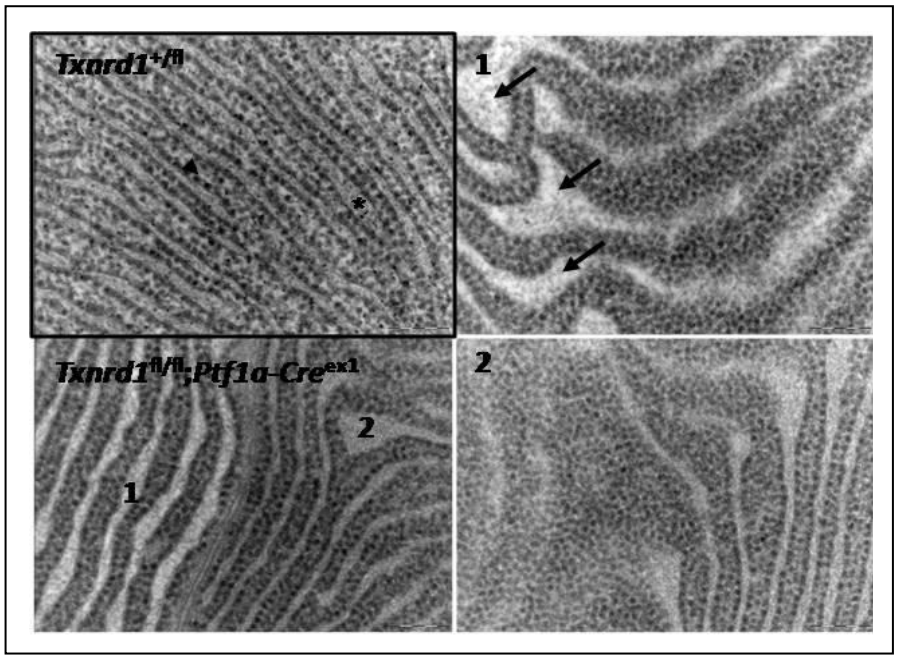

Fig.44: Alterations in the rough endoplasmic reticulum. Rough endoplasmic reticulum of control (upper left, black frame) with typical ergastoplasma and of knockout pancreatic acinar cells with different types of alterations. (1) Bright cell with dilated rER (arrow). (2) Electron dense cell with total loss of structure of the rER. (TEM, 80000x).

Whether the ultrastructure alterations had an effect on the integrity of the acinus cells was investigated by analyzing blood serum samples for the pancreas-specific parameters α-amylase and lipase. Also a lipid absorption test was performed.

For the serum analysis the ages four, twelve and twenty-four weeks and one year were chosen. The level of amylase (Fig.45,A) in four weeks old *Txnrd1* knockout mice was significantly lower than in the control mice ($p < 0.01$, student t-test). Also in the other analysed ages amylase was slightly decreased in the knockout mice, although this was not statistically significant. A similar picture could be seen for levels of serum lipase (Fig.45,B). Lipase was also significantly decreased in *Txnrd1* knockout mice at an age of 4 weeks compared to the controls ($p < 0.001$, student t-test). Also at an age of twelve weeks knockout mice showed reduced serum lipase levels compared to their controls, but this was not statistically significant. At an age of twenty-four weeks there was nearly no difference between knockout and control mice, whereas at an age of one year the serum lipase level was slightly increased in the knockout mice compared to controls. Taken the lipase levels together, a continuously increase could be observed in the knockout mice.

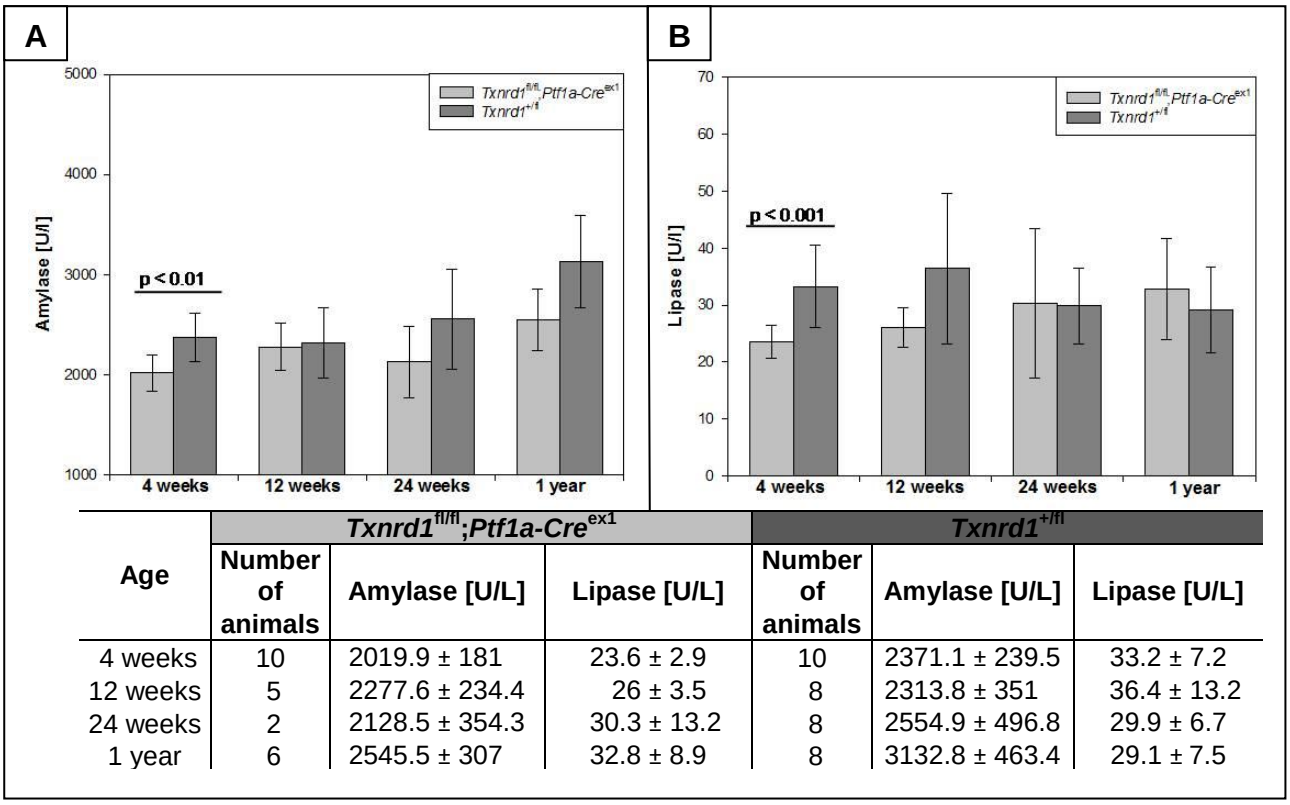

Age	*Txnrd1*$^{fl/fl}$;*Ptf1a-Cre*^{ex1}			*Txnrd1*$^{+/fl}$		
	Number of animals	**Amylase [U/L]**	**Lipase [U/L]**	**Number of animals**	**Amylase [U/L]**	**Lipase [U/L]**
4 weeks	10	2019.9 ± 181	23.6 ± 2.9	10	2371.1 ± 239.5	33.2 ± 7.2
12 weeks	5	2277.6 ± 234.4	26 ± 3.5	8	2313.8 ± 351	36.4 ± 13.2
24 weeks	2	2128.5 ± 354.3	30.3 ± 13.2	8	2554.9 ± 496.8	29.9 ± 6.7
1 year	6	2545.5 ± 307	32.8 ± 8.9	8	3132.8 ± 463.4	29.1 ± 7.5

Fig.45: Serum amylase and lipase levels in *Txnrd1* knockout and control mice. (A) Blood serum amylase levels. (B) Blood serum lipase levels. Serum amylase and lipase were significantly reduced in knockouts at 4 weeks of age. Data are expressed as means ± standard deviation.

Pancreatic maldigestion is characterised by an increased presence of lipids in the faeces, which is called steatorrhea. To detect triglycerides, a lipid absorption test was performed. To quantify this test, in each animal lipid globules were counted in 20 fields of vision. Figure 46,A depicts samples of stool pellets of *Txnrd1* knockout and control mice, which did not differ in colour or consistency. Representative examples of the stool smears, stained with Oil Red O, are depicted in figure 46,B. The stool smears did not differ in the number of fat droplets (Fig.46,B). Figure 46,C depicts the results of quantification of six *Txnrd1* knockout and seven control mice. The data endorsed, that lipid digestion was not different between knockout and control mice.

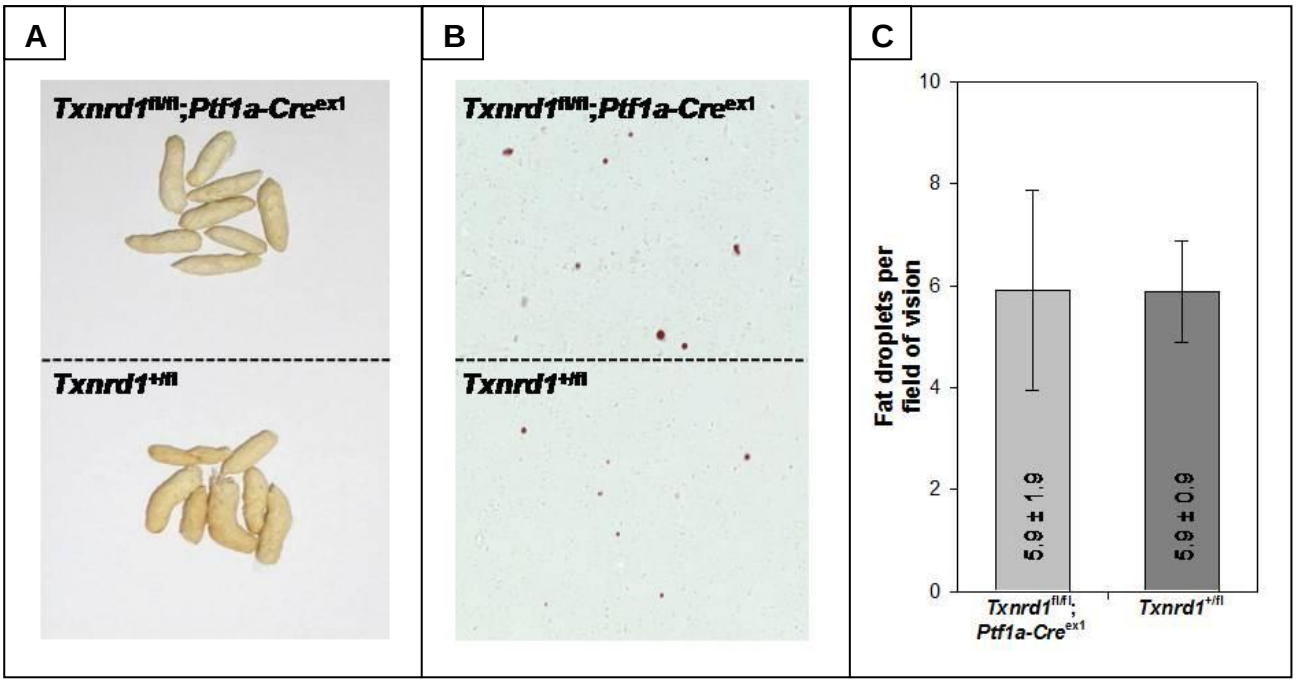

Fig.46: Lipid absorption in *Txnrd1* knockout and control mice. (A) Faecal pellets of knockout (*Txnrd1*$^{fl/fl}$;*Ptf1a-Cre*^{ex1}) and control mice (*Txnrd1*$^{+/fl}$). (B) Representative Oil Red O stained stool smears of knockout and control mice (1000x). (C) Quantification of Oil red O positive lipid droplets. *Txnrd1* knockout mice showed normal lipid digestion. Data are expressed as means ± standard deviation.

3.3.6 Characterisation of endocrine functional parameters

The endocrine pancreas, consisting of the islets of Langerhans, was characterized histological and its metabolic function was tested by observation of blood glucose level and with a glucose tolerance test.

The same set of samples as described in 3.3.3 was analysed. Immunohistochemical staining with guinea pig anti-insulin (Fig.47,A) and rabbit anti-glucagon (Fig.47,B) were done. The β-cells of the islets of Langerhans were positively stained for insulin in the knockout as well as in the control mice. There was no difference observed in comparison of genotype or age (Fig.47,A). Also, there was no difference evident for the glucagon producing α-cells which were stained with the rabbit anti-glucagon antibody (Fig.47,B). Both proteins were produced in the knockout and there were also neither difference in location nor in the quantity of producing cells.

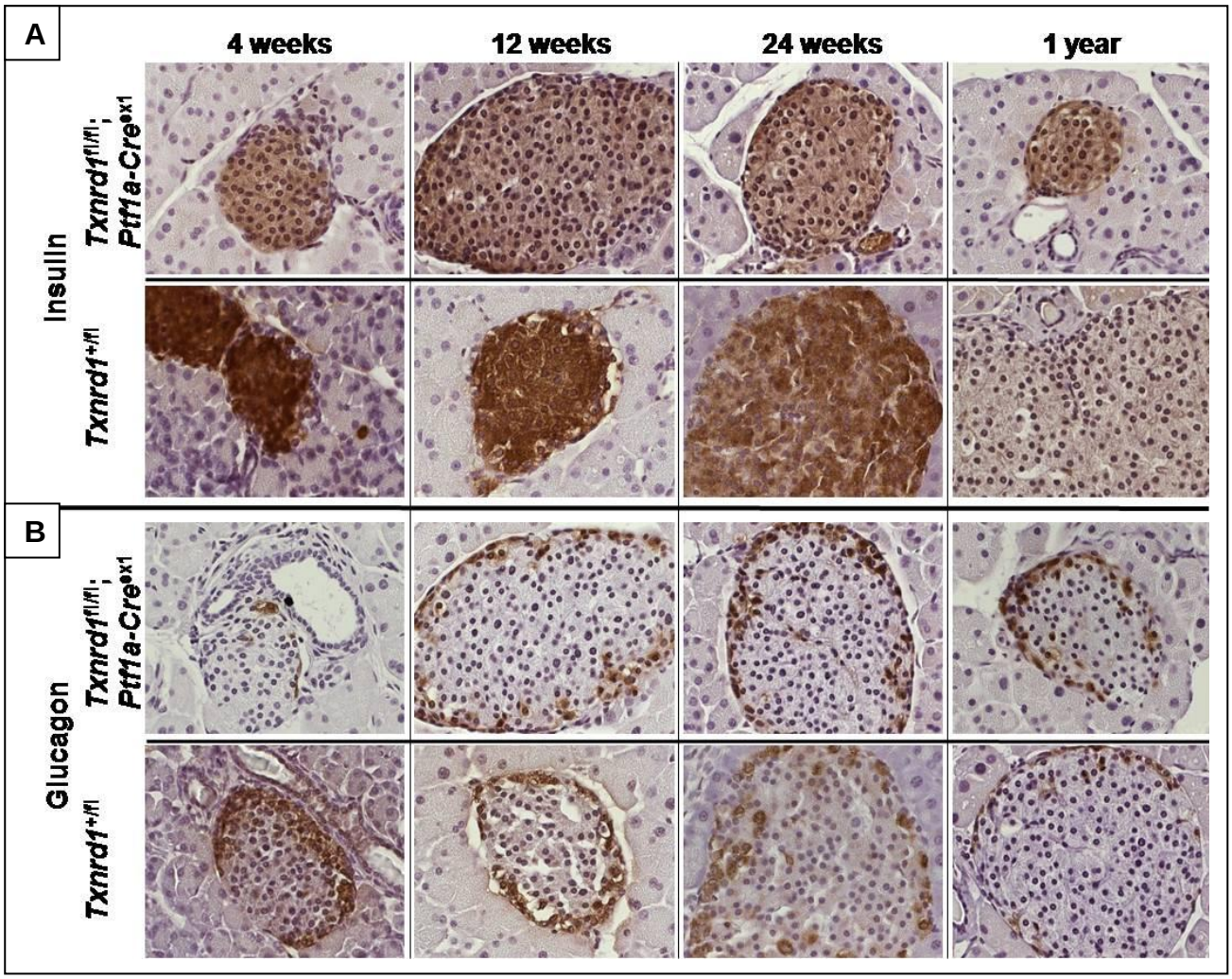

Fig.47: Immunohistochemical analyses of the endocrine pancreas *Txnrd1* knockout and control mice. (A) Pancreatic β-cells stained with a guinea pig anti-insulin antibody in knockout (upper row) and control (lower row) islet of Langerhans (630x). (B) Pancreatic α-cells stained with a rabbit anti-glucagon antibody in knockout (upper row) and control (lower row) islet of Langerhans (630x). Expression of insulin and glucagon was not influenced by the genotype. Differences in staining intensity are due to individual reactions of samples on the staining solution and do not correspond to stronger expression levels.

The physiological function of the islets of Langerhans was tracked by measuring blood glucose levels every two weeks over one year after fasting overnight. *Txnrd1* knockout as well as control mice (each n = 8) had a blood glucose level of around 60 mg/dL which is within the physiological range in C57BL/6 mice of up to 120 mg/dL (Klempt *et al*., 2006) (Fig.48).

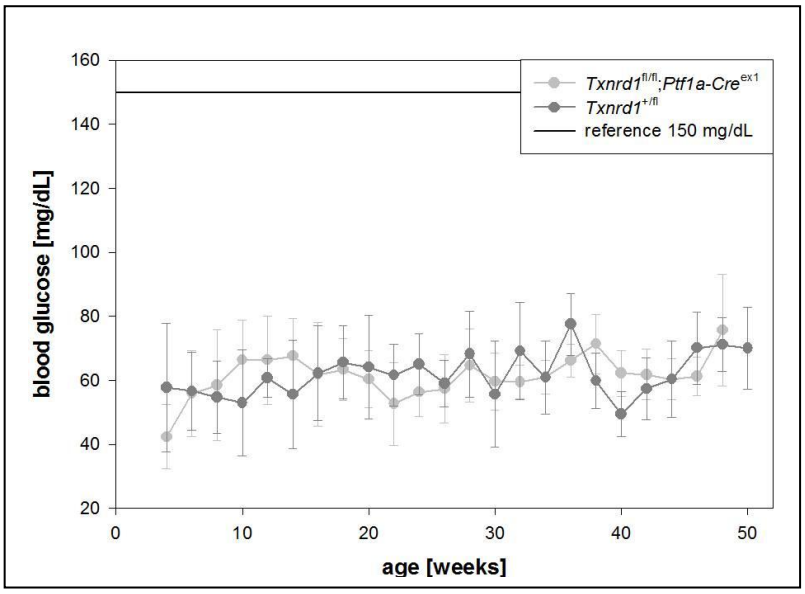

Fig.48: Blood glucose levels in *Txnrd1* knockout and control mice. Glucose levels were obtained after fasting the mice over night. The blood glucose levels in knockout and control mice remained considerably below the critical level for diabetic blood glucose (150 µg/dL).

An intraperitoneal glucose tolerance test (IP-GTT) was performed to determine how quickly glucose was cleared from the blood as a parameter of the metabolical function of the endocrine pancreas. Figure 49 depicts the results: on the left both sexes together and on the right splitted in males and females. For the test, one-year-old mice were used (*Txnrd1*$^{fl/fl}$;*Ptf1a-Cre*^{ex1}: males n = 3, females n = 2, *Txnrd1*$^{+/fl}$: males n = 3, females n = 4). The blood glucose levels were measured directly before and after injection of glucose and then 15, 30, 60, 90 and 120 minutes after injection. The blood glucose levels increased faster in the knockout mice and to a higher level after injection in comparison to controls. The glucose was cleared from blood slower in knockout mice than in the control mice. There was no difference between males and females. The results highlighted an impaired glucose clearance in the knockout mice.

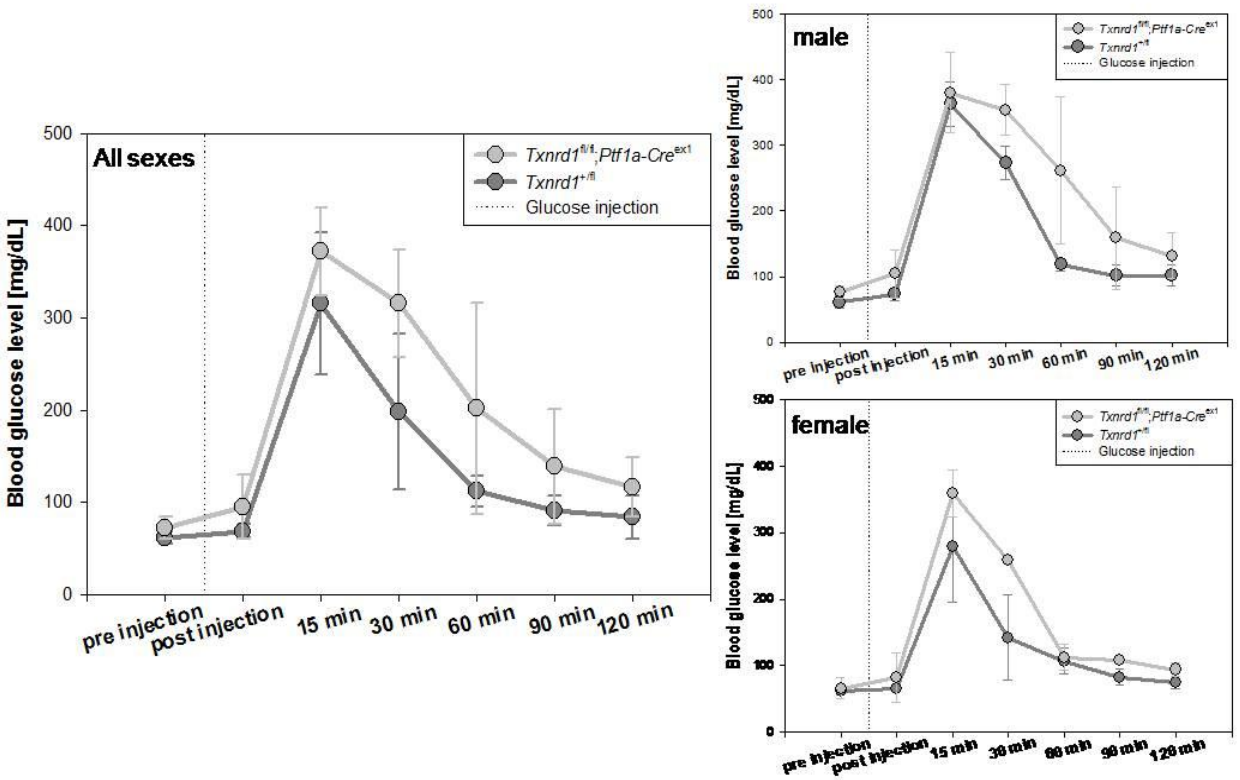

	***Txnrd1*$^{fl/fl}$;*Ptf1a-Cre*^{ex1} IP-GTT blood glucose levels [mg/dL]**						
	pre injection	**post injection**	**15 min**	**30 min**	**60 min**	**90 min**	**120 min**
both sexes	72.6 ± 11.7	95 ± 34.7	372 ± 48	315.6 ± 58.5	201.8 ± 114.2	138.8 ± 61.8	116.6 ± 32.6
males	77 ± 8.9	104 ± 37.4	380 ± 61.1	353.3 ± 38.7	261.3 ± 112.2	159 ± 78.1	131.7 ± 35
females	66 ± 15.6	81.5 ± 37.5	360 ± 35.4	259 ± 1.4	112.5 ± 19.1	108.5 ± 2.1	94 ± 9.9

	***Txnrd1*$^{+/fl}$ IP-GTT blood glucose levels [mg/dL]**						
	pre injection	**post injection**	**15 min**	**30 min**	**60 min**	**90 min**	**120 min**
both sexes	61.3 ± 6.8	69 ± 7.8	315.4 ± 77.1	198.3 ± 84.5	112 ± 16.4	90.9 ± 16.3	83.9 ± 23
males	61.3 ± 10	73 ± 9.8	363.3 ± 33.7	273 ± 26.1	118.7 ± 9.6	101.7 ± 16	96.3 ± 32.6
females	61.3 ± 4.9	66 ± 5.4	279.5 ± 84.4	142.3 ± 63.8	107 ± 19.9	82.8 ± 12.4	74.5 ± 8.8

Fig.49: Intraperitoneal glucose tolerance test in *Txnrd1* knockout and control mice. 2 mg dextrose per g body weight was injected and glucose levels were measured at the time points indicated. Both sexes together (left side) or separately (right side) were analysed. Blood glucose rose faster and to a higher level in knockout mice (*Txnrd1*$^{fl/fl}$;*Ptf1a-Cre*^{ex1}) in comparison to controls (*Txnrd1*$^{+/fl}$). Also glucose was cleared slower from blood in knockout mice than in controls. Data are expressed in means ± standard deviation. (Dotted line = dextrose injection)

3.3.7 Monitoring of other target organs of *Cre*-expression under the control of the *Ptf1a*-promotor

The promoter *Ptf1a* directs *Cre*-expression also to GABAergic neuronal cells of the cerebellum, which are the purkinje cells, as well as cells of the neuroretina of the eye (Nakhai *et al*., 2007; Hoshino *et al*., 2005). To investigate potential effects in *Txnrd1* knockout mice in these tissues, an eye screen was performed and the cerebellum was examined by behavioural and functional tests and histological methods.

The routine eye screen of the German Mouse Clinic showed that one-year-old *Txnrd1* knockout mice had full vision in comparison to their age matched controls. Only some age related malfunctions in both genotypes were found.

Observation of the behaviour did not suggest of a defect in the cerebellum of one-year-old knockout mice. In addition, the histological morphology did not show any alterations in knockout mice. Figure 50 depicts representative examples of knockout and control cerebellum stained with H&E and an immunohistchemical staining of purkinje cells, which showed no alterations in knockout mice.

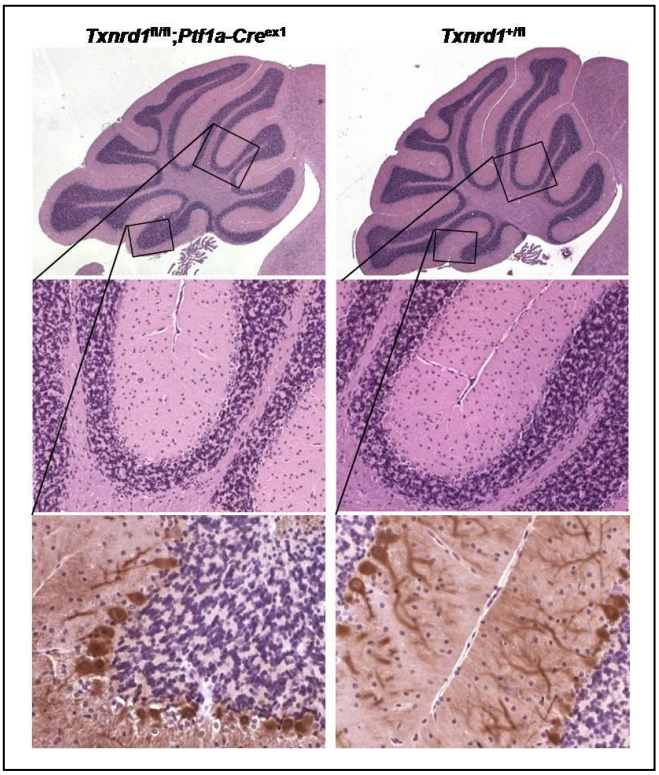

Fig.50: Cerebellar morphology of *Txnrd1* knockout and control mice. H & E stained paraffin sections of low magnification for overview (upper panel, 40x). Magnifications from the upper panel are shown in the middle panel (200x). The lower panel shows immunohistochemical staining of Purkinje cells with an rabbit anti- calbindin antibody (400x). Rectangles indicate the areas chosen for higher magnifications. No alteration in the knockout (*Txnrd1*$^{fl/fl}$;*Ptf1a-Cre*^{ex1}) cerebellum has been present.

3.4 Pancreas-specific knockout of *Txnrd2*

The results presented in 3.2 demonstrated a very high thioredoxin reductase activity in the mitochondria of pancreatic cells. Interestingly, in contrast to all other organs studied, the activity of thioredoxin reductase in mitochondria even increased under selenium deficient conditions. Homozygous knockout mice for mitochondrial thioredoxin reductase (*Txnrd2*) died around embryonic day (E) 13.5 (Conrad *et al*., 2004). In order to study pancreatic *Txnrd2* knockout, the *Cre-/loxP* technology was used to bypass embryonic lethality. To clarify the role of *Txnrd2* in the pancreas, the floxed conditional knockout mouse strain was crossed with a Cre-recombinase knockin mouse strain under the control of the *Ptf1a-p48* promoter to generate pancreas-specific *Txnrd2* knockout mice, which then were examined in this part of the study. Below, the designation "*Txnrd2* knockout mouse" was used for the genotype *Txnrd2*$^{fl/fl}$;*Ptf1a-Cre*^{ex1}, whereas "*Txnrd2* control" for the genotype *Txnrd2*$^{+/fl}$. In case other genotypes were used, they were indicated separately.

3.4.1 Validation of pancreas-specific *Txnrd2* knockout

Pancreas-specific *Cre*-expression was demonstrated by crossing the *Txnrd2* mouse strain with the ROSA26 Cre reporter mouse strain (R26R) (Soriano, 1999). The validation of the conditional knockout was done on three levels: genomic DNA, mRNA expression and enzyme activity.

To monitor pancreas-specific *Cre*-expression, the *Txnrd2* mouse strain was crossed with the Cre reporter mouse strain R26R (Soriano, 1999). Three-weeks-old *Txnrd2* knockout (*Txnrd2*$^{fl/fl}$;*Ptf1a-Cre*^{ex1};R26R$^{\Delta/+}$) and control (*Txnrd2*$^{+/fl}$;R26R$^{\Delta/+}$) mice from this breed were sacrificed and the pancreas as well as a part of the duodenum and the spleen were prepared. The whole organs as well as cryosections were stained for β-galactosidase activity. Figure 51 depicts representative examples of this staining. The pancreas of the knockout mice stained blue for β-galactosidase activity indicating positive *Cre*-expression, whereas the duodenum and the spleen remained unstained (Fig.51,A). The pancreas, duodenum and spleen of the control mice also remained unstained (Fig.51,B). The restricted tissue specific activity of β-galactosidase further became apparent in the cryosections of pancreatic tissue. The pancreatic tissue stained positively for β-galactosidase activity in the knockout pancreas, whereas the intra-pancreatic lymph node

(Ln) remained unstained (Fig.51,C). Also, the pancreatic tissue of control mice did not show a blue staining (Fig.51,D). These results demonstrated a restricted pancreas-specific *Cre*-expression in *Txnrd2* knockout mice.

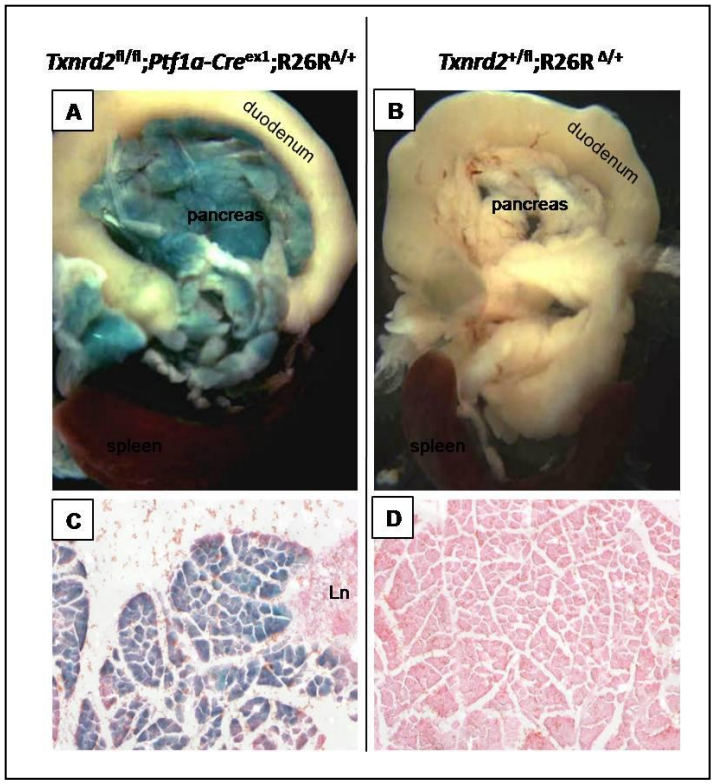

Fig.51: Cre-recombinase expression in pancreatic *Txnrd2* knockout tissue. (A,B) Whole mount β-galactosidase staining of knockout and control pancreata with duodenum and spleen. (C,D) β-galactosidase staining of cryosections of the pancreas (100x). Only the pancreas of *Txnrd2* knockout mice (*Txnrd2*$^{fl/fl}$;*Ptf1a-Cre*^{ex1};R26R$^{\Delta/+}$) stained blue for β-galactosidase activity as a result of *Cre*-expression. The pancreas of *Txnrd2* control mice (*Txnrd2*$^{+/fl}$) remained unstained. (Ln = lymph node).

Deletion of exon 15 to 18 of the mitochondrial thioredoxin reductase gene in the knockout pancreas was validated on genomic DNA-level by PCR. Therefore DNA from the pancreas and the tail biopsy was isolated. The tail DNA was chosen as a representative for non-pancreatic tissues. Floxed alleles were validated with a primer pair (TR3flox1 / TR3flox2) amplifying a 181 bp long template spanning the *loxP* site upstream exon 15 (Fig.52,B). In the wild type situation a 133 bp long template was amplified with the same primer pair (Fig.52,B). In the *Txnrd2* knockout mice both alleles contained *loxP* sites upstream exon 15 and downstream exon 18, whereas *Txnrd2* control mice contained one floxed and one wild type allele (Fig.52,A; floxed allele). Another primer pair (TR3Del1 / TR3Del2) was used to confirm the excision of exon 15 to 18 in the pancreas of knockout mice. This

primer pair amplified a 500 bp long template only in the knockout mice. As depicted in figure 52,A (deleted allele), these alleles were deleted only in the pancreas, but not in the tail or in the control mice. Cre-recombinase was present only in the knockout mice, but not in the controls.

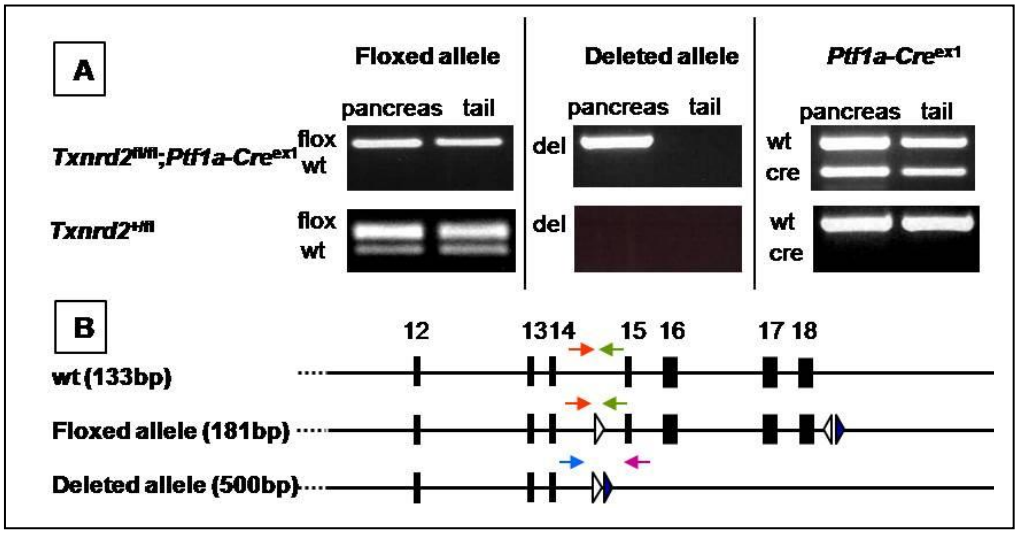

Fig.52: *Txnrd2* knockout validation on DNA level. The conditional knockout was first verified on DNA level by PCR with specific primer pairs. (A) PCR results for the different Txnrd2 alleles in pancreas and tail. *Txnrd2* knockout mice showed two floxed *Txnrd2* alleles (floxed allele) together with one *Ptf1a-Cre* allele (*Ptf1a-Cre*^{ex1}). Excision of *Txnrd2* exon 15 to 18 was restricted to the pancreas (deleted allele). *Txnrd2* control mice showed one floxed and one wt *Txnrd2* allele (floxed allele) together with a wt allele in the *Ptf1a* locus (*Ptf1a-Cre*^{ex1}) and no excision of exon 15 to 18 (deleted allele). (B) Primer binding sites (arrows). Only in the knockout mice (*Txnrd2*$^{fl/fl}$;*Ptf1a-Cre*^{ex1}) a template spanning the deleted exons 15 to 18 in the pancreas could be amplified, but not in the tail or control mice (*Txnrd2*$^{+/fl}$).

To validate the expression of mitochondrial thioredoxin reductase on mRNA-level, a semiquantitative RT-PCR was performed. Therefore RNA was isolated from the pancreas as target organ and from liver as a reference organ, each from *Txnrd2* knockout and *Txnrd2* control mice (each genotype n = 3). Oligo(dT) primer were used to transcribe mRNA into cDNA. The housekeeping genes *aldolase* and *GAPDH* were used as standards (Fig.53). The primer pair TR2 E6 / E10 bound upstream of exon 15 was used to amplify a region not affected by the knockout, whereas TR2 E15 / E18 synthesized a template spanning the knockout target region. Upstream the knockout region, mRNA of a truncated form of *Txnrd2* was slightly reduced in the knockout pancreas in comparison to control. The liver remained unaffected (Fig. 53). Expression of mRNA of exon 15 to 18 was

conspicuously reduced in the pancreas of knockout in comparison to control mice (Fig. 53). Again, the liver remained unaffected.

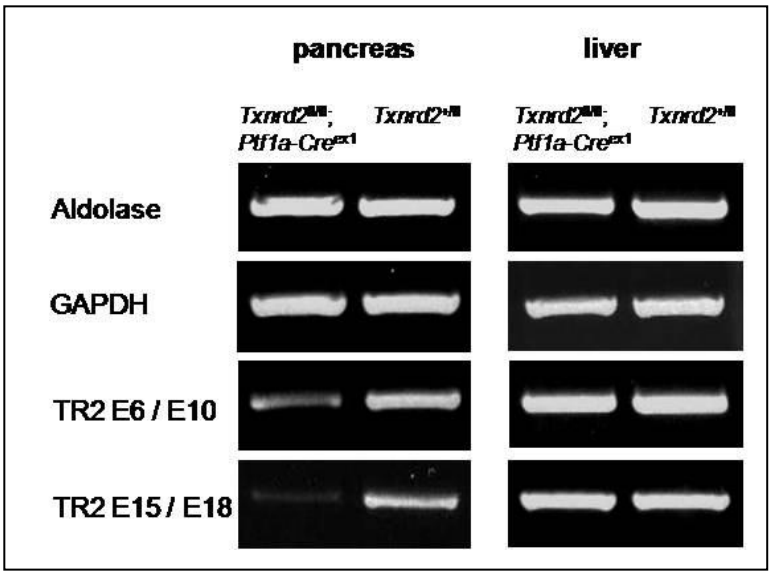

Fig.53: *Txnrd2* knockout validation on mRNA level. *Txnrd2* mRNA containing the deleted region was strongly reduced, truncated mRNAs detected by primers TR2 E6 / E10 was moderately reduced and *Txnrd2* expression in the liver was not affected in knockout mice.

Enzymatic activity of TXNRD2 in the pancreas as target organ and in the liver and kidney as reference organs (all n = 5) from three weeks old *Txnrd2* knockout and control mice was measured by a colorimetric enzyme activity assay. In the pancreas of knockout mice, enzymatic activity was significantly reduced compared to the controls ($p < 0.01$, student-t-test) (Fig.54). In the liver and kidney, the enzymatic activity was higher in the knockout mice than in the controls, which was not statistically significant.

Taken together the results of the validation experiments showed an effective and pancreas- specific knockout of mitochondrial thioredoxin reductase.

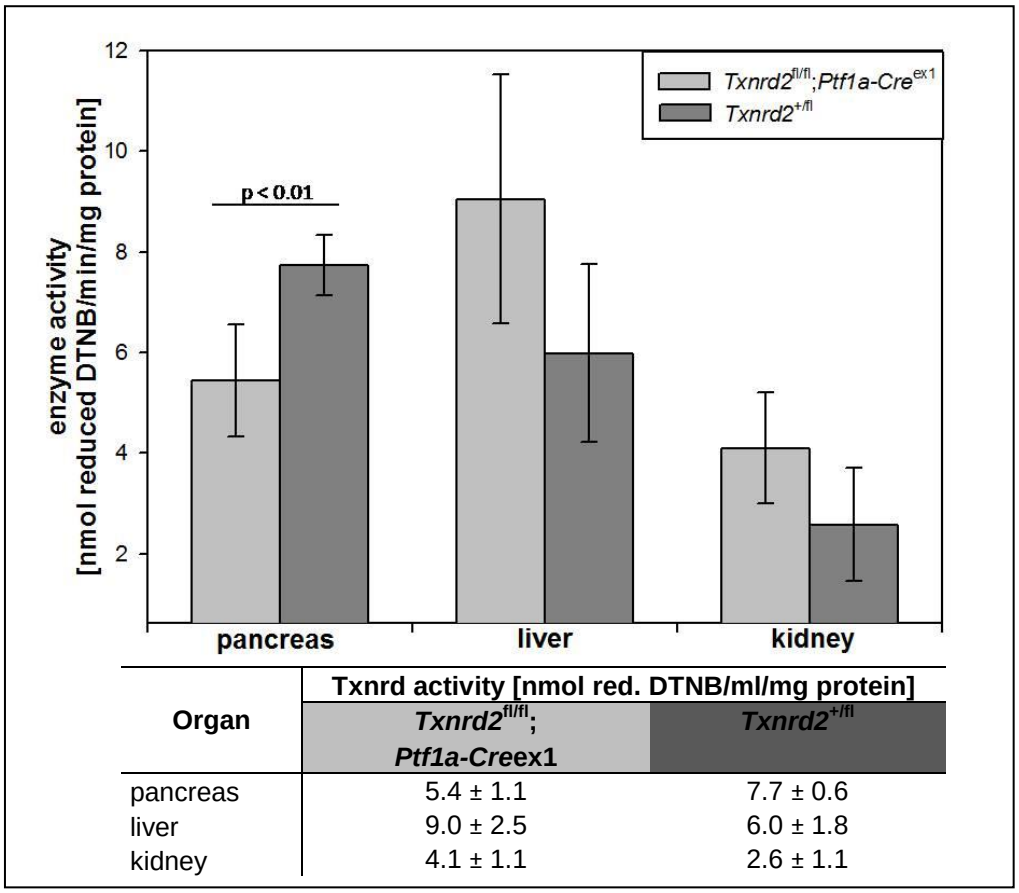

Organ	Txnrd activity [nmol red. DTNB/ml/mg protein]	
	***Txnrd2*$^{fl/fl}$; *Ptf1a-Cre*ex1**	***Txnrd2*$^{+/fl}$**
pancreas	5.4 ± 1.1	7.7 ± 0.6
liver	9.0 ± 2.5	6.0 ± 1.8
kidney	4.1 ± 1.1	2.6 ± 1.1

Fig.54: TXNRD2 activity in *Txnrd2* knockout mice. Enzymatic activity of thioredoxin reductase in the mitochondrial protein fraction of the pancreas of knockout mice (*Txnrd2*$^{fl/fl}$;*Ptf1a-Cre*^{ex1}) was significantly reduced in comparison to control mice (*Txnrd2*$^{+/fl}$). Data are expressed as means ± standard deviation.

3.4.2 General observations

Both, pancreas-specific *Txnrd2* knockout mice and control mice showed similar appearance and behaviour over an observation period of one year. They were also fertile.

Effects of the knockout on digestion, growth or metabolism, was tested by weighing mice every two weeks after fasting over night over an observation period of one year. The body weight development of the mice did not differ significantly (Fig.55). Even when sexes were analyzed separately, there were no significantly differences between mice with pancreas-specific *Txnrd2* knockout and controls (Fig.55).

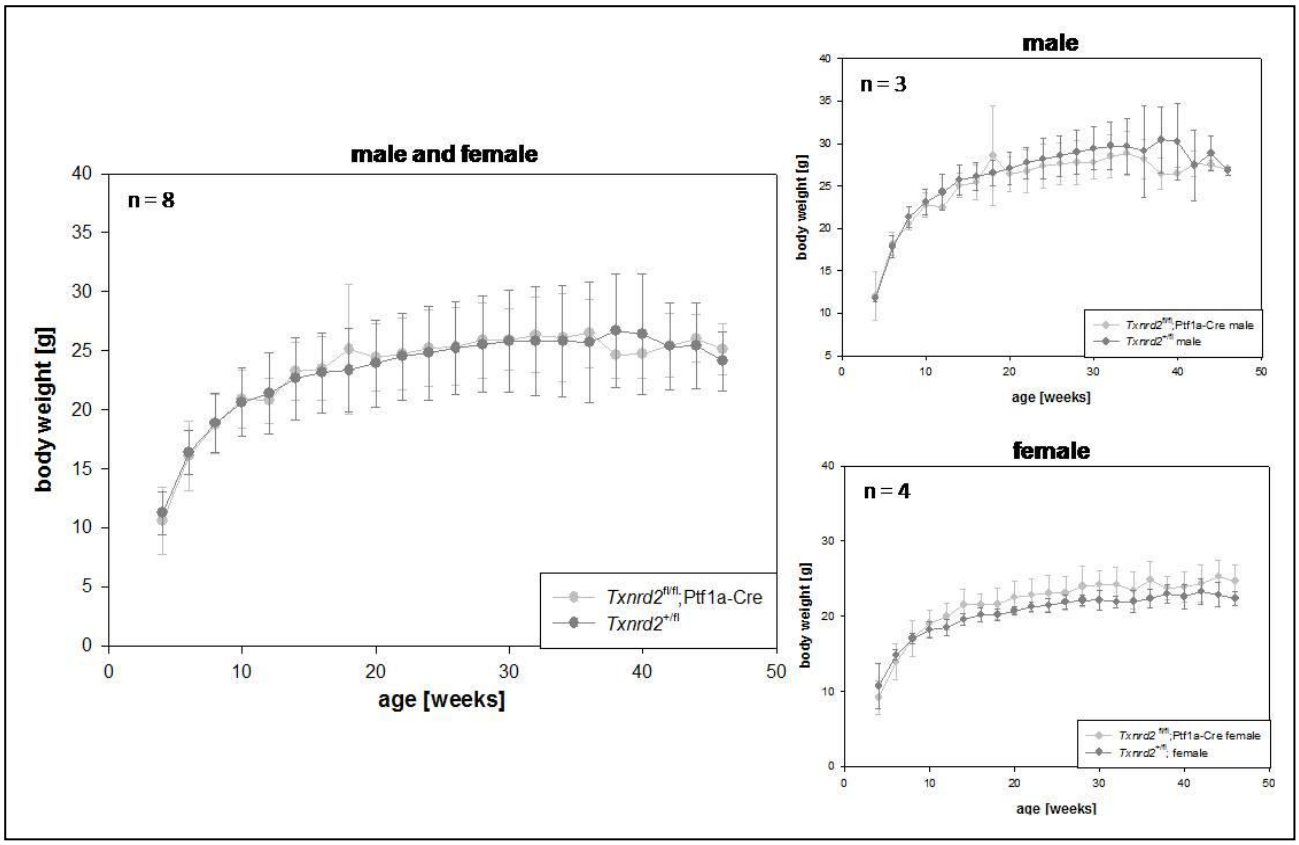

Fig.55: Body weight development in *Txnrd2* knockout and control mice. Mice were fasted over night and weight in the morning. Each dot represents the mean body weight of the mouse group ± standard deviation observed over one year. Data showed no difference in weight development in knockout (*Txnrd2*$^{fl/fl}$;*Ptf1a-Cre*^{ex1}) and control (*Txnrd2*$^{+/fl}$) mice.

3.4.3 Pancreatic gross morphology

Mice were checked for gross morphological changes during necropsy, especially in the pancreas. *Txnrd2* knockout mice and controls were sacrificed at an age of one, two, three, four, twelve, twenty-four weeks and one year (each time point and genotype n = 4 males and n = 4 females, except one year old *Txnrd2*$^{fl/fl}$;*Ptf1a-Cre*^{ex1} n = 3 males and n = 4 females). Ages one to three weeks are depicted in figure 56. This is the suckling period where infant mice do not yet eat chow. Figure 57 depicts the juvenile stadium of four weeks of age at which mice start to eat chow. Also, this figure depicts the adult ages of twelve weeks to one year. Part A in each of these figures depicts the pancreas *in situ* in relation to liver, duodenum and stomach as indicated, whereas part B depicts a direct comparison of the pancreas of *Txnrd2* knockout and control mice with spleen as a size standard. At the infant stages there were no gross morphological changes (Fig.56,A). This was also true for the direct comparison of knockout and control pancreata at the age of

three weeks (Fig.56,B). Direct comparison of earlier ages was not possible because the genotype, necessary for direct comparison, was not available at the time of necropsy.

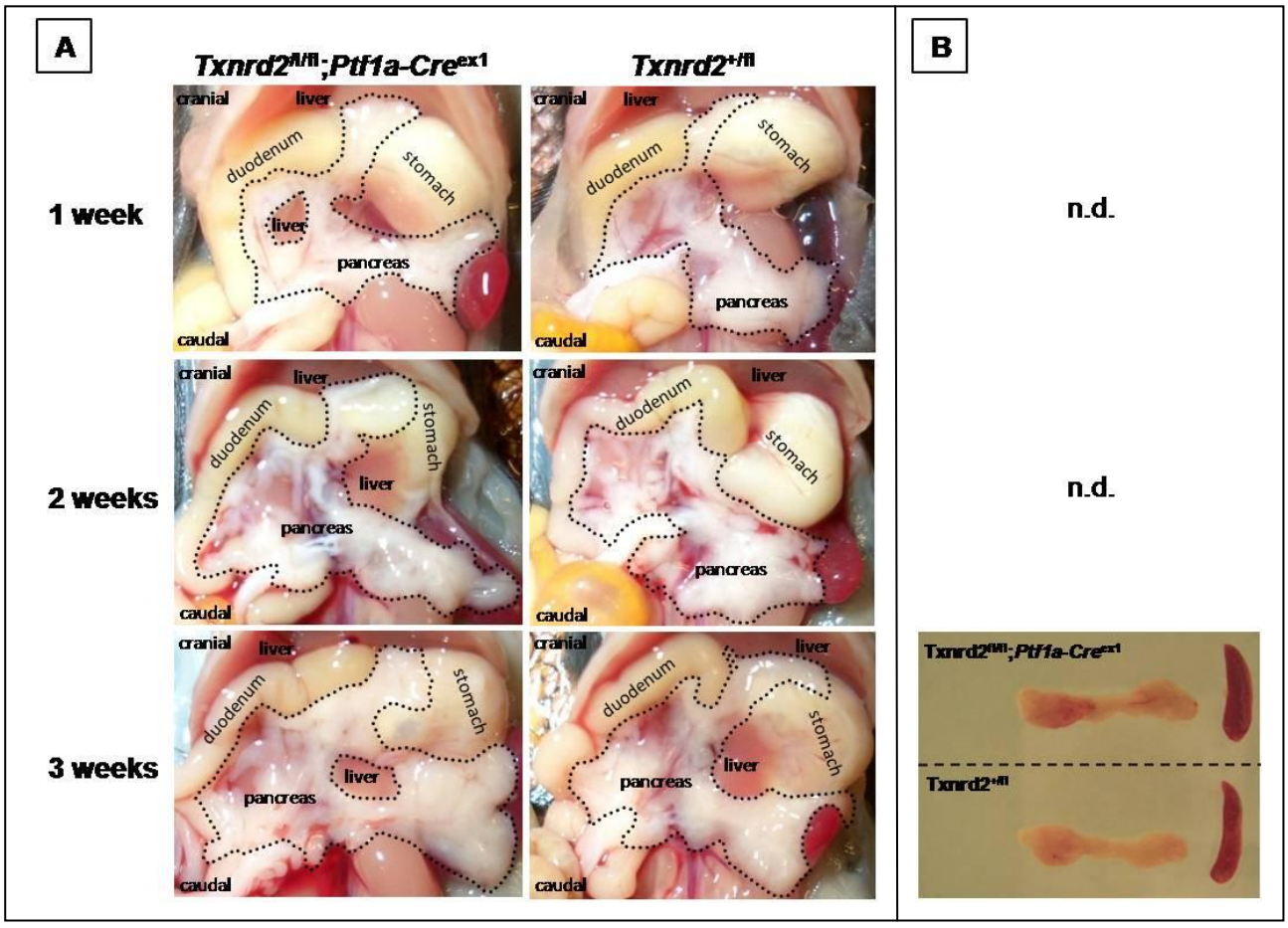

Fig.56: Gross morphology of infant *Txnrd2* knockout and control mice. (A) Gross morphological situation *in situ* in *Txnrd2* knockout and control mice at an age of one to three weeks. (B) Direct comparison of *Txnrd2* knockout and control pancreata at an age of three weeks. Gross morphological changes could not be observed in knockout (*Txnrd2*$^{fl/fl}$;*Ptf1a-Cre*^{ex1}) sucklings of an age of one to three weeks in comparison to controls (*Txnrd2*$^{+/fl}$). Even in direct comparison of pancreata at an age of three weeks there was no difference observable.

At the juvenile stage of four weeks the pancreas of *Txnrd2* knockout mice seemed slightly more transparent *in situ* than that of controls (Fig.57,A), but in direct comparison no clear difference was observed (Fig.57,B). In the adult stages of twelve and twenty-four weeks and one year the knockout pancreas was more transparent in comparison to controls and looked sometimes slightly reddish (Fig.57,A). Also, in direct comparison, the knockout pancreas showed a clear reduction in size (Fig.57,B).

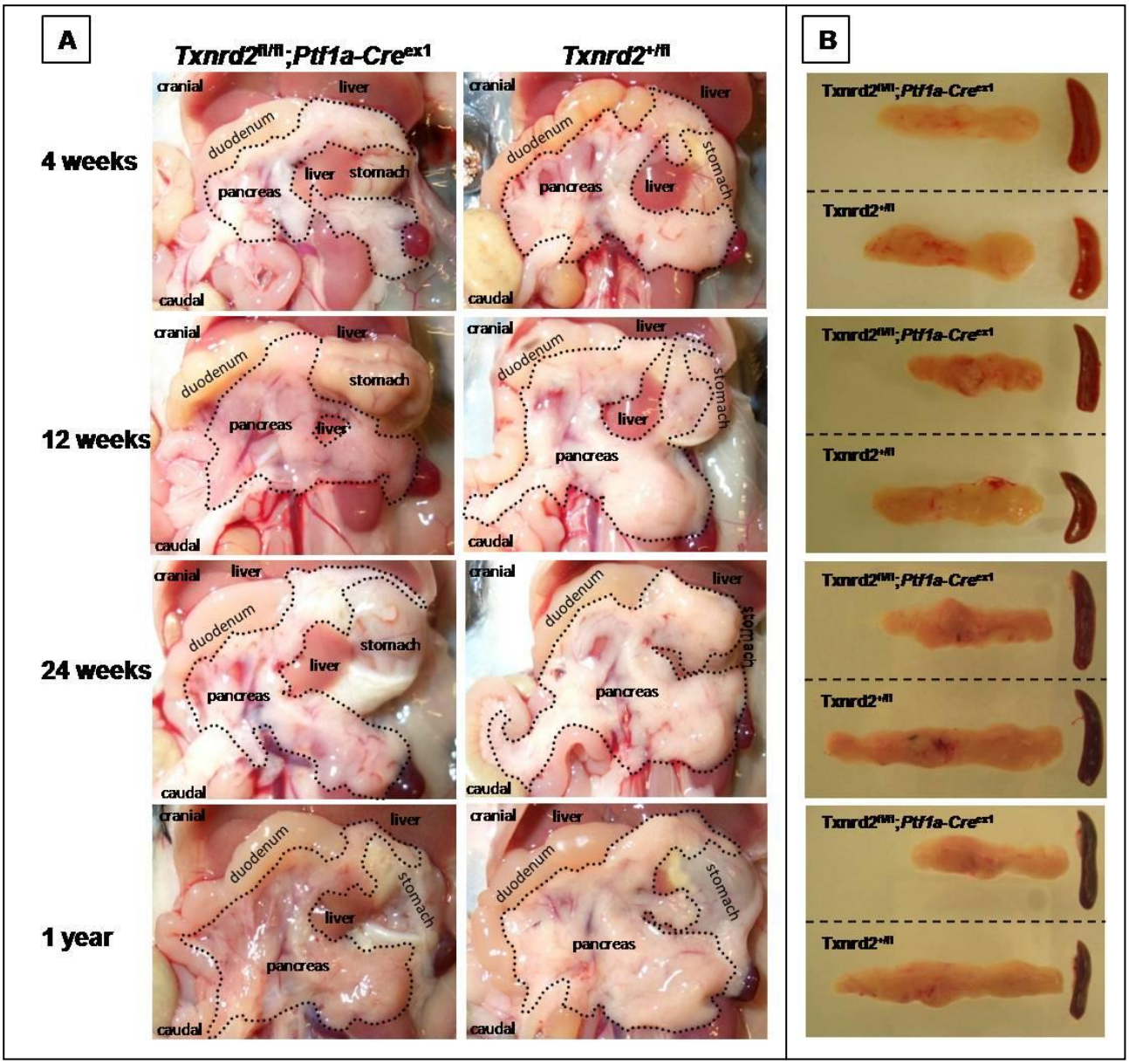

Fig.57: Gross morphology of juvenile and adult *Txnrd2* knockout and control mice. (A) Gross morphological situation *in situ* in knockout and control mice at an age of four to twenty-four weeks and one year. (B) Direct comparison of knockout and control pancreata at an age of four to twenty-four weeks and one year with spleen as a size standard. The pancreas of *Txnrd2* knockout mice (*Txnrd2*$^{fl/fl}$;*Ptf1a-Cre*^{ex1}) showed a progressive reduction in size in comparison to controls (*Txnrd2*$^{+/fl}$).

The relative pancreatic weight was determined as a parameter for pancreatic development and integrity during an observation period of one year at stages of four, twelve and twenty-four weeks and one year. The same mice as for the gross morphological analysis were used. At the juvenile stage of four weeks, the relative pancreatic weight of *Txnrd2* knockout mice was slightly reduced compared to control mice (Fig.58). A highly significant

progressive reduction in specific pancreas weight was observed at later stages ($p < 0.001$, student-t-test).

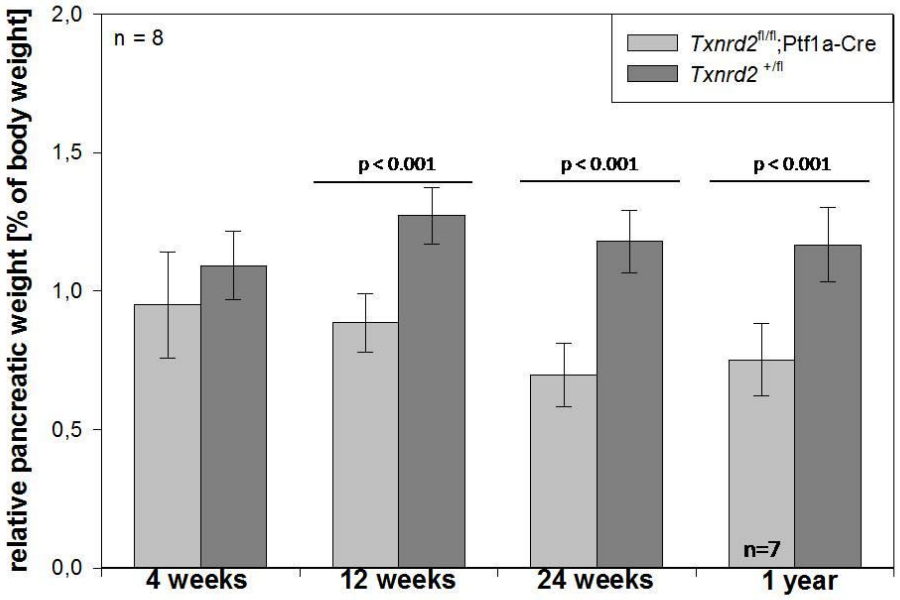

Age	Relative pancreatic weight [% of body weight]	
	***Txnrd2*$^{fl/fl}$; *Ptf1a-Cre*^{ex1}**	***Txnrd2*$^{+/fl}$**
4 weeks	0.95 ± 0.19	1.09 ± 0.12
12 weeks	0.89 ± 0.11	1.27 ± 0.10
24 weeks	0.7 ± 0.11	1.2 ± 0.11
1 year	0.75 ± 0.13	1.2 ± 0.13

Fig.58: Relative pancreatic weight in *Txnrd2* knockout and control mice. The relative pancreatic weight of *Txnrd2* knockout (*Txnrd2*$^{fl/fl}$;*Ptf1a-Cre*^{ex1}) or control mice (*Txnrd2*$^{+/fl}$) was not influenced by the genotype. Data are expressed as means ± standard deviation in % of body weight.

3.4.4 Pancreatic tissue morphology

The morphology of the pancreas was analyzed at different infant, juvenile and adult stages. The same mice as in 3.4.3 were used. Histological samples were prepared and sections were stained with H&E and examined for histological alterations.

Postnatal, the pancreatic structure was already fully developed. Figure 59 depicts representative pancreatic samples of *Txnrd2* knockout and control mice (*Txnrd2*$^{fl/fl}$) at the three first postnatal weeks where infant mice suckle. Morphological changes in comparison of genotypes could not be observed during this period.

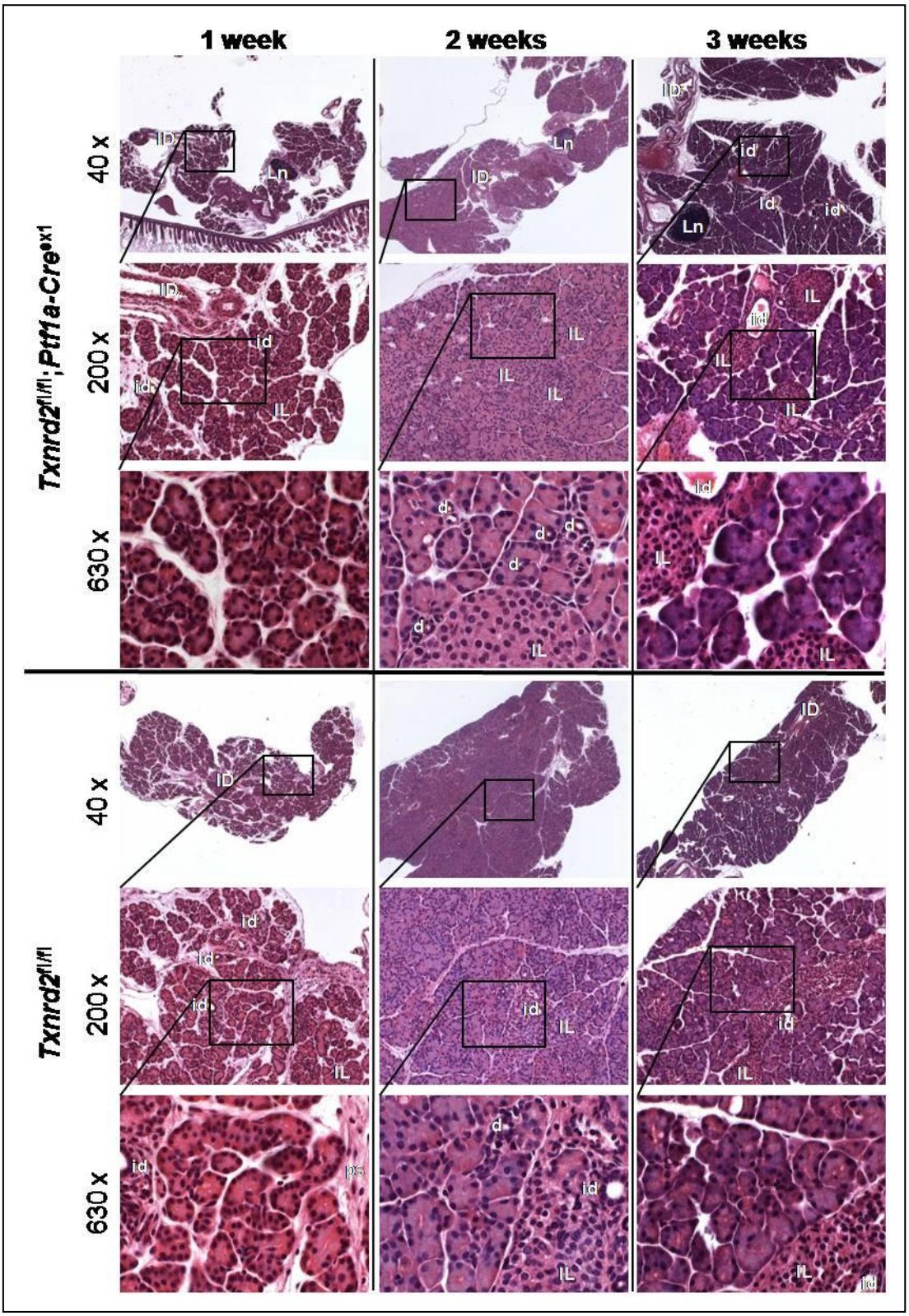

Fig.59: Pancreatic tissue morphology in *Txnrd2* knockout and control mice (age 1-3 weeks). The upper panel depicts H & E stained slides of knockout pancreata at different ages and magnifications. Rectangles indicate the areas chosen for higher magnifications. *Txnrd2* knockout mice (*Txnrd2*$^{fl/fl}$;*Ptf1a-Cre*^{ex1}) as well as control mice (*Txnrd2*$^{fl/fl}$) showed a typical age-based pancreas. (ID= interlobular duct, id = intralobular duct, d= intercalated duct, IL= islet of Langerhans, LN= lymph node, ps= pancreatic stellate cells)

At an age of four weeks, four out of eight *Txnrd2* knockout mice developed acute pancreatitis, characterized by an inflammatory infiltrate and an oedematous fluid in the extracellular space separating the lobules and acini. Figure 60 depicts a representative example of one of those mice with acute pancreatitis compared to a healthy control. The inflammatory cells were only present in the interacinar space (Fig.60, left and central panels) and did not infiltrate the islets of Langerhans (Fig.60, left panel). Also, a strong oedematous area is depicted (Fig.60, right panel).

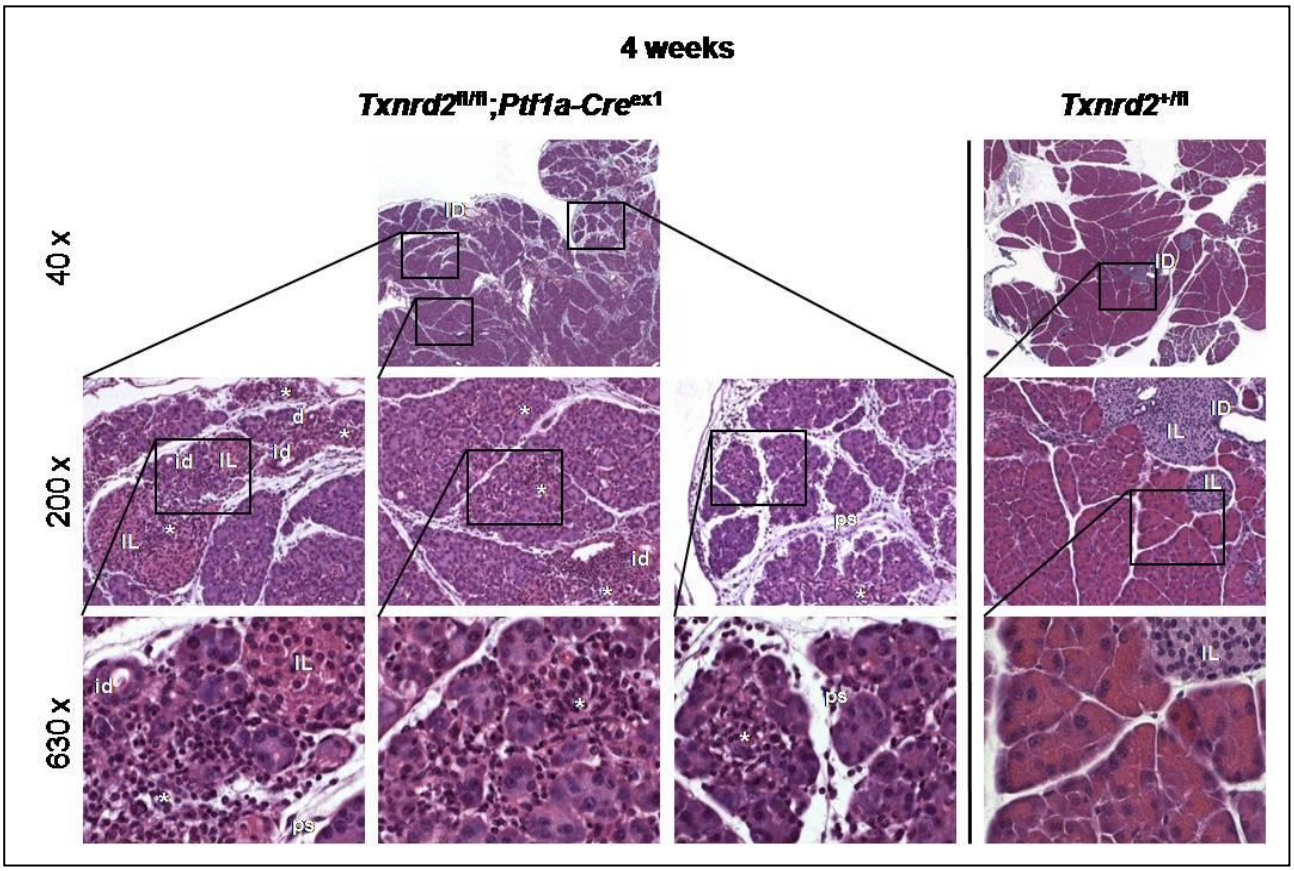

Fig.60: Pancreatic tissue morphology of four-weeks-old *Txnrd2* knockout and control mice. The left panel shows typical lesions found in *Txnrd2* knockout mice at different magnifications as indicated. Control pancreas is shown on the right panel for comparison. Rectangles indicate the areas chosen for higher magnifications. *Txnrd2* knockout mice showed signs of acute pancreatitis. Inflammatory cells did not afflict the islets of Langerhans (*Txnrd2*$^{fl/fl}$;*Ptf1a-Cre*^{ex1}, left panel) and infiltrated generalized mainly the interacinar space (*Txnrd2*$^{fl/fl}$;*Ptf1a-Cre*^{ex1}, central panel). The mice had a very oedematous pancreas (*Txnrd2*$^{fl/fl}$;*Ptf1a-Cre*^{ex1}, right panel). Controls did not exhibit signs of pancreatitis (*Txnrd2*$^{+/fl}$). (ID= interlobular duct, id = intralobular duct, IL = islet of Langerhans, LN = lymph node, ps = pancreatic stellate cells, asterix = infiltrating inflammatory cells)

At the first analyzed adult stadium of twelve weeks, eight out of eight *Txnrd2* knockout mice showed advanced inflammation of pancreas. Figure 61 depicts a representative example of a knockout and a control mouse. The pancreas of the knockout mice was oedematous as shown by figure 61 (magnification 40x) and inflammatory cells were observed in some areas in the interacini space (Fig.61, right panel), but mainly found in clusters (Fig.61, left panel). Chronic inflammation of the pancreas is known to result in the formation of metaplastic lesions of a ductal phenotype. Already in this twelve weeks old knockout mice first responses to chronic injury, which means the formation of metaplastic lesions and development of fibrosis, were observed (Fig.61, central panel). Metaplastic lesions are classified in an additional chapter (3.4.8).

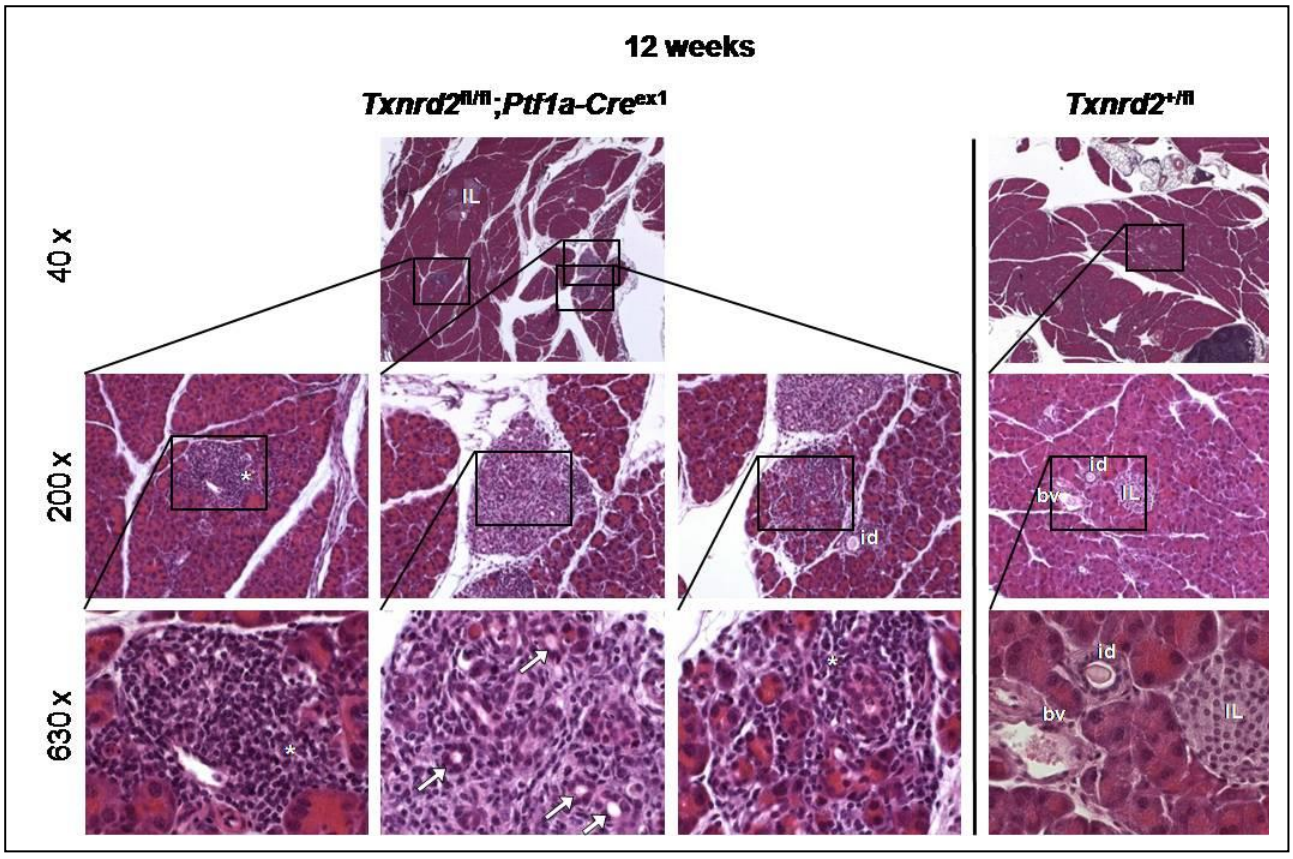

Fig.61: Pancreatic tissue morphology of twelve-weeks-old *Txnrd2* knockout and control mice. The left panel shows typical lesions of twelve-weeks-old knockout mice at different magnification. Control pancreas is shown on the right panel for comparison. Rectangles indicate the areas chosen for higher magnifications. Signs indicating a chronic course of disease including infiltrating cells in clusters (*Txnrd2*$^{fl/fl}$;*Ptf1a-Cre*^{ex1}, left panel) or in the interacini space (*Txnrd2*$^{fl/fl}$;*Ptf1a-Cre*^{ex1}, right panel) and metaplastic lesions surrounded by fibrotic tissue (*Txnrd2*$^{fl/fl}$;*Ptf1a-Cre*^{ex1}, central panel, arrows). None of these pathological findings were present in the control mice. (bv = blood vessels, id = intralobular duct, IL = islet of Langerhans, arrow = metaplastic lesions – tubular complex, asterix = infiltrating inflammatory cells)

At an age of twenty-four weeks, eight out of eight analyzed *Txnrd2* knockout mice showed a severe pancreatitis with characteristics of a chronically course of disease, whereas *Txnrd2* control mice remained healthy. Clusters of inflammatory cells only infiltrated acinar tissue and did not enter the islets of Langerhans (Fig.62, *Txnrd2*$^{fl/fl}$;*Ptf1a-Cre*^{ex1}, middle panel). Developing fibrosis surrounding acini and formation of metaplastic lesions as already seen in twelve weeks old mice could be observed (*Txnrd2*$^{fl/fl}$;*Ptf1a-Cre*^{ex}, right and left panel). Fat necrosis in accumulations of adipocytes in and around the pancreas was evident (Fig.62, *Txnrd2*$^{fl/fl}$;*Ptf1a-Cre*^{ex1}, 40x panel and left panel). The appearance of fat necrosis is often the result of dilated acini and tissue atrophy.

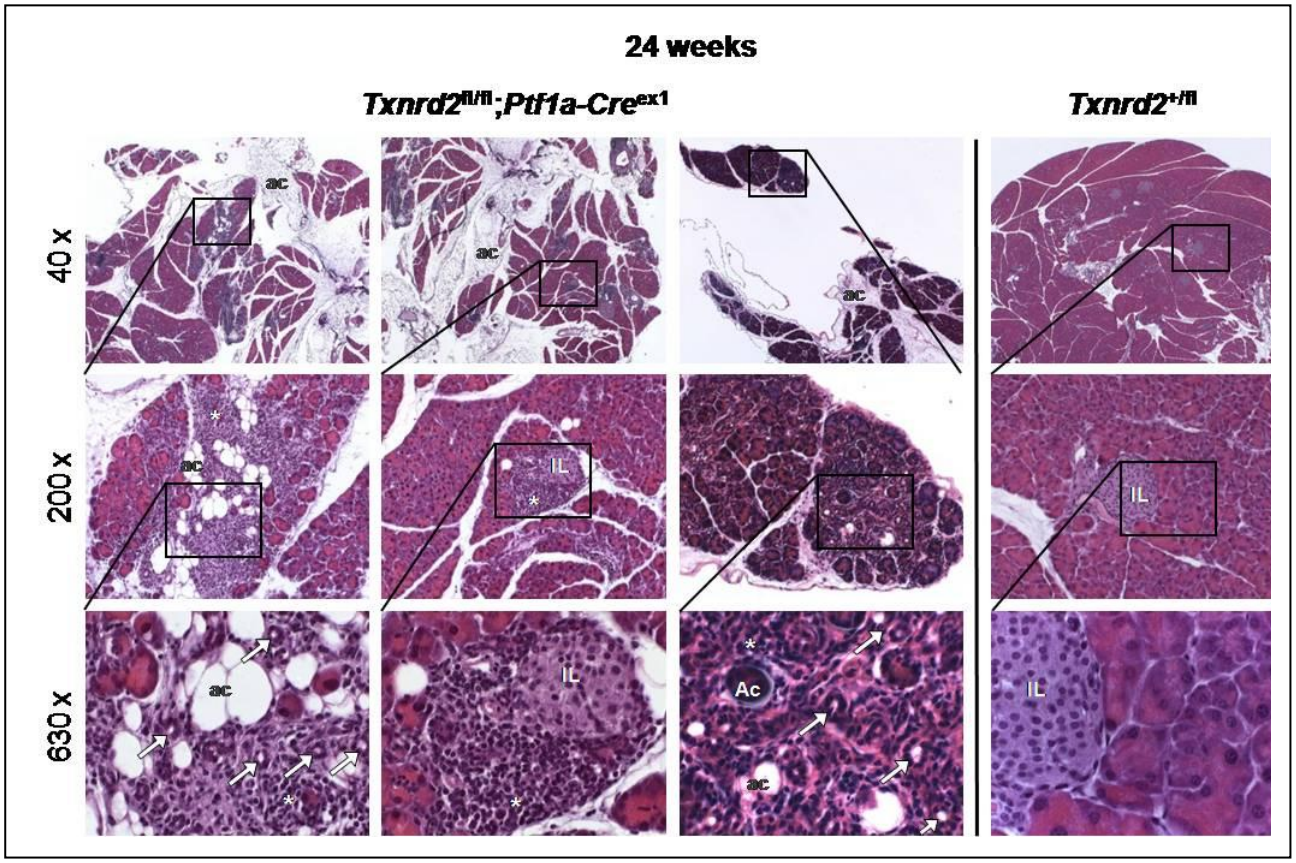

Fig.62: Pancreatic tissue morphology of twenty-four-weeks-old *Txnrd2* knockout and control mice. The left panel shoes three typical lesions for chronic pancreatitis shown in different magnifications. Control pancreas is shown on the right panel for comparison. Rectangles indicate the areas chosen for higher magnifications. Pancreatic atrophy (40x) with fat necrosis and fibrosis surrounding the acini (*Txnrd2*$^{fl/fl}$;*Ptf1a-Cre*^{ex1}, left and right panel). Inflammatory cells did not infiltrate islets of Langerhans (*Txnrd2*$^{fl/fl}$;*Ptf1a-Cre*^{ex1}, middle panel). Controls remained unaffected (*Txnrd2*$^{+/fl}$). (Ac = acinus, ac = adipocytes, IL = islets of Langerhans, arrow = metaplastic lesions – tubular complex, asterix = infiltrating inflammatory cells).

At the age of one year, eight out of eight *Txnrd2* knockout mice showed chronic pancreatitis (Fig.68). Control mice remained healthy (see fig.64). The pancreas of these mice showed typical pathological alterations of chronic pancreatitis, characterized by severe atrophic pancreatic tissue with fat necrosis (Fig.63, central right panel) and fibrosis (Fig.68 , both left panel). Multiple metaplastic lesions of different types could be observed, which will be addressed in an additional chapter (Fig.63, both left panel). Islets of Langerhans remained unaffected and were often surrounded by fibrosis, metaplastic lesions or adipocytes and fatty necrosis (Fig.63, central right panel). Also, for the first time necrotic acinar tissue could be observed in one animal, which is also a typical sign of chronic pancreatitis (Fig.63, right panel).

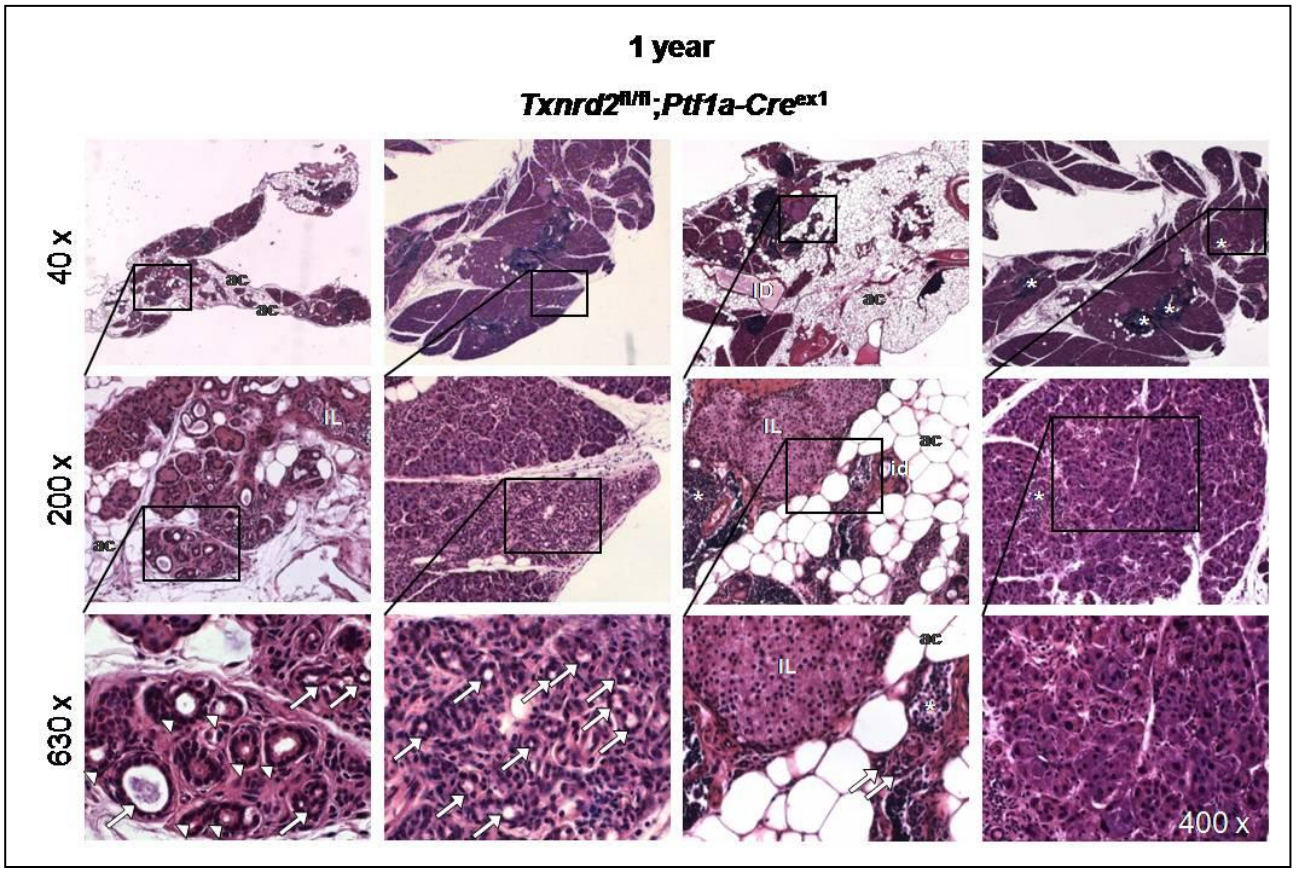

Fig.63: Pancreatic tissue morphology of one-year-old *Txnrd2* knockout and control mice. Four typical lesions indicating chronic pancreatitis with metaplastic lesions surrounded by massive fibrosis. Rectangles indicate the areas chosen for higher magnifications. Different types of metaplastic lesions surrounded by fibrosis (*Txnrd2*$^{fl/fl}$;*Ptf1a-Cre*^{ex1}, both left panel). The islets of Langerhans remained unaffected and were often surrounded by adipocytes or fibrotic areas (*Txnrd2*$^{fl/fl}$;*Ptf1a-Cre*^{ex1}, central right panel). In one animal necrotic acinar tissue could be observed (*Txnrd2*$^{fl/fl}$;*Ptf1a-Cre*^{ex1}, right panel). (ac = adipocytes, id = intralobular duct, IL = islets of Langerhans, arrow = metaplastic lesions – tubular complex, arrow head = metaplastic lesion – mucinous type, asterix = infiltrating inflammatory cells).

So far, no homozygous null mutations of *TXNRD2* have been described in humans, but several heterozygous point mutations leading to amino acid exchanges leading to reduced enzymatic activity have been described (Gromer *et al*., 2006; Ma *et al*., 2002; Oblong *et al*., 1994). Pancreas-specific heterozygous knockout mice (*Txnrd2*$^{+/fl}$;*Ptf1a-Cre*^{ex1}) were examined at several ages. Interestingly at the ages four, twelve and twenty-four weeks (each n = 8), no mouse out of eight mice showed a phenotype. But at an age of one year, four out of eight heterozygous *Txnrd2* knockout mice showed clusters of infiltrating inflammatory cells (Fig.64). The islets of Langerhans remained unaffected (Fig.64,left panel).

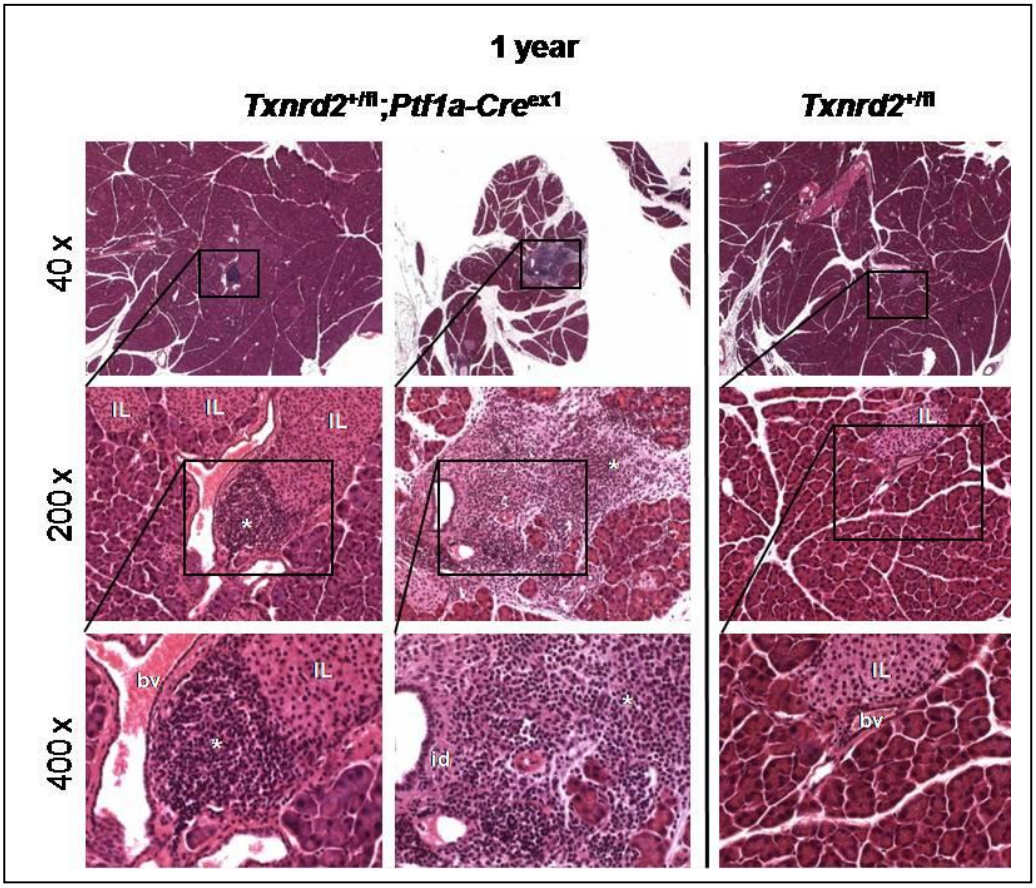

Fig.64: Pancreatic tissue morphology of one-year-old *Txnrd2* heterozygous knockout and control mice. The left panel shows typical pancreatic inflammatory lesions found in heterozygous knockout mice at an age of one year. Control pancreas is shown on the right panel for comparison. Rectangles indicate the areas chosen for higher magnifications. Clusters of infiltrating inflammatory cells (*Txnrd2*$^{+/fl}$;*Ptf1a-Cre*^{ex1}, both panel). Islets of Langerhans remained unaffected (*Txnrd2*$^{+/fl}$;*Ptf1a-Cre*^{ex1}, left panel). Control mice showed a normal pancreas (*Txnrd2*$^{+/fl}$). (bv = blood vessels, id = intralobular duct, IL = islet of Langerhans, asterix = infiltrating inflammatory cells)

3.4.5 Characterisation of exocrine functional parameters

The exocrine pancreatic knockout phenotype was characterized by immunohistochemical methods, serum analysis and by a lipid absorption test.

Histological, the pancreas was characterized at the age of four, twelve and twenty-four weeks and one year. The same mice as in 3.4.3 were used. Acinar cells were immunohistochemically stained with a rabbit anti-α-amylase antibody. In *Txnrd2* knockout mice, staining for α-amylase in acinus cells surrounded by inflammatory cells was inhomogeneous and some acinus cells were stained stronger than others in these areas. Except in these inflamed areas, there were no further differences in staining compared to control mice (Fig.65).

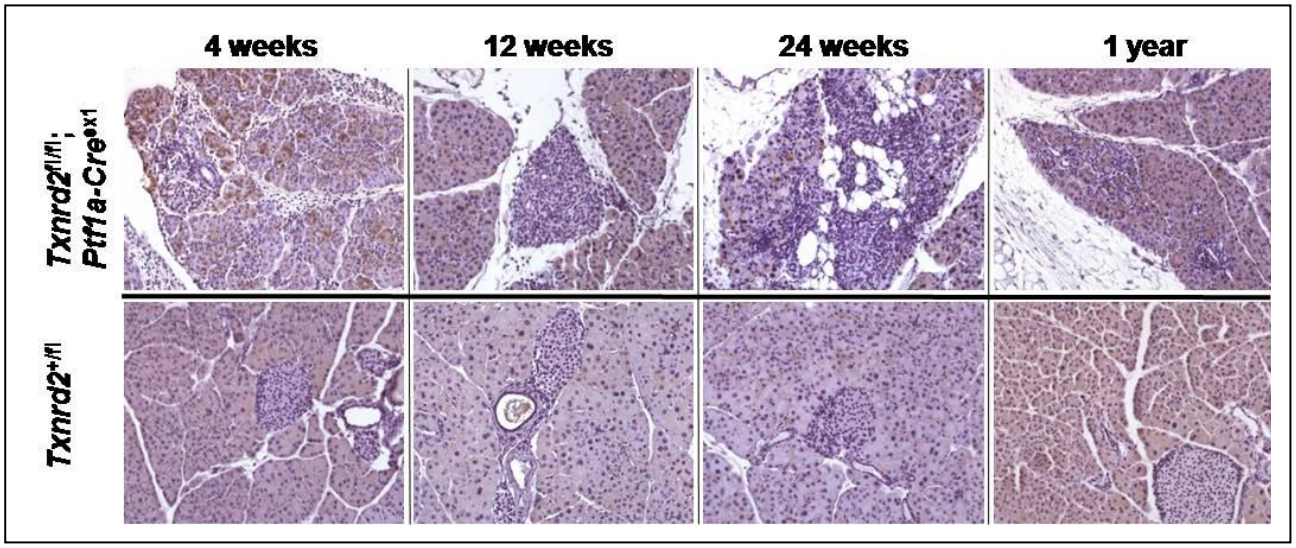

Fig.65: Amylase expression in the pancreas of *Txnrd2* knockout and control mice. At all stages examined the acinar cells of the pancreas were positively stained for α-amylase with similar expression in knockout (*Txnrd1*$^{fl/fl}$;*Ptf1a-Cre*^{ex1}) and control (*Txnrd1*$^{+/fl}$) mice. Acinus cells in the pancreas of *Txnrd2* knockout mice (*Txnrd2*$^{fl/fl}$;*Ptf1a-Cre*^{ex1}), surrounded by inflammatory cells, stained inhomogeneous. (Rabbit anti-α-amylase; 200x)

Proliferation of the exocrine pancreas was investigated as a parameter for regenerative activity of the organ. A proliferation index of the acinar cells was determined by injecting knockout and control mice at an age of four, twelve and twenty-four weeks and one year (each age and genotype n = 5) with BrdU. Afterwards, mice were sacrificed, histological samples were prepared and stained immunohistochemically with a rat anti-BrdU antibody. The proliferation index was determined and expressed as percentage of proliferating

acinar cells of all acinar cells. Already, at the age of four weeks, there were significantly more proliferative acinar cells in the *Txnrd2* knockout mice compared to the *Txnrd2* control mice ($p < 0.05$, student t-test) (Fig.66). Also, at the age of twelve weeks, as well as the age of twenty-four weeks and one year, the acinar cells of knockout mice showed a statistically significant increase in the proliferation index in comparison to controls ($p < 0.001$, student t-test). These results showed that in the knockout mice the exocrine pancreas had more proliferative activity in comparison to control mice, which might be a result of regenerative activity. Figure 66 also depicts representative histological samples of all analyzed stages and genotypes.

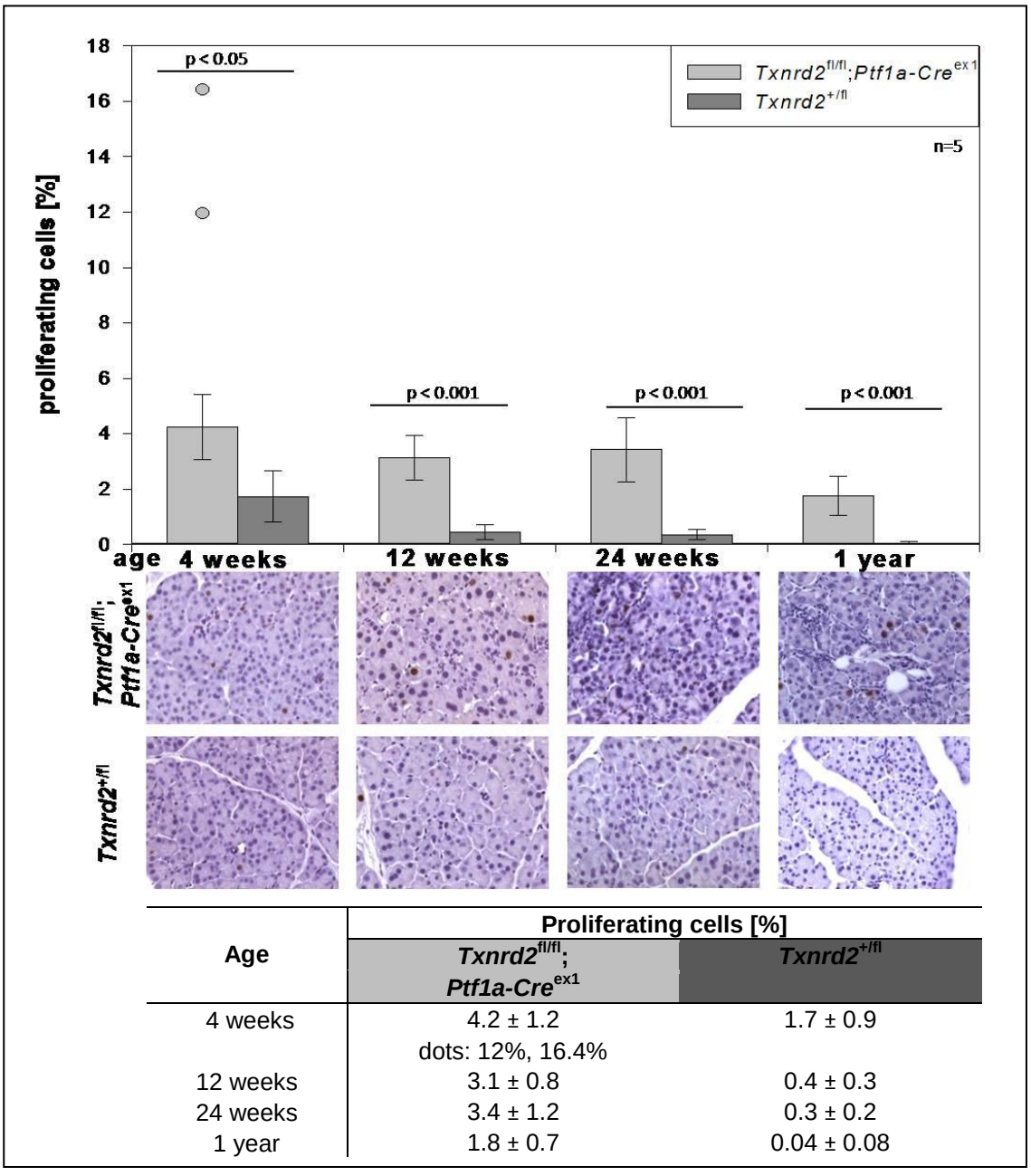

Age	Proliferating cells [%]	
	Txnrd2$^{fl/fl}$; *Ptf1a-Cre*^{ex1}	*Txnrd2*$^{+/fl}$
4 weeks	4.2 ± 1.2 dots: 12%, 16.4%	1.7 ± 0.9
12 weeks	3.1 ± 0.8	0.4 ± 0.3
24 weeks	3.4 ± 1.2	0.3 ± 0.2
1 year	1.8 ± 0.7	0.04 ± 0.08

Fig.66: Proliferation index of the exocrine pancreatic tissue in *Txnrd2* knockout and control mice. The number of BrdU-positive proliferating cells was determined by staining pancreatic slides with a rat anti-BrdU antibody (middle panel). Quantification of counted BrdU-positive cells (upper panel). At all analyzed ages, the exocrine pancreatic tissue showed more proliferative acinar cells in the knockout mice (*Txnrd2*$^{fl/fl}$;*Ptf1a-Cre*^{ex1}) than in the control mice (*Txnrd2*$^{+/fl}$). Data are expressed in means ± standard deviation. Representative histological samples of all analyzed stages and genotypes are depicted (rat anti-BrdU, 400x).

Ultrastructural analysis of the exocrine pancreas of one year old *Txnrd2* knockout and control mice was done by transmission electron microscopy (TEM). In *Txnrd2* knockout mice, severe apoptotic cell destruction was observed (Fig.67,G-H). The mitochondria of acinus cells in these mice were swollen and showed total loss of the inner mitochondrial cristae structure (Fig.67,J-L). The *Txnrd2* control mice did not show ultrastructural alterations.

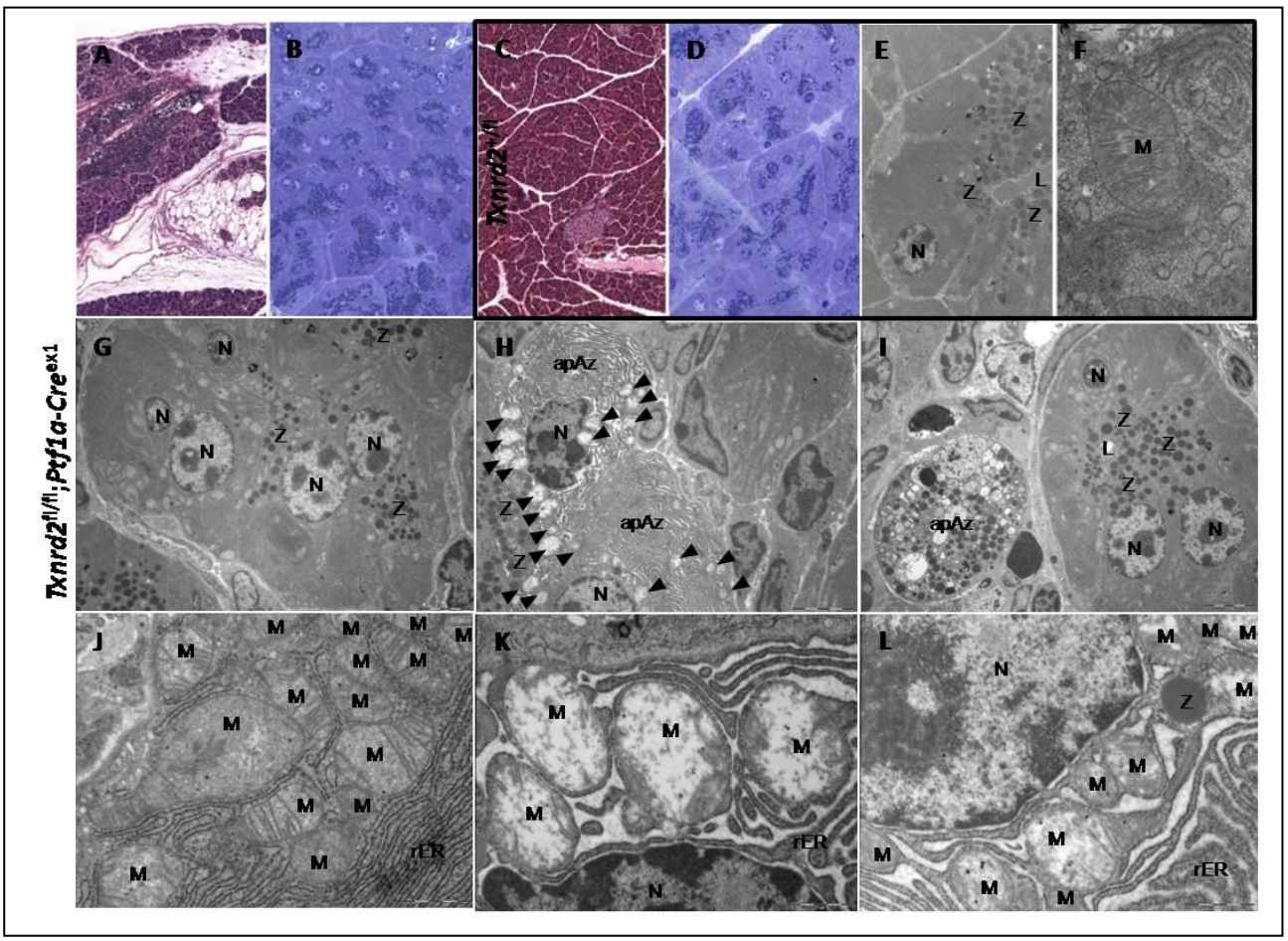

Fig.67: Ultrastructural analysis of *Txnrd2* knockout and control mice. The pancreas of one year old knockout (*Txnrd2*$^{fl/fl}$;*Ptf1a-Cre*^{ex1}) and control (*Txnrd2*$^{+/fl}$) mice is depicted. (A) Overview of a *Txnrd2* knockout pancreas (H & E, 100x). (B) Semi thin cut of a *Txnrd2* knockout pancreas (Toluidine blue, 630x). (C) Overview of a control pancreas (H & E, 100x). (D) Semi thin cut of a control pancreas (Toluidine blue, 630x).

(E) Acinus of a control pancreas (TEM, 2520x). (F) Mitochondrium in an acinus cell of a control pancreas (TEM, 10000x). (G,H) Apoptotic cell debris in acinus cells of *Txnrd2* knockout pancreas (TEM, 2520x, arrowheads = alternated mitochondria). (J–L) Swollen and destructed mitochondria in an acinus cell of *Txnrd2* knockout pancreas (TEM, 10000x). In the knockout mice severe cell destruction and mitochondrial swelling could be observed, while the control mice did not show any alterations. (ApAZ = apoptotic acinus cell, arrowheads = alternated mitochondria, L = lumen of an acinus, N = nucleus, M = mitochondria, cristae type, rER = rough endoplasmic reticulum, Z = zymogen granules)

As a parameter for the destruction of the exocrine pancreas, the pancreatic enzymes amylase and lipase were measured in blood serum samples of *Txnrd2* knockout and control mice. For the serum analysis the ages of three weeks, when a histological phenotype could not yet be observed, and of four, twelve and twenty-four weeks and one year, when destruction of the exocrine pancreas was evident, were chosen. There was no significant difference either in the case of amylase (Fig.68,A) or lipase (Fig.68,B), although a continuous increase in the serum amylase level in the knockout mice could be observed.

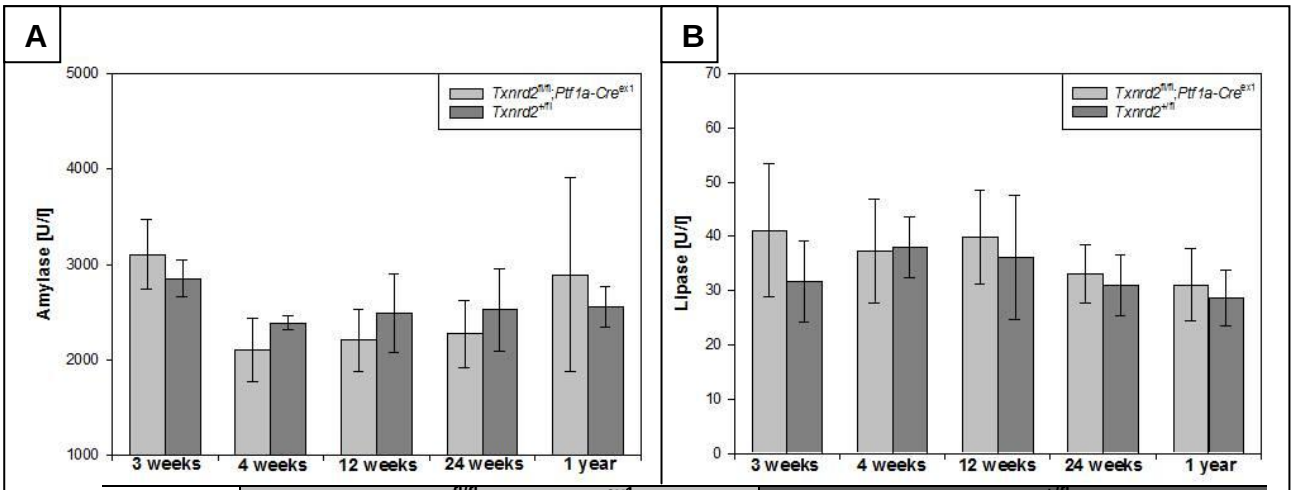

Age	*Txnrd2*$^{fl/fl}$;*Ptf1a-Cre*^{ex1}			*Txnrd2*$^{+/fl}$		
	Number of animals	Amylase [U/L]	Lipase [U/L]	Number of animals	Amylase [U/L]	Lipase [U/L]
3 weeks	3	3102.0 ± 365.2	41.1 ± 12.3	4	2848.5 ± 191.7	31.7 ± 7.5
4 weeks	8	2106.4 ± 334.7	37.3 ± 9.7	4	2385.0 ± 73.3	38.0 ± 5.6
12 weeks	8	2206.1 ± 322.9	39.9 ± 8.6	6	2484.5 ± 411.5	36.1 ± 11.5
24 weeks	6	2273.0 ± 351.0	33.1 ± 5.4	7	2523.4 ± 430.7	31.0 ± 5.7
1 year	6	2829.5 ± 1020.3	31.1 ± 6.7	8	2553.4 ± 214.4	28.6 ± 5.1

Fig.68: Serum amylase and lipase in *Txnrd2* knockout and control mice. (A) Blood serum amylase levels. (B) Blood serum lipase levels. Data are expressed as means ± standard deviation. The amylase and lipase levels in blood serum of *Txnrd2* knockout mice (*Txnrd2*$^{fl/fl}$;*Ptf1a-Cre*^{ex1}) did not significantly differ to controls (*Txnrd2*$^{+/fl}$), but the amylase levels increased continuously.

To detect the presence of lipids in the faeces, as a sign of pancreatic maldigestion, a lipid absorption test was performed. Therefore, one year old *Txnrd2* knockout and control mice were used (*Txnrd2*$^{fl/fl}$;*Ptf1a-Cre*^{ex1} n = 7, *Txnrd2*$^{+/fl}$ n = 8). To quantify this test, lipid globules were counted in each animal in 20 fields of sight. The colour of the faecal pellets differed between knockout and control mice and the brighter colour indicated already steatorrhea in knockout mice (Fig.69,A). In stool smears of knockout mice, the number of red lipid was increased in comparison to controls (Fig.69,B) ($p < 0.001$, students t-test). This result indicated, that lipid digestion in knockout animals was disturbed compared to control mice.

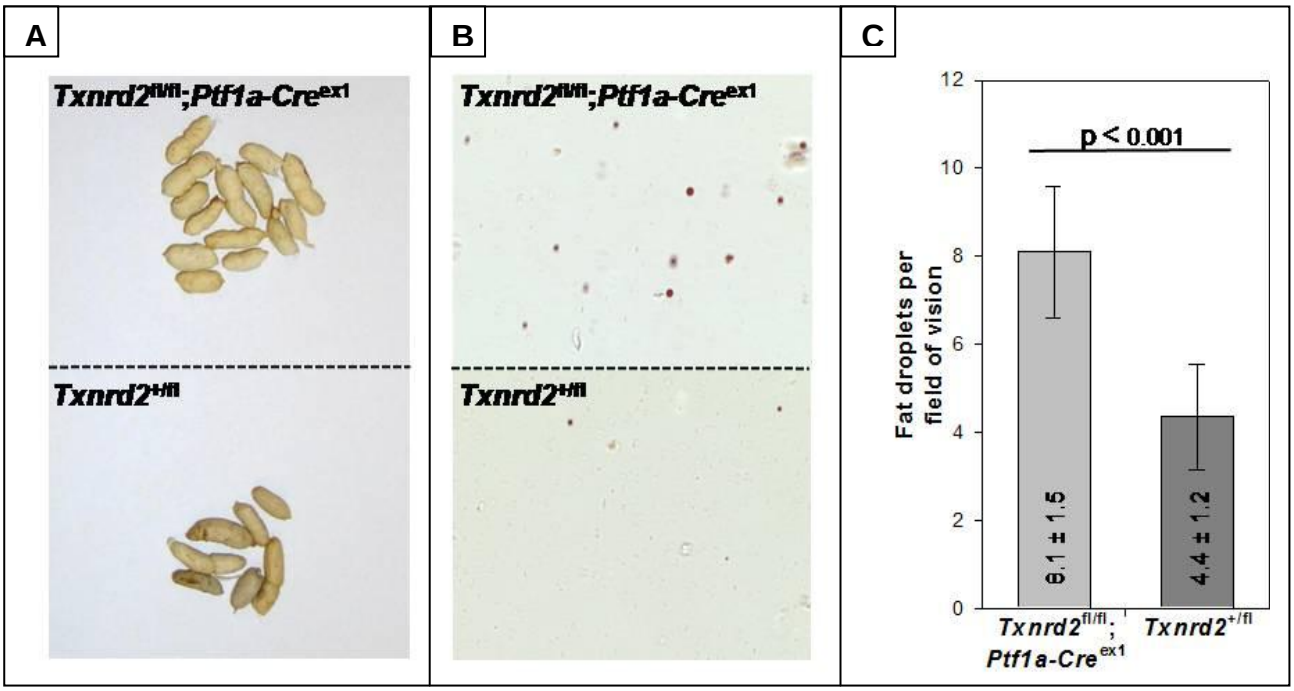

Fig.69: Steatorrhea in *Txnrd2* knockout mice. (A) Faecal pellets of knockout (*Txnrd2*$^{fl/fl}$;*Ptf1a-Cre*^{ex1}) and control mice (*Txnrd2*$^{+/fl}$). (B) Representative Oil red O stained stool smears of knockout and control mice (1000x). (C) Quantification of Oil Red O positive lipid droplets. Lipid digestion in *Txnrd2* knockout mice was disturbed. Data are expressed as means ± standard deviation.

3.4.6 Characterisation of endocrine functional parameters

The endocrine pancreatic phenotype was characterized by immunohistological methods, and the metabolical function was tested by determing of blood glucose levels and a glucose tolerance test.

Histological samples of knockout and control mice at the ages of four, twelve, twenty-four weeks and one year were analysed. The same mice as in 3.4.3 were used. Figure 70 depicts immunohistochemical staining of islets of Langerhans with a guinea pig anti-insulin (Fig.70,A) and a rabbit anti-glucagon (Fig.70,B) antibody. The β-cells stained positive for insulin in the knockout mice as well as in the control mice. There was no difference observable in comparison of genotypes or age (Fig.70A). Also, there was no difference evident for the glucagon producing α-cells in these mice (Fig.70,B). Figure 70 also shows, that the infiltrating inflammatory cells did not penetrate the islets of Langerhans, but surrounded them.

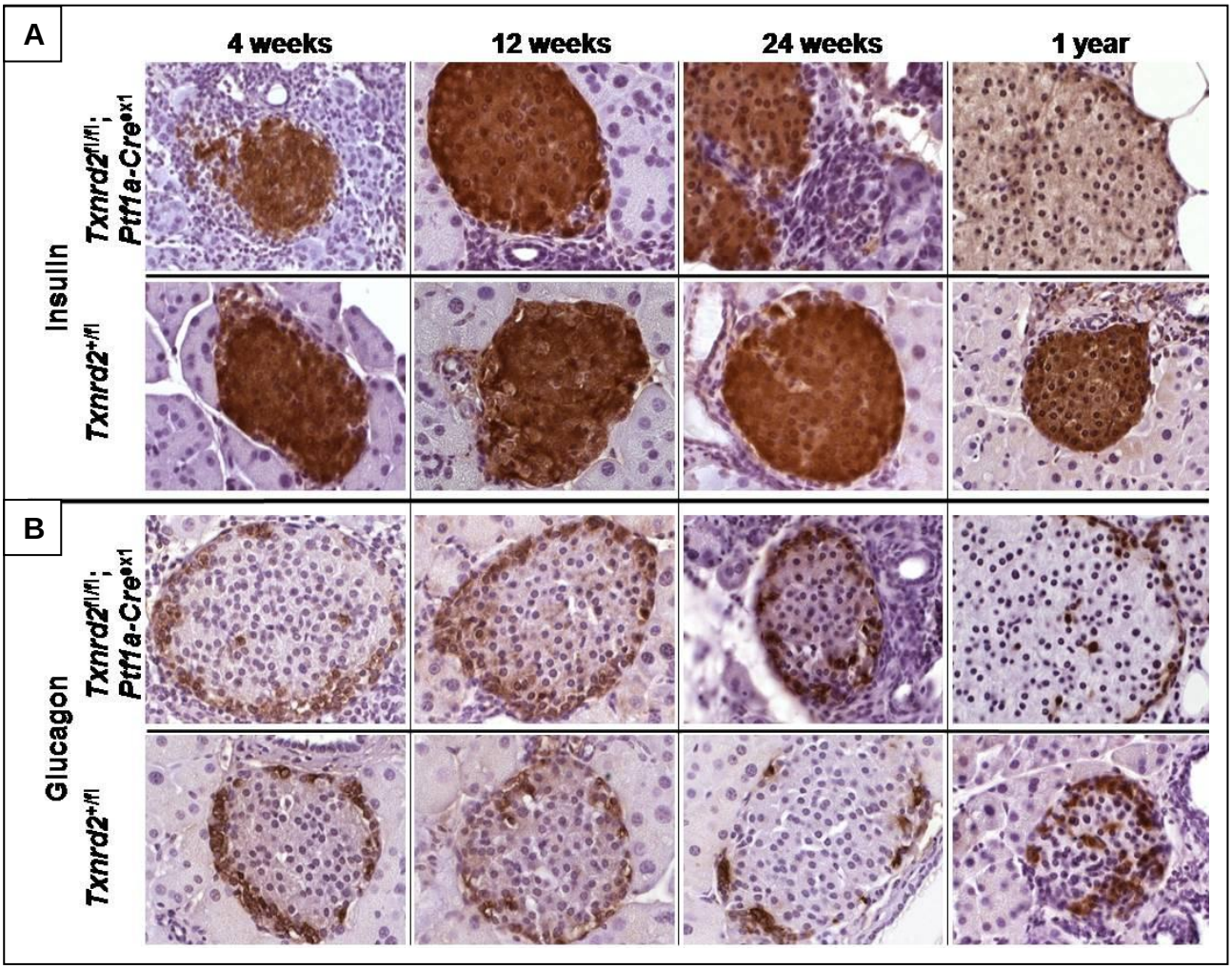

Fig.70: Immunohistochemical analyses of the endocrine pancreas *Txnrd2* knockout and control mice. (A) Pancreatic β-cells stained with a guinea pig anti-insulin antibody in knockout (upper row) and control (lower row) islet of Langerhans (630x). (B) Pancreatic α-cells stained with a rabbit anti-glucagon antibody in knockout (upper row) and control (lower row) islet of Langerhans (630x). Expression of insulin and glucagon was not influenced by the genotype. Differences in staining intensity are due to individual reactions of samples on the staining solution and do not correspond to stronger expression levels.

The physiological function of the islets of Langerhans was investigated by measuring blood glucose levels every two weeks over one year after fasting overnight. Knockout (*Txnrd2*$^{fl/fl}$;*Ptf1a-Cre*^{ex1}, n = 8) as well as control mice (*Txnrd2*$^{+/fl}$, n = 8) had a blood glucose level of around 60 mg/dL which is within the physiological range in C57BL/6 mice of up to 120 mg/dL (Klempt *et al*., 2006) (Fig.71).

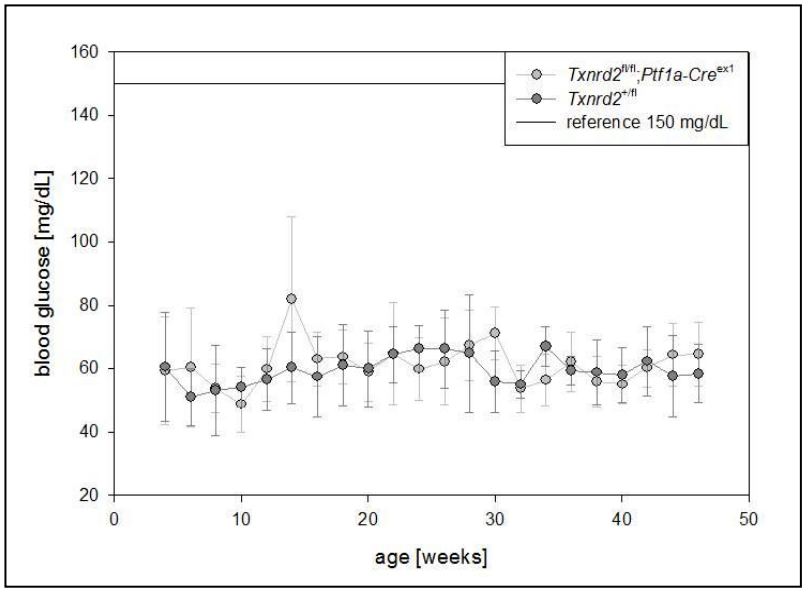

Fig.71: Blood glucose levels in *Txnrd2* knockout and control mice. Glucose levels were obtained after fasting the mice over night. The blood glucose levels in knockout and control mice remained considerably below the critical level for diabetic blood glucose (150 µg/dL).

An intraperitoneal glucose tolerance test (IP-GTT) was performed to determine how quickly glucose was cleared from the blood as a parameter of metabolical function of the endocrine pancreas. Figure 72 depicts these results: on the left both sexes together and on the right splitted into males and females. For the test, one year old mice were used (*Txnrd2*$^{fl/fl}$;*Ptf1a-Cre*^{ex1} males n = 3, females n = 4 and control mice (*Txnrd2*$^{+/fl}$) males n = 3, females n = 4). The blood glucose levels were measured directly before and after injection of glucose and then 15, 30, 60, 90 and 120 minutes after injection. Analysing both sexes together no difference was seen between knockout and control mice. When males and females were analyzed separately, males reacted inversely to females. In knockout males blood glucose levels increased faster, to a higher extend and glucose was cleared slower from blood. In contrast, in knockout females the blood glucose levels did not increase so fast and glucose was cleared much faster from blood as in controls.

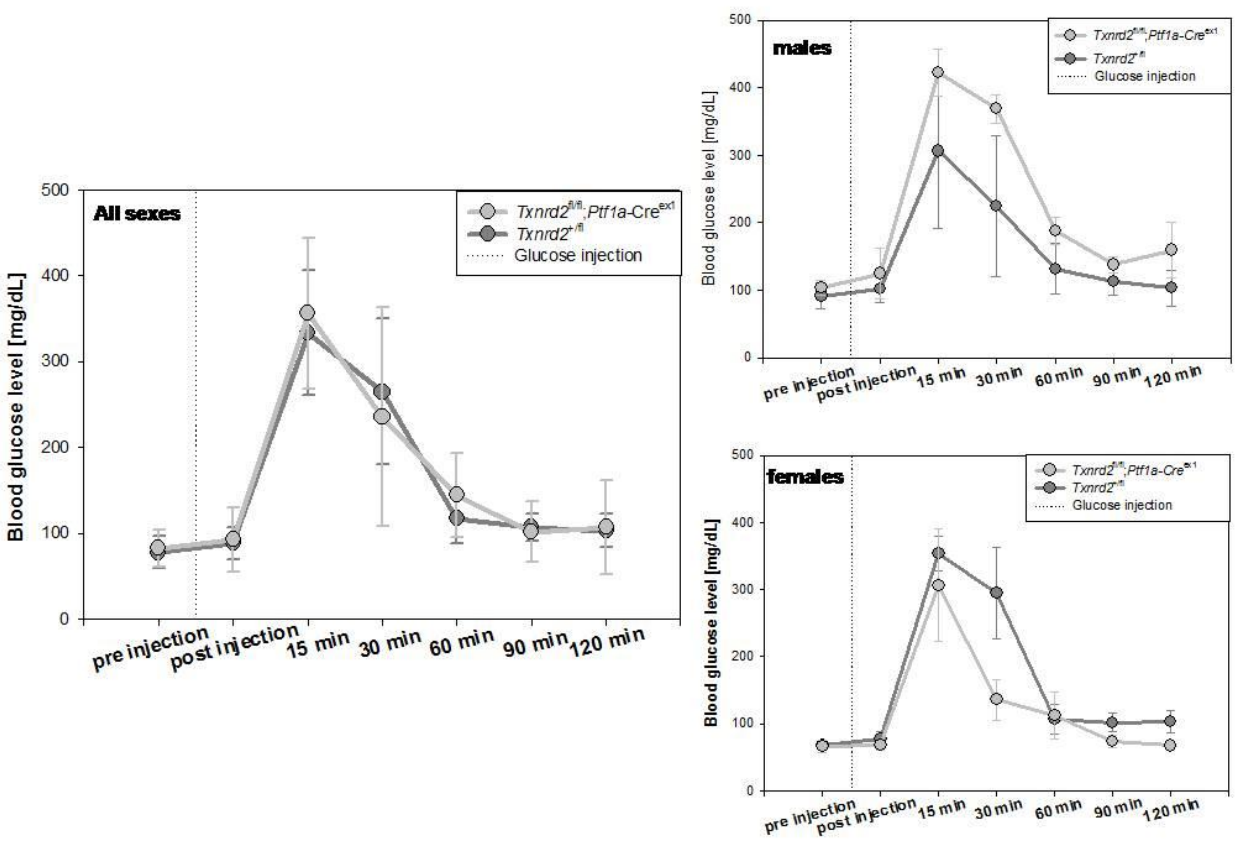

	***Txnrd2*$^{fl/fl}$;*Ptf1a-Cre*^{ex1} IP-GTT blood glucose levels [mg/dL]**						
	pre injection	**post injection**	**15 min**	**30 min**	**60 min**	**90 min**	**120 min**
both sexes	82.7 ± 22	92.7 ± 37.4	356 ± 88.1	235.6 ± 126.9	144.4 ± 49	101.4 ± 35.5	106.9 ± 55.0
males	104 ± 11.3	125 ± 37.3	422.3 ± 34.6	368.7 ± 20.6	188 ± 20.1	138 ± 12.1	159.7 ± 41.1
females	66.8 ± 9.3	68.5 ± 7.0	306.3 ± 84	135.8 ± 30.4	111.8 ± 34.9	74 ± 9.1	67.3 ± 6.9

	***Txnrd2*$^{+/fl}$ IP-GTT blood glucose levels [mg/dL]**						
	pre injection	**post injection**	**15 min**	**30 min**	**60 min**	**90 min**	**120 min**
both sexes	78 ± 18.2	88.1 ± 19.4	333.3 ± 72.8	265 ± 85.4	117.4 ± 29.7	106.9 ± 16.3	103.1 ± 19.1
males	92 ± 19.9	102.3 ± 21.1	306.3 ± 113.8	225 ± 114	132 ± 37.3	113.7 ± 20.3	103.3 ± 26
females	67.5 ± 7.4	77.5 ± 10.1	353.5 ± 26.4	295 ± 67.7	106.5 ± 21.6	101.8 ± 13.4	103 ± 16.7

Fig.72: Intraperitoneal glucose tolerance test in *Txnrd2* knockout and control mice. 2 mg dextrose per g body weight was injected and glucose levels were measured at the time points indicated. Both sexes together (left side) or separately (right side) were analysed. There was no difference of the clearance of blood glucose when both sexes were analyzed together. Male and female knockouts, in separate, showed impaired glucose tolerance, whereas female knockouts showed improved glucose clearing (Dotted line = dextrose injection)

3.4.7 Characterisation of infiltrating inflammatory cells

The cells infiltrating the pancreas of the knockout mice were characterized by immunohistochemical staining against different specific markers. Figure 73 depicts pancreatic sections from four weeks and one year old mice. As already described in chapter 3.4.4, the pancreas of four weeks old knockout mice corresponds to the pathological picture of acute pancreatitis, whereas the pancreas of one year old knockout mice corresponds to chronic pancreatitis. By treating mice with BrdU it could be shown, that the infiltrating cells were proliferating in four weeks as well as in one year old mice (Fig.73,BrdU). A rabbit anti-CD3 antibody was used for detecting T lymphocytes. Most of the infiltrating cells stained positive for CD3 in four weeks and one year old knockout mice (Fig.73,CD3). B lymphocytes were detected with a rat anti-CD45R/B220 antibody. Only a few positive stained cells could be observed in four weeks old knockout mice, but in one year old knockout mice the number increased drastically (Fig.73,CD45R/B220). Neutrophile granulocytes were detected by using an antibody against myeloperoxidase (MPO). In four weeks old knockout mice several neutrophile granulocytes could be detected and also in one year old knockout mice there were a few positively stained cells (Fig.73,MPO). The antibody rat anti-F4/80-BM8 detects specifically mouse macrophages. In four weeks old knockout mice no macrophages could be detected in the pancreas, but in one year old knockout mice (Fig.73,F4/80). All these staining confirmed acute inflammation in four weeks old knockout mice and a chronic inflammation in one year old mice.

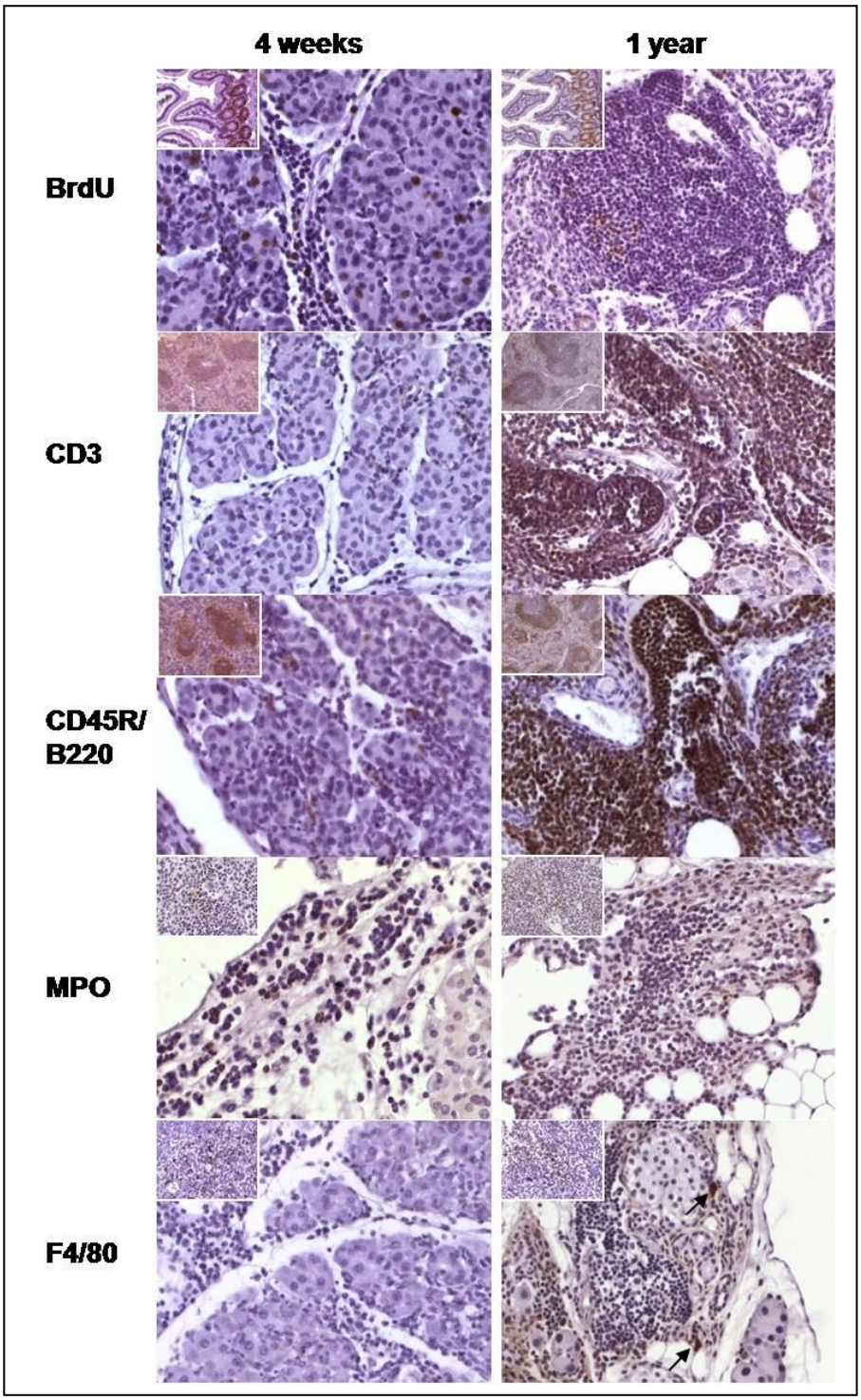

Fig.73: Characterisation of infiltrating inflammatory cells in *Txnrd2* knockout mice. Immuno-histochemical staining characterizing main populations of infiltrating cells in four weeks and one year old mice are shown. (BrdU) The infiltrating cells showed proliferative activity (rat anti-BrdU, 400x). The inlays depict sections of the duodenum as a positive control for proliferating cells (rat anti-BrdU, 400x). (CD3) Most infiltrating cells were T lymphocytes (rabbit anti-CD3, 400x). The inlays depict sections of the spleen as a positive control for $CD3^+$ cells (rabbit anti-CD3, 100x). (CD45R/B220) The number of B lymphocytes increased with age (rat anti-CD45R/B220, 400x). The inlays depict sections of the spleen as a positive control for $CD45R/B220^+$ cells (rat anti-CD45R/B220, 100x). (MPO) Neutrophile granulocytes were detected

in four weeks and one year old knockout mice (rabbit anti-MPO, 400x). The inlays depict sections of the spleen as a positive control for MPO^+ cells (rabbit anti-MPO, 400x). (F4/80) Macrophages were only detected in one year old mice (rat anti-F4/80, 400x, arrows). The inlays depict sections of the spleen as a positive control for $F4/80^+$ cells (rat anti-F4/80, 400x). The results approved acute pancreatitis in four weeks and chronic pancreatitis in one year old *Txnrd2* knockout mice.

3.4.8 Characterisation of metaplastic lesions

Metaplastic lesions found in the exocrine pancreas were classified according to Strobel and colleagues (Strobel *et al*., 2007). Histological samples were stained with H&E for an overview (Fig.74,A). PAS-staining was performed for detection of mucins (Fig.74,B). Immunohistochemical staining was performed for α-amylase as a marker for acinar cells (Fig.74,C,E). Ductal pancreatic cells were stained with the epithelial cell marker cytokeratin 19 (CK19) (Fig.74,D,F). Figure 74 depicts the pancreatic morphology of a one-year-old knockout mouse with metaplastic lesion surrounded by fibrosis. Three different types of metaplasias could be observed. Tubular complexes with an empty lumen lined by many small flat cells (TCs) were first observed at an age of twelve weeks and also in later stages (Fig.61, and Fig.74,E,F). They were only slightly positive for α-amylase (Fig.79,E, arrows) compared to normal acinus cells (Fig.74,E, arrowheads) and they were also positive for CK19 (Fig.74,F). Only a few tubular complexes with a wide empty lumen lined by a few large flat cells with spares cytoplasm (TCL) were found (Fig.74,B). Most metaplasias found in one-year-old mice were mucinous metaplastic lesions (MML). The epithelial cells of MML expressed mucin (Fig.74,B arrows) and varied in height according to the extent of mucin expression. Some lesions exhibited abundant supranuclear mucin and flat, basally located nuclei. Also these lesions stained positive for α-amylase and CK19 (Fig.74,C,D, arrows). The expression of both, acinar and ductal phenotypes in these cells is typical for the formation of acinar to ductal metaplasia.

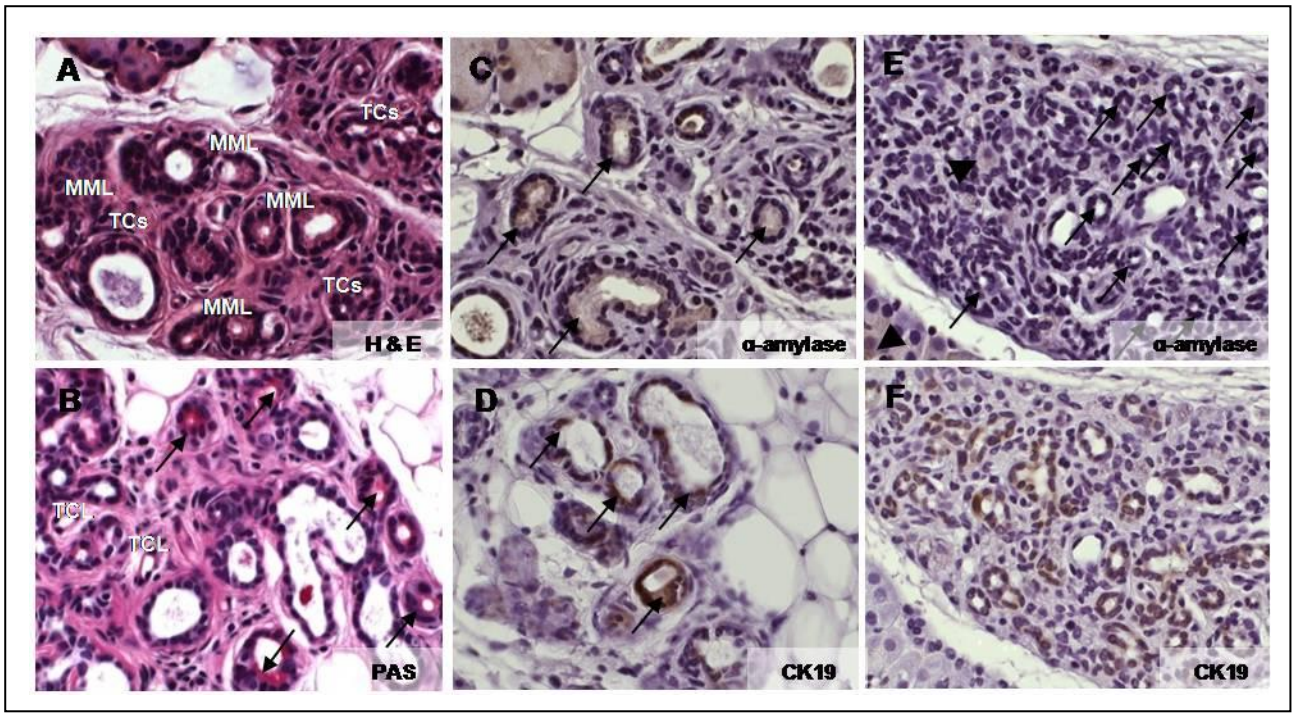

Fig.74: Metaplastic lesions in one year old *Txnrd2* knockout mice. Immunohistochemical characterization of different types of metaplastic lesions observed. (A) Overview (H&E, 630x). (B) Mucin producing MML (PAS, 630x, arrows). (C) α-amylase expressing MML (rabbit anti-α-amylase, 630x, arrows). (D) CK19 expressing MML (rabbit anti-cytokeratin 19, 630x, arrows). (E) α-amylase expressing TCs in field formation (rabbit anti-α-amylase, 630x, arrows, arrowheads = α-amylase expressing normal acinus cells). (F) CK19 expressing TCs in field formation (rabbit anti-cytokeratin 19, 630x). (TCL = tubular complex, lumen surrounded by a few large cells; TCs = tubular complex, lumen surrounded by several small cells; MML = mucinous metaplastic lesion)

3.4.9 Characterisation of fibrosis

The cumulative fibrosis in *Txnrd2* knockout mice was examined after staining the connective tissue with the Masson-Trichrom method. The collagen of the connective tissue is stained in blue. Histological samples of knockout and control mice at the ages of four, twelve and twenty-four weeks and one year were analysed. The same mice as in 3.4.3 were used. Figure 75 depicts representative histological sections of knockout and control mice in an overview magnification of 40x and an indicated area in a magnification of 400x. In the knockout mice fibrosis was observed mainly in areas of metaplastic lesions. Fibrosis increased with age. In the control mice only pancreatic ducts or blood vessels were surrounded by connective tissue, which is a normal finding.

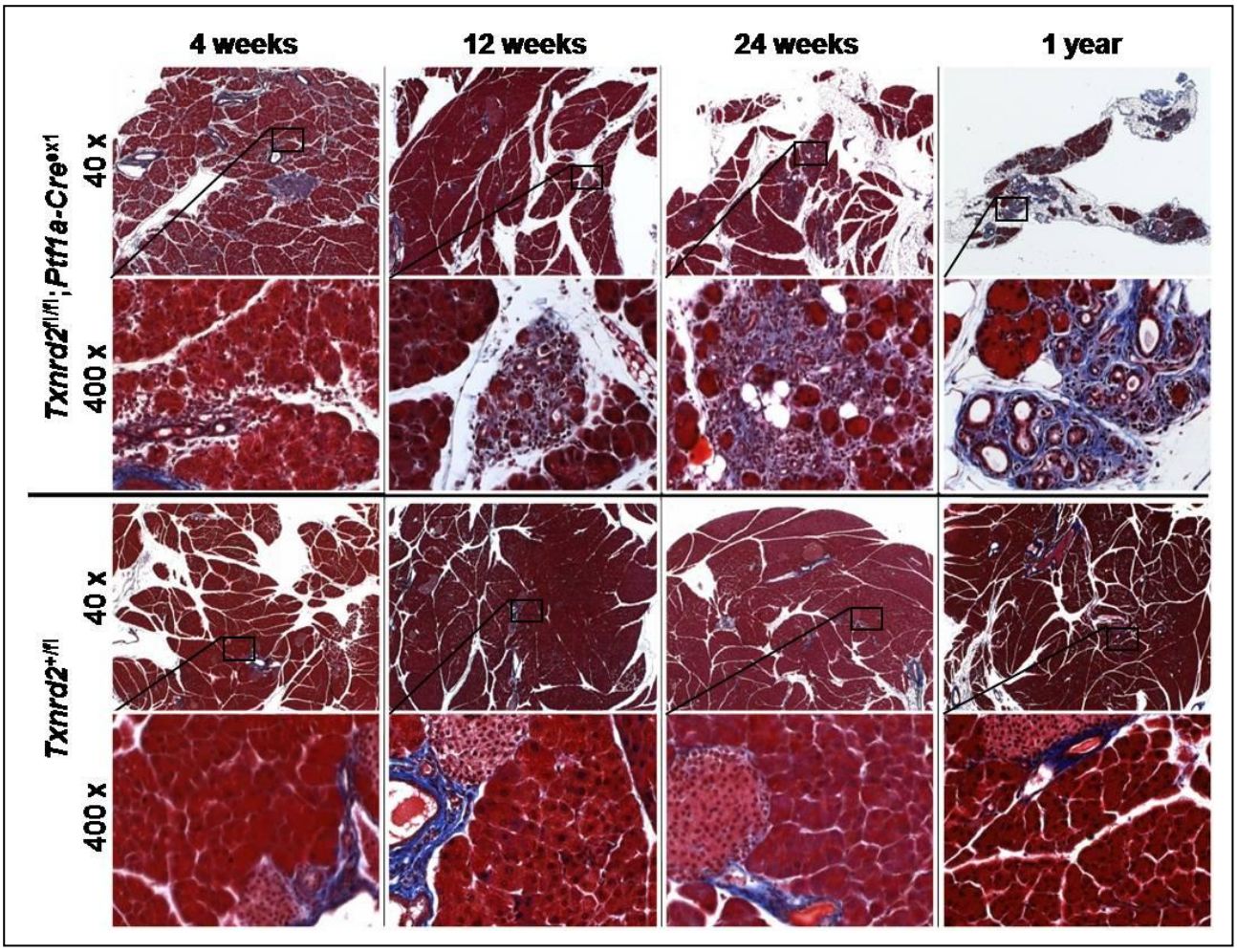

Fig.75: Fibrosis in *Txnrd2* knockout mice. Fibrosis was detected by Masson-Trichrom staining in knockouts (*Txnrd2*$^{fl/fl}$;*Ptf1a-Cre*^{ex1}) and controls (*Txnrd2*$^{+/fl}$). Rectangles indicate the areas chosen for higher magnifications. In *Txnrd2* knockout mice fibrosis was mainly observed in areas with metaplastic lesions and increased with age. In control mice only pancreatic ducts and blood vessels were surrounded by connective tissue, which is a normal finding.

3.4.10 Observation of the lung

Acute pancreatitis is often paralleled by an acute respiratory distress syndrome, which causes a serious lung injury. It is characterized by a diffuse inflammation of the lung parenchyma. In order to find out whether pancreatitis in our genetic model is also paralleled by pneumonia, the lung of *Txnrd2* knockout mice and controls was stained with H&E and examined. The same mice as in 3.4.3 were used. In four weeks old knockout mice 0 out of 8, in twelve weeks old 2 out of 8, in twenty-four weeks old 0 out of 8 and in one year old mice also 0 out of 8 showed areas of inflammation. All other mice were free of inflammation in the lung. The affected areas appeared only in punctual clusters of

infiltrating cells, whereas the remaining lung parenchyma did not show pathological alterations (Fig.76). Focal inflammation was also found in lungs of control mice (four weeks: 0/8, twelve weeks: 2/8, twenty-four weeks: 1/8 and in one year old mice 1/8) (Fig.76). An acute respiratory distress syndrome was excluded by these investigations.

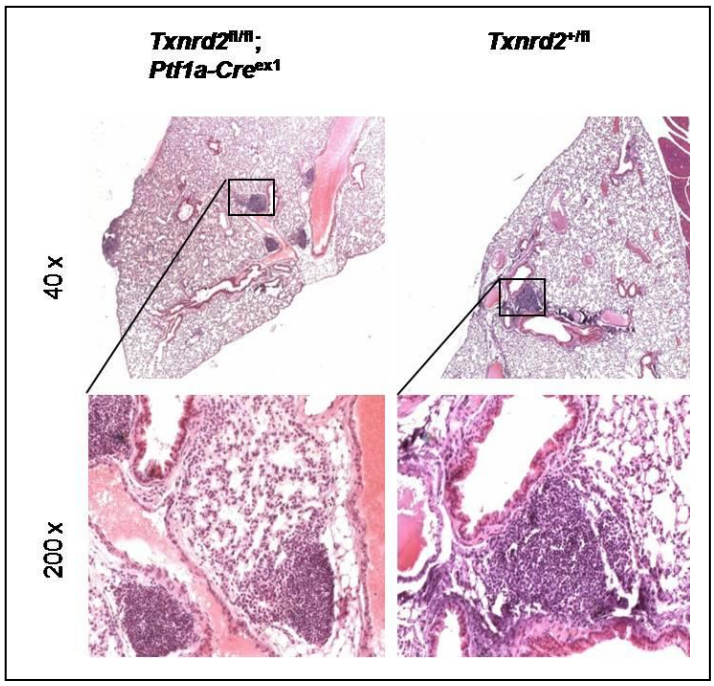

Fig.76: Lung of *Txnrd2* knockout and control mice. Focal sites of inflammation found in the lung of some *Txnrd2* knockout (*Txnrd2*$^{fl/fl}$;*Ptf1a-Cre*^{ex1}) and control mice (*Txnrd2*$^{+/fl}$). Such focal lesions have been found independent of the genotype. Rectangles indicate the areas chosen for higher magnifications. (H&E, 40x and 200x)

3.4.11 Monitoring of other target organs of *Cre*-expression under the control of the *Ptf1a*-promotor

Apart from directing *Cre*-expression to the pancreas, the promoter *Ptf1a* drives *Cre*-expression also in GABAergic cells in the neuroretina of the eye, as well as in neuronal cells of the cerebellum (Hoshino *et al*., 2005; Nakhai *et al*., 2007). The affected cell type in the cerebellum is the purkinje cell. To monitor potential effects of the knockout of mitochondrial thioredoxin reductase in these tissues, the eye and the cerebellum were screened by behavioural and functional tests and histological methods.

The eye screen routinely performed by the German Mouse Clinic showed, that one-year-old *Txnrd2* knockout mice had the full vision compared to age matched controls. Only some age-related alterations were found in both genotypes.

Behavioural observations did not indicate a defect of the cerebellum of one-year-old knockout mice, as compared to control mice. Further, the histological appearance did not show any alterations in knockout mice. Figure 77 depicts representative examples of the cerebellum stained with H & E of *Txnrd2* knockout and control mice and an immunohistchemical staining of the purkinje cells.

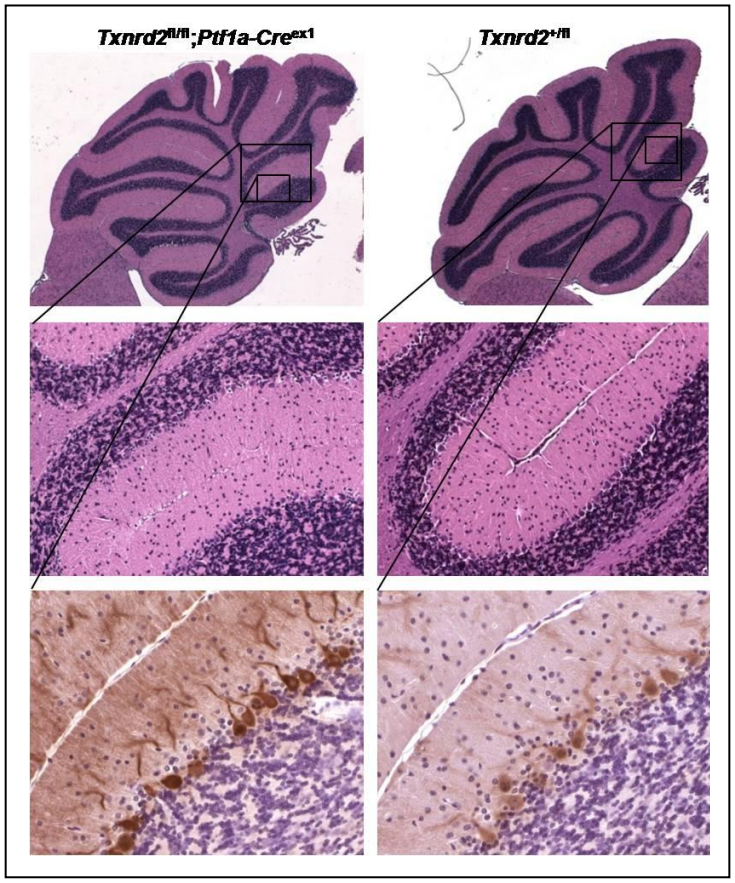

Fig.77: Cerebellar morphology of *Txnrd2* knockout and control mice. H & E stained paraffin sections of low magnification for overview (upper panel, 40x). Magnifications from the upper panel are shown in the middle panel (200x). The lower panel shows immunohistochemical staining of Purkinje cells with an rabbit anti- calbindin antibody (400x). Rectangles indicate the areas chosen for higher magnifications. No alteration in the knockout (*Txnrd2*$^{fl/fl}$;*Ptf1a-Cre*^{ex1}) cerebellum have been present.

4 Discussion

Despite rapid progress in understanding molecular mechanisms leading to pancreatic cancer, this cancer is still considered a fatal disease. The five-year survival rate is less than 5% which is a result of ineffective early detection methods, nonspecific symptoms hampering diagnosis and poor efficacy of the therapies for advanced disease (Hruban *et al*., 2006b; Welch *et al*., 2000). Today, pancreatic cancer is the fourth leading cause of cancer-related deaths in Germany and in the United States (Jemal *et al*., 2007; DKFZ, 2006). Most pancreatic cancers are ductal adenocarcinomas, occur sporadically and show a very aggressive course of disease. Among all cases of this cancer, there are approximately 5-10% of patients with a family history of pancreatic cancer (Klein *et al*., 2001). Preventive strategies in individuals with familial pancreatic carcinoma are therefore highly desirable. Based on the following findings we chose selenium as potential chemopreventive agent in pancreatic carcinogenesis.

Several epidemiological studies showed an inverse correlation between selenium-intake and age-adjusted mortality of certain types of cancer (Clark *et al*., 1991; Yu *et al*., 1985; Shamberger *et al*.,1976). Clinical data also showed cancer-preventive properties of selenium, when added to the normal diet, in all and particularly in gastrointestinal cancers (Rayman, 2005; Bjelakovic *et al*., 2004; Whanger, 2004). Until now, no controlled or randomized interventional study has been published, proving the specific effect of selenium on pancreatic cancer. Yet, data from epidemiological and case-control studies supported a protective effect (Knekt *et al*., 1990; Burney *et al*., 1989). Previous animal studies on the effect of antioxidants, including selenium, on pancreatic carcinogenesis were based on chemically induced models (Woutersen *et al*., 1999; Appel *et al*., 1996; Nishikawa *et al*., 1992; Birt *et al*., 1988; Curphey *et al*., 1988). In contrast, in the present study, the influence of the selenium status was investigated in a genetically defined pancreatic cancer mouse model, the EL-TGFα$^{tg/+}$;*p53*$^{+/-}$ mouse strain, recapitulating the genetic changes seen in human patients (Schreiner *et al*., 2003; Wagner *et al*., 2001).

In the study presented here, in the hyperacute phase of disease, all mice developed cancer. Due to *p53* hemizygousity, the mice showed a broad spectrum of tumour types (Jacks *et al*., 1994; Donehower *et al*., 1992). Sometimes even more than one tumour type was found in one mouse. Although the different tumour types have been diagnosed and the numbers counted, tumours other than pancreatic carcinomas have not been analyzed in detail and the influence of selenium on these tumours was not the focus of this study.

There was no obvious cancer-preventive effect of selenium in tumour latency or prevalence. This was unexpected, since as outlined above clinical data showed a cancer-protective effect in gastrointestinal cancers (Rayman, 2005; Bjelakovic *et al*., 2004; Whanger, 2004) (Fig.23). Although, in selenium-deficient mice a smaller percentage of the tumours were pancreatic carcinomas than in selenium-adequate mice.

As a major finding, the pancreatic carcinomas in this mouse model showed different grades of differentiation. The differentiation grade of pancreatic carcinomas was strongly influenced by the selenium status (Fig.28). In the selenium-deficient group there were more non-differentiated pancreatic carcinomas than in the selenium-adequate group, which highlighted the implication of selenium or selenoproteins in tumour differentiation. This phenomenon was also seen with other non-selenoprotein, redox active enzymes such as manganese superoxide dismutase (MnSOD). Men with a homozygous mutation of MnSOD showed an increased risk for high-grade prostate cancer. A positive correlation between low/baseline selenium levels in these patients and the development of more aggressive cancer was also observed (Li *et al*., 2005), indicating an effect of selenium / selenoproteins. Further, *in vitro* studies with pancreatic adenocarcinoma cell lines also showed a correlation between decreased activity of MnSOD and grade of differentiation of the tumour cell lines (Cullen *et al*., 2003).

In the present study, sodium selenite was chosen as selenium source. This inorganic selenium compound is incorporated predominantly into selenoproteins, since, in contrast to organic selenium compounds, it cannot be incorporated non-specifically into proteins (Rayman, 2004). Therefore, effects seen in this study are primarily selenoprotein associated effects. Low levels of selenoproteins may therefore enforce dedifferentiation or impair differentiation programs in the tumour or tumour precursor cells as shown for the maturation program of spermatozoa during spermatogenesis (Olson *et al*., 2005; Su *et al*., 2005).

In a study with knockouts of selenoprotein P (SePP), a selenium transport protein, more malignant tumours were found in the APC^{min} model of colon carcinoma (L. Schomburg, personal communication).

Within the selenoproteins, *Txnrd1* is a strong candidate, because it is strongly associated with tumour cell proliferation in vitro and with the function of the tumour suppressor p53. The fact, that administration of selenite causes the inhibition of tumour cell proliferation *in vivo* and the finding, that thioredoxin reductase showed higher levels in malignant cells, prompted *in vitro* investigations on selenite as an inducer of the mammalian thioredoxin

system. In contrast to what was expected, it was discovered that selenite is a direct substrate of thioredoxin reductase as well as an efficient oxidant of thioredoxin (Kumar *et al*., 1992). Until that finding it was assumed, that selenite and glutathione react to form selenodiglutathione (GS-Se-SG), which has been suggested to be a major metabolite of inorganic selenium salts in mammalian tissue (Hsieh and Ganther, 1975). It was also demonstrated, that GS-Se-SG is reduced by glutathione reductase. Therefore, it has been proposed to be a source of selenide in cells as well as an inhibitor of neoplastic growth (Shamberger, 1985; Ganther, 1971). With a synthetic GS-Se-SG it was shown that this compound is a direct substrate for mammalian thioredoxin reductase and a highly efficient oxidant of reduced thioredoxin (Luthman and Holmgren, 1982; Holmgren, 1977).

In summary, using a genetically defined mouse model of pancreatic carcinogenesis, our data suggest that selenium in physiological concentrations does not prevent or decelerate pancreatic adenocarcinoma, but significantly alters the differentiation status of the tumour. These findings point to a new role for this trace element in cancer development and cancer cell differentiation, which may serve for new intervention or treatment strategies.

Until now, no specific data about selenium-content and Txnrd activity in the pancreas have been published, but it is well established, that a hierarchy exists, in which order organs are provided with selenium. In selenium deficiency mainly liver, kidney and skeletal muscle are reduced in the selenium-content, whereas brain, endocrine and reproductive organs are preferentially supplied with selenium (Hill *et al*., 1992; Behne *et al*. 1988). In these organs also the activity of some selenoproteins like Txnrd, SelW is hardly affected, wheras the activity of other selenoproteins vanishes (Whanger, 2001; Yeh, 1997). This is due to a second hierarchy, the hierarchy in selenoprotein expression in various conditions in a given organ. In selenium-deficiency, the levels of GPx1 and SePP are drastically reduced, while iodothyronine deiodinase 1 (DIs1) and GPx4 are nearly unaffected (Brigelius-Flohe, 1999; Bermano *et al*., 1995). In the work presented here it was shown, that the pancreas has a moderate ability to store selenium and the selenium content is significantly reduced in selenium-deficiency, although the content of selenium in the islets of Langerhans has not been determined specifically (Fig.19). This leads to the suggestion, that at least the exocrine pancreas is not a “selenium priority organ” like brain, reproductive and other endocrine organs. The influence of selenium deficiency on the activity of TXNRD1 and TXNRD2 in the pancreas was different. Only the activity of TXNRD1 in the cytosol was reduced (Fig.29). Unexpectedly, in the mitochondria the activity of TXNRD2 was the

highest upon all organs tested and more importantly its activity was raised under selenium deficiency (Fig.30).

After identifying them as important selenoproteins in the pancreas, the role of Txnrd1 and Txnrd2 was investigated by pancreas-specific knockout mice. The embryonic lethality of mice which hampered analysis of a total knockout of these enzymes in adult mice (Jakupoglu *et al*., 2005; Conrad *et al*., 2004) was bypassed by the use of the *Cre*/*loxP* technology. To create pancreas-specific knockout mice, *Cre*-expression was directed to the pancreas under the control of the *Ptf1a-p48* promoter (Nakhai *et al*., 2007). In both mouse strains, the knockout was validated on DNA, mRNA and enzymatic activity level.

Enzymatic activity in the *Txnrd1* knockout mice was not totally eliminated by the knockout, but significantly reduced (Fig.37). This might be due to the fact, that *Ptf1a-Cre*^{ex1} is only expressed in about 50% of endocrine cells (R. Schmid, personal communication). It is also possible, that not 100% of the exocrine pancreatic cells were knocked out. Regarding the situation in humans, this partial reduction in TXNRD1 activity is highly relevant for two reasons. In the area of Germany, the selenium content of the soil and subsequently the intake of selenium by nutrition in humans and animals is low (Sill, 1999). In this respect, the pancreas-specific *Txnrd1* knockout mice represent the situation in humans. The enzymatic activity ranged around the activity of TXNRD1 in selenium-deficient mice (Fig.31). Since homozygous *TXNRD1* null mutations in humans have not been described and most probably are lethal like in mice, mutations might still be present on one allele and this situation causing a hypomorph gene phenotype is also mimicked by our conditional model.

The *Txnrd1* knockout mice did not show an obvious phenotype. The mice behaved normal and the pancreas did not show any gross morphological alterations. The endocrine pancreas of *Txnrd1* knockout mice did not show morphological alterations (Fig.47), which might be a result of the fact, that the *Ptf1a-Cre*^{ex1} is only expressed in about 50% of endocrine cells (R. Schmid, personal communication). Also the blood glucose levels did not show any differences between knockout and control mice over an observation period of one year (Fig.48). Surprisingly, in an intraperitoneal glucose tolerance test, knockout mice showed an impaired glucose tolerance (Fig.49). It was already shown, that Txnrd and Txn are expressed in the islets of Langerhans and the expression is increased during starvation (Hansson *et al*., 1986). Also, selenium-deficient animals have low serum insulin, and their islets show impaired protein secretion that can be normalized by selenium and vitamin E (Tong and Wang, 1998). To get a better insight into the role of Txnrd1 in the

endocrine pancreas further investigations in knockout mice with a Cre-recombinase directed by a specific promoter to the endocrine pancreas are needed.

The exocrine pancreatic function was unimpaired, but interestingly, in one-year-old knockout mice, the ultrastructure of acinus cells showed a mosaic of bright and electron dense cells (Fig.43). A similar picture was observed in ethanol-fed alcohol dehydrogenase-deficient (ADH^-) mice (Bhopale *et al*., 2006). In the bright cells of the ADH^- mice, a dilated rough endoplasmic reticulum was observed, which was also seen in the bright acinus cells of the *Txnrd1* knockout mice. It is assumed, that such an effect is the result of alterations in the structure of several proteins, resulting in ER stress due to their impaired exit from the ER as found in alcoholic liver disease (Ji and Kaplowitz, 2004). ER stress can be a result of suppression of protein glycosilation, disruption of calcium homeostasis or redox alterations (Shen *et al*., 2004). These perturbations all lead to protein misfolding or unfolding, which in turn initiates a series of transducer pathways as a self-protective mechanism. This so-called unfolded protein response is characterized by an immediate stop of new protein synthesis and growth arrest, followed by adaptive survival or apoptosis, if the rescue effort is exhausted (Kadowaki *et al*., 2004; Ma and Hendershot, 2004; Shen *et al*., 2004). In the electron-dense cells loss of the rER membrane was observed which maybe a further result of ER stress but which cannot yet be classified. Further experiments are necessary to soundly characterise study ER stress and its consequences in our model.

Despite these alterations in the rER, in a lipid absorption test the knockout pancreas did not show altered integrity and the mice were was able to digest fat (Fig.46). Also the blood serum markers for the function of the exocrine pancreas, amylase and lipase, were not significantly influenced in quantity in one-year-old knockout mice. Only amylase was slightly reduced. In contrast, in four-weeks-old knockout mice, blood serum amylase and lipase were significantly reduced and increased over the observation period (Fig.45). This observation warrants further investigations.

Like in *Txnrd1* knockout mice, the enzymatic activity of TXNRD2 was not totally eliminated in *Txnrd2* knockout mice, but significantly reduced (Fig.54). As figured out for *Txnrd1* knockouts this is a highly relevant situation for humans. Studies are under way to determine whether mutations in the human *TXNRD2* gene are linked to familial cases of pancreatic disease (R. Schmid, personal communication).

Already at an age of four weeks, *Txnrd2* knockout mice showed signs of mild pancreatitis. First, loss in organ size (Fig.57) and weight (Fig.58) was discovered and the pancreatic

connective tissue was infiltrated with inflammatory cells (Fig.60). The inflammatory cells were a composition of T- and B-lymphocytes as well as neutrophile granulocytes. Additionally, oedematous fluid was present in the extracellular space, but there were no further changes in the parenchyma. These are all characteristic features of acute pancreatitis (Bockman, 1997). Remarkably, this phenotype was not evident in three-weeks- old or younger mice (Fig.59). At an age of three weeks, infant mice were separated from their mothers; therefore their nutrition changed from milk to standard rodent chow. Also, at an age of three weeks, TXNRD2 activity in the control pancreas was quite low (Fig.54) compared to the activity in older wild type mice (Figs.30 and 32). It is possible, that pancreatic activity is boosted when weaned mice start to ingest standard chow and need the full spectrum of pancreatic enzymes for digestion of the nutritive components of that diet and that this change in diet is paralleled by an increase in TXNRD2 activity. There is nearly no data available on the physiology of the pancreas in infant mice, and this needs therefore further efforts.

The exact mechanisms that provoke acute pancreatitis are still unknown, but it is believed that intra-acinar cell activation of digestive enzymes is an early event of acinar and ductal cell injury (Rubin and Farber, 1990). Inappropriate activation of trypsinogen to trypsin causes autodigestion of the organ which leads to pancreatic inflammation. Also, reactive oxygen species (ROS) can attack polyunsaturated fatty acids, which results in peroxidation of lipids (Slater, 1984; Stocks and Dormandy, 1971; Frees *et al*., 1967). Polyunsaturated fatty acids are present in high concentrations in cellular membranes and are most susceptible to free radical attacks. Reactions of ROS with these membrane constituents can lead to disintegration of the cells and subsequently cell death (Slater, 1984). It is therefore tempting to assume that oxidative damage by ROS marks the start of pancreatitis in our model. ROS have been implicated in the induction of acute human or experimental pancreatitis (Dabrowski *et al*., 1999; Tsai *et al*., 1998). At an early stage of acute pancreatitis, before morphological alterations could be observed, lipid peroxidation products were found to be increased. It was also shown, that oxidized glutathione (GSSG) increased at the expense of reduced glutathione (GSH) at an early stage of cerulein-induced pancreatitis, which was interpreted as a manifestation of oxidative stress (Schonberg *et al*., 1994, 1990; Dabrowski and Chwiecko, 1990). Experiments testing the expression of oxidative stress markers like HO-1 by western blot technique are under way to examine if oxidative stress is also the reason for acute pancreatitis in the case of *Txnrd2* knockout mice.

Acute pancreatitis is often paralleled by an acute respiratory syndrome (Whitcomb, 2006; Baron and Morgan, 1999). In our mouse model, no generalized pneumonia was observed. The small, punctual sites of inflammation (Fig.76) found in our animals are a common finding also in mice from other animal husbandries and have not been correlated to the genotype of the mice (H. Algül, personal communication). This is therefore regarded as an effect not related to pancreatitis.

In twelve-weeks-old mice, first signs of chronic injury of the pancreatic tissue were observed and became more evident at twenty-four weeks and in one-year-old mice. The lesions were characterized by acinar atrophy, apoptotic cell death of acinar cells, fat necrosis, fibrosis and infiltration of inflammatory cells as well as formation of metaplastic lesions. Also, in one-year-old heterozygous *Txnrd2* knockout mice inflammatory infiltrates were observed. In contrast to the acute pancreatitis observed in four-weeks-old *Txnrd2* knockout mice, the inflammatory infiltrates in older *Txnrd2* knockout mice were present in clusters and consisted mainly of B- and T-lymphocytes. A few neutrophile granulocytes and infiltrating macrophages appeared. This composition of infiltrating inflammatory cells has been described as a typical feature of chronic pancreatitis with fat necrosis (Shimizu *et al*., 2006; Rubin and Farber, 1990).

Chronic pancreatitis often leads to destruction of the endocrine pancreas (Etemad and Whitcomb, 2001). In our model the endocrine pancreas was widely unaffected and the infiltrating cells did not enter the islets of Langerhans (Fig. 60, 62-64, 70). Also, blood glucose homeostasis was not affected over an observation period of one year (Fig.71). It is highly interesting to see that in our genetically induced model of pancreatitis only the exocrine pancreas is affected in contrast for example to alcohol abuse induced pancreatitis. It seems that damage is limited to those cells without thioredoxin reductase activity and the endocrine cells expressing it are able to remain integrity even in an inflamed environment.

In a glucose tolerance test, sex-dependent, marginally impaired glucose tolerance has been observed in males. The expression of several selenoproteins shows, sex- and age-related effects (Schomburg *et al*., 2007; Riese *et al*., 2006) Further investigations, e.g. with mice where *Txnrd2* is deleted specifically in the endocrine pancreas are needed to address this topic in further detail.

Chronic pancreatitis often leads to total destruction of the pancreas and results in malabsorption of dietary nutrients (Etemad and Whitcomb, 2001). Exocrine pancreatic function of *Txnrd2* knockout mice was tested by a lipid absorption test as well as by testing

the serum markers amylase and lipase. In the lipid absorption test, *Txnrd2* knockout mice showed mild steatorhea. The amylase and lipase levels in the blood serum were not increased. This was unexpected because of the massive acinar cell destruction and the possible release of pancreatic enzymes into the blood. It is conceivable, that cell destruction in this model appears so slow that the low amounts of constantly released pancreatic enzymes can be cleared from blood without reaching aberrant levels.

Destruction of the pancreas and dilation of acinar cells were observed by an ultrastructural analysis. Here, clear signs of apoptotic cell death were found in acinus cells (Fig.67). The cell death in these *Txnrd2* knockout mice might therefore be a result of the mitochondrial destruction observed in the acinus cells (Fig.67). The mitochondria were swollen and had lost the structure of their cristae. Similar mitochondrial alterations have been observed in the heart-specific *Txnrd2* knockout (Conrad *et al*., 2004). Therefore, this seems to be a typical cellular *Txnrd2* knockout feature marking a critical step in cell death in our model.

Txnrd2 knockout mice developed several types of acinar to ductal metaplasias (Fig.74). The origin of these metaplastic lesions is unknown but they can be grouped into two different types, tubular complexes and mucinous metaplasia including pancreatic intraepithelial neoplasia (Bockman *et al*., 2003; Hruban *et al*., 2001). Most of the metaplastic lesions found in *Txnrd2* knockout mice were tubular complexes with an empty lumen lined by many small flat cells (TCs) (Fig.61, and fig.74,E,F). This type of tubular complexes was first observed at an age of twelve weeks and was evident until an age of one year. Only a few tubular complexes with a wide empty lumen lined by a few large flat cells with sparse cytoplasm (TCL) were found (Fig.74,B). In one-year-old mice also mucinous metaplastic lesions (MML) were found (Fig.74,A). There is a strong association between chronic pancreatitis and an increased risk of developing pancreatic ductal adenocarcinoma (PDA) (Howes *et al*., 2004; Malka, *et al*., 2002; Whitcomb and Pogue-Geile, 2002; Lowenfels *et al*., 1997, 1993). In this respect, mucinous metaplastic lesions showed characteristic features of early pancreatic intraepithelial neoplasia, like production of abundant supranuclear mucin and flat, basally located nuclei (Hruban *et al*., 2006a). Pancreatic intraepithelial neoplasias are commonly accepted precursor lesions of pancreatic ductal adenocarcinomas (Hruban *et al*., 2006a). The role of candidate genes mediating the passage from chronic pancreatitis to pancreatic carcinomas, like activating K-ras mutations (Guerra *et al*., 2007; Aguirre *et al*., 2003; Grippo *et al*., 2003; Hingorani *et al*., 2003) have to be studied in future experiments in order to identify molecular pathways underlying this phenomenon.

Experimental chronic pancreatitis in mice is normally induced by a laborious cerulein treatment schedule over several months that is very stressful for the animals. Until now, there was no genetically defined mouse model, which shows the spontaneous development of acute pancreatitis followed by a chronic course of the disease. The *Txnrd2* knockout mice developed a large spectrum of characteristics known from human acute and chronic pancreatitis. They showed pancreatic oedema with patterns of inflammatory cells typical for acute and chronic pancreatitis. Pancreatic atrophy and fat necrosis as a consequence of severe apoptotic cell death was present. As a result of this pancreatic injury, the mice developed steatorrhea. The most interesting finding in these mice was the development of acinar to ductal metaplasias, which in part showed features of early pancreatic intraepithelial neoplasias, the precursor lesion of pancreatic ductal adenocarcinomas. The *Txnrd2* knockout mice therefore represent a unique and powerful tool to model the pathogenesis of pancreatic diseases in several risk groups of humans prone to familial chronic pancreatitis and pancreatic cancer. Recently, another genetically modified mouse model for hereditary pancreatitis has been published (Archer *et al*., 2006). These transgenic mice harbour a missense mutation of the trypsinogen gene. Pancreata displayed an early-onset of acinar cell injury and inflammatory cell infiltration. With progressing age, they developed pancreatic fibrosis and acinar cell dedifferentiation, but only upon cerulein treatment, the mice developed chronic pancreatitis.

As already discussed for heart and brain (Conrad *et al*., 2006), *Txnrd1* and *Txnrd2* seem to have widely non-redundant functions also in the pancreas. In wild type mice TXNRD1 shows moderate activity in the pancreas, whereas TXNRD2 is highly active, also in comparison to other organs. Under selenium-deficient conditions, TXNRD1 activity decreased, whereas TXNRD2 activity even increased. These observations gave already a cue on different roles of these enzymes in the pancreas. The characterisation of the two pancreas-specific knockout mouse strains confirmed this assumption. The strains developed completely different phenotypes.

In the first part of this study it was shown that selenium influences the differentiation status of pancreatic carcinomas in a genetically defined mouse model. This finding initiate further studies since it points to a new role of the trace element. Understanding the role of selenium in differentiation and apoptosis may serve in future for new intervention or treatment strategies. As sodium selenite was used in the study, the effects seen can be attributed to selenoproteins. Within those, the thioredoxin reductases represent strong candidates mediating selenium effects. The following parts of this study therefore attended

to the role of the selenoproteins TXNRD1 and TXNRD2 in the pancreas. In the pancreas-specific knockout mice different phenotypes were observed. The pancreas-specific knockouts of *Txnrd1* lead to an altered rER and impaired glucose tolerance. Further investigations are needed to characterise the alterations of the rER and to evaluate the consequences of ER stress. Because of the observed impaired glucose tolerance in this mouse model also the role of *Txnrd1* in the endocrine pancreas should be investigated in more detail. The best way to do this might be the use of a conditional knockout mouse model in which Cre-expression will be directed to the endocrine pancreas with a tissue-specific promoter.

In contrast to the pancreas-specific knockout of *Txnrd1*, the pancreas-specific knockout of *Txnrd2* lead to acute and chronic pancreatitis with formation of acinar-ductal metaplasias, which in part showed features of early precursor lesions of pancreatic ductal adenocarcinomas. This mouse model harbours enormous possibilities to investigate the link between acute and chronic pancreatitis and pancreatic carcinogenesis. However, to get a more detailed insight into the role of *Txnrd2* in pancreatic carcinogenesis, further laborious experiments will be necessary. It is planed to cross *Txnrd2* knockout mice into different pancreatic cancer mouse models.

So far, the most important finding out of the *Txnrd2* knockout mice is the fact, that this is the first mouse model which spontaneously develops a phenotype resembling this important human disease. As one consequence of these findings, human samples can be screened now for alterations in the *TXNRD2* gene to evaluate a potential risk-group for pancreatic diseases. In addition, this mouse model will serve in the near future for studies on the pathogenic mechanism of pancreatic diseases, prevention studies and therapeutic concepts.

5 Summary

Pancreatic ductal adenocarcinoma (PDA) is one of the most aggressive cancers in humans. It is the fourth leading cause of cancer related deaths in Germany and in the United States. Most PDA occurs sporadically, but there are also approximately 5-10% of patients with a family history of pancreatic cancer. The high mortality of PDA is attributed to a lack of early detection methods and poor efficacy in therapies for advanced disease. As an alternative, preventive strategies in individuals with familial pancreatic carcinoma should be considered. Several epidemiological studies showed an inverse correlation between selenium-intake and mortality of certain types of cancer and particularly in gastrointestinal cancers.

To this end, in the first part of this study, the influence of selenium as a preventive nutritional additive was investigated in a genetically defined pancreatic cancer mouse model, the EL-TGFα$^{tg/+}$;*p53*$^{+/-}$ mouse strain. As a major finding, the differentiation grade of the pancreatic carcinomas was heavily influenced by the selenium status. In the selenium-deficient group there were more non-differentiated pancreatic carcinomas than in the selenium-adequate group, which highlighted the implication of selenium or selenoproteins in tumour differentiation. Unexpectedly, however, there was no protective effect of selenium on total or pancreatic tumour latency.

Within the selenoproteins, the thioredoxin reductases are strong candidates which may influence cell death and differentiation in pancreatic carcinogenesis. Their function is generally associated with tumour proliferation and also linked to the activation of the tumour suppressor p53. Consequently, the role of the thioredoxin reductases in the pancreas was studied in the second part of this thesis.

The enzymatic activity of cytosolic (TXNRD1) and mitochondrial (TXNRD2) thioredoxin reductase in the pancreas and other organs was determined in relation to the selenium-status. TXNRD1 activity in the pancreas was moderate and decreased under selenium deficiency. TXNRD2, instead, showed very high pancreatic activity in relation to other organs and its activity was even increased under selenium-deficiency emphasising its special role in this organ.

To further investigate the function of Txnrd1 and Txnrd2 in the pancreas, tissue-specific knockout mice were created and characterized. The *Txnrd1* knockout mice did not show an overt phenotype. Interestingly although, pancreatic acinus cells in one year old mice showed a disturbed rough endoplasmic reticulum and alterations in serum amylase and

lipase. These mice also had an impaired glucose tolerance. The pancreas of *Txnrd2* knockout mice showed severe chronic pancreatitis and pancreatic atrophy at the end of an observation period of one year. The progressive pathogenic process started with mild pancreatitis, developing spontaneously at an age of four weeks. The chronic stage was characterized by the formation of different types of acinar-to-ductal metaplastic lesions, which could be classified in part as early precursor lesions of pancreatic carcinomas. The endocrine pancreas was not affected.

The pancreas-specific *Txnrd2* knockout mouse strain is the first genetically modified mouse model spontaneously developing acute and chronic pancreatitis. This strain constitutes a unique and powerful tool to model pancreatic pathogenesis, especially the yet unresolved process of transformation from inflammatory to malignant disease.

6 Zusammenfassung

Das duktale Adenokarzinom des Pankreas gehört zu den aggressivsten Krebsarten des Menschen. In Deutschland wie auch in den USA bilden Krebserkrankungen des Pankreas die viert häufigste durch Krebs hervorgerufene Todesursache. Obwohl die molekularen Mechanismen des duktalen Adenokarzinoms immer besser verstanden werden, nimmt diese Krebserkrankung meist einen tödlichen Verlauf. Die hohe Sterblichkeitsrate wird vor allem durch fehlende Möglichkeiten der Früherkennung und mangelnde Effektivität der Behandlungsmethoden bei fortgeschrittener Krankheit begründet. Zumeist tritt das Pankreaskarzinom spontan auf, jedoch bei 5-10% der Patienten lässt sich ein familiärer Hintergrund nachweisen. Für diese Patientengruppe sollten präventive Maßnahmen angestrebt werden. In epidemiologischen Studien konnten Hinweise zu einer inversen Korrelation von Selenaufnahme und altersabhängiger Sterblichkeit bei verschiedenen Krebsarten und vor allem bei gastrointestinalen Krebserkrankungen erarbeitet werden.

Im ersten Teil der hier vorliegenden Studie wurde daher der Einfluss von Selen auf das Pankreaskarzinom des genetisch definierten EL-TGFα$^{tg/+}$;*p53*$^{+/-}$ Mausmodelles beforscht. Selen-defiziente Mäuse wurden mit Selen-adäquat ernährten Mäusen verglichen. Interessanter Weise wurde der Differenzierungsgrad der entstandenen Pankreaskarzinome hoch signifikant durch den Selenstatus der Mäuse beeinflusst. Selen-defizient ernährte Mäuse entwickelten hauptsächlich anaplastische Pankreaskarzinome, wohingegen Selen-adäquat ernährte Mäuse mehr differenzierte Tumoren aufwiesen. Unerwarteter Weise konnte jedoch kein protektiver Einfluss von Selen weder auf die Latenzzeit aller auftretender Tumoren, noch im einzelnen auf Pankreaskarzinome festgestellt werden.

Innerhalb der Gruppe der Selenoproteine sind die Thioredoxinreduktasen potentielle Kandidaten welche den Zelltod und die Differenzierung von Pankreaskarzinomen beeinflussen. Ihre Funktion wird im Allgemeinen mit der Proliferation von Tumoren und der Aktivierung des Tumorsupressors p53 in Verbindung gebracht. Folglich wurde die Rolle der Thioredoxinreduktasen im Pankreas im zweiten Teil dieser Studie bearbeitet.

Die enzymatische Aktivität der cytosolischen (TXNRD1) und mitochondrialen (TXNRD2) Thioredoxinreduktase im Pankreas und anderen Organen wurde im Allgemeinen und in Bezug auf den Selenstatus der Tiere bestimmt. Die enzymatische Aktivität von TXNRD1 im Pankreas war eher mäßig und sank unter Selen-defizienten Bedingungen noch weiter ab. TXNRD2 hingegen zeigte eine sehr starke enzymatische Aktivität im Pankreas und in

Selen-defizienten Tieren erhöhte sich die enzymatische Aktivität von TXNRD2 im Pankreas sogar noch, was auf eine wichtige Rolle dieses Enzyms in diesem Organ schließen lässt.

Um die Rolle von Txnrd1 und Txnrd2 im Pankreas aufzuklären wurden Gewebe-spezifische Knockout-Mäuse gezüchtet und charakterisiert. *Txnrd1* Knockout-Mäuse zeigten zuerst keinen offensichtlichen Phänotyp. Interessanter Weise jedoch, konnte in Azinus-Zellen des Pankreas von ein Jahr alten Mäusen ein dilatatives bis hin zu völlig zerstörtem rauen Endoplasmatischem Retikulum beobachtet werden. Des Weiteren wurden Veränderungen der Amylase und Lipase Werte im Blutserum gemessen. Die Tiere hatten auch eine veränderte Glucose Toleranz. Das Pankreas der *Txnrd2* Knockout-Mäuse wies eine schwerwiegende chronische Pankreatitis und voranschreitende Atrophie des Pankreasgewebes gegen Ende des Beobachtungszeitraums von einem Jahr auf. Die Mäuse entwickelten spontan eine akute Pankreatitis im Alter von vier Wochen. In der chronischen Pankreatitis wurden verschiedene Arten von azinären-duktalen Metaplasien gefunden, die zum Teil als frühe Vorläuferstadien von Pankreaskarzinomen klassifiziert werden konnten. Das endokrine Pankreas wies keine Veränderungen auf.

Dieser Pankreas-spezifische *Txnrd2* Knockout-Mausstamm ist das erste genetische Model welches spontan akute und chronische Pankreatitis entwickelt und bietet daher enorme Möglichkeiten für die Erforschung dieser inflamatorischen Erkrankung und ihrer Verbindung zu Krebserkrankungen des Pankreas.

7 References

Adrian, T.E., Bloom, S.R., Bryant, M.G., Polak, J.M., Heitz, P.H., Barnes, A.J. (1976) Distribution and release of human pancreatic polypeptide. Gut 17(12):940-4.

Aguirre, A.J., Bardeesy, N., Sinha, M., opez, L., Tuveson, D.A., Horner, J., Redston, M.S., DePhino, R.A. (2003) Activated Kras and Ink4a/Arf deficiency cooperate to produce metastatic pancreatic ductal adenocarcinoma. Genes Dev 17(24):3112-26.

Algül, H., Treiber, M., Lesina, M., Schmid, R.M. (2007) Mechanism of disease: chronic inflammation and cancer in the pancreas-a potential role for pancreatic stellate cells? Nat Clin Pract Gastroenterol Hepatol 4(8):454-62.

Almoguera, C., Shibata, D., Forrester, K., Martin, J., Arnheim, N., Perucho, M. (1988) Most human carcinomas of the exocrine pancreas contain mutant c-K-*ras* genes. Cell 53(4):549-554.

Andersson, M., Holmgren, A., Spyrou, G. (1996) NK-lysin, a disulfide-containing effector peptide of T-lymphocytes, is reduced and inactivated by human thioredoxin reductase. Implication for a protective mechanism against NK-lysin cytotoxicity. J Biol Chem 271(17):10116-20.

Apple, M.J., van Garderen-Hoetmer, A., Woutersen, R.A. (1996) Lack of inhibitory effects of beta-carotene, vitamin C, vitamin E and selenium on development of ductular adenocarcinomas in exocrine pancreas of hamsters. Cancer Lett 103(2):157-62.

Applebaum-Shapiro, S.E., Finch, R., Pfützer, R.H., Hepp, L.A., Gates, L., Amann, S., Martin, S., Ulrich, C.D., Whitcomb, D.C. (2001) Hereditary pancreatitis in North America: The Pitsburg-Midwest Multi-Center Study Group study. Pancreatology 1(5):439-43.

Apte, M.V., Haber, P.S., Applegate, T.L., Norton, I.D., McCaughan, G.W., Korsten, M.A., Pirola, R.C., Wilson, J.S. (1998) Periacinar stellate shaped cells in rat pancreas: identification, isolation, and culture. Gut 43(1):128-33.

Apte, M.V.,Park, S., Phillips, P.A., Santucci, N., Goldstein, D., Kumar, R.K., Ramm, G.A., Bichler, M., Friess, H., McCarroll, J.A., Keogh, G., Merrett, N., Pirola, R., Wilson, J.S. (2004) Desmoplastic reaction in pancreatic cancer: role of pancreatic stellate cells.

Archer, H., Jura, N., Keller, J., Jacobsen, M., Bar-Sagi, D. (2006) A mouse model of hereditary pancreatitis by transgenic expression of R122H trypsinogen. Gastroenterology 131(6):1844-55.

Arner, E.S.J., Holmgren, A. (2000) Physiological functions of thioredox and thioredoxin reductase. Eur J Biochem 267(20):6102-9.

Bachem, M.G., Schneider, E., Gross, H., Weidenbach, H., Schmid, R.M., Menke, A., Siech, M., Beger, H., Grunert, A., Adler, G. (1998) Identification, culture, and characterisation of pancreatic stellate cells in rats and humans. Gastroenterology 155(2):421-32.

Barton, C.M., Hall, P.A., Hughes, C.M., Gullick, W.J., Lemoine, N.R. (1991a) Transforming growth factor alpha and epidermal growth factor in human pancreatic cancer. J Pathol 163(2):111-6.

Barton, C.M., Staddon, S.L., Hughes, C.M., Hall, P.A., O´Sullivan, C., Klöppel, G., Theis, B., Russell, R.C.G., Neoptolemos, J., Williamson, R.C.N., Lane, D.P., Lemoine, N.R. (1991b) Abnormalities of the p53 tumour suppressor gene in human pancreatic cancer. Br J Cancer 64(6):1076-82.

Baron, T.H., Morgan, D.E. (1999) Acute necrotizing pancreatitis. N Engl J Med 340(18):1412-7.

Basran, G.S., Ramasubramanian, R., Verma, R. (1987) Intrathoracic complications of acute pancreatitis. Br J Dis Chest 81(4):326-31.

Becker, K., Gromer, S., Schirmer, R.H., Müller, S. (2000) Thioredoxin reductase as a physiological factor and drug target. Eur J Biochem 267(20:6118-25.

Behne, D., Hilmert, H., Scheid, S., Gessner, H., Elger, W. (1988) Evidence for specific selenium target tissues and new biologically important selenoproteins. Biochim Biophys Acta 966(1):12-21.

Behne, D., Kyrikopoulos, A., Scheid, S., Greener, H. (1991) Effects of chemical form and dosage on the incorporation of selenium into tissue proteins in rats. J Nutr.121(6):806-14.

Berggren, M.M., Mangin, J.F., Gasdaska, J.R., Powis, G. (1999) Effect of selenium on rat thioredoxin reductase activity: increase by supranutritional selenium and decrease by selenium deficiency. Biochem Pharmacol 57(2):187-93.

Bermano, G., Nicol, F., Deyer, J.A., Sunde, R.A., Beckett, G.J., Arthur, J.R., Hesketh, J.E. (1995) Biochem J 311(Pt2):425-30.

Berry, M.J., Banu, L., Chen, Y.Y., Mandel, S.J., Kieffer, J.D., Harney, J.W., Larsen, P.R. (1991) Recognition of UGA as a selenocystein codon in type I deiodinase requires sequences in the 3´untranslated region. Nature 353(6341):273-6.

Berry, M.J., Banu, L., Harney, J.W., Larsen, P.R. (1993) Functional characterisation of the eukaryotic SECIS elements which direct selenocysteine insertion at UGA codons. EMBO J 12(8):3315-22.

Bhopale, K.K., Wu, H., Boor, P.J., Popov, V.L., Ansari, G.A.S., Kaphalia, B.S. (2006) Metabolic basis of ethanol-induced hepatic and pancreatic injury in hepatic alcohol dehydrogenase deficient deer mice. Alcohol 39(3):179-88.

Birt, D.F., Julius, A.D., Runice, C.E., White, L.T., Lawson, T., Pour, P.M. (1988) Enhancement of BOP-induced pancreatic carcinogenesis in selenium-fed Syrian golden hamsters under specific dietary conditions. Nutr Cancer 11(1):21-33.

Bjelakovic, G., Nikolova, D., Simonetti, R.G., Gluud, C. (2004) Antioxidant supplements for prevention of gastrointestinal cancers: a systemic review and meta-analysis. Lancet 364(9441):1219-28.

Blot , W.J., Li, J.Y., Taylor, P.R., Guo, W., Dawsey, S., Wang, G.Q., Yang, C.S., Zheng, S.F., Gail, M., Li, G.Y., et al. (1993) Nutrition intervention trials in Linxian, China: supplementation with specific vitamin/mineral combinations, cancer incidence, and disease-specific mortality in the general population. J NAtl Cancer Inst 85(18):1483-92.

Burk, R.F., Norsworthy, B.K., Hill, K.E., Motley, K.E., Byrne, D.W. (2006) Effects of chemical form of selenium on plasma biomarkers in a high-dose human supplemention trial. Cancer Epidemiol Biomarkers Prev 15(4):804-10.

Burney, P.G.J., Comstock, G.W., Morris, J.S. (1989) Serologic precursors of cancer: serum micronutrients and the subsequent risk of pancreatic cancer. Am J Clin Nutr. 49(5):895-900.

Bock,A., Forchhammer, K., Heider, J., Leinfelder, W., Sawers, G., Veprek, B., Zinoni, F. (1991) Selenocystein: the 21st aminoacid. Mol Microbiol 5(3):515-20.

Bockman, D.E. (1997). Morphology of the exocrine pancreas related to pancreatitis. Microsc Res Tech. Jun 1-15;37(5-6):509-19.

Bockman, D.E., Boydston W.R., Anderson, M.C. (1982) Origin of tubular complexes in human chronic pancreatitis. Am J Surg 144(2):243-9.

Bockman, D.E., Guo, J., Büchler, P., Müller, M.W., Bergmann, F., Friess, H. (2003) Origin and development of the precursor lesions in experimental pancreatic cancer in rats. Lab Invest 83(6):853-9.

Bockman, D.E., Guo J., Müller, M.W., Friess, H., Büchler, M.W. (2004). Cell wounding in early experimental acute pancreatitis. Lab Invest 84, 362-367.

Bode, A.M., Dong, Z. (2004) Post-translational modification of p53 in tumorigenesis. Nat Rev Cancer 4(10):793-805.

Brigelius-Flohe, R. (1999) Tissue-specific functions of individual glutathione peroxidases. Free Radic Biol Med 27(9-10):951-65.

Caldas, C.; Hahn, S.A., da Costa, .T., Redston, M.S., Schutte, M., Seymour, A.B., Weinstein, C.L., Hruban, R.H., Yeo, C.J., Kern, S.E. (1994) Frequent somatic mutations and homozygous deletions of the p16 (MTS1) gene in pancreatic adenocarcinoma. Nat Genet 8(1):27-32.

Calvert, C.C., Nesheim, M.C., Scott, M.L. (1962) Effectiveness of selenium in prevention of nutritional muscular dystrophy in the chick. Proc Soc Exp Biol Med 109:16-18.

Casini, A., Galli, A., Pignalosa, P., Frulloni, L., Grappone, C., Milani, S., Pederzoli, P., Cavallini, G., Surrenti, C. (2000) Collagen type I synthesized by pancreatic stellate cells (PSC) co.localizes with lipid peroxidation-derived aldehydes in chronic alcoholic pancreatitis. J Pathol 192(1):81-9.

Clark, L.C., Cantor, K.P, Allaway, W.H. (1991) Selenium in forage crops and cancer mortality in U.S. Counties. Arch Environ Health 46(1):37-42.

Clark, L.C., Combs, G.F.Jr., Turnbull, B.W., Slate, E.h., Chalker, D.K., Chow, J., Davis, L.S., Glover, R.A., Graham, G.F., Gross, E.G., Kongrad, A., Lesher, J.L., Park, H.K., Sanders, B.B.Jr., Smith, C.L., Taylor, J.R. (1996) Effects of selenium supplementation for cancer prevention in patients with carcinoma of the skin. A randomized controlled trial. JAMA 276:1857-63.

Cohn, J.A., Friedman, K.J., Noone, P.G., Knowles, M.R., Silverman, L.M., Jowell, P.S. (1998) Relation between mutations of the cystic fibrosis gene and idiopathic pancreatitis. N Engl J Med 339(10):653-8.

Combs, G.F., Jr. (2005) Current evidence and research needs to support a health claim for selenium and cancer prevention. J Nutr. 2005; 135, 343-7.

Conrad, M., Bornkamm, G.W., Brielmeier, M. (2006) Mitochondrial and cytosolic thioredoxin reductase knockout mice. In: Hatfield, G., Berry, M.J., Gladyshev, V.N. Selenium: It´s molecular biology and role in human health. Springer Verag, New York, Berlin.

Conrad, M., Jakupoglu, C., Moreno, S.G., Lippl, S., Banjac, A., Schneider, M., Beck, H., Hatzopoulos, A.K., Just, U., Sinowatz, F., Schmahl, W., Chien, K.R., Wurst, W., Bornkoamp, G.W., Brielmeier, M. (2004) Essential role for mitochondrial thioredoxin reductase in hematopoiesis, heart development, and heart function. Mol Cell Biol 24(21):9414-23.

Contempre, B., Morreale de Escobar, G., Denef, J-F., Dumont, J.E., Many, M-C. (2004) Thiocyanate Induces Cell Necrosis and Fibrosis in Selenium- and Iodine-Deficient Rat Thyroids: A Potential Experimental Model for Myxedematous Endemic Cretinism in Central Africa. Endocrinology 145(2):994-1002.

Copeland, P.R., Fletcher, J.E., Carlson, B.A., Hatfield, D.L., Driscoll, D.M. (2000) A novel RNA binding protein, SBP2, is required for the translation of mammalian selenoprotein mRNAs. EMBO J 19(2):306-14.

Copeland, P.R., Stepanik, V.A., Driscoll, D.M. (2001) Insight into selenocysteine insertion: domain structure and ribosome binding properties of Sec insertion sequence binding protein 2. Mol Cell Biol 21(5):1491-8.

Cubilla, A.L., Fitzgerald, P.J. (1976) Morphological lesions associated with human primary invasive nonendocrine pancreas cancer. Cancer Res 36(7PT2):2690-98.

Cubilla, A.L., Fitzgerald, P.J. (1975) Morphological patterns of primary nonendocrine human pancreas carcinoma. Cancer res 35(8):2234-48.

Cullen, J.J., Weydert, C., Hinkhouse, M.M., Ritchie, J., Domann, F.E., Spitz, D., Oberley, L.W. (2003) The role of manganese superoxide dismutase in the growth of pancreatic adenocarcinoma. Cancer Res 63(6):1297-303.

Curphey, T.J., Kuhlmann, E.T., Roebuck, B.D., Longnecker, D.S. (1988) Inhibition of pancreatic and liver carcinogenesis in rats by retinoid- and selenium-supplemented diets. Pancreas 3(1):36-40.

Dabrowski, A., Chwiecko, M. (1990) Oxigen radicals mediate depletion of pancreatic sulfhydryl compounds in rats with cerulein-induced acute pancreatitis. Digestion 47(1):15-9.

Dabrowski, A., Konturek, S.J., Konturek, J.W., Gabryelewicz, A. (1999) Role of oxidative stress in the pathogenesis of caerlein-induced acute pancreatitis. Eur J Pharmacol 377(1):1-11.

Dalke, C., Löster, J., Fuchs, H., Gailus-Durner, V., Soewarto, D., Favor, J., Neuhäuser-Klaus, A., Pretsch, W., Gekeler, F., Shinoda, K., Zrenner, E., Meitinger, T., Hrabé de Angelis, M., Graw, J. (2004) Electroretinography as a screening method for mutations causing retinal dysfunction in mice. Invest Ophthalmol Vis Sci 45(2):601-9.

Day, J.D., Digiuseppe, J.A., Yeo, C., Lai-Goldman, M., Anderson, S., Goodman, S.N., Kern, S.E., Hruban, R.H. (1996) Immunohistochemical evaluation of HER-2/neu expression in pancreatic adenocarcinoma and pancreatic intraepithelial neoplasms. Hum Pathol 27(2):119-24.

Demols, A., Van Laethem, J.L., Quertimont, E., Legros, F., Louis, H., LE Moine, O., Deviere, J. (2000) N-acetylcysteindecreases severity of acute pancreatitis in mice. Pancreas 20:161-169.

Deutsch, G., Jung, J., Zheng, M., Lora, J., Zaret, K.S. (2001) A bipotential precursor population for pancreas and liver within the embryonic endoderm. Development. 2001 Mar;128(6):871-81.

DKFZ-Deutsches Krebsforschungszentrum, Krebsatlas. www.dkfz.de/de/krebsatlas/gesamt/mort_6.html

Dodd, D.C., Blakelay, A., Thornburry, S., Dewesh, F. (1960) Muscel degeneration and yellow fat disease in foals. N Z Vet J 8:45-50.

Donwhower, L.A., Harvey, M., Slale, B.L., McArthur, M.J., Montgomery, C.A., Butel, J.S., Bradley, A. (1992) Mice deficient for p53 are developmentally normal but susceptible to spontaneous tumours. Nature 356(6366):215-21.

Downs, K.M., Davies, T. (1993) Staging of gastrulating mouse embryos by morphological landmarks in the dissecting microscope. Development 118(4):1255-66.

Drake, E.N. (2006) Cancer chemoprevention: Selenium as a prooxidant, not an antioxidant. Med Hypotheses 67(2):318-22.

Du, W.D, Yuan, Z.R., Sun, J., Tang, J.X., Cheng, A.Q., Shen, D.M., Huang, C.J., Song, X.H., Yu, X.F., Zheng, S.B. (2003) Therapeutic efficacy of high dose vitamin c on acute pancreatitis and its potential mechanism. World J Gastroenterol 9:2565-2569.

Durbec J.P., Sarles, H. (1978) Multicenter survey of the etiology of pancreatic diseases. Relationship between the relative risk of developing chronic pancreatitis and alcohol, protein and lipid consumption. Digestion 18(5-6):337-50.

Eggert, G., Patterson, E., Akers, W.T., Stockstad, E.LR. (1957) The role of vitamine e and selenium in the nutrition of the pig. J Anim Sci 16:1037.

Elsässer, H.P., Adler, G., Kern, H.F. (1986) Time course and cellular source of pancreatic regeneration following acute pancreatitis in the rat. Pancreas 1:421-9

Esaki, N., Nakamura, T., Tanaka, H., Soda, K. (1982) Selenocysteine lyase, a novel enzyme that specifically acts on selenocysteine. Mammalian distribution and purification and properties of pig liver enzyme. J Biol Chem 257(8):4386-91.

Esrefoglu, M., Gül, M., Ates, B., Yilmaz, I. (2006) Ultrastructural clues for the protective effect of ascorbic acid and n-acetylcysteine against oxidative damage on caerulein-induced pancreatitis. Pancreatology 6:477-485.

Etemad, B., Whitcomb, D.C. (2001) Chronic pancreatitis: diagnosis, classification and new genetic developments. Gastroenterology 120:682-707.

Fagegaltier, D., Hubert, N., Yamada, K., Mizutani, T., Carbon, P., Krol, A. (2000) Characterisation of mSelB, a novel mammalian elongation facor for selenoprotein translation. EMBO J 19(17):4796-805.

Favor, J. (1983) A comparison of the dominant cataract and recessive specific-locus mutation rates induced by treatment of male mice with ethylnitrosourea. Mutat Res 110(2):367-82.

Franke, K.W. (1934) A new toxicant occurring naturally in certain samples of plant food stuffs. I. Results obtained in preliminary feeding trials. J Nutr 8:597-608.

Freese, E.B., Gerson, J., Taber, H., Rhaese, H.J., FreeseE. (1967) Inactivating DNA alterations induced by peroxides and peroxide-producing agents. Mutat Res 4(5):517-31.

Foster, S.J., Kraus, R.J., Ganther, H.E. (1986) The metabolism of selenomethionine, Se-methylselenocystein, their seleno derivates, and trimethylselenonium in the rat. Arch Biochem Biophys 251(1):77-86.

Gan, L., Yang, X.L., Liu, Q., Xu, H.B. (2005) Inhibitory effects of thioredoxin reductase antisense RNA on the growth of human hepatocellular carcinoma cells. J Cell Biochem 96(3):653-64.

Ganther, H.E. (1971) Reduction of the selenotrisulfide derivate of glutathione to a persulifide along by glutathione reductase. Biochemistry 10(22):4089-98.

Gasdaska, P.Y., Berggren, M.M., Berry, M.J., Powis, G. (1999a) Cloning, sequencing and functional expression of a novel human thioredoxin reductase. FEBS Lett 442(1):105-11.

Gasdaska, J.R., Harney, J.W., Gasdaska, P.Y., Powis, G., Berry, M.J. (1999b) Regulation of human thioredoxin reductase expression and activity by 3'-untranslated region selenocysteine insertion sequence and mRNA instability elements. J Biol Chem 274(36):25379-85.

Gasdaska, P.Y., Gasdaska, J.R., Cochran, S., Powis, G. (1995) Cloning and sequencing of a human thioredoxin reductase. FEBS Lett 373(1):5-9.

Gasdaska, P.Y., Oblong, J.E., Cotgreave, I.A., Powis, G. (1994) The predicted amino acid sequence of human thioredoxin is identical to that of the autocrine growth factor human adult T-cell derived factor (ADF): thioredoxin mRNA is elevated in some human tumors. Biochim Biophys Acta 1218(3):292-6.

Genovese, T., Mazzon, E., Di Paola, R., Muia, C., Crisafulli, C., Malleo, G., Esposito, E., Cuzzocera, S. (2006) Role of peroxisome proliferator-activated reseptor-α in acute pancreatitis induced by cerulein. Immunology 1881:559-570.

Gladyshev, V.N., Jeang, K.T., Stadtman, T.C. (1996) Selenocysteine, identified as the penultimate C-terminal residue in human T-cell thioredoxin reductase, corresponds to TGA in the human placental gene. Proc Natl Acad Sci USA 93(12):6146-51.

Goyens, P., Golstein, J., Nsombola, B., Vis, H., Dumont, J.E. (1987) Acta Endocrinol (Copenh) 114(4):497-502.

Grapin-Botton, A. (2005) Ductal cells of the pancreas. Int J Biochem Cell Biol 37(3):504-10.

Grattaglino, I., Palmieri, V., Vendemiale, G., Portincasa, P., Altomare, E., Palpasciano, G. (1999) Chronic ethanol administration induces oxidative alterations and functional impairment of pancreatic mitochondria in rat. Digestion 60:549-53.

Grippo, P.J., Nowlin, P.S., Demeure, M.J., Longnecker, D.S., Sandgren, E.P. (2003) Preinvasive pancreatic neoplasia of ductal phenotype induced by acinar cell targeting of mutant Kras in transgenic mice. Cancer Res 63(9):2016-19.

Gromer, S., Wissing, J., Behne, D., Ashman, K., Schirmer, R.H., Flohe, L., Becker, K. (1998) A hypothesis on the catalytic mechanism of the selenoenzyme thioredoxin reductase. Biochem J 332(Pt2):591-2.

Guerra, C., Schuhmacher, A.J., Canamero, M., Grippo, P.J., Verdguer, L., Perez-Gallego, L., Dubus, P., Sandgren, E.P., Barbacid, M. (2007) Chronic pancreatitis is essential for induction of pancreatic ductal adenocarinomaby K-Ras oncogenes in adult mice. Cancer Cell 11(3):291-302.

Gukovskaya, A.S., Mouria, M. Gukovsky, I., Reyes, C.N., Kasho, V.N., Faller, L.D., Pandol, S.J. (2002) Ethanol metabolism and transcription factor activation in pancreatic acinar cells in rats. Gastroenterology 122(3):106-118.

Haapasalo, H., Kylamiemi, M., Paunul, N., Kinnula, V.L., Soini, Y. (2003) Expression of antioxidant enzymes in astrocytic brain tumors. Brain Pathol 13(2):155-64.

Haber, P.S., Keogh, G.W., Apte, M.V., Moran, C.S., Stewart, N.L., Crawford, D.H., Pirola, R.C.,McCaughan, G.W., Ramm, G.A., Wilson, J.S. (1999) Activation of pancreatic stellate cells in human and experimental pancreatic fibrosis. Am J Pathol 155(4):1087-95.

Hahn, S.A., Schutte, M., Hoque, A.T., Moskaluk, C.A., da Costa, L.T., Rozenblum, E., Weinstein, C.L., Fisher, A., Yeo, C.J., Hruban, R.H., Kern, S.E. (1996) DPC4, a candidate tumor suppressor gene at human chromosome 18q21.1. Science 271(5247):350-3.

Hainhaut, P., Milner, J. (1993) Redox modulation of p53 conformation and sequence-specific DNA binding in vitro. Canser Res 53(19):4469-73.

Hansson, H.A., Holmgren, A., Rozell, B., Täljedal, I.B. (1986) Immunohistochemical localization of thioredoxin and thioredoxin reductase in mouse exocrine and endocrine pancreas. Cell Tissue Res 245:189-195.

Harrison, K.A., Thaler, J., Pfaff, S.L., Gu, H., Kehrl, J.H. (1999) Pancreas dorsal lobe agenesis and abnormal islets of Langerhans in Hlxb9-deficient mice. Nat Genet 23(1):71-5.

Hartley, W.J., Grant, A.B. (1961) A review of selenium responsive disease of New Zealand livestock. Fed Proc 20:679-688.

Hatfield, D.L.; Gladyshev, V.N. (2002) How selenium has altered our understanding of the genetic code. Mol Cell Biol 22(11):3565-76.

Hawkins, P. (2002) Recognizing and assessing pain, suffering and distress in laboratory animals: a survey of current practice in the UK with recommendations. Lab Anim,36,378-95.

Hazelwood, R.L. (1993) The pancreatic polypeptide (PP-fold) family: gastrointestinal, vascular, and feeding behavioral implications. Proc Soc Exp Biol Med 202(1):44-63.

Hebrok M, Kim SK, St Jacques B, McMahon AP, Melton DA. (2000) Regulation of pancreas development by hedgehog signaling. Development 127(22):4905-13.

Hill, K.E., McCollum, G.W., Boeglin, M.E., Burk, R.F. (1997) Thioredoxin reductase activity is decreased by selenium deficiency. Biochem Biophys Res Commun 234(2):293-5.

Hill, K.E., Lyons, P.R., Burk, R.F. (1992) Differential regulation of rat liver selenoprotein mRNAs in selenium deficiency. Biochem Biophys Res Commun 185(1):260-3.

Hingorani, S.R., Petricoin, E.F., Maitra, A., Rajapakse, V., King, C., Jacobetz, M.A., Ross, M.A., Conrads, T.P., Veenstra, T.D., Hitt, B.A., Kawaguchi, Y., Johann, D., Liotta, L.A., Crawford, H.C., Putt, M.E., Jacks, T., Wright, C.V., Hruban, R.H., Lowy, A.M., Tuveson, D.A. (2003) Preinvasive and invasive ductal pancreatic cancer and its early detection in the mouse. Cancer Cell 4(6):437-50.

Hisaoka, M., Haratake, J., Hashimoto, H. (1993) Pancreatic morphogenesis and extracellular matrix organization during rat development. Differentiation 53(3):163-72.

Holland, A.M., Hale, M.A., Kagami, H, Hammer, R.E., MacDonald, R.J. (2002) Experimental control of pancreatic development and maintenance. Proc Natl Acad Sci U S A. 2002 Sep 17;99(19):12236-41. Epub 2002 Sep 9.Holmgren, A., Bjornstedt, M. (1995) Thioredoxin and thioredoxin reductase.Methods Enzymol.1995;252:199-208.

Holmgren, A. (1977) Bovine thioredoxin system. Purification of thioredoxin reductase from calf liver and thymus and studies of its function in disulfide reduction. J Biol Chem 252(13):4600-6.

Hoshino, M., Nakamura, S., Mori, K., Kawaguchi, T., Terao, M., Nishimura, Y.V., Fukuda, A., Fuse, T., Matsuo, N., Sone, M., Watanabe, M., Bito, H., Terashima, T., Wright, C.V., Kawaguchi, Y., Nakao, K., NabeshimaY. (2005) Ptf1a, a bHLH transcriptional gene, defines GABAergic neuronal fates in cerebellum. Neuron 47(2):201-13.

Howes, N., Greenhalf, W., Stocken, D.D., Neoptolemos, J.P. (2004) Cationic trypsinogen mutations and pancreatitis. Gastroenterol Clin North Am 33(4):767-87.

Hruban, R.H., Adsay, N.V., Albores-Saavedra, J., Anver, M.R., Biankin,A.V., Boivin, G.P., Furth, E.E., Furukawa, T., Klein, A., Klimstra, D.S., Kloppel, G., Lauwers, G.Y., Longnecker, D.S., Luttges, J., Maitra, A., Offerhaus, G.J., Perez-Gallego, L., Redston, M., Tuveson, D.A. (2006a) Pathology of genetically engineered mouse models of pancreatic exocrine cancer: consensus report and recommendations. Cancer Res. 2006 Jan 1;66(1):95-106.

Hruban, R.H., Adsay, V., Albores-Saavedra, J., Compton, C., Garrett, E.S., Goodman, S.N., Kern, S.E., Klimstra, D.S., Klöppel, G., Longnecker, D.S., Lüttges, J., Johan, G., Offerhaus, A. (2001) Pancreatic intraepithelial neoplasia: a new nomenclature and classification system for pancreatic duct lesions. Am J Surg Pathol 25(5):579-86.

Hruban, R.H., Rustgi, A.K., Brentnall, T.A., Tempero, M.A., Wright, C.V., Tuveson, D.A. (2006b) Pancreatic cancer in mice and man: the Penn Workshop 2004. Cancer Res 66(1):14-7.

Hsieh, H.S., Ganther, H.E. (1975) Acid-Volatile selenium formation catalyzed by glutathione reductase. Biochemistry 14(8):1632-6.

Ikejiri, N. (1990) The vitamin A-storing cells in the human and rat pancreas. Kurume Med J 37(2):67-81.

Iovanna, J.L., Redifferentiation and apoptosis of pancreatic cells during acute pancreatitis. Int J Pancreatol 20(2):77-84.

Ip, C., Hayes, C., Budnick, R.M., Ganther, H.E. (1991) Chemical form of selenium, critical metabolites, and cancer prevention. Cancer Res 51(2):595-600.

Jacks, T., Remington, L., Williams, B.O., Schmitt, E.M., Halachmi, S., Bronson, R.T., Weinberg, R.A. (1994) Tumor spectrum analysis in p53-mutant mice. Curr Bio 4(1):1-7.

Jakupoglu, C., Przermeck, G.K., Schneider, M., Moreno, S.G., Mayer, N., Hatzopoulos, A.K., deAngelis, M.H., Wurst, W., Bornkomp, G.W., Brielmeier, M., Conrad, M. (2005) Cytoplasmic thioredoxin reductase is essential for embryogenesis but dispensable for cardiac development. Mol Cell Biol. 2005 Mar;25(5):1980

Jemal, A., Siegel, R., Ward, E., Murray, T., Ku, J., Thun, M.J. (2007) Cancer statistics, 2007. CA Cancer J Clin 57(1):43-66.

Ji, C., Kaplowitz, N. (2004) Hyperhomocysteinemia, endoplasmic reticulum stress, and alcoholic liver injury. World J Gastroenterol 10(12):1699-708.

Kadowaki, H., Nishitoh, H., Ichijo, H. (2004) Survival and apoptosis signals in ER stress: the role of protein kinases. J Chem Neuroanat 28(1-2):93-100.

Karimpour, S., Lou, J., Lin, L.L., Rene, L.M., Lagunas, L., Ma, X., Karra, S., Bradbury, C.M., Markovina, S., Goswami, P.C., Spitz, D.R., Hirota, K., Kalvakolanu, D.V., Yodoi, J., Gius, D. (2002) Thioredoxin reductase regulates AP-1 activity as well as thioredoxin nuclear localization via active cysteines in response to ionizing radiation. Oncogene 21(41):6317-27.

Kawaguchi, Y., Cooper, B., Gannon, M., Ray M, MacDonald R.J, Wright C.V (2002) The role of the transcriptional regulator Ptf1a in converting intestinal to pancreatic progenitors. Nat Genet 32(1):128-34.

Kim, S.K, Hebrok, M, Melton, D.A. (1997) Notochord to endoderm signaling is required for pancreas development. Development. 1997 Nov;124(21):4243-52.

Kim, S.K., MacDonald, R.J. (2002) Signaling and transcription control of pancreatic organogenesis. Curr Opin Genet Dev. 2002 Oct;12(5):540-7.

Kishi, S., Takeyama, Y., Ueda, T., Yasuda, T. Shinzeki, M., Kuroda, Y., Yokozaki, H. (2003) Pancreatic duct obstruction itself induces expression of alpha smooth muscle actin in pancreatic stellate cells. J Sur Res 114(1):6-14.

Klein, A.P., Hruban, R.H., Brune, K.A., Petersen, G.M., Goggins, M. (2001) Familial pancreatic cancer. Cancer J 7(4):266-73.

Klempt, M., Rathkolb, B., Fuchs, E., Hrabe de Angelis, M., Wolf, E., Aigner, B. (2006) Genotype-specific environmental impact oft he variance of blood values in inbred and F1 hybrid mice. Mamm Genome (2):93-102.

Klimstra, D.S., Longnecker, D.S. (1994) K-ras mutations in pancreatic ductal proliverative lesions. Am J Pathol 145(6):1547-50.

Knekt, P., Aromaa, A., Maatela, J., Alfthan, G., Aaran, R-K., Hakama, M., Hakulinen, T., Peto, R., Teppo, L. (1990) Serum selenium and subsequent risk of cancer among Finnish men and women. J Natl Cancer Inst 82(10):864-8.

Kobayashi, Y., Orga, Y., Ishiwata, K., Takayama, H., Aimi, N., Suzuki, K.T. (2002) Seneosuggars are key and urinary metabolites for selenium excretion within the required to low-toxic range. Proc Natl Acad Sci USA 99(25):15932-6.

Koehrle, J. (2000) The deiodinase family: selenoenzymes regulating thyroid hormone availability and action. Cell Mol Live Sci 57(13-14):1853-63.

Krapp, A., Knofler, M., Frutiger, F., Hughes, G.J., Hagenbuchle, O., Wellauer, P.K. (1996) The p48 DANN-binding subunit of transcription factor PTF1 ia a new exocrine pancreas-specific basic helix-loop-helix protein. EMBO J 15(16):4317-4329.

Krapp, A., Knöfler, M., Ledermann, B., Bürki, K., Berney, C., Zoerkler, N., Hagenbüchle, O., Wellauer, P.K. (1998) The bHLH protein PTF1-p48 is essential for the formation of the exocrine and the correct spatial organization of the endocrine pancreas. Genes Dev 12(23):3752-63.

Krüger, B., Albrecht, E., Lerch, M.M. (2000) The role of intracellular calciumsignalling in premature protease activation and the onset of pancreatitis. Am J Pathol 157(1):43-50.

Kryukov, G.V., Castellano, S., Novoselov, S.V., Lobanov, A.V., Zehtab, O., Guigo, R., Gladyshev, V.N. (2003) Characterisation of mammalian selenoproteoms. Science 300 (5624):1439-43.

Kubisch, C.H., Sans, M.D., Arumugam, T., Ernst, S.A., Williams, J.A., Logsdon, C.D. (2006) Early activation of endoplasmatic reticulum stress is associated with arginin-induced acute pancreatitis. Am J Physiol Gastrointerst Liver Physiol 291:G238-G245.

Kumar, S., Björnstedt, M., Holmgren, A. (1992) Selenite is a substrate for calf thymus thioredoxin reductase and thioredoxin and elicits a large non-stoichiometric oxidation of NADPH in the presence of oxygen. Eur J Biochem 207(2):435-39.

Lechene dlP, P., Iovanna, J., Odaira, C., Choux, R., Sarles, H., Berger, Z. (1991) Involvement of tubular complexes in pancreatic regeneration after acute necrohemorrhagic pancreatitis. Pancreas 6:298-306.

Lee, B.J., Worland, P.J., Davis, J.N., Stadtman, T.C., Hatfield, D.L. (1989) Identification of a selenocysteyl-tRNA(Ser) in mammalian cells that recognizes the nonsense codon, UGA. J Biol Chem 264(17):9724-7.

Leinfelder, W., Zehelein, E., Mandrand-Berthelot, M.A., Boeck, A. (1988) Gene for a novel tRNA species that accepts L-serine and cotranslationally inserts selenocystein. Nature 331(6158):723-5.

Li, H, Arber, S, Jessell, TM, Edlund, H. (1999) Selective agenesis of the dorsal pancreas in mice lacking homeobox gene Hlxb9. Nat Genet. 1999 Sep;23(1):67-70.

Li, H, Edlund, H. (2001) Persistent expression of Hlxb9 in the pancreatic epithelium impairs pancreatic development. Dev Biol. 2001 Dec 1;240(1):247-53.

Li, H., Kantoff, P.W., Giovannucci, E., Leitzmann, M.F., Gaziano, J.M., Stampfer, M.J., Ma, J. (2005) Manganese superoxide dismutase polymorphism, prediagnostic antioxidant status, and risk of clinical significant prostate cancer. Cancer Res 65(6):2498-504.

Li, H.S., Zhag, J.Y., Thompson, B.S., Deng, X.Y., Ford, M.E., Wood, P.G., Stolz, D.B., Eagon, P.K., Whitcomb, D.C. (2001) Rat mitochondrial ATP synthase ATP5G3: cloning and upregulation in pancreas after chronic ethanol feeding. Physiol Genomics 6(2):91-8.

Loeb, W.F., Quimby, F.W. (1999) The clinical chemistry of laboratory animals. Taylor & Francis, London.

Low, S.C., Berry, M.J. (1996) Knowing when not to stop: selenocysteine incorporation in eukaryotes. Trends Biochem Sci 21(6):203-8.

Low, S.C., Gundner-Culemann, E., Harney, J.W., Berry, M.J. (2000) SECIS-SBP2 interaction dictate selenocysteine incorporation efficiency and selenoprotein hierarchy. EMBO J 19(24):6882-90.

Lowenfels, A.B., Maisonneuve, P., Cavallini, G., Ammann, R.W., Lankisch, P.G., Andersen, J.R., DiMagno, E.P., Andren-Sandberg, A., Domellöf, L. (1993) Pancreatitis and the risk of pancreatic cancer. International Pancreatitis Study Group. N Engl J Med 328(20):1433-7).

Lowenfels, A.B., Maisonneuve, P., DiMagno, E.P., Elitsur, Y., Gates, L.K.Jr., Perrault, J., Whitcomb, D.C. (1997) Hereditary pancreatitis and the risk of pancreatitic cancer. International Hereditary Pancreatitis Study Group. J Natl Cancer Inst 89(6):442-6.

Lu, J., Jiang, C., Kaeck, M., Ganther, H., Vadhanavikit, S., Ip, C., Thompson, H. (1995) Dissociation of the genotoxic and growth inhibitory effects of selenium. Biochem Pharmacol 50(2):213-9.

Lugea, A., Nan, L., French, S.W., Bezerra, J.A., Gukovskava, A.S., Pandol, S.J. (2006) Pancreas recovery following cerulean-induced panceatitis is impaired in plasminogen-deficient mice. Gastroenterology 131(3):885-99.

Luthman, A., Holmgren, A. (1982) Rat liver thioredoxin and thioredoxin reductase: purification and characterisation. Biochemistry 21(26):6628-33.

Luty-Frackiewicz, A. (2005) The role of selenium in cancer and viral infection prevention. Int J Occup Med Environ Health 18(4):305-11.

Ma, Y., Hendershot, L.M. (2004) ER chaperon functions during normal and stress conditions. J Chem Neuroanat 28(1-2):51-65.

MacKenzie, P.I., Messer, M. (1976) Sstudies on the origin and excretion of serum alpha-amylase in the mouse. Comp Biochem Physiol B 54(1):103-6.

Malka, D., Hammel, P., Maire, F., Rufat, P., Madeira, I., Pessione, F., Levy, P., Ruszniewski, P. (2002) Risk of pancreatic adenocarcinoma in chronic pancreatitis.

Marino, C.R., Matovcik, L.M.,Gorelick, F.S., Cohn, J.A. (1991) Localization of the cystic fibrosis transmembrane conductance regulator in pancreas. J Clin Invest 88(2):712-6.

Matsui, M., Oshima, M., Oshima, H., Takaku, K., Maruyama, T., Yodoi, J., Taketo, M.M. (1996) Early embryonic lethality caused by targeted disruption of the mouse thioredoxin gene. Dev Biol 178(1):179-85.

Matsuzaka, Y., Okamoto, K., Mabuchi, T., Iizuka, M., Ozawa, A., Oka, A., Tamiya, G., Kulski, J.K., Inoko, H. (2005) Identification and characterisation of novel variants of the thioredoxin reductase 3 new transcript 1 TXNRD3NT1. Mamm Genome 16(1):41-9.

McCuskey, R.S., Chapman, T.M. (1969) Microscopy of the living pancreas in situ. Am J Anat 126(4):395-407.

Meuillet, E., Stratton, S., Cherukuri, D.P., Goulet, A-C., Kagey, J., Porterfield, B., Nelson, M.A. (2004) Chemoprevention of prostate cancer with selenium: An update on current clinical trials and preclinical findings. J Cell Biochem 91(3):443-58.

Moxon, A.L., Olson, O.E., Seawright, W.V. (1939) Selenium in rocks, soils and plants. S D Agric Exp Stn Tech Bull 2:88-90.

Mustacich, D., Powis, G. (2000) Thioredoxin reductase. Biochem J 346(Pt1):1-8.

Muth, O.H., Odfield, J.E., Remmert, L.F., Schubert, J.R. (1958) Effects of selenium ans vitamine E on white muscel disease. Science(Washington, DC) 128:1090.

Nakhai, H., Sel, S., Favor, J., Mendoza-Torres, L., Paulsen, F., Duncker, G.I., Scmid, R.M. (2007) Ptf1a is essential for the differentiation of GABAergic and glycinergic amacrine cells and horizontal cells in the mouse retina. Development 134(6):1151-60.

Naruse, S. (2003) Molecular pathophysiology of pancreatitis. Intern Med 42(3):288-9.

Nicklas, W., Baneux, P., Boot, R., Decelle, T., Deeny, A.A., Fumanelli, M., Illgen-Wilcke, B., FELASA (Federation of European Laboratory Animal Science Associations Working Group on Health Monitoring of Rodent and Rabbit Colonies) (2002) Recommendations for the health monitoring of rodent and rabbit colonies in breeding and experimental units. Lab Anim 36(1):20-42

Nishikawa, A., Furukawa, F., Imazawa, T., Yoshimura, H., Mitsumori, K., Takahashi, M. (1992) Effects of caffeine, nicotine, ethanol and sodium selenite on pancreatic carcinogenesis in hamsters after initiation with N-nitrosobis(2-oxoproyl)amine. Carcinogenesis 13(8):1379-82.

Nishinake, Y., Nakamura, H., Yodoi, J. (2002) Thioredoxin cytokine action. Methods Enzymol 347:332-8.

Nonn, L., Williams, R.R., Erickson, R.P., Powis, G. (2003) The absence of mitochondrial thioredoxin 2 causes massive apoptosis, exencephaly, and early embryonic lethality in homozygous mice. Mol Cell Biol 23(3):916-22.

Nordberg, J., Arner, E.S. (2001) Reactive oxygen species, antioxidants, and the mammalian thioredoxin system. Free Radic Biol Med 31(11):1287-312.

Obata, J., Yano, M., Mimura, H., Toto, T., Nakayama, R., Mibu, Y., Oka, C., Kawaichi, M. (2001) p48 subunit of mouse PTF1 binds to RBP-KI/CBF-1, the intracellular mediator of Notch signaling, and is expressed in the neural tube of early stage embryos. Genes Cells 6(4):345-360.

Olson, G.E., Winfrey, V.P., Nagdas, S.K., Hill, K.E., Burk, R.F. (2005) Selenoprotein P is required for mouse sperm development. Biol Reprod 73(1):201-11.

Omary, M.B., Lugea, A., Lowe, A.W., Pandol, S.J. (2007) The pancreatic stellate cell: a star on the rise in pancreatic diseases. J. Clin. Invest 117(1):50-9.

Ornitz, D.M., Palmiter, R.D., Hammer, R.E., Brinster, R.L., Swift, G.H., MacDonald, R.J. (1985) Specific expression of an elastase-human growth hormone fusion gene in pancreatic acinar cells of transgenic mice. Nature 313(6003):600-2.

Papp, L.V., Lu, J., Holmgren, A., Khanna, K.K. (2007) From selenium to selenoproteins: synthesis, identity, and their role in human health. Antioxid Redox Signal 9(7):775-806.

Parks, D., Bolinger, R., Mann, K. (1997) Redox state regulates binding of p53 to sequence-specific DNA, but not to non-specific or mismatched DNA. 25(6):1289-95.

Pastor, C.M., Vonlaufen, A., Georgi, F., Hadengue, A., Morel, P., Frossard, J-L. (2006) Neutrophil depletion-but not prevention of kupffer cell activation-decreases the severity of cerulein-induced acute pancreatitis. World J Gastroenterol 12(8):1219-1224.

Pavelka, M., Roth, J. (2005) Funktionelle Ultrastruktur. Springer- Verlag, Wien, New York.

Pictet, R.L., Clark, W.R., Williams, R.H., Rutter, W.J. (1972) An ultrastructural analysis of the developing embryonic pancreas. Dev. Biol. 1972, 29, 436-467

Poston, H.A., Combs, G.F.Jr, Leibovitz, L. (1976) Vitamine E and selenium interrelation in the diet of Atlantic salmon: gross histological and biochemical deficiency. J Nutr 106:892-904.

Pubolos, M.H., Bartelt, D.C., Greene, L.J. (1974) Trypsin inhibitor from human pancreas and pancreatic juice. J Biol Chem 249(7):2235-42.

Qin, J., Clore, G.M., Kennedy, W.M., Huth, J.R., Gronenborn, A.M. (1995) Solution structure of human thioredoxin in a mixed disulfide intermediate complex with its target peptide from the transcription factor NF kappa B. Structure 3(3):289-97.

Raraty, M., Ward, J., Erdemil, G., Vaillant, C., Neoptolemos, J.P., Sutton, R., Petersen , O.H. (2000) Calcium-dependent enzyme activation and vacuole formation in the apical granular region of pancreatic acinar cells. Proc Natl Acad Sci USA 97(24):13126-31.

Rayman, M.P. (2004). The use of high-selenium yeast to raise selenium status: how does it measure up? Br J Nutr 2004, 92, 557-73.

Rayman, M.P. (2005) Selenium in cancer prevention: a review of the evidence and mechanism of action. Proc Nutr Soc 64(4):527-42.

Reid, M.E., Stratton, M.S., Lillico, A.J., Fakhi, M., Natarajan, R., Clark, L.C., Marshall, J.R. (2004) A report of high-dose selenium supplementation; response and toxicities. J Trace Elem Med Biol 18(1):69-74.

Rhee, S.G., Kang, S.W., Chang, T.S., Jeong, W., Kim, K. (2001) Peroxiredoxin, a novel family of peroxidases. IUBMB Life 52(1-2):35-41.

Richards, C., Fitzgeralds, P.J., Carol, B., Rosenstock, L., Lipkin, L. (1964) Segmental division of the rat pancreas for experimental procedures. Lab Invest 13:1303-21.

Riese, C., Michaelis, M., Mentrup, B., Götz, F., Köhrle, J., Schweizer, U., Schomburg, L. (2006) Selenium-dependent pre- and posttranscriptional mechanisms are responsible for sexual dimorphic expression of selenoproteins in murine tissue. Endocrinology 147(12):5883-92.

Rose, S.D., Swift, G.H., Peyton, M.J., Hammer, R.E., MacDonald, R.J. (2001) The role of PTF1-P48 in pancreatic acinar gene expression. J Biol Chem 276(47):44018-44026.

Rotruck, J.T., Pope, A.L., Ganther, H.E., Swanson, A.B., Hafeman, D.G., Hoekstra, W.G. (1973) Selenium: biochemical role as a component of glutathione peroxidase. Science 179(73):588-90.

Rubin, E., Farber, J.L. (1990). Essential Pathology. J.B. Lippincott Company, Philadelphia, Pennsylvania, USA.

Sabichi, A.L., Lee, J.J., Taylor, R.J., Thompson, I.M., Miles, B.J., Tangen, C.M., Minasian, L.M., Pister, L.L., Caton, J.R., Basler, J.W., Lerner, S.P., Menter, D.G., Marshall, J.R., Crawford, E.D., Lippman, S.M. (2006) Selenium accumulation in prostate tissue during a randomized, controlled short-term of L-selenomethionine: a Southwest Oncology Group Study. Clin Cancer Res 12(7Pt1):2178-84.

Sahin-Tóth, M., Tóth, M. (2000) Gain-of-function mutations associated with hereditary pancreatitis enhance autoactivation of human cationic trypsinogen. Biochem Biophys Res Commun 278(2):286-9.

Sandalova, T., Zhong, L., Lindquist, Y., Holmgren, A., Schneider, G. (2001) Three-dimensional structure of a mammalian thioredoxin reductase: implications for mechanism and evolution of a selenocysteine-dependent enzyme. Proc Natl Acad Sci USA 98(17):9533-8.

Sandgren, E.P., Luetteke, N.C., Palmiter, R.D., Brinster, R.L., Lee, D.C. (1990) Overexpression of TGF alpha in transgenic mice: induction of epithelial hyperplasia, pancreatic metaplasia, and carcinoma of the breast. Cell 61(6):1121-35.

Sandren, E.P., Luetteke, N.C., Qiu, T.H., Palmiter, R.D., Brinster, R.L., Lee, D.C. (1993) Transforming growth factor alpha dramatically enhances oncogene-induced carcinogenesis in transgenic mouse pancreas and liver. Mol Cell Biol 13(1):320-30.

Saluja, A.K., Bhagat, L., Lee, H.S., Bhatia, M., Frossard, J.L, Steer, M.L. (1999). Secretagogue-induced digestive enzyme activation and cell injury in rat pancreatic acini. Am J Physiol 276:G835-G842.

Scherb, H. (2001) Determination of uniformly most powerful tests in discrete sample spaces. Metrika 53(1):71-84.

Schmucker, C., Schaeffel, F. (2004) In vivo biometry in the mouse eye with low coherence interferometry. Vision Res 44(21):2445-56.

Schmucker, C., Seeliger, M., Humphries, P., Biel, M., Schaeffel, F. (2005) Grating aculity at different luminances in wild.type mice and in mice lacking rod or corne function. Invest Ophthalmol Vis Sci 46(1):398-407.

Schneider, A., Whitcomb, D.C. (2002) Hereditary pancreatitis: a model for inflammatory diseases of the pancreas. Best Pract Res Clin Gastronterol 16(3):347-63.

Schomburg, L., Riese, C., Renko, K., Schweizer, U. (2007) Effect on age on sexually dimorphic selenoprotein expression in mice. Biol Chem 388(10):1035-41.

Schrauzer, G.N., White, D.A., Schneider, C.J. (1977a) Cancer mortality correlation studies—III: statistical associations with dietary selenium intakes. Bioinorg Chem 7(1):23-31.

Schrauzer, G.N., White, D.A., Schneider, C.J. (1977b) Cancer mortality correlation studies—IV: associations with dietary intakes and blood levels of certain trace elements, notably Se-antagonists. Bioinorg Chem 7(1):35-56.

Schrauzer, G.N. (2000) Selenomethionine: a review of its nutritional significance, metabolism and toxicity. J Nutr 130(7):1653-6.

Schrauzer, G.N. (2003) The nutritional significance, metabolism and toxicology of selenomethionine. Adv Food Nutr Res 47:73-112.

Schreiner, B., Baur, D.M., Fingerle, A.A., Zechner, U., Greten, F.R., Adler, G., Sipos, B., Klöppel, G., Hameister, H., Schmid, R.M. (2003) Pattern of secondary genomic changes in pancreatic tumors of Tgf alpha/Trp53+/- transgenic mice. Genes Chromosomes Cancer 38(3):240-8.

Schwarz, K., Foltz, C.M. (1957) Selenium as an integral part of factor 3 against dietary necrotic liver degeneration. J Am Chem Soc 79:3292-93.

Schweizer, U., Michaelis, M., Köhrle, J., Schomburg, L. (2004) Efficient selenium transfer from mother to offspring in selenoprotein-P-deficient mice enables dose-dependent rescue of phenotypes associated with selenium deficiency. Biochem J 378(Pt1):21-6.

Seemann, S., Hainaut, P. (2005) Roles of thioredoxin reductase 1 and APE/Ref-1 in the control of basal p53 stability and activity. Oncogene 24(24):3853-63.

Shamberger, R.J. (1985) The genotoxicity of selenium. Mutat Res 154(1):29-48.

Shamberger, R.J., Tytko, S.A., Willis, C.E.(1976) Antioxidants and cancer. Arch Environ Health 31(5):231-5.

Sharer, N., Schwarz, M., Malone, G., Howarth, A., Painter, J., Super, M., Braganza, J. (1998) Mutations of the cystic fibrosis gene in patients with chronic pancreatitis. N Engl J Med 339(19):645-52.

Shen, X., Zhang, K., Kaufman, R.J. (2004) The unfolded protein respunce – a stress signaling pathway of the endoplasmic reticulum. J Chem Neuroanat 28(1-2):79-92.

Shiobara, Y., Yoshida, T., Suzuki, K.T. (1998) Effects of dietary selenium species on se concentrations in hair, blood, and urine. Toxicol Appl Pharmacol 152(2):1237-14.

Silbernagl, S., Despopoulos, A. (2001) Taschenatlas der Physiologie. Georg Thieme Verlag, Stuttgart.

Sill, R. (1999) Bedeutung von Selen in Prävention und komplementärer Therapie. Pharm. Ztg. 32:2508-2513.

Slater, T.F. (1984) Overview of methods used for detecting lipid peroxidation. Methods Enzymol 105:283-93.

Soriano, P. (1999) Generalized lacZ expression with the ROSA26 Cre reporter strain. Nat Genet 21(1):70-1.

Spooner, B.S., Walther, B.T., Rutter, W.J. (1970) The development of the dorsal and ventral mammalian pancreas in vivo and in vitro. J Cell Biol 47(1):235-46.

Stadtman, T.C. (1996) Selenocystein. Annu Rev Biochem 65:83-100.

Stocks, J., Dormandy, T.L. (1971) The autoxidation of human red cell lipids induced by hydrogen peroxide. Br J Haematol 20(1):95-111.

Strobel, O., Dor, Y., Stirman, A., Trainor, A., Fernandez-del Castillo, C., Warshaw, A.L., Thayer, S.P. (2007) ß cell transdifferentiation does not contribute to preneoplastic/metaplastic ductal lesions of the pancreas by genetic lineage tracing *in vivo*. PNAS 104(11):4419-24.

Su, D., Novoselov, S.V., Sun, Q.A., Moustafa, M.E., Zouh, Y., Oko, R., Hatfield, D.L., Gladyshev, V.N. (2005) Mammalian selenoprotein thioredoxin-glutathione reductase. Roles in disulfide bond formation and sperm maturation. J Biol Chem. 280(28):26491-8.

Sun, Q.A., Kirnarsky, L., Sherman, S., Gladyshev, V.N. (2001) Selenoprotein oxidoreductase with specificity for thioredoxin and glutathione systems. Proc Natl Acad Sci USA 98(7):3673-8.

Sun. Q.A., Wu, Y., Zappacosta, F., Jeang, K.T., Lee, B.J., Hatfield, D.L., Gladyshev, V.N. (1999) Redox regulation of cell signaling by selenocysteine in mammalian thioredoxin reductases. J Biol Chem 274(35):24522-30.

Surrai (2006) Selenium in nutrition and health. Nottingham University Press, Nottingham, United Kingdom.

Tamura, T., Stadtman, T.C. (1996) A new selenoprotein from human lung adenocarcinoma cells: purification, properties, and thioredoxin reductase activity. Proc Natl Acad Sci USA 93(3):1006-11.

Tanaka, T., Reddy, B.S., el-Bayoumy, K. (1985) Inhibition by dietary organoselenium, p-methoxybenzene-selenol, of hepatocarcinogenesis induced by azoxymethane in rats. Jpn J Cancer Res 76(6):462-7.

Thompson, J.N., Scott, M.L. (1970) Impaired lipid and vitamin E absorption related to atrophy of the pancreas in selenium-deficent chicks. J Nutr 100:797-809.

Tong, W.M., Wang, F. (1998) Alterations in rat pancreatic islet β cells induced by Keshan disease pathogenic factors: protective action of selenium and vitamin E. Metabolism 47(4):415-9.

Tsai, K., Wang, S.S., Chen, T.S., Kong, C.W., Chang, F.Y., Lee, S.D., Lu, J. (1998) Oxidative stress: an important phenomenon with pathogenic significance in the progression of acute pancreatitis. Gut 42:850-855

Tujebajeva, R.M., Copeland, P.R., Xu, X.M., Carlson, B.A., Harney, J.W., Driscoll, D.M., Hatfield, D.L., Berry, M.J. (2000) Decoding apparatus for eukaryotic selenocysteine insertion. EMBO Rep 1(2):158-63.

Turunen, N., Karihatala, P., Mantymiemi, A., Sormunen, R., Holmgren, A., Kinula, V.L., Soini, Y. (2004) Thioredoxin is associated with proliferation, p53 expression and negative estrogen and progesterone receptor status in breast carcinoma. APMIS 112(2):123-32.

Ueno, M., Masutani, H., Arai, R.J., Yamauchi, A., Hirota, K., Sakai, T., Inamoto, T., Yodoi, J., Nikaido, T. (1999) Thioredoxin-dependent redox regulation of p53-mediated p21 activation. J Biol Chem 274(50):35809-15.

Urunuela, A., Sevillano, S., de la Mano, A.M., Manso, M.A., Orfao, A., de Dios I (2002) Time-course of oxygen free radical production in acinar cells during acute pancreatitis induced by pancreatic duct obstruction. Biochim Biophys Acta 1588:159-164.

Van Vleet, J.F., Ferrans, V.J. (1977) Ultrastructural alterations in skeletal muscle of selenium-vitamin E deficient ducklings. Am J Vet Res 38:1231-36.

Vinceti, M., Wei, E.T., Malagoli, C., Bergomi, M., Vivoli, G. (2001) Adverse health effects of selenium in human health. Rev Environ Health 16(4):233-51.

Voet, D., Voet, J.G. (2004) Biochemistry. John Wiley & Sons, Inc, Hoboken, USA.

Voronina, S., Longbottom R., Sutton, R., Petersen, O.H., Tepikin, A. (2002) Bile acids induce calcium signals in mouse pancreatic acinar cells: implications for bile-induced pancreatic pathology. J Physiol 540(Pt1):49-55.

Wagner, M., Greten, F.R., Weber, C.K., Koschnick, S., Mattfeldt, T., Deppert, W., Kern, H., Adler, G., Schmid, R.M. (2001) A murine tumor progression model for pancreatic cancer recapitulating the genetic alterations of the human disease. Genes Dev. 2001 Feb 1;15(3):286-93.

Wagner, M., Lührs, H., Klöppel, G., Adler, G., Schmid, R.M. (1998) Malignant transformation of duct-like cells originating from acini in transforming growth factor α transgenic mice. Gastroenterology 115(5):1254-62.

Walter, E.D., Jensen, L.S. (1964) Serum glutamic-oxalacetic acid transaminase levels, muscular dystrophy and certain hematological measurements in chicks and poults as influenced by vitamine E, selenium and methionine. Poult Sci 43:919-26.

Watari, N., Hotta, Y., Mabuchi, Y. (1982) Morphological studies on a vitamin A-storing cell and its complex with macrophage observed in mouse pancreatic tissue following excess vitamin A administration. Okajimas Folia Anat Jpn 58(4-6):837-58.

Welch, H.G., Schwartz, L.M., Woloshin, S. (2000) Are increasing 5-year survival rates evidence of success against cancer? JAMA 283(22):2975-78.

Wells, J.M., Melton, D.A. (2000) Early mouse endoderm is patterened by soluble factors from adjacent germ layers. Development. Apr;127(8):1563-72.

Wessels, N.K., Cohen, J. (1967) Early pancreas organogenesis: morphogenesis, tissue interactions, and mass effects. Dev Biol 15:237-270.

Whanger, P.D. (2001) Selenium and the brain: a review. Nutr Neurosci 4(2):81-97.

Whanger, P.D. (2004) Selenium and its relationship to cancer: an update dagger. Br J Nutr 91(1):11-28.

Whanger, P.D., Weswig, P.H. (1975) Effects of selenium, chromium and antioxidants on growth, eye cataracts, plasma cholesterol and blood glucose in selenium-deficient, vitamine E supplemented rats. Nutr Rep Int 12:345-58.

Whitcomb, D.C. (2004) Value of genetic testing in management of pancreatitis. Gut 53(11):1710-7.

Whitcomb, D.C. (1999) Hereditary pancreatitis: New insights into acute and chronic pancreatitis. Gut 45(3):317-22.

Whitcomb, D.C. (1996). Hereditary pancreatitis is caused by a mutation in the cationic trypsinogen gene. Nat Genet. 14:141-5

Whitcomb, D.C., Pogue-Geile, K. (2002) Pancreatitis as a risk for pancreatic cancer. Gastroenterol Clin North Am 31(2):663-78.

Willemer, S., Adler, G. (1989) Histochemical and ultrastructural characteristics of tubular complexes in human acute pancreatitis. Dig Dis Sci 34(1):46-55.

Williams, C.H.Jr., Arscott, L.D., Müller, S., Lennon, B.W., Ludwig, M.L., Wang, P.F., Veine, D.M., Becker, K., Schirmer, R.H. (2000) Thioredoxin reductase two modes of catalysis have evolved. Eur J Biochem 267(20):6110-7.

Witt, H., Luck, W., Hennies, H.C., Classen, M., Kage, A., Lass, U., Landt, O., Becker, M. (2000) Mutations in the gene encoding the serine protease inhibitor, kazal type 1 are associated with chonic pancreatitis. Nat Genet 25(2):213-16

Woutersen, R.A., Appel, M.J., van Garderen-Hoetmer, A. (1999) Modulation of pancreatic carcinogenesis by antioxidants. Food Chem Toxicol 37(9-19):981-4.

Wu, A.S.H., Oldfield, J.E., Whanger, P.D., Weswig, P.H. (1973) Effect of selenium, vitamin E and antioxidants on teticular function in rats. Biol Reprod 8:625-29.

Xia, L., Nordman, T., Olsson, J.M., Damdimopoulos, A., Bjorkhem-Bergman, L., Nalvarte, I., Erikkson, L.C., Arner, E.S., Spyrou, G., Bjornsted, M. (2003) The mammalian cytosolic selenoenzyme thioredoxin reductase reduces ubiquinone. A novel mechanism for defense against oxidative stress. J Biol Chem 278(4):2141-6.

Yeh, J.Y., Vendeland, S.C., Gu, Q., Butler, J.A., Ou, B.R., Whanger, P.D. (1997) Dietary selenium increases selenoprotein W levels in rat tissues. J Nutr. 127(11):2165-72.

Yokota, T., Denham, W., Murayama, K., Pelham, C., Joehl, R., Bell, R.H.Jr. (2002) Pancreatic stellate cell activation and MMP production in experimental pancreatic fibrosis. J Surg Res 104(2):106-11.

Yoo, M.H., Xu, X.M., Carlson, B.A., Gladyshev, V.N., Hatfield, D.L. (2006) Thioredoxin reductase 1 deficiency reverses tumor phenotype and tumorigenicity of lung carcinoma cells. J Biol Chem 281(19):13005-8.

Yu, S.Y., Zhu, Y.J., Li, W.G. (1997) Protective role of selenium arainst hepatitis B virus and primary liver cancer in Qidong. Biol Trace Elem Res. 56(1):117:24.

Zhong, L., Arner, E.S., Holmgren, A. (2000) Structure and mechanism of mammalian thioredoxin reductase: the active site is a redox-active selenolthiol/selenenylsulfide formed from the conserved cysteine-selenocysteine sequence. Proc Natl Acad Sci USA 97(11):5854-9.

Zhong, L., Arner, E.S., Ljung, J., Aslund, F., Holmgren, A. (1998) Rat and calf thioredoxin reductase are homologous to glutathione reductase with a carboxyl-terminal elongation containing a conserved catalytically active penultimate selenocysteine residue. J Biol Chem 273(15):8581-91.

Zhong, L., Holmgren, A. (2000) Essential role of selenium in the catalytic activities of mammalian thioredoxin reductase revealed by characterisation of recombinant enzymes with selenocysteine mutations. J Biol Chem 275(24):18121-8.

8 Appendix

8.1 List of figures

8.2 List of tables

Abbreviations

ABC	avidin-biotin complex
AP-1	activator protein 1
bp	base pair
BrdU	5-bromo-2´-deoxyuridine
cDNA	copy deoxyribonucleic acid
CFTR	cystic fibrosis transmembrane conductance regulator
dATP	deoxyadenosine triphosphate
dCTP	deoxycytidine triphosphate
dGTP	deoxyguanosine triphosphate
DIs	iodothyronine deiodinase
DMF	N,N-dimethylformamide
DNA	deoxyribonucleic acid
dNTP	deoxynucleoside triphosphate
DTNB	5,5´-dithio-bis-(2-nitrobenzoic acid)
dTTP	deoxythymidine triphosphate
E	embryonic day
EDTA	ethylenediamine-tetraacetic acid
EFSec	selenocystein specific elongation factor
EGF	epidermal growth factor
FAD	flavin adenine dinucleotide
Fig	figure
GPx	glutathione peroxidase
GSH	glutathione
GSSG	oxidized glutathione
HCL	hydrochloric acid
H&E	haematoxylin and eosin
HEPES	4-(2-hydroxyethyl)-1-piperazine-ethanesulfonic acid
hGH	human growth hormone
Hlxb9/Mnx1	motor neuron and pancreas homeobox 1
IP-GTT	intra peritoneal-glucose tolerance test
IL	interleukin
Ipf1	Insulin promoter factor 1

PBS	phosphate buffered saline
Pdx1	pancreas duodenum homeobox 1
MnSOD	manganese superoxide dismutase
MPO	myeloperoxidase
mRNA	messenger ribonucleic acid
NADPH	nicotinamideadeninedinucleotidephosphate
NF-κB	nuclear factor-kappa B
PanIn	pancreatic intraepithelial neoplasia
PAS	periodic acid schiff
PCR	polymerase chain reaction
PDA	pancreatic ductal adenocarcinoma
Ptf1	pancreas transcription factor 1
Ptf1a-p48	pancreas transcription factor 1a-subunit 48
PRSS1	cationic trypsinogen
PSTI	pancreatic secretory trypsin inhibitor
RNA	ribonucleic acid
rER	rough endoplasmic reticulum
rRNA	ribosomal ribonucleic acid
ROS	reactive oxygen species
RT-PCR	reverse transcription-polymerase chain reaction
R26R	Cre reporter strain ROSA26R
SAPE	sentinel acute pancreatitis event
SBP2	selenocysteine insertion sequence binding protein 2
Sec	selenocysteine
SECIS	selenocysteine insertion sequence
SePP	selenoprotein P
SelW	selenoprotein W
SDS	sodium dodecylsulfate
SPINK1	pancreatic secretory trypsin inhibitor
TBE	Tris borate EDTA
TEM	transmission electron microscopy
TGF-α	transforming growth factor-alpha
TGF-β	transforming growth factor-beta
TGR	thioredoxin-glutathione- reductase

Tris	Tris(hyoroxymethyl)-aminomethane
tRNA	transfer ribonucleic acid
Txn1	thioredoxin 1
Txn2	thioredoxin 2
Txnrd1	cytosolic thioredoxin reductase
Txnrd2	mitochondrial thioredoxin reductase
Txnrd3	testis associated thioredoxin reductase
UTR	untranslated region
wt	wild type
X-Gal	5-bromo-4-chloro-3-indolyl-B-D-galactopyranosidase

According to the international standards for gene and protein-notation in mice, proteins are notated in capital letters (e.g. TXNRD1), genes cursive, first a capital letter, followed by small letters (e.g. *Txnrd1*). This stands in contrast to human protein and gene notation.

Acknowledgments

This work has been carried out at the Helmholtz Center Munich – German Research Center for Environmental Health (GmbH), formerly GSF-National Research Center for Environment and Health, Neuherberg, Germany, Department of Comparative Medicine, during the years 2005 – 2007.

First of all, I would like to thank Prof. Dr. Jörg Schmidt, head of the Department of Comparative Medicine for committing me the following thesis. His unlimited support and ever present interest in the progress of this work was a great motivation. I also want to thank him for giving me the chance to discuss my research on several conferences.

I would like to express my deepest gratitude to Prof. Dr. Lutz Graeve for being my supervisor at the university, especially as I was an external student. I want to thank him for his willingness for discussion and his support.

Especially, I would like to thank Dr. Markus Brielmeier for being my supervisor at the Department of Comparative Medicine. As he established the whole selenium project, I had the great chance to take part in this exciting research field. He was never tired of spending time in meetings and discussions, and letting me develop my own ideas. His continuous support for and confidence in my work and my person were of great help and motivation. He also encouraged me to discuss my research projects on several conferences. I am grateful for his patient proof-reading of this manuscript and my scientific drafts.

Furthermore, I am indebted to Prof. Dr. Roland Schmid, head of the 2nd Medical Clinic, Kinikum Rechts der Isar, Technical University, Munich, for letting me take part and benefit of his great knowledge, enthusiasm and research spirit. It was a pleasure to meet and work with him. He gave me a first insight into the fascinating world of the pancreas. The EL-TGFα-hGH transgenic mice, the p53$^{+/-}$ knockout mice and the *Ptf1a-Cre*^{ex1} mice were a kind gift from him. Also, I would like to thank his research group, especially Dr. Hana Algül, Dr. Matthias Treiber, Dr. Henrik Einwächter and Dr. Jens Siveke for supporting me with theoretical and technical knowhow and the CK19 antibody.

I would like to thank Dr. Claudia Kiermayer for teaching me the enzyme assay.

Warmest thanks go to Claudia Ludwig for technical assistance. Especially, during my stay in hospital she helped me in keeping the 16 mouse strains.

My deepest thank I would like to express to all other persons from the Helmholtz Center Munich – German Research Center for Environmental Health who supported my work with technical and theoretical help and always having time for great discussions: Univ. Doz. Dr. Bernhard Michalke and Peter Grill from the Institute of Ecological Chemistry, Central Inorganic Service Analytics, for selenium analytics, Dr. Leticia Quintanilla-Fendt, Dr. Gabriele Hölzlwimmer and Elenore Samson, from the Institute of Pathology for technical support and their help in analyzing the sections of the EL-TGF-$\alpha^{tg/+}$;*p53*$^{+/-}$ mice, PD Dr. Axel Walch and Luise Jennen also form the Institute of Pathology for their help with transmission electron microscopy, Prof. Dr. Joachim Graw, Dr. Claudia Dahlke, Dr. Oliver Puk, Erika Bürkle and Maria Kugler from the German Mouse Clinic for the eye screens, Dr. Hagen Scherb, Institute of Biomathematics and Biometry for his kind help with and discussions about biostatistics, Dr. Lutz Ruprecht, animal welfare officer, for always having an open ear and advising me in animal handling questions and last but not least all the animal caretakers for their excellent work and expertise.

All my friends, who never stopped believing in me and encouraged me to do and finish this Ph.D. thesis, receive my warmest thanks: Isa and Thomas, Flo, Colonel … and all the rest, and of course Susi and Peter. To Susi a special thanks for great administrative work and technical support in the Department of Comparative Medicine.

My studies and Ph.D. theses would not have been possible without the love and financial support of my parents, Gerda and Bernd Aichler. Never was a distance too far, never a hole too deep, never a problem too big. They have always been there for me. I would like to express my warmest thanks for everything they did for me.

And, last but not least, I also would like to express my deepest thanks to Tom, having always a warm shoulder and a kiss for me.

Unterschleißheim, December 2007 Michaela Aichler

Curriculum Vitae

Not published in the electronic version.

Declaration / Erklärung

This thesis with the topic:
Diese Arbeit mit dem Thema:

“Influence of selenium on pancreatic carcinogenesis and the role of the selenoproteins cytosolic and mitochondrial thioredoxin reductase in the pancreas.”

is presented in the fulfilment of the requirement for the degree of Doctor rerum naturalis in the Faculty of Natural Sciences at the University of Hohenheim. I herby certify that this thesis is entirely my own work. All materials and references which were required for this work are indicated.

entspricht den Anforderungen zur Erlangung des Grades eines Doctor rerum naturalis in der Fakultät Naturwissenschaften der Universität Hohenheim. Hiermit erkläre ich, dass ich die vorliegende Dissertation selbständig und unter Verwendung der angegebenen Quellen und Hilfsmittel angefertigt habe.

Ort, Datum

Unterschrift